ANTIBODY THERAPY OF CANCER

FC RECEPTOR-MEDIATED MECHANISMS OF ACTION

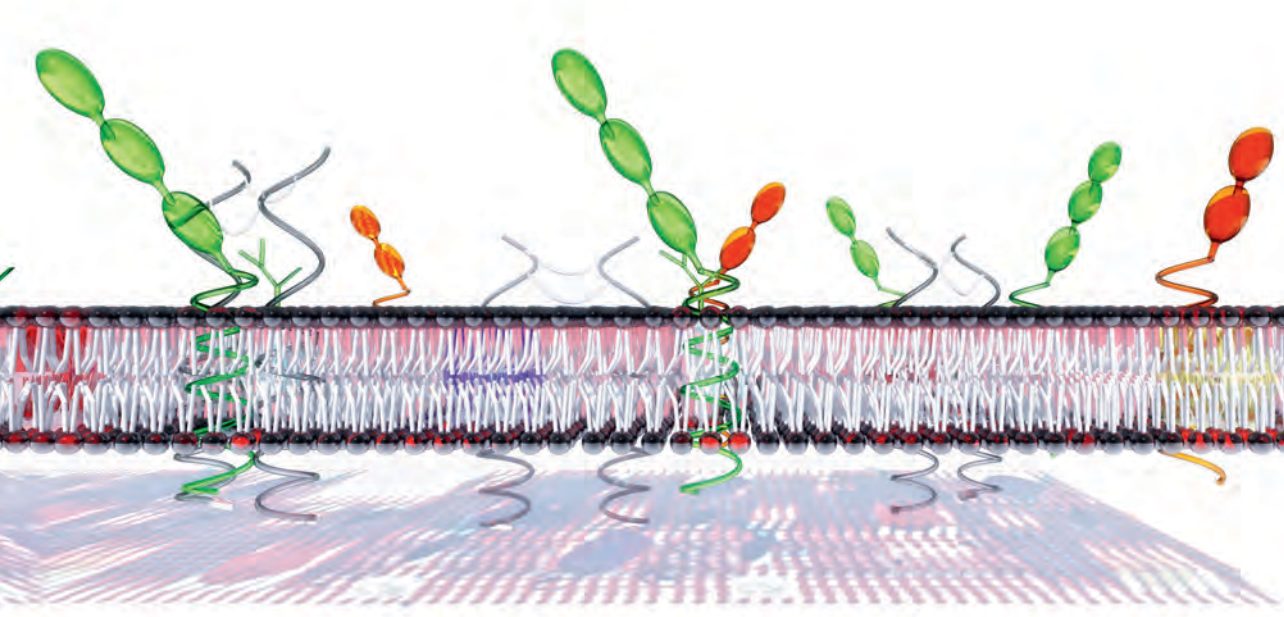

MARIJE B. OVERDIJK

Antibody therapy of cancer

Fc receptor-mediated mechanisms of action

Marije Berber Overdijk

Beoordelingscommissie:
Prof. dr. C.E. Hack
Prof. dr. M.H.M. Wauben
Prof. dr. H.M. Lokhorst
Prof. dr. J.J.W. de Haard
Prof. dr. F.G.M. Kroese

Cover art: Roel de Ruiter
Layout: Ferdinand van Nispen, Citroenvlinder-dtp.nl, Bilthoven, The Netherlands
Printed by GVO drukkers & vormgevers B.V. | Ponsen & Looijen, Ede

ISBN/EAN: 978-90-6464-716-1

Proefschrift Universiteit Utrecht, Faculteit Geneeskunde

Antibody therapy of cancer

Fc receptor-mediated mechanisms of action

Antistof therapie voor kanker

Fc receptor-gemedieerde werkingsmechanismen

(met een samenvatting in het Nederlands)

Proefschrift

ter verkrijging van de graad van doctor aan de Universiteit Utrecht op gezag van de rector magnificus, prof.dr. G.J. van der Zwaan, ingevolge het besluit van het college voor promoties in het openbaar te verdedigen op donderdag 28 november 2013 des middags te 12.45 uur

door

Marije Berber Overdijk
geboren op 6 januari 1980, te Sneek

Promotor:	Prof. dr. J.G.J. van de Winkel
Co-promotoren:	Dr. P.W.H.I. Parren Dr. W. K. Bleeker

Dit proefschrift werd mede mogelijk gemaakt met financiële steun van Genmab.

List of abbreviations

Ab	antibody
ADC	antibody drug conjugate
ADCC	antibody-dependent cellular cytotoxicity
ADCP	antibody-dependent cellular phagocytosis
Ag	antigen
BL	burkitt's lymphoma
BM	bone marrow
CDC	complement-dependent cytotoxicity
CRC	colorectal cancer
CTC	circulating tumor cell
DARA	daratumumab (human IgG1 CD38 mAb)
E:T	Effector : Target ratio
EGFR	epidermal growth factor receptor
ELISA	enzyme-linked immunosorbent assay
EMA	European Medicines Agency
Fab-region	fragment antigen binding-region
FACS	fluorescence activated cell sorting
Fc-region	fragment crystallizable-region
FcγR	Fc-gamma receptor
FDA	Food and drug administration
i.v.	intravenous
IgG	immunoglobulin G
mAb	monoclonal antibody
MFI	mean fluorescence intensity
MM	multiple myeloma
MNC	mononuclear cells
MoA	mechanism of action
Mφ	macrophage
NK cell	natural killer cell
PBMC	peripheral blood mononuclear cell
PCD	programmed cell death
PMN	polymorphonuclear leukocyte
s.c.	subcutaneous
SCID mouse	severe combined immunodeficiency mouse
TR-FRET	time-resolved fluorescence resonance energy transfer
WT	wild type
Zalu	zalutumumab (human IgG1 EGFR mAb)

Table of contents

1

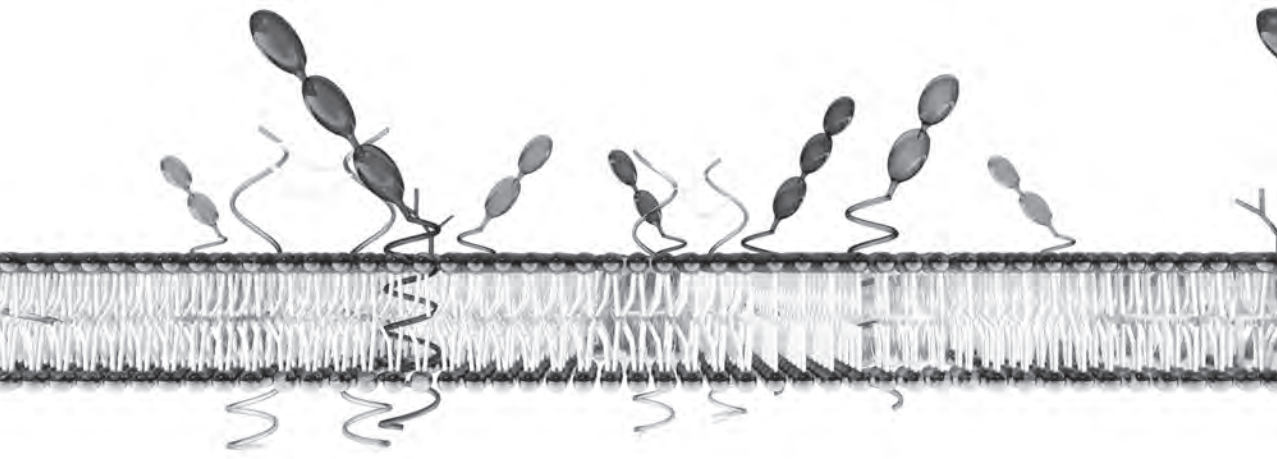

General outline and aim of the thesis

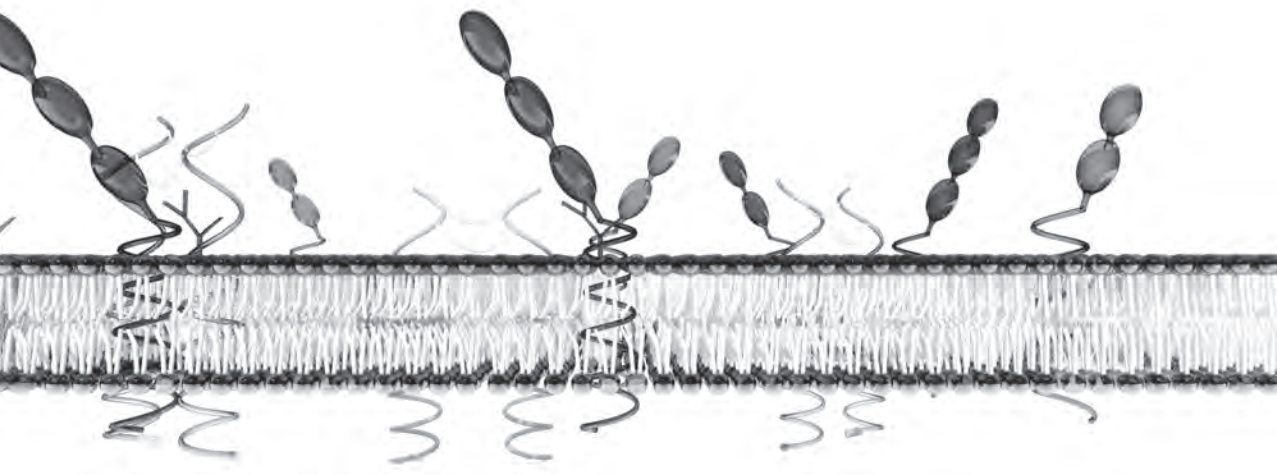

Antibodies (Abs) form the basis of the adaptive humoral immune response, which protects the body against pathogens. Antibodies are produced by B-cells, which originate from hematopoietic stem cells in the bone marrow. B-cells enter the bloodstream after successful expression of a unique B-cell receptor (BCR), consisting of membrane bound immunoglobulin (Ig). Recognition of pathogen specific antigens (Ags) results in B-cell activation and selection for B cells with high affinity BCR which will mature into Ab-secreting B cells.

Antibodies are built up by a pair of identical light chains and a pair of identical heavy chains, which are connected via multiple disulfide bonds (hinge region) (Fig. 1). The light chains are formed by one variable domain (V_L) and one constant domain (C_L). The heavy chain is formed by one variable domain (V_H) and three or four constant domains (C_H1, C_H2, C_H3, C_H4), depending on the class of the Ab.

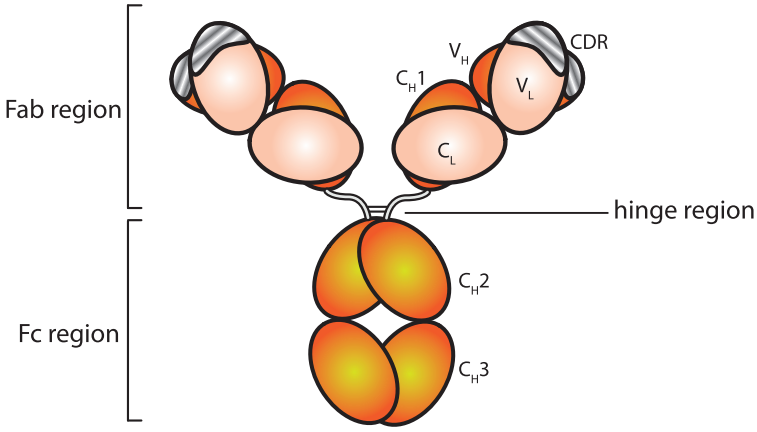

Figure 1. *IgG1 antibody structure.* Depicted are the two light chains (light orange) and the two heavy chains (dark orange).

Antibodies contain two Fab (fragment antigen binding) regions, each composed of one light chain (V_L, C_L) and two domains of a heavy chain (V_H, C_H1). The Fab-regions determine the selectivity for the antigen via the hypervariable complementary determining regions (CDRs) located at the top of the Fab-regions. The Fc (fragment crystallizable) region, composed of the remaining constant domains of both heavy chains, determines the class of the Ab.

In humans there are five different Ab classes, namely IgA, IgD, IgE, IgG and IgM. The most abundant class in the bloodstream is IgG, which can potently initiate either Fab and/or Fc-mediated immunity against invading pathogens. Binding

of the Fab-regions to the Ag may result in preventing entry of the pathogen or toxin into healthy cells, also referred to as Ab-mediated neutralization. The Fab-mediated binding to Ag may also result in coating of the pathogen surface, so-called opsonization, leading to activation of an immune response via the clustered Fc-region. A cellular immune response is activated by binding of clustered IgG Fc-regions to Fc-gamma receptors (FcγRs) expressed on immune effector cells such as NK-cells, macrophages and neutrophils. Subsequently, the FcγRs become activated and may induce antibody-dependent cellular cytotoxicity (ADCC) and/or antibody-dependent cellular phagocytosis (ADCP). A non-cellular immune response is activated by binding of proteins of the complement system to the clustered Fc-regions which activates complement-dependent cytotoxicity (CDC). In addition, considerable interactions between the cellular and complement system exist with substantial cross-activation and synergies.

Cancer is a class of malignant diseases which is characterized by unregulated cell growth caused by either genetic alterations or environmental factors (1). Radiation or chemotherapy combined with surgical removal of the tumor when possible, often represents the standard of care. However, limitations of a narrow therapeutic index and frequently acquired resistance for radiation and chemotherapy stimulated the development of targeted therapies (2). The high specificity of Abs and the (near) absence of off-target effects, combined with the ability to engage multiple mechanisms of action (MoA), made them attractive agents for treatment of cancer. The introduction of the hybridoma technique (fusion of an immortalized myeloma cell line with an Ab-producing B cell) by Kohler and Milstein (3), made it possible to produce large quantities of monoclonal antibodies (mAbs) derived from one B-cell *in vitro*. Therefore, it became feasible to produce mAbs directed against tumor Ags and this started a revolution in anti-cancer treatment, which continues to date. The first therapeutic mAbs were of murine origin, however to reduce the risk for immunogenicity and provide optimal interactions with the human immune system human(ized) mAbs were developed (4). As of January 2013, 15 antibody products are being marketed for cancer treatment in various countries around the globe, all of the IgG class (**Chapter 2,** Fig. 2). The possible Fab and Fc-mediated MoA of therapeutic mAbs inducing anti-tumor activity are addressed in **Chapter 2**. To develop novel, more effective mAbs and therapies, a better understanding of the role for the different MoA is required. Therefore, the aim

of this thesis was to study the FcγR-mediated effects of mAbs to gain insight into which, when and where FcγR-mediated antibody effector functions contribute to anti-tumor activity.

In **Chapter 2** we reviewed pre-clinical and clinical studies with therapeutic mAbs, with emphasis on the role of Fc-FcγR mediated effector functions. In humans there are five activating FcγRs (hFcγRI, hFcγRIIa, hFcγRIIc, hFcγRIIIa, hFcγRIIIb) and one inhibitory FcγR, (hFcγRIIb), which all contain a ligand-binding extracellular α-chain. Most activating FcγRs are linked to a dimer of γ-chains that are critical for outside-in signaling and effector cell activation (Fig. 2). For the different FcγRs single nucleotide polymorphisms have been described (5), which result in FcγR polymorphic variants with an amino acid substitution. These polymorphic variants differ in functionality and are further explained in **Chapter 2**. The IgG Abs are subdivided in four isotypes, IgG1, IgG2, IgG3 and IgG4, which each have a unique affinity for the different FcγRs. Table I shows the affinity order of the different IgG isotypes for the different FcγRs (6, 7), which is reflected in their biological activities (8-10). Mice have only three activating FcγRs; (mFcγRI, mFcγRIII, mFcγRIV) and also one inhibitory FcγR (mFcγRIIb) (Fig. 2) (11). Since mouse models still represent a crucial step in the pre-clinical development of therapeutic mAbs, we addressed the question how different human IgG isotypes interact with murine FcγR-expressing effector cells in **Chapter 3.**

Table 1. Interactions of human FcγRs with the different IgG isotypes

		Human	
FcγR	**Isoform expressed**	**Polymorphic Variant**	**IgG specificity**
FcγRI (CD64)	FcγRIa	-	IgG3≥1>4, no binding IgG2
FcγRII (CD32)	FcγRIIa	R131	IgG3≥1>4>>>>IgG2
		H131	IgG3≥1=2>> IgG4
	FcγRIIb	-	IgG3≥1≥4>2
FcγRIII (CD16)	FcγRIIIa	F158	IgG3>>IgG1, no binding IgG2,4
		V158	IgG3>IgG1>>IgG4>IgG2
	FcγRIIIb	NA-1, NA-2	IgG3≥IgG1, no binding IgG2,4

Based on data Bruhns et al. (6)

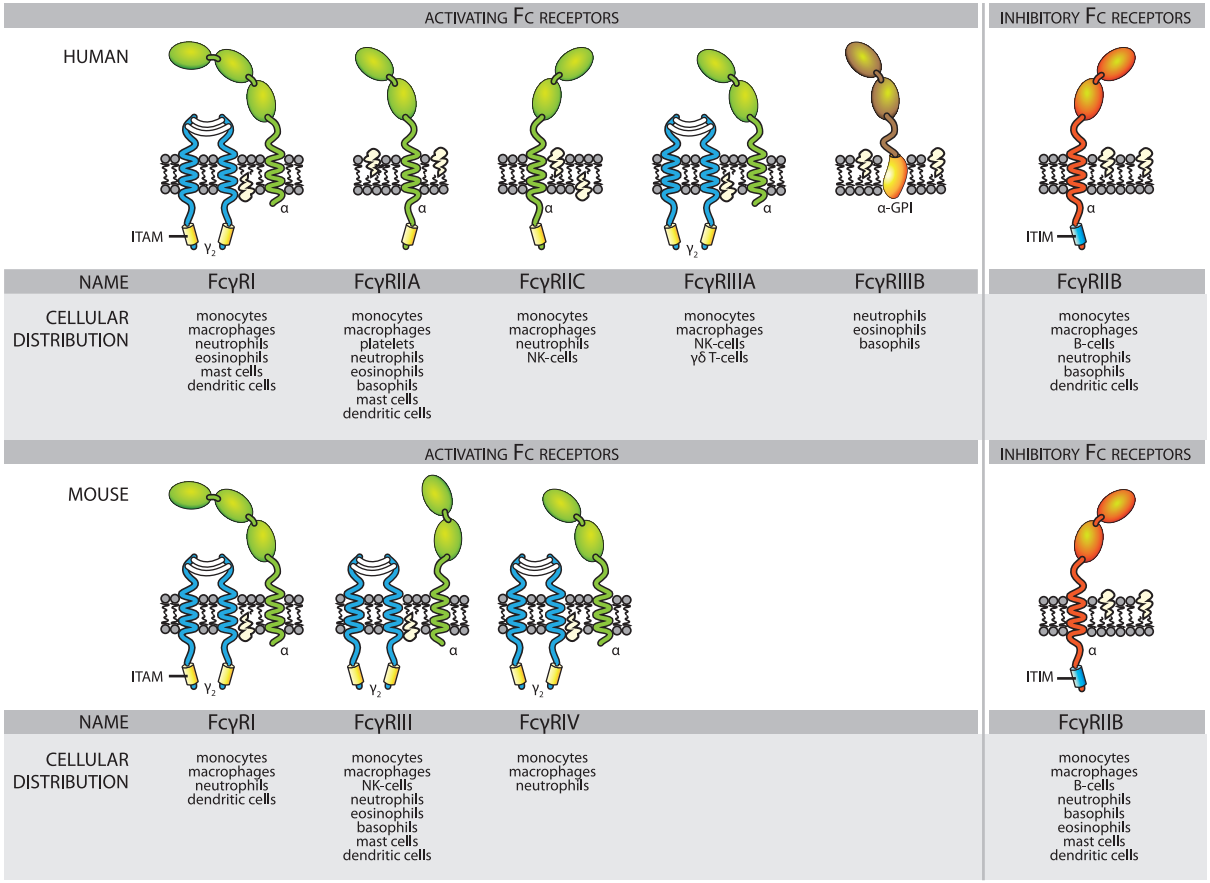

Figure 2. *Schematic representation of the human (upper panel) and mouse (lower panel) FcγRs.*

After mapping the interplay of the murine cellular immune effector system with different human IgG isotypes, we studied the contribution of several FcγR-mediated effector functions to the MoA of therapeutic mAbs in more detail. In **Chapter 4** the contribution of antibody-dependent cellular phagocytosis (ADCP) to the MoA for daratumumab (human IgG1 CD38 mAb) was explored. The role of FcγR-mediated crosslinking of daratumumab, resulting in induction of tumor cell programmed cell death, was studied in **Chapter 5**. In **Chapter 6** the *in vivo* contribution of antibody-dependent cellular cytotoxicity (ADCC) in the MoA for epidermal growth factor receptor (EGFR) targeting mAbs was addressed. In **Chapter 7** we studied the potential of EGFR as a target for peri-operative treatment of colon carcinoma. A general discussion is provided in **Chapter 8,** addressing the key findings of this thesis and putting them in context of future antibody therapeutic approaches of cancer.

References

1. Anand, P., A. B. Kunnumakkara, C. Sundaram, K. B. Harikumar, S. T. Tharakan, O. S. Lai, B. Sung, and B. B. Aggarwal. 2008. Cancer is a preventable disease that requires major lifestyle changes. *Pharm Res* 25:2097-2116.
2. Vanneman, M., and G. Dranoff. 2012. Combining immunotherapy and targeted therapies in cancer treatment. *Nat Rev Cancer* 12:237-251.
3. Kohler, G., and C. Milstein. 1975. Continuous cultures of fused cells secreting antibody of predefined specificity. *Nature* 256:495-497.
4. Ruuls, S. R., J. J. Lammerts van Bueren, J. G. van de Winkel, and P. W. Parren. 2008. Novel human antibody therapeutics: the age of the Umabs. *Biotechnol J* 3:1157-1171.
5. Concetti, F., and V. Napolioni. 2010. Insights into the role of Fc gamma receptors (FcgammaRs) genetic variations in monoclonal antibody-based anti-cancer therapy. *Recent Pat Anticancer Drug Discov* 5:197-204.
6. Bruhns, P., B. Iannascoli, P. England, D. A. Mancardi, N. Fernandez, S. Jorieux, and M. Daeron. 2009. Specificity and affinity of human Fcgamma receptors and their polymorphic variants for human IgG subclasses. *Blood* 113:3716-3725.
7. van de Winkel, J. G., and C. L. Anderson. 1991. Biology of human immunoglobulin G Fc receptors. *J Leukoc Biol* 49:511-524.
8. Parren, P. W., P. A. Warmerdam, L. C. Boeije, J. Arts, N. A. Westerdaal, A. Vlug, P. J. Capel, L. A. Aarden, and J. G. van de Winkel. 1992. On the interaction of IgG subclasses with the low affinity Fc gamma RIIa (CD32) on human monocytes, neutrophils, and platelets. Analysis of a functional polymorphism to human IgG2. *J Clin Invest* 90:1537-1546.
9. Parren, P. W., P. A. Warmerdam, L. C. Boeije, P. J. Capel, J. G. van de Winkel, and L. A. Aarden. 1992. Characterization of IgG FcR-mediated proliferation of human T cells induced by mouse and human anti-CD3 monoclonal antibodies. Identification of a functional polymorphism to human IgG2 anti-CD3. *J Immunol* 148:695-701.
10. Bruggemann, M., G. T. Williams, C. I. Bindon, M. R. Clark, M. R. Walker, R. Jefferis, H. Waldmann, and M. S. Neuberger. 1987. Comparison of the effector functions of human immunoglobulins using a matched set of chimeric antibodies. *J Exp Med* 166:1351-1361.
11. Nimmerjahn, F., and J. V. Ravetch. 2008. Fcgamma receptors as regulators of immune responses. *Nat Rev Immunol* 8:34-47.

2

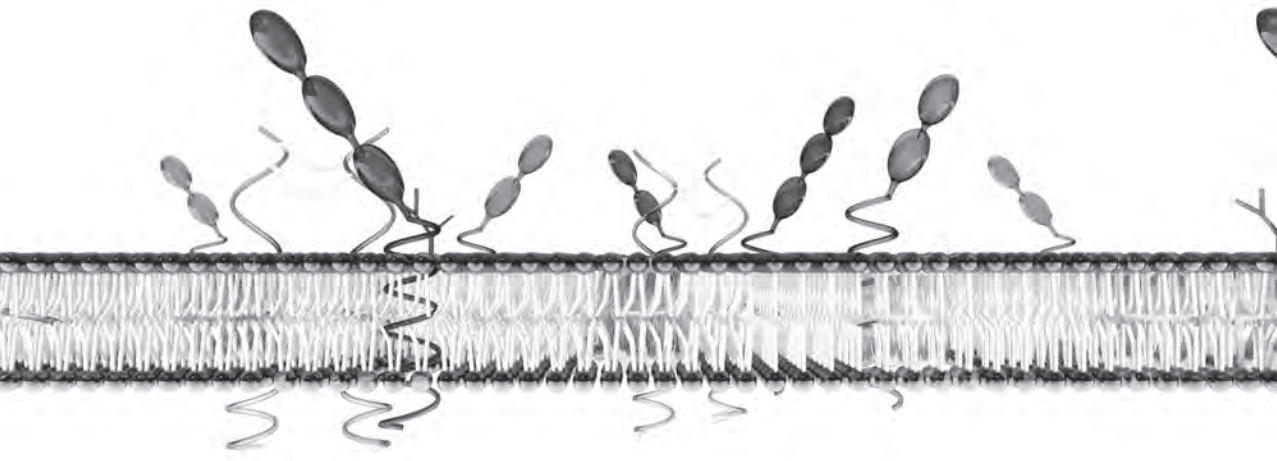

Role of IgG Fc Receptors in Monoclonal Antibody Therapy of Cancer

Marije B. Overdijk[*], Sandra Verploegen[*], Wim K. Bleeker[*] and Paul W.H.I. Parren[*]
[*]Genmab, Utrecht, The Netherlands

Chapter 13, *Antibody Fc: Linking Adaptive and Innate Immunity*, page 239-255, ISBN 9780123948021,

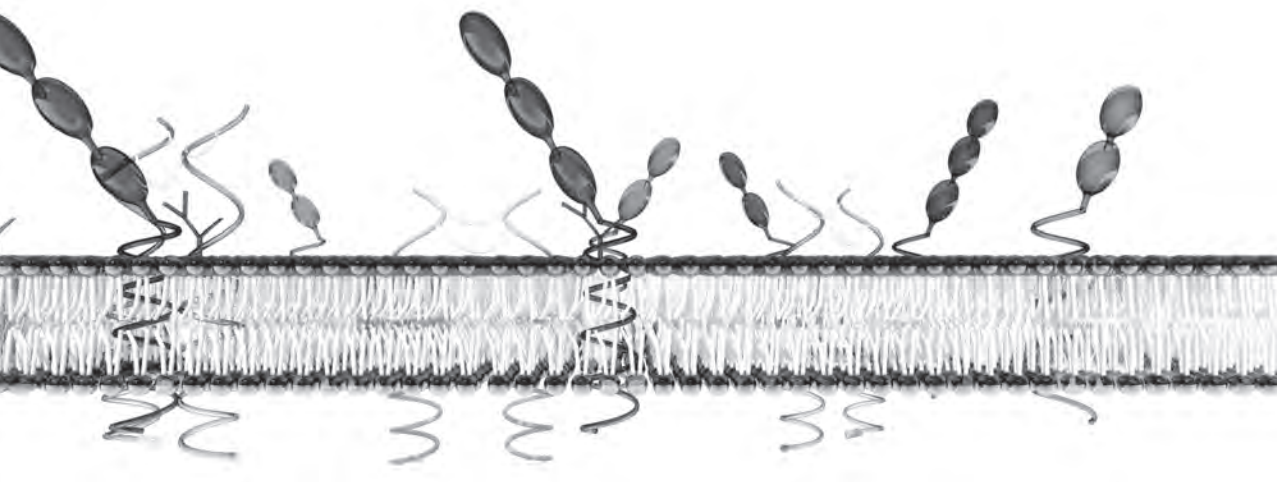

Abstract

Historically, lack of specificity for cancer cells has been a major problem in cancer treatment. However, the development of monoclonal antibodies (mAbs), which combine high specificity with multiple mechanisms of action (MoA), started a revolution in anti-cancer treatment options which continues to date. As of January 2013, 15 major antibody products are being marketed for cancer treatment in various countries around the globe; 10 of which are unmodified mAbs, which generally have multiple potential MoA, and may act via direct, Fab-domain related effects, or indirect, Fc-domain related effects. Fc-domain related effects consist of immune-mediated effector functions which include complement-dependent cytotoxicity (CDC), antibody-dependent cellular cytotoxicity (ADCC) and antibody-dependent cellular phagocytosis (ADCP). ADCC and ADCP depend on the engagement of Fcγ-receptors (FcγR) on immune effector cells by Fc-domains clustered due to antibody-antigen binding. Similarly, CDC depends on the engagement of proteins of the complement system by clustered antibody Fc domains. In this chapter, preclinical and clinical studies with approved anti-cancer mAbs are reviewed with an emphasis on the role of FcγR-mediated effector functions. The importance of therapeutic antibody - FcγR interactions for human treatment can be deduced from correlations of clinical responses with FcγR polymorphisms, results supported by a wealth of preclinical and *in vitro* studies.

Mechanisms of action of monoclonal antibodies in oncology

Unmodified therapeutic monoclonal antibodies (mAbs) can achieve clinical effect by one or several potential direct or indirect mechanisms of action (MoAs), consistent with the activities of natural antibodies (1). For oncology targets, direct, or Fab-domain-related effects, are induced by binding of the mAb to its target via its antigen-binding site, resulting in ligand binding inhibition, receptor cross-linking and/or internalization, which may lead to growth inhibition or apoptosis (Fig. 1). Indirect, or Fc-domain-related effects, are mediated by the antibody constant regions (Fc) and may result in the antibody-mediated effector functions, which include complement-dependent cytotoxicity (CDC), antibody-dependent cellular cytotoxicity (ADCC) and antibody-dependent cellular phagocytosis (ADCP) (Fig. 1). Indeed, the first publication of mAb therapy in a human dates back to 1980 and describes treatment of a patient with non-Hodgkin's lymphoma (NHL), in which a murine IgG directed against a unique tumor-associated antigen induced adherence of the patient's tumor cells to macrophages and tumor cell lysis via CDC (1, 2). This study demonstrated for the first time that tumor cell depletion with a mAb could occur with minimal toxicity in man and might employ tumor killing mechanisms including CDC and cell clearance via the reticuloendothelial system. It was rapidly followed by others (see text below), giving rise to a growing class of approved therapeutics, as well as to more recent efforts to expand upon the natural activities of antibodies.

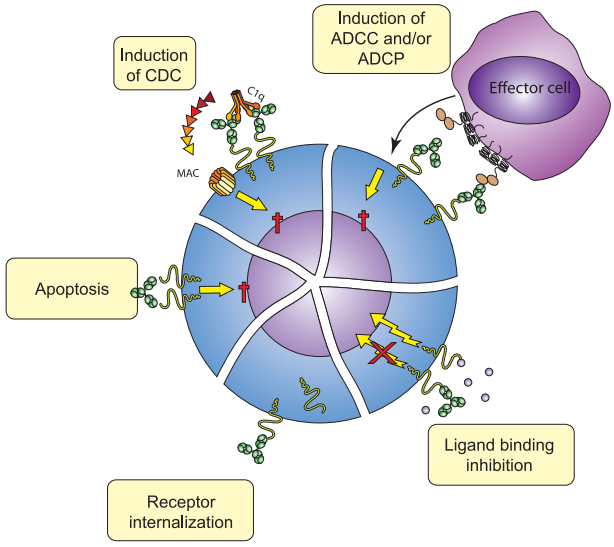

Figure 1. *Possible therapeutic antibody mechanisms of action.* MoA of therapeutic antibodies can be divided in Fab-domain-related effects and Fc-domain-related effects. Fab-domain or direct effects are represented by ligand binding inhibition, receptor internalization and apoptosis. Fc-domain or indirect effects are represented by complement-dependent cytotoxicity, antibody-dependent cellular cytotoxicity (ADCC) and antibody-dependent cellular phagocytosis (ADCP).

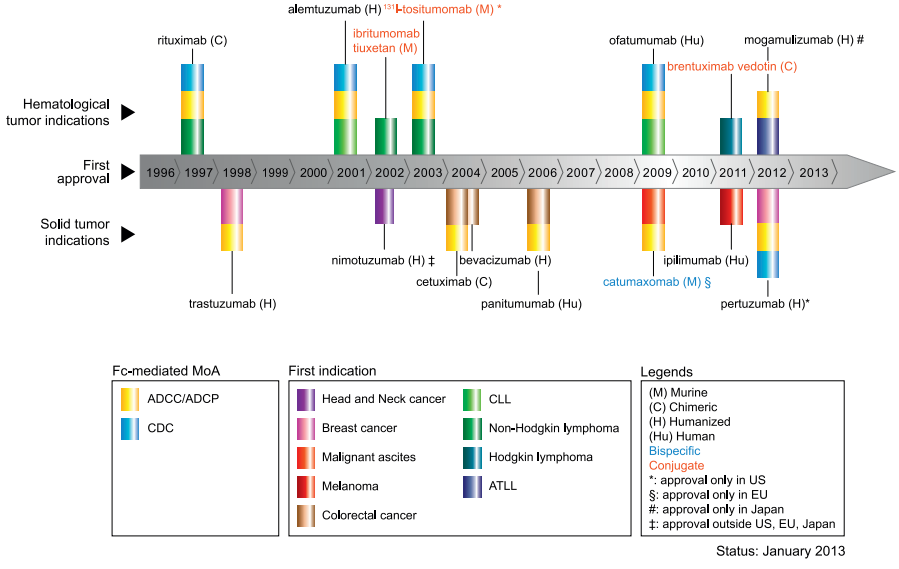

Figure 2. *MAbs currently approved for use in cancer therapy.* Therapeutic antibodies approved for use in cancer by the regulatory authorities are shown by their time of first registration. Note that nimotuzumab is only approved outside the United States, European Union, and Japan. Catumaxomab was only approved by the European Medicines Agency (EMA) for the treatment of malignant ascites.

Mogamulizumab is thus far only approved by the Japanese authorities. Clinical trials for these three antibodies are currently underway in the other territories. The colors for the indications in the figure describe the first therapeutic area for which the antibodies were approved. The yellow and blue bars indicate whether the mAb is described to induce Fc-related effects as ADCC/ADCP or CDC respectively. (Figure is adapted from Parren, P.W. and van de Winkel, J.G. *Curr. Opin. Immunol.,* **20**(4):426-430, 2008; Reichtert, J.M., *MAbs*, **4**(3): 413-415, 2012.)

Development of therapeutic monoclonal antibodies for the treatment of cancer

Since their introduction into the clinic, therapeutic antibodies have continuously evolved in terms of species origin, isotype, and MoA, as well as composition, including sequence and chemical modifications (2, 3). Initially, murine mAbs were developed, followed by the generation of chimeric and human(ized) mAbs. The principal drivers behind this evolution were the aim to reduce immunogenicity and to increase efficacy to permit serial administration and optimize interaction of the antibody Fc domain with the patients' innate immune system. Currently, most mAbs approved for human use are full-length, unmodified, human(ized) mAbs. The first antibody marketed for the treatment of cancer was rituximab, a chimeric IgG1 CD20 mAb in 1997. This was rapidly followed in 1998 by the approval of trastuzumab, a humanized IgG1 against HER2. In 2006, panitumumab, the first mAb solely consisting of human antibody sequences, was approved. Panitumumab is a human IgG2 mAb against epidermal growth factor receptor (EGFR) which was isolated via immunization of human antibody transgenic mice. Today, 10 unmodified mAbs are being used for the treatment of cancer (Fig. 2), most often in conjunction with classical treatments such as radio- and chemotherapy, and hundreds more are at various stages of clinical and preclinical development.

Novel antibody formats to potentiate or optimize the activity of unmodified antibodies with the aim to increase clinical efficacy have been investigated for decades, but their development has only recently come of age. Among others, these formats include mAb-payload conjugates comprised of toxins or radioisotopes (4), bispecific mAbs (5), and mAbs with enhanced immune effector function due to Fc-domain mutations or glycoengineering (6, 7). The first mAb-payload conjugate, gemtuzumab ozogamicin, an IgG4 mAb against CD33 conjugated to the DNA-cleaving agent calicheamycin was approved in 2000 but was subsequently withdrawn from the market in 2010 due to an unfavorable safety profile. Currently there are three mAb-payload conjugates

approved for treating cancer (Fig. 2). The first two, ibritumomab tiuxetan and ^{131}I-tositumomab, are CD20 mAb-radioconjugates and have been available for human use for about a decade. The third is brentuximab vedotin, which is a CD30 mAb conjugated to the tubulin inhibitor auristatin which was approved in the United States (2011) and the European Union (2012) for the treatment of Hodgkin's lymphoma and anaplastic large-cell lymphoma (ALCL).

Mogamulizumab, an anti-CCR4 mAb, recently approved in Japan for the treatment of adult T-cell leukemia-lymphoma (ATLL), represents the first marketed effector-function enhanced mAb. NK cell-mediated ADCC for this antibody has been improved by decreased fucosylation of the Fc domain-associated carbohydrate (8, 9). Mogamulizumab is being assessed in a number in clinical trials in the United States and Eurpean Union, along with other afucosylated mAbs such as the CD20 mAb obinutuzumab (10, 11) and the CD19 mAb MEDI-551 (12, 13).

Finally, bispecific mAbs, which combine the ability to bind two distinct epitopes or targets, are an area of high interest (5). Most clinical validation has been generated for bispecific antibodies that can recruit a novel effector reservoir (i.e. T cells) for antibody-mediated tumor cell killing. The bispecific mAb catumaxomab, a murine IgG2a anti-EpCAM/rIgG2b CD3 mAb approved for the treatment of malignant ascites (Fig. 2), thus represents a novel, highly potent approach to recruit innate immune cells for cancer therapy (14).

In the following sections, we will specifically address the MoAs of unmodified therapeutic mAbs in cancer, in both in pre-clinical experiments and the clinical setting, with an emphasis on Fcγ receptor (FcγR)-mediated effector functions.

Fc-mediated effector functions, pre-clinical data

Evidence for the role of Fc-mediated effector functions including CDC, ADCC and ADCP, in the MoAs of therapeutic mAbs was first established in pre-clinical studies. CDC is induced by binding of C1q to the Fc-domain, leading to deposition of C3b on the surface of Ab-coated tumor cells. The presence of C3b catalyzes formation of the C5-C9 membrane attack complex (MAC), resulting in tumor cell lysis. ADCC and ADCP are mediated by recognition of clustered antibody Fc-domains on tumor cells by specific FcγRs on immune-effector cells such as NK cells, macrophages, and neutrophils. The potency of a

mAb to induce Fc-mediated effector functions depends on a number of factors, including the species origin, the isotype and subclass, the glycosylation profile, and the cognate epitope of the mAb.

In pre-clinical studies, rituximab (15, 16), ofatumumab (IgG1 CD20 mAb) (17, 18) and alemtuzumab (IgG1 CD52 mAb) (19-21) were found to induce potent ADCC and CDC, and may also induce direct cell killing via apoptosis following receptor cross-linking. Trastuzumab (anti-HER2) (22, 23) and cetuximab (anti-EGFR) (24), also of the IgG1 isotype, can induce killing via ADCC and apoptosis. The IgG1 isotype is highly effective in triggering ADCC via NK cells, which represent the principal effector cells in the peripheral blood mononuclear cell (PBMC) populations commonly used in *in vitro* ADCC assays. As human IgG2 is not able to recruit NK cells (25), panitumumab, a human IgG2 mAb, was originally reported to induce ADCC poorly; however, panitumumab was later shown to be able to induce effective ADCC via myeloid cells (i.e. neutrophils and monocytes) with comparable efficacy to an IgG1 mAb (26), highlighting the subclass dependence of effector cell recruitment.

The role of Fc-mediated effector functions for immunotherapy was investigated in more detail using various Fc receptor knock-out mouse models. Clynes et al. (27) were the first to demonstrate a critical role for FcγR-mediated effector functions for antibody therapy by demonstrating loss of efficacy of trastuzumab and rituximab in common γ-chain knock-out mice (FcR$\gamma^{-/-}$, mice lacking expression of activating IgG Fc receptors). Their experiments therefore strongly suggest a critical role for ADCC in the MoAs of these mAbs, at least under the early treatment conditions employed in their study. Similarly, efficacy of alemtuzumab in a murine ATL model was lost in the FcR$\gamma^{-/-}$ mouse model. The authors suggest ADCC as the MoA, but argued that a role for FcγR-induced cross-linking, leading to apoptosis could not be excluded (28). The potential of apoptosis induction via FcγR-induced cross-linking was demonstrated by Wilson et al. with a DR5-specific mAb (29). To settle this question for CD20 antibody therapy, de Haij et al. (30) developed a novel mouse model with normal expression of common γ-chain–associated FcγRs in which signal transduction and thereby ADCC, was inactivated through an intracellular mutation in this γ-chain. These studies confirmed that ADCC indeed represents a critical MoA for rituximab and ofatumumab.

It is important to note, however, that timing of treatment as well as tumor load impact the importance of ADCC as an effector mechanism. Thus, Boross et al. (31) demonstrated that *in vivo* ADCC may be enhanced by concomitant complement

activation through recognition of complement deposits by macrophage complement receptors. Interestingly, it was shown that whereas complement alone was sufficient to eliminate a low tumor burden, high tumor burdens required both active complement as well as activating FcγR. Also Gong et al. (32) demonstrated a requirement of multiple effector mechanisms for optimal cell depletion. Thus, a CD20 mAb rapidly cleared circulating B cells in a human CD20 transgenic mouse model via monocytes and macrophages, whereas depletion of resident B cells within the marginal zone compartment required both CDC and ADCC. Finally, our own study employing EGFR-specific mAbs suggests that ADCC induction can prevent tumor outgrowth or metastasis *in vivo*, but that ADCC alone, however, is not effective against established solid tumors (33).

The studies above indicate an important role for FcγR-mediated effector functions in antibody therapy in which a major contribution of ADCC can be observed in early treatment, metastasis as well as against circulating cells. The engagement of ADCC alone appears to be inadequate in therapy of established tumors or resident cells, which appear to require the engagement of multiple effector mechanisms for treatment to be effective. An important question is whether these pre-clinical findings will be confirmed in the clinic.

Role for FcγR-mediated effector functions, clinical data

Several studies have explored the potential role of FcγR-mediated effector functions as MoAs of trastuzumab in patients. ADCC of patient PBMCs and lymphoid cell infiltration into tumors were analyzed in a study in which trastuzumab was administered prior to surgery in patients with primary operable breast tumors overexpressing HER2. ADCC activity correlated with clinical response, and larger tumor lymphoid cell infiltrates were observed in responding compared to the non-responding patients, suggesting that FcγR-mediated effector functions are beneficial in this setting. A study by Repka et al. (34) explored the potential of interleukin-2 (IL-2) treatment to enhance NK cell numbers, thereby increasing trastuzumab activity via NK cell-mediated ADCC. Patients receiving IL-2 indeed showed increased NK cell numbers, and combining IL-2 with trastuzumab resulted in enhanced ADCC of several breast cancer cell lines *ex-vivo*. In a study of the potential role of different immune cells in the clinical response to trastuzumab Arnould et al. (35) demonstrated that

in primary systemic therapy of HER2-positive primary breast cancer patients, trastuzumab treatment influences the number and trafficking of various immune cells, including T- and B lymphocytes and NK cells, into tumor infiltrates. The presence of increased numbers of NK cells, as well as the detection of cytotoxic proteins such as granzyme B, lends support to a role for NK cells in trastuzumab-induced tumor regression. Maréchal et al. (36) assessed the potential impact of intratumoral immune cells and efficacy of first-line cetuximab in combination with chemotherapy in metastatic colorectal cancer (M-CRC) patients. Although cetuximab treatment did not influence NK cell influx into the tumor compared to controls, if present, tumor-infiltrating NK cells were an independent predictor for progression-free survival (PFS) and objective response rate (ORR) in the cetuximab-treated group. Overall, these translational studies of trastuzumab- and cetuximab-treated patients suggest a role for FcγR-mediated effector functions, specifically NK cell-mediated ADCC in clinical responses.

Polymorphisms in FcγRs

FcγRs are expressed by different immune cells and become activated upon aggregation by multivalent antigen-antibody complexes (37). Functional polymorphisms in the coding regions of the different FcγRs impact the affinity for IgG. In addition, mutations that modulate the expression level of FcγR have been described (Table 1).

In the field of therapeutic mAbs, many studies have focused on functional polymorphisms identified in FcγRII and FcγRIII. First, FcγRIIa, expressed by myeloid cells, platelets, a subset of T cells and endothelial cells, harbors a functional polymorphism due to an arginine (R) to histidine (H) amino acid substitution at position 131 (FcγRIIa-131H) (38-40) which results in a higher binding affinity for complexed IgG2 and IgG3 compared to FcγRIIa-131R (41). Second, FcγRIIb, expressed by B cells, monocytes and macrophages, harbors a functional polymorphism resulting in an isoleucine (I) to threonine (T) amino acid substitution at position 232 (42), which impairs the association of FcγRIIb-232T with lipid rafts and attenuates its inhibitory effect (43). Third, FcγRIIIa, expressed by NK cells, macrophages, a subset of monocytes and a subset of T-cells, has a polymorphism with a phenylalanine (F) to valine (V) substitution at amino acid position 158 (44, 45), which results in a higher binding affinity

Table 1. Main FcγR polymorphisms and their physiological effects

Receptor family	Human genes	Variants	Effect
FcγRI (CD64)	FcγRIA	R92X	X92: undetectable expression of FcγRIA on phagocyte
FcγRII (CD32)	FcγRIIA	R131H	H131: higher affinity for IgG2
	FcγRIIB	I232T	T232: lower affinity for lipid rafts/decreased inhibitory activity
	FcγRIIC	CNV	Gene copy number variation (CNV) resulting in higher or lower number of the receptor leading to an altered balance of activating and inhibitory FcγRs
FcγRIII (CD16)	FcγRIIIA	V158F	V158: higher affinity for IgG1 and IgG3, binds IgG4
		CNV	CNV resulting in higher or lower number of the receptor leading to an altered balance of activating and inhibitory FcγRs
	FcγRIIIb	NA 1/2	NA 1: higher affinity for IgG1 and IgG3
		CNV	CNV resulting in higher or lower number of the receptor leading to an altered balance of activating and inhibitory FcγRs

Source: Adapted from Concetti, F. and Napolioni, V., *Recent Pat. Anticancer Drug Discov.*, **5**(3):197-204, 2010.

of FcγRIIIa-158V to complexed IgG1, IgG3 and IgG4 (46). Finally, FcγRIIIb, expressed by neutrophils and eosinophils, bears the neutrophil antigen (NA) polymorphisms NA-1 or NA-2 in its membrane-distal Ig-like domain (47), in which IgG1- or IgG3-opsonized particles are more efficiently ingested upon interaction with the FcγRIIIb-NA-1 allotype (48). Bruhns et al. (49) studied the specificity and affinity of the individual FcγRs and their polymorphic variants for the four human IgG isotypes, confirming the findings described above. Interestingly, FcγR polymorphisms have been identified as genetic factors that may impact susceptibility to autoimmune or infectious diseases (50), and they also correlated with therapeutic efficacy of therapeutic mAbs, where FcγR-mediated effector functions are part of the *in vivo* MoA.

Impact of FcγR polymorphisms on mAb treatment, pre-clinical *in vitro* data

Several *in vitro* studies demonstrated the impact of FcγR polymorphisms on FcγR-mediated effector functions. We previously demonstrated that monocytes expressing only the FcγRIIA-131H allele support IgG2 anti-CD3 induced T cell proliferation efficiently, whereas monocytes homozygous for the FcγRIIA-131R

allele do not (51). For cetuximab it was found that ADCC against squamous cell carcinoma of head and neck (SCCHN) cells was significantly higher with NK cells homozygous or heterozygous for the high affinity FcγRIIIA-158V allele than NK cells homozygous for the low affinity FcγRIIIA-158F (52, 53). FcγRIIIa-158V was also related to significantly higher expression of NK activation markers CD69 and CD107a and significantly higher secretion levels of IFN-γ, MIP-1α, MIP-1β, RANTES and TNF-α. Dall'Ozzo et al. (54) compared ADCC of rituximab-opsonized human Burkitt's lymphoma cells by NK cells. This study demonstrated that rituximab was about four times more potent in ADCC with NK cells homozygously expressing FcγRIIIa-158V. Comparable results were found for the CD20 mAb, ofatumumab (18). For trastuzumab, ADCC efficacy of a human breast cancer cell line was significantly higher, with PBMCs only expressing FcγRIIIa-158V compared to 158F carriers (55); no significant differences were found for FcγRIIa-131H versus 131R. These *in vitro* studies clearly demonstrate that FcγR polymorphisms, with an emphasis on the FcγRIIIa-158V/F polymorphism, may affect mAb efficacy and indicates that exploring the relation between FcγR polymorphisms and clinical responses may provide additional evidence for the contributions of FcγR-mediated effector functions to mAb therapy.

Impact of FcγR polymorphisms in mAb treatment, clinical data

Studies on the correlation of FcγR polymorphisms with clinical outcome have been reported for four mAbs; rituximab, alemtuzumab, cetuximab and trastuzumab. The findings of these studies are summarized in Table 2. The CD20 mAb, rituximab was the first therapeutic mAb for which the influence of the functional polymorphism in FcγRIIIa was studied. Cartron et al. (56) observed a significantly higher ORR in patients homozygous for FcγRIIIa-158V compared to FcγRIIIa-158F carriers, indicating a significant role for FcγRIIIa-mediated effector functions in the treatment of follicular lymphoma (FL) patients with rituximab. The FcγRIIIa-158F carriers nonetheless did show significant clinical responses to rituximab. This can be explained by the *in vitro* observation that reduction in FcγR affinity reduces, but does not abrogate, ADCC, as well as by the contribution of multiple additional MoA (such as CDC and apoptosis), as discussed above. Two other studies confirmed homozygous FcγRIIIa-158V

expression to be associated with a higher clinical response to monotherapy with rituximab in FL (57, 58). Ghielmini et al. (59) observed that homozygosity for 158V correlated with significantly longer event-free survival (EFS) in FL patients compared to 158F carriers, although they did not see significantly enhanced ORR. Cornec et al. (57) analyzed response rates in association with genetic polymorphisms in low grade NHL (FL and marginal zone (MZ) lymphoma) and found 158V homozygotes exhibited a significantly higher complete response rate (CR). Additionally, a correlation with the FcγRIIIa polymorphism was also demonstrated in Waldenström's macroglobulinemia (WM) (60). In WM patients the ORR was significantly higher in patients expressing only FcγRIIIa-158V, but this was not observed for PFS. However, the correlation between the FcγRIIIa polymorphism and response to rituximab has not been observed in all B-cell malignancies; for example, no correlation was found in chronic lymphocytic leukemia (CLL) (61) and mantle cell lymphoma (MCL) (59).

In addition to FcγRIIIa polymorphisms, the impact of the FcγRIIa polymorphisms has been studied. *In vitro*, only very limited differences in IgG1 binding to the polymorphic forms of FcγRIIa have been observed (41). In patients, Weng et al. (58, 62) found that not only homozygous FcγRIIIa-158V expression but also homozygous expression of FcγRIIa-131H was associated with a higher ORR and PFS in rituximab treatment of FL. The question has been raised whether this association was due to a non-random association of the FcγRIIa-131H and FcγRIIIa-158V alleles, as may be caused by linkage disequilibrium, due to the close proximity of all FcγR genes on Chromosome 1 (63). In view of this Weng and Levy (62) provided additional arguments that both polymorphisms independently correlate with response rates in a second study with an extended patient population and longer follow-up. However, the correlation between the FcγRIIa polymorphism and rituximab response rates in monotherapy was not confirmed by Cornec et al. (57) in a smaller study of FL/MZ patients, with CR as read-out. Altogether, the response to rituximab monotherapy therefore displays only a clear correlation with the FcγRIIIa polymorphism in FL, MZ and WM, suggesting a role for FcγR-mediated effector functions in the *in vivo* MoA in Ab therapy of these diseases.

Abbreviations: N, number of patients; CR, complete response; ORR, objective response rate;, EFS, event-free survival; PFS, progression-free survival;, OS, overall survival; FL, follicular lymphoma; MZ, marginal zone lymphoma; WM, Waldenström macroglobulinemia; CLL, chronic lymphatic leukemia; MCL, mantle-cell lymphoma; M-CRC, metastatic colorectal cancer; MBC, metastatic breast cancer; +, significant effect high-affinity polymorphism compared to the low affinity polymorphism (158VV vs. 158FF, 131HH vs. 131RR, 232TT vs. 232II); -, no significant effect; +/-, a beneficial trend; ND, not determined; *, V carrier.

Table 2. Impact of FcγR polymorphisms on clinical outcome

Therapy	FcγR	N	N (polymorphism)	Indication	Clinical outcome				Ref.
					CR	ORR	EFS/PFS	OS	
Monotherapy									
Rituximab	FcγRIIIa	49	10 (158V/V)	FL	ND	+	+	ND	(56)
	FcγRIIIa	101	15 (158V/V)	FL	ND	+	+	ND	(58, 62)
	FcγRIIa		21 (131H/H)		ND	+	+	ND	
	FcγRIIIa	30	6 (158V/V)	CLL	ND	-	ND	ND	(61)
	FcγRIIIa	58	10 (158V/V)	WM	ND	+	-	ND	(60)
	FcγRIIIa	171	32 (158V/V)	FL	ND	-	+	ND	(59)
				MCL	ND	-	-	ND	
	FcγRIIb	101	15 (232I/T)	FL	ND	-	-	ND	(62)
	FcγRIIIa	50	6 (158V/V)	FL/MZ	+	ND	ND	ND	(57)
	FcγRIIa		13 (131H/H)		-	ND	ND	ND	
Alemtuzumab	FcγRIIIa	33	4 (158V/V)	CLL	ND	-	ND	ND	(72)
	FcγRIIa		6 (131H/H)		ND	-	ND	ND	
Cetuximab	FcγRIIIa	35	5 (158V/V)	M-CRC	ND	ND	-	-	(74)
	FcγRIIa		9 (131H/H)		ND	ND	+	-	
Trastuzumab	FcγRIIIa	35	15 (158V/V)	MBC	ND	+/-	+/-	ND	(78)
	FcγRIIa		15 (131H/H)		ND	+	+	ND	
Combination therapy									
R-CHOP	FcγRIIIa	113	53 (158V/V)	DLBCL	+	+	-	-	(64)
	FcγRIIa		60 (131H/H)		-	-	-	-	
	FcγRIIIa	94	18 (158V/V)	FL	-	-	-	ND	(70)
	FcγRIIa		30 (131H/H)		-	-	-	ND	
	FcγRIIIa	58	16 (158V/V)	DLBCL	-	ND	-	-	(68)
	FcγRIIa		23 (131H/H)		-	ND	-	-	
R+chemo	FcγRIIa	55	11 (131H/H)	NHL	+	-	-	-	(92)
R-FC	FcγRIIIa	210	20 (158V/V)	CLL	ND	-	-	-	(71)
	FcγRIIa		54 (131H/H)		ND	-	-	-	
R-CHOP	FcγRIIIa	87	15 (158V/V)	DLBCL	-	ND	-	-	(66)
	FcγRIIa		27 (131H/H)		-	ND	-	-	
	FcγRIIIa	263	76 (158V/V)	DLBCL	-	ND	-	-	(67)
	FcγRIIa		111 (131H/H)		-	ND	-	-	
	FcγRIIIa	30	1 (158V/V)	FL	ND	ND	-	+	(65)
	FcγRIIa		9 (131H/H)		ND	ND	-	-	
Cetuximab+ irinotecan	FcγRIIIa	69	10 (158V/V)	M-CRC	ND	-	+	-	(75)
	FcγRIIa		17 (131H/H)		ND	-	-	-	
Cetuximab+ chemo	FcγRIIIa	44	31* (158V carrier)	M-CRC	ND	+/-	ND	ND	(76)
	FcγRIIa		12 (131H/H)		ND	+	ND	ND	
Trastuzumab+ chemotaxane	FcγRIIIa	54	11 (158V/V)	MBC	ND	+	+	ND	(55)
	FcγRIIa		10 (131H/H)		ND	+/-	+/-	ND	
Trastuzumab+ chemo	FcγRIIIa	15	7 (158V/V)	MBC	ND	-	ND	ND	(78)
	FcγRIIa		7 (131H/H)		ND	+	ND	ND	

In standard-of-care cancer therapy, however, rituximab is most often used in combination with chemotherapy, resulting in a significantly enhanced response compared to either agent alone. Several studies have explored whether the enhanced efficacy in combination therapy is impacted by FcγR-mediated effector functions. Kim et al. (64) observed no correlation between the FcγRIIa polymorphism with response rate, whereas the FcγRIIIa polymorphism was found predictive for CR and ORR in treatment with rituximab in combination with cyclophosphamide/doxorubicin/vincristine/prednisone (R-CHOP) in patients with diffuse large B-cell lymphoma (DLBCL). However, the FcγRIIIa polymorphism was not predictive for event-free survival (EFS) or overall survival (OS), suggesting that FcγR-mediated effector functions are most important in initial responses. Also Persky et al. (65) found the FcγRIIIa polymorphism to be predictive of survival in FL patients given treatments containing a CD20 antibody but not by treatment with chemotherapy alone. Conversely, in other studies neither FcγRIIa nor FcγRIIIa polymorphisms influenced the EFS or OS to R-CHOP (66-68). These results suggest that FcγR-mediated effects are not a dominant MoA in R-CHOP therapy in DLBCL. Boettcher et al. (69) and Carlotti et al. (70) also did not observe a correlation of CR, ORR or PFS in FL patients treated with R-CHOP with FcγRIIa or FcγRIIIa polymorphisms. Dornan et al. (71) retrospectively analyzed FcγRIIa and FcγRIIIa polymorphisms of patients enrolled in a controlled randomized study of relapsed CLL, which were treated with either fludarabine and cyclophosphamide (FC) or rituximab plus FC (R-FC). Also in this study, neither the FcγRIIa nor the FcγRIIIa polymorphism significantly influenced ORR, PFS or OS.

Overall, there seems to be a contrast between the convincing association of FcγRIIIa polymorphism and rituximab efficacy in monotherapy, and the limited correlation when rituximab is used in combination with chemotherapy. These conflicting data may imply that FcγR-mediated responses are not the principal MoA when rituximab is used in combination with chemotherapy; however, the lack of a clear correlation may be due to the immunosuppressive effect of most chemotherapeutic drugs, causing effector cells to be less responsive to mAbs and thereby impacting FcγR-mediated effector functions. Also, chemotherapy enhances the efficacy of the treatment, which potentially results in a smaller difference in responses between high- and low-affinity polymorphic FcγR. Overall, therefore, for rituximab, the role of FcγR-mediated effector functions as suggested by FcγR polymorphisms have only been convincingly demonstrated for monotherapy in FL, MZ and WM.

A correlation between FcγR polymorphisms and efficacy of alemtuzumab (CD52 mAb) treatment has been studied in CLL patients. Lin et al. (72) could not demonstrate a correlation between the FcγRIIa and FcγRIIIa polymorphisms and alemtuzumab ORR, similar to rituximab treatment in CLL. No further studies investigating the role of FcγR polymorphisms in combination with alemtuzumab treatment are available.

Cetuximab, an EGFR-targeting mAb used for the treatment of M-CRC, has been shown to induce ADCC *in vitro* (73). In a small study of only 35 patients containing a limited number of homozygotes, Zhang et al. (74) explored whether FcγRIIa and FcγRIIIa polymorphisms could serve as molecular markers to predict cetuximab response, OS, and toxicity in M-CRC. Indeed, homozygous expression of FcγRIIa-131H correlated with a longer PFS after monotherapy with cetuximab in M-CRC. Unexpectedly, homozygotes for the high-affinity FcγRIIIa-158V demonstrated a shorter PFS compared to 158F carriers. In contrast, Bibeau et al. (75) demonstrated in a retrospective study comprising 69 M-CRC patients, of whom 10 were 158V and 17 were 131H homozygotes, that FcγRIIIa-158V significantly improved PFS of patients treated with cetuximab in combination therapy with irinotecan. A recent study of Rodríguez (76) of M-CRC patients treated with cetuximab combined with standard chemotherapy showed a significantly stronger ORR and a trend for a beneficial effect for FcγRIIa-131H and FcγRIIIa-158V carriers, respectively. Overall, therefore, patients appear to benefit from carrying the 158V and 131H polymorphisms in cetuximab treatment. The data available, however, are incomplete and this point therefore requires more study.

Finally, ADCC induction was demonstrated *in vitro* for the HER2 mAb trastuzumab (35, 77). Musolino et al. (55) investigated the potential role of FcγR-mediated effector functions in trastuzumab plus taxane treatment of HER2-positive metastatic breast cancer (MBC) patients. Indeed, patients homozygous for FcγRIIIa-158V, alone and in combination with the FcγRIIA-131HH genotype showed significantly better ORR and PFS upon trastuzumab treatment. Tamura et al. (78) conducted a prospective study in MBC patients, treated either with trastuzumab monotherapy or trastuzumab plus taxane, to determine the predictive value of the FcγR polymorphisms. In both trastuzumab monotherapy and in combination with taxane, homozygosity for FcγRIIa-131H was significantly associated with a stronger anti-tumor response and a longer PFS. Patients homozygous for FcγRIIIa-158V only showed a favorable trend in PFS after trastuzumab monotherapy.

In summary, studies correlating FcγR polymorphisms with clinical response suggest a role for FcγR-mediated effector functions in mAb therapy. Results from monotherapy treatments in this respect are more clear cut than from antibody-chemotherapy combination regimens. The contribution also seems to be more pronounced in hematological tumors compared to solid tumors, although within the hematological tumors not all malignancies seem to have a similar sensitivity to FcγR-mediated effector functions. Differences for a particular mAb between indications may in addition be due to differences in target expression or expression of soluble forms of the target, differential expression of regulatory molecules, mutations downstream of the target, differences in the numbers of immune effector cells between patients or differences between patient groups studied. There indeed are some remarkable differences in results between similar studies, such as between studies on R-CHOP treatment of DLBCL patients. The study of Kim et al. (64) showed a significant benefit of the homozygous FcγRIIIA-158V genotype, while three other studies (66-68) did not reveal such a benefit. An important difference between these studies is that Kim et al. studied Asian DLBCL patients, in which the proportion of the FcγRIIIA-158VV genotype is much higher (79); that is, 41.5% of the patients were homozygous for FcγRIIIa-158V in the study by Kim et al. versus only 27%, 17% and 28% in the other three studies. Finally, factors such as small patient groups, the use of retrospective analysis, differences in treatment regimes and differences in time for OS or ORR might also account for the observation that the beneficial effect of FcγR polymorphisms are more pronounced in some studies than in others.

Opportunities to enhance FcγR-mediated effector functions

As already stated above, the impact of FcγR polymorphisms is most evident in mAb monotherapy compared to mAb combined with chemotherapy. However, in standard-of-care cancer therapy, most mAbs are used in combination with chemotherapy, which seems to reduce the contribution of FcγR-mediated effector functions to the overall therapeutic effect. Two strategies have been followed to take greater advantage of the benefit of FcγR-mediated effect, which include increasing the activation status of effector cells and modulating the strength of the antibody Fc-FcγR interaction.

Combination therapy with immune-modulatory drugs (IMiDs) impacts the activation status of effector cells. Lenalidomide is a structural analog of thalidomide with similar but more potent immune modulatory activities (80). Its NK cell stimulatory properties suggest that lenalidomide could be highly effective in combination with therapeutic mAbs capable of inducing NK cell-mediated ADCC, thereby enhancing efficacy of the mAb. Indeed, lenalidomide synergistically increased lysis of multiple myeloma (MM) cells by daratumumab, a human IgG1 mAb targeting CD38, both in primary cultures of patient bone-marrow-derived mononuclear cells and in ADCC assays using PBMC from lenalidomide-treated patients (81-83). Additionally, the impact of several undefined IMiDs was studied by Hayashi et al. (84). These IMiDs do not directly activate NK cells, but rather induce T-cells to produce IL-2, which subsequently activates the NK cells. They demonstrated that ADCC induced by a chimeric CD20 mAb was enhanced with the IMiDs, again providing a preclinical rationale for the use of IMiDs in combination with mAb therapy. Chemotherapeutic taxane, which synergizes with trastuzumab, is described to inhibit tumor growth and inducing immunosuppression of adaptive immunity, but also selectively increases NK cell activity (77, 85). In combination studies with taxanes, immune effector functions are probably not the main MoA; however, the enhanced NK activity can likely contribute to an enhanced FcγR-mediated efficacy of the mAb.

A second strategy to enhance FcγR-mediated effector functions is to increase the affinity of the Fc-domain for FcγRs by Ab engineering, either via mutations in the Fc-domain or by changing the glycosylation of the Fc-domain. Desjarlais and Lazar (6) provided an overview of the clinical stage of mAbs with improved effector functions. Several *in vitro* studies showed the effect of Fc engineering on binding to the different FcγR variants. Fc-domain single mutants S239D or I332E and the double and triple mutants S239D/I332E and S239D/I332E/A330L exhibited significantly higher affinities for FcγRIIIa-158F, even higher than the affinity of WT IgG1 mAb for the FcγRIIIa-158V polymorphism (86). XmAb5574, a CD19 IgG1 mAb, contains the S239D and I332E mutations in the Fc-domain which showed enhanced ADCC efficacy compared to its WT IgG1 analog (87). Pretreating NK cells with lenalidomide could enhance ADCC efficacy of CD19 mAb XmAb5574 even more. Enhanced ADCC was also demonstrated for the glycoengineered CD20 mAb obinutuzumab, which bound more strongly to FcγRIIIa-158V and -158F (88), resulting in increased ADCC activity (10, 89). Enhanced ADCC activity was also observed for MEDI 551, a CD19 mAb which is

afucosylated by using a fucosyltransferase-deficient producer cell line (12). The same technology was used for the generation of the afucosylated anti-CCR4 antibody mogamulizumab (KW-0761), which demonstrated positive results in Phase II study for the treatment of ATLL (8, 9) and was recently approved in Japan (Fig 2). Niwa et al. (90) demonstrated enhanced ADCC mediated by a low-fucose version of rituximab compared to rituximab. Low-fucose mAb displayed a 3 to 4 fold higher affinity to the homozygous FcγRIIIa-158F polymorphism than the WT IgG1 for homozygous FcγRIIIa-158V, suggesting that this enhancement is achieved independently of the FcγRIIIa functional polymorphism. This result was confirmed by a study with a low-fucose mAb targeting EGFR (91). However, this latter study also demonstrated that ADCC with polymorphonuclear cells (PMN) is less effective with defucosylated EGFR mAb than with the high-fucose form, which may have implications for therapeutic mAbs that recruit PMNs for their *in vivo* therapeutic effects.

Future perspectives

Overall, preclinical studies performed *in vitro* and *in vivo* have identified FcγR-mediated effector functions as important mechanisms for tumor cell killing. These findings have been translated to the clinic by studies that demonstrate positive correlations between clinical response and effector cell activation, or the influx of effector cells into tumors. The correlation of certain functional FcγR polymorphisms with clinical responses furthermore provides additional evidence for the role of FcγR-mediated effector functions in clinical efficacy of unmodified mAbs. That said, it should be noted, however, that the impact of FcγR polymorphisms on clinical efficacy may be modulated by multiple factors such as target expression, indication, patient population, dosing regimen, effector cells availability and concomitant therapy, resulting in more or less pronounced effects. Because of this variability, FcγR polymorphisms therefore currently do not seem to provide particularly useful predictive biomarkers for patient selection. The evidence for the impact of antibody-FcγR interactions in mAb therapy indicates that there may be room for further improvement of such therapies by optimizing mAb- FcγR interactions, as well as by strategies to effectively recruit, activate or retain effector cell compartments.

References

1. Oldham, R. K., and R. O. Dillman. 2008. Monoclonal antibodies in cancer therapy: 25 years of progress. *J Clin Oncol* 26:1774-1777.
2. Nadler, L. M., P. Stashenko, R. Hardy, W. D. Kaplan, L. N. Button, D. W. Kufe, K. H. Antman, and S. F. Schlossman. 1980. Serotherapy of a patient with a monoclonal antibody directed against a human lymphoma-associated antigen. *Cancer Res* 40:3147-3154.
3. Parren, P. W., and J. G. van de Winkel. 2008. An integrated science-based approach to drug development. *Curr Opin Immunol* 20:426-430.
4. FitzGerald, D. J., A. S. Wayne, R. J. Kreitman, and I. Pastan. 2011. Treatment of hematologic malignancies with immunotoxins and antibody-drug conjugates. *Cancer Res* 71:6300-6309.
5. Muller, D., and R. E. Kontermann. 2010. Bispecific antibodies for cancer immunotherapy: Current perspectives. *BioDrugs* 24:89-98.
6. Desjarlais, J. R., and G. A. Lazar. 2011. Modulation of antibody effector function. *Exp Cell Res* 317:1278-1285.
7. Labrijn, A. F., R. C. Aalberse, and J. Schuurman. 2008. When binding is enough: nonactivating antibody formats. *Curr Opin Immunol* 20:479-485.
8. Ishida, T., T. Joh, N. Uike, K. Yamamoto, A. Utsunomiya, S. Yoshida, Y. Saburi, T. Miyamoto, S. Takemoto, H. Suzushima, K. Tsukasaki, K. Nosaka, H. Fujiwara, K. Ishitsuka, H. Inagaki, M. Ogura, S. Akinaga, M. Tomonaga, K. Tobinai, and R. Ueda. 2012. Defucosylated Anti-CCR4 Monoclonal Antibody (KW-0761) for Relapsed Adult T-Cell Leukemia-Lymphoma: A Multicenter Phase II Study. *J Clin Oncol* 30:837-842.
9. Ishii, T., T. Ishida, A. Utsunomiya, A. Inagaki, H. Yano, H. Komatsu, S. Iida, K. Imada, T. Uchiyama, S. Akinaga, K. Shitara, and R. Ueda. 2010. Defucosylated humanized anti-CCR4 monoclonal antibody KW-0761 as a novel immunotherapeutic agent for adult T-cell leukemia/lymphoma. *Clin Cancer Res* 16:1520-1531.
10. Mossner, E., P. Brunker, S. Moser, U. Puntener, C. Schmidt, S. Herter, R. Grau, C. Gerdes, A. Nopora, E. van Puijenbroek, C. Ferrara, P. Sondermann, C. Jager, P. Strein, G. Fertig, T. Friess, C. Schull, S. Bauer, J. Dal Porto, C. Del Nagro, K. Dabbagh, M. J. Dyer, S. Poppema, C. Klein, and P. Umana. 2010. Increasing the efficacy of CD20 antibody therapy through the engineering of a new type II anti-CD20 antibody with enhanced direct and immune effector cell-mediated B-cell cytotoxicity. *Blood* 115:4393-4402.
11. Salles, G., F. Morschhauser, T. Lamy, N. J. Milpied, C. Thieblemont, H. Tilly, G. Bieska, E. Asikanius, D. Carlile, J. Birkett, P. Pisa, and G. Cartron. 2012. Phase 1 study results of the type II glycoengineered humanized anti-CD20 monoclonal antibody obinutuzumab (GA101) in B-cell lymphoma patients. *Blood*.
12. Herbst, R., Y. Wang, S. Gallagher, N. Mittereder, E. Kuta, M. Damschroder, R. Woods, D. C. Rowe, L. Cheng, K. Cook, K. Evans, G. P. Sims, D. S. Pfarr, M. A. Bowen, W. Dall'Acqua, M. Shlomchik, T. F. Tedder, P. Kiener, B. Jallal, H. Wu, and A. J. Coyle. 2010. B-cell depletion in vitro and in vivo with an afucosylated anti-CD19 antibody. *J Pharmacol Exp Ther* 335:213-222.
13. Ward, E., N. Mittereder, E. Kuta, G. P. Sims, M. A. Bowen, W. Dall'Acqua, T. Tedder, P. Kiener, A. J. Coyle, H. Wu, B. Jallal, and R. Herbst. 2011. A glycoengineered anti-CD19 antibody with potent antibody-dependent cellular cytotoxicity activity in vitro and lymphoma growth inhibition in vivo. *Br J Haematol* 155:426-437.
14. Seimetz, D. 2011. Novel monoclonal antibodies for cancer treatment: the trifunctional antibody catumaxomab (removab). *J Cancer* 2:309-316.
15. Liu, A. Y., R. R. Robinson, E. D. Murray, Jr., J. A. Ledbetter, I. Hellstrom, and K. E. Hellstrom. 1987. Production of a mouse-human chimeric monoclonal antibody to CD20 with potent Fc-dependent biologic activity. *J Immunol* 139:3521-3526.
16. Golay, J., L. Zaffaroni, T. Vaccari, M. Lazzari, G. M. Borleri, S. Bernasconi, F. Tedesco, A. Rambaldi, and M. Introna. 2000. Biologic response of B lymphoma cells to anti-CD20 monoclonal antibody rituximab in vitro: CD55 and CD59 regulate complement-mediated cell lysis. *Blood* 95:3900-3908.
17. Pawluczkowycz, A. W., F. J. Beurskens, P. V. Beum, M. A. Lindorfer, J. G. van de Winkel, P. W. Parren, and R. P. Taylor. 2009. Binding of submaximal C1q promotes complement-dependent cytotoxicity (CDC) of B cells opsonized with anti-CD20 mAbs ofatumumab (OFA) or rituximab (RTX): considerably higher levels of CDC are induced by OFA than by RTX. *J Immunol* 183:749-758.

18. Craigen, J. L., W. J. M. Mackus, P. Engleberts, S. R. Miller, S. Speller, L. C. Chamberlain, B. G. Davis, S. M. McHugh, E. Bullmore, C. J. Cox, S. Wetten, G. Perdock, J. M. Bakker, J. G. J. van de Winkel, and P. W. H. I. Parren. 2009. Ofatumumab, a Human Mab Targeting a Membrane-Proximal Small-Loop Epitope On CD20, Induces Potent NK Cell-Mediated ADCC. *ASH Annual Meeting Abstracts* 114:1725-.
19. Crowe, J. S., V. S. Hall, M. A. Smith, H. J. Cooper, and J. P. Tite. 1992. Humanized monoclonal antibody CAMPATH-1H: myeloma cell expression of genomic constructs, nucleotide sequence of cDNA constructs and comparison of effector mechanisms of myeloma and Chinese hamster ovary cell-derived material. *Clin Exp Immunol* 87:105-110.
20. Nuckel, H., U. H. Frey, A. Roth, U. Duhrsen, and W. Siffert. 2005. Alemtuzumab induces enhanced apoptosis in vitro in B-cells from patients with chronic lymphocytic leukemia by antibody-dependent cellular cytotoxicity. *Eur J Pharmacol* 514:217-224.
21. Siders, W. M., J. Shields, C. Garron, Y. Hu, P. Boutin, S. Shankara, W. Weber, B. Roberts, and J. M. Kaplan. 2010. Involvement of neutrophils and natural killer cells in the anti-tumor activity of alemtuzumab in xenograft tumor models. *Leuk Lymphoma* 51:1293-1304.
22. Sliwkowski, M. X., J. A. Lofgren, G. D. Lewis, T. E. Hotaling, B. M. Fendly, and J. A. Fox. 1999. Nonclinical studies addressing the mechanism of action of trastuzumab (Herceptin). *Semin Oncol* 26:60-70.
23. Spector, N. L., and K. L. Blackwell. 2009. Understanding the mechanisms behind trastuzumab therapy for human epidermal growth factor receptor 2-positive breast cancer. *J Clin Oncol* 27:5838-5847.
24. Roda, J. M., T. Joshi, J. P. Butchar, J. W. McAlees, A. Lehman, S. Tridandapani, and W. E. Carson, 3rd. 2007. The activation of natural killer cell effector functions by cetuximab-coated, epidermal growth factor receptor positive tumor cells is enhanced by cytokines. *Clin Cancer Res* 13:6419-6428.
25. Bruggemann, M., G. T. Williams, C. I. Bindon, M. R. Clark, M. R. Walker, R. Jefferis, H. Waldmann, and M. S. Neuberger. 1987. Comparison of the effector functions of human immunoglobulins using a matched set of chimeric antibodies. *J Exp Med* 166:1351-1361.
26. Schneider-Merck, T., J. J. Lammerts van Bueren, S. Berger, K. Rossen, P. H. van Berkel, S. Derer, T. Beyer, S. Lohse, W. K. Bleeker, M. Peipp, P. W. Parren, J. G. van de Winkel, T. Valerius, and M. Dechant. 2010. Human IgG2 antibodies against epidermal growth factor receptor effectively trigger antibody-dependent cellular cytotoxicity but, in contrast to IgG1, only by cells of myeloid lineage. *J Immunol* 184:512-520.
27. Clynes, R. A., T. L. Towers, L. G. Presta, and J. V. Ravetch. 2000. Inhibitory Fc receptors modulate in vivo cytoxicity against tumor targets. *Nat Med* 6:443-446.
28. Zhang, Z., M. Zhang, C. K. Goldman, J. V. Ravetch, and T. A. Waldmann. 2003. Effective therapy for a murine model of adult T-cell leukemia with the humanized anti-CD52 monoclonal antibody, Campath-1H. *Cancer Res* 63:6453-6457.
29. Wilson, N. S., B. Yang, A. Yang, S. Loeser, S. Marsters, D. Lawrence, Y. Li, R. Pitti, K. Totpal, S. Yee, S. Ross, J. M. Vernes, Y. Lu, C. Adams, R. Offringa, B. Kelley, S. Hymowitz, D. Daniel, G. Meng, and A. Ashkenazi. 2011. An Fcgamma receptor-dependent mechanism drives antibody-mediated target-receptor signaling in cancer cells. *Cancer Cell* 19:101-113.
30. de Haij, S., J. H. Jansen, P. Boross, F. J. Beurskens, J. E. Bakema, D. L. Bos, A. Martens, J. S. Verbeek, P. W. Parren, J. G. van de Winkel, and J. H. Leusen. 2010. In vivo cytotoxicity of type I CD20 antibodies critically depends on Fc receptor ITAM signaling. *Cancer Res* 70:3209-3217.
31. Boross, P., J. H. Jansen, S. de Haij, F. J. Beurskens, C. E. van der Poel, L. Bevaart, M. Nederend, J. Golay, J. G. van de Winkel, P. W. Parren, and J. H. Leusen. 2011. The in vivo mechanism of action of CD20 monoclonal antibodies depends on local tumor burden. *Haematologica* 96:1822-1830.
32. Gong, Q., Q. Ou, S. Ye, W. P. Lee, J. Cornelius, L. Diehl, W. Y. Lin, Z. Hu, Y. Lu, Y. Chen, Y. Wu, Y. G. Meng, P. Gribling, Z. Lin, K. Nguyen, T. Tran, Y. Zhang, H. Rosen, F. Martin, and A. C. Chan. 2005. Importance of cellular microenvironment and circulatory dynamics in B cell immunotherapy. *J Immunol* 174:817-826.
33. Overdijk, M. B., S. Verploegen, J. H. van den Brakel, J. J. Lammerts van Bueren, T. Vink, J. G. van de Winkel, P. W. Parren, and W. K. Bleeker. 2011. Epidermal Growth Factor Receptor (EGFR) Antibody-Induced Antibody-Dependent Cellular Cytotoxicity Plays a Prominent Role in Inhibiting Tumorigenesis, Even of Tumor Cells Insensitive to EGFR Signaling Inhibition. *J Immunol* 187:3383-3390.

34. Repka, T., E. G. Chiorean, J. Gay, K. E. Herwig, V. K. Kohl, D. Yee, and J. S. Miller. 2003. Trastuzumab and interleukin-2 in HER2-positive metastatic breast cancer: a pilot study. *Clin Cancer Res* 9:2440-2446.

35. Arnould, L., M. Gelly, F. Penault-Llorca, L. Benoit, F. Bonnetain, C. Migeon, V. Cabaret, V. Fermeaux, P. Bertheau, J. Garnier, J. F. Jeannin, and B. Coudert. 2006. Trastuzumab-based treatment of HER2-positive breast cancer: an antibody-dependent cellular cytotoxicity mechanism? *Br J Cancer* 94:259-267.

36. Maréchal, R., J. De Schutter, N. Nagy, P. Demetter, A. Lemmers, J. Deviere, I. Salmon, S. Tejpar, and J. L. Van Laethem. 2010. Putative contribution of CD56 positive cells in cetuximab treatment efficacy in first-line metastatic colorectal cancer patients. *BMC Cancer* 10:340.

37. Daeron, M. 1997. Fc receptor biology. *Annu Rev Immunol* 15:203-234.

38. Clark, M. R., S. B. Clarkson, P. A. Ory, N. Stollman, and I. M. Goldstein. 1989. Molecular basis for a polymorphism involving Fc receptor II on human monocytes. *J Immunol* 143:1731-1734.

39. Tax, W. J., H. W. Willems, P. P. Reekers, P. J. Capel, and R. A. Koene. 1983. Polymorphism in mitogenic effect of IgG1 monoclonal antibodies against T3 antigen on human T cells. *Nature* 304:445-447.

40. Warmerdam, P. A., J. G. van de Winkel, A. Vlug, N. A. Westerdaal, and P. J. Capel. 1991. A single amino acid in the second Ig-like domain of the human Fc gamma receptor II is critical for human IgG2 binding. *J Immunol* 147:1338-1343.

41. Parren, P. W., P. A. Warmerdam, L. C. Boeije, J. Arts, N. A. Westerdaal, A. Vlug, P. J. Capel, L. A. Aarden, and J. G. van de Winkel. 1992. On the interaction of IgG subclasses with the low affinity Fc gamma RIIa (CD32) on human monocytes, neutrophils, and platelets. Analysis of a functional polymorphism to human IgG2. *J Clin Invest* 90:1537-1546.

42. Kyogoku, C., H. M. Dijstelbloem, N. Tsuchiya, Y. Hatta, H. Kato, A. Yamaguchi, T. Fukazawa, M. D. Jansen, H. Hashimoto, J. G. van de Winkel, C. G. Kallenberg, and K. Tokunaga. 2002. Fcgamma receptor gene polymorphisms in Japanese patients with systemic lupus erythematosus: contribution of FCGR2B to genetic susceptibility. *Arthritis Rheum* 46:1242-1254.

43. Kono, H., C. Kyogoku, T. Suzuki, N. Tsuchiya, H. Honda, K. Yamamoto, K. Tokunaga, and Z. Honda. 2005. FcgammaRIIB Ile232Thr transmembrane polymorphism associated with human systemic lupus erythematosus decreases affinity to lipid rafts and attenuates inhibitory effects on B cell receptor signaling. *Hum Mol Genet* 14:2881-2892.

44. Ravetch, J. V., and B. Perussia. 1989. Alternative membrane forms of Fc gamma RIII(CD16) on human natural killer cells and neutrophils. Cell type-specific expression of two genes that differ in single nucleotide substitutions. *J Exp Med* 170:481-497.

45. Wu, J., J. C. Edberg, P. B. Redecha, V. Bansal, P. M. Guyre, K. Coleman, J. E. Salmon, and R. P. Kimberly. 1997. A novel polymorphism of FcgammaRIIIa (CD16) alters receptor function and predisposes to autoimmune disease. *J Clin Invest* 100:1059-1070.

46. Koene, H. R., M. Kleijer, J. Algra, D. Roos, A. E. von dem Borne, and M. de Haas. 1997. Fc gammaRIIIa-158V/F polymorphism influences the binding of IgG by natural killer cell Fc gammaRIIIa, independently of the Fc gammaRIIIa-48L/R/H phenotype. *Blood* 90:1109-1114.

47. Huizinga, T. W., M. Kleijer, P. A. Tetteroo, D. Roos, and A. E. von dem Borne. 1990. Biallelic neutrophil Na-antigen system is associated with a polymorphism on the phospho-inositol-linked Fc gamma receptor III (CD16). *Blood* 75:213-217.

48. Salmon, J. E., S. S. Millard, N. L. Brogle, and R. P. Kimberly. 1995. Fc gamma receptor IIIb enhances Fc gamma receptor IIa function in an oxidant-dependent and allele-sensitive manner. *J Clin Invest* 95:2877-2885.

49. Bruhns, P., B. Iannascoli, P. England, D. A. Mancardi, N. Fernandez, S. Jorieux, and M. Daeron. 2009. Specificity and affinity of human Fcgamma receptors and their polymorphic variants for human IgG subclasses. *Blood* 113:3716-3725.

50. van Sorge, N. M., W. L. van der Pol, and J. G. van de Winkel. 2003. FcgammaR polymorphisms: Implications for function, disease susceptibility and immunotherapy. *Tissue Antigens* 61:189-202.

51. Parren, P. W., P. A. Warmerdam, L. C. Boeije, P. J. Capel, J. G. van de Winkel, and L. A. Aarden. 1992. Characterization of IgG FcR-mediated proliferation of human T cells induced by mouse and human anti-CD3 monoclonal antibodies. Identification of a functional polymorphism to human IgG2 anti-CD3. *J Immunol* 148:695-701.

52. Lopez-Albaitero, A., S. C. Lee, S. Morgan, J. R. Grandis, W. E. Gooding, S. Ferrone, and R. L. Ferris. 2009. Role of polymorphic Fc gamma receptor IIIa and EGFR expression level in cetuximab mediated, NK cell dependent in vitro cytotoxicity of head and neck squamous cell carcinoma cells. *Cancer Immunol Immunother* 58:1853-1864.

53. Taylor, R. J., S. L. Chan, A. Wood, C. J. Voskens, J. S. Wolf, W. Lin, A. Chapoval, D. H. Schulze, G. Tian, and S. E. Strome. 2009. FcgammaRIIIa polymorphisms and cetuximab induced cytotoxicity in squamous cell carcinoma of the head and neck. *Cancer Immunol Immunother* 58:997-1006.

54. Dall'Ozzo, S., S. Tartas, G. Paintaud, G. Cartron, P. Colombat, P. Bardos, H. Watier, and G. Thibault. 2004. Rituximab-dependent cytotoxicity by natural killer cells: influence of FCGR3A polymorphism on the concentration-effect relationship. *Cancer Res* 64:4664-4669.

55. Musolino, A., N. Naldi, B. Bortesi, D. Pezzuolo, M. Capelletti, G. Missale, D. Laccabue, A. Zerbini, R. Camisa, G. Bisagni, T. M. Neri, and A. Ardizzoni. 2008. Immunoglobulin G fragment C receptor polymorphisms and clinical efficacy of trastuzumab-based therapy in patients with HER-2/neu-positive metastatic breast cancer. *J Clin Oncol* 26:1789-1796.

56. Cartron, G., L. Dacheux, G. Salles, P. Solal-Celigny, P. Bardos, P. Colombat, and H. Watier. 2002. Therapeutic activity of humanized anti-CD20 monoclonal antibody and polymorphism in IgG Fc receptor FcgammaRIIIa gene. *Blood* 99:754-758.

57. Cornec, D., A. Tempescul, S. Querellou, P. Hutin, J. O. Pers, C. Jamin, B. Bendaoud, C. Berthou, Y. Renaudineau, and P. Youinou. 2012. Identification of patients with indolent B cell lymphoma sensitive to rituximab monotherapy. *Ann Hematol* 91:715-721.

58. Weng, W. K., and R. Levy. 2003. Two immunoglobulin G fragment C receptor polymorphisms independently predict response to rituximab in patients with follicular lymphoma. *J Clin Oncol* 21:3940-3947.

59. Ghielmini, M., K. Rufibach, G. Salles, L. Leoncini-Franscini, C. Leger-Falandry, S. Cogliatti, M. Fey, G. Martinelli, R. Stahel, A. Lohri, N. Ketterer, M. Wernli, T. Cerny, and S. F. Schmitz. 2005. Single agent rituximab in patients with follicular or mantle cell lymphoma: clinical and biological factors that are predictive of response and event-free survival as well as the effect of rituximab on the immune system: a study of the Swiss Group for Clinical Cancer Research (SAKK). *Ann Oncol* 16:1675-1682.

60. Treon, S. P., M. Hansen, A. R. Branagan, S. Verselis, C. Emmanouilides, E. Kimby, S. R. Frankel, N. Touroutoglou, B. Turnbull, K. C. Anderson, D. G. Maloney, and E. A. Fox. 2005. Polymorphisms in FcgammaRIIIA (CD16) receptor expression are associated with clinical response to rituximab in Waldenstrom's macroglobulinemia. *J Clin Oncol* 23:474-481.

61. Farag, S. S., I. W. Flinn, R. Modali, T. A. Lehman, D. Young, and J. C. Byrd. 2004. Fc gamma RIIIa and Fc gamma RIIa polymorphisms do not predict response to rituximab in B-cell chronic lymphocytic leukemia. *Blood* 103:1472-1474.

62. Weng, W. K., and R. Levy. 2009. Genetic polymorphism of the inhibitory IgG Fc receptor FcgammaRIIb is not associated with clinical outcome in patients with follicular lymphoma treated with rituximab. *Leuk Lymphoma* 50:723-727.

63. Lejeune, J., G. Thibault, D. Ternant, G. Cartron, H. Watier, and M. Ohresser. 2008. Evidence for linkage disequilibrium between Fcgamma RIIIa-V158F and Fcgamma RIIa-H131R polymorphisms in white patients, and for an Fcgamma RIIIa-restricted influence on the response to therapeutic antibodies. *J Clin Oncol* 26:5489-5491; author reply 5491-5482.

64. Kim, D. H., H. D. Jung, J. G. Kim, J. J. Lee, D. H. Yang, Y. H. Park, Y. R. Do, H. J. Shin, M. K. Kim, M. S. Hyun, and S. K. Sohn. 2006. FCGR3A gene polymorphisms may correlate with response to frontline R-CHOP therapy for diffuse large B-cell lymphoma. *Blood* 108:2720-2725.

65. Persky, D. O., D. Dornan, B. Goldman, R. Braziel, R. Fisher, M. Leblanc, D. G. Maloney, O. Press, T. Miller, and L. M. Rimsza. 2012. Fc gamma receptor 3a genotype predicts overall survival in follicular lymphoma patients treated on SWOG trials with combined monoclonal antibody plus chemotherapy but not chemotherapy alone. *Haematologica*.

66. Fabisiewicz, A., E. Paszkiewicz-Kozik, M. Osowiecki, J. Walewski, and J. A. Siedlecki. 2011. FcgammaRIIA and FcgammaRIIIA polymorphisms do not influence survival and response to rituximab, cyclophosphamide, doxorubicin, vincristine, and prednisone immunochemotherapy in patients with diffuse large B-cell lymphoma. *Leuk Lymphoma* 52:1604-1606.

67. Ahlgrimm, M., M. Pfreundschuh, M. Kreuz, E. Regitz, K. D. Preuss, and J. Bittenbring. 2011. The impact of Fc-gamma receptor polymorphisms in elderly patients with diffuse large B-cell lymphoma treated with CHOP with or without rituximab. *Blood* 118:4657-4662.

68. Mitrovic, Z., I. Aurer, I. Radman, R. Ajdukovic, J. Sertic, and B. Labar. 2007. FCgammaRIIIA and FCgammaRIIA polymorphisms are not associated with response to rituximab and CHOP in patients with diffuse large B-cell lymphoma. *Haematologica* 92:998-999.

69. Boettcher, S., C. Pott, M. Ritgen, W. Hiddemann, M. Unterhalt, and M. Kneba. 2004. Evidence for Fc{gamma} Receptor IIIA-Independent Rituximab Effector Mechanisms in Patients with Follicular Lymphoma Treated with Combined Immuno-Chemotherapy. *ASH Annual Meeting Abstracts* 104:590-.

70. Carlotti, E., G. A. Palumbo, E. Oldani, D. Tibullo, S. Salmoiraghi, A. Rossi, J. Golay, A. Pulsoni, R. Foa, and A. Rambaldi. 2007. FcgammaRIIIA and FcgammaRIIA polymorphisms do not predict clinical outcome of follicular non-Hodgkin's lymphoma patients treated with sequential CHOP and rituximab. *Haematologica* 92:1127-1130.

71. Dornan, D., O. Spleiss, R. F. Yeh, G. Duchateau-Nguyen, A. Dufour, J. Zhi, T. Robak, S. I. Moiseev, A. Dmoszynska, P. Solal-Celigny, K. Warzocha, J. Loscertales, J. Catalano, B. V. Afanasiev, L. Larratt, V. A. Rossiev, I. Bence-Bruckler, C. H. Geisler, M. Montillo, M. K. Wenger, and M. Weisser. 2010. Effect of FCGR2A and FCGR3A variants on CLL outcome. *Blood* 116:4212-4222.

72. Lin, T. S., I. W. Flinn, R. Modali, T. A. Lehman, J. Webb, S. Waymer, M. E. Moran, M. S. Lucas, S. S. Farag, and J. C. Byrd. 2005. FCGR3A and FCGR2A polymorphisms may not correlate with response to alemtuzumab in chronic lymphocytic leukemia. *Blood* 105:289-291.

73. Bier, H., T. Hoffmann, I. Haas, and A. van Lierop. 1998. Anti-(epidermal growth factor) receptor monoclonal antibodies for the induction of antibody-dependent cell-mediated cytotoxicity against squamous cell carcinoma lines of the head and neck. *Cancer Immunol Immunother* 46:167-173.

74. Zhang, W., M. Gordon, A. M. Schultheis, D. Y. Yang, F. Nagashima, M. Azuma, H. M. Chang, E. Borucka, G. Lurje, A. E. Sherrod, S. Iqbal, S. Groshen, and H. J. Lenz. 2007. FCGR2A and FCGR3A polymorphisms associated with clinical outcome of epidermal growth factor receptor expressing metastatic colorectal cancer patients treated with single-agent cetuximab. *J Clin Oncol* 25:3712-3718.

75. Bibeau, F., E. Lopez-Crapez, F. Di Fiore, S. Thezenas, M. Ychou, F. Blanchard, A. Lamy, F. Penault-Llorca, T. Frebourg, P. Michel, J. C. Sabourin, and F. Boissiere-Michot. 2009. Impact of Fc{gamma} RIIa-Fc{gamma}RIIIa polymorphisms and KRAS mutations on the clinical outcome of patients with metastatic colorectal cancer treated with cetuximab plus irinotecan. *J Clin Oncol* 27:1122-1129.

76. Rodriguez, J., R. Zarate, E. Bandres, V. Boni, A. Hernandez, J. J. Sola, B. Honorato, N. Bitarte, and J. Garcia-Foncillas. 2012. Fc gamma receptor polymorphisms as predictive markers of Cetuximab efficacy in epidermal growth factor receptor downstream-mutated metastatic colorectal cancer. *Eur J Cancer*.

77. Gennari, R., S. Menard, F. Fagnoni, L. Ponchio, M. Scelsi, E. Tagliabue, F. Castiglioni, L. Villani, C. Magalotti, N. Gibelli, B. Oliviero, B. Ballardini, G. Da Prada, A. Zambelli, and A. Costa. 2004. Pilot study of the mechanism of action of preoperative trastuzumab in patients with primary operable breast tumors overexpressing HER2. *Clin Cancer Res* 10:5650-5655.

78. Tamura, K., C. Shimizu, T. Hojo, S. Akashi-Tanaka, T. Kinoshita, K. Yonemori, T. Kouno, N. Katsumata, M. Ando, K. Aogi, F. Koizumi, K. Nishio, and Y. Fujiwara. 2011. FcgammaR2A and 3A polymorphisms predict clinical outcome of trastuzumab in both neoadjuvant and metastatic settings in patients with HER2-positive breast cancer. *Ann Oncol* 22:1302-1307.

79. Wang, J., J. Feng, L. Zhang, Y. Hu, B. Luan, W. Yue, H. Wang, S. Zhu, and Y. Xu. 2003. Distribution of variant genotypes of Fc gamma receptor IIIa in healthy Chinese population of Zhengzhou City. *J Huazhong Univ Sci Technolog Med Sci* 23:239-241.

80. Armoiry, X., G. Aulagner, and T. Facon. 2008. Lenalidomide in the treatment of multiple myeloma: a review. *J Clin Pharm Ther* 33:219-226.

81. de Weers, M., Y. T. Tai, M. S. van der Veer, J. M. Bakker, T. Vink, D. C. Jacobs, L. A. Oomen, M. Peipp, T. Valerius, J. W. Slootstra, T. Mutis, W. K. Bleeker, K. C. Anderson, H. M. Lokhorst, J. G. van de Winkel, and P. W. Parren. 2011. Daratumumab, a novel therapeutic human CD38 monoclonal antibody, induces killing of multiple myeloma and other hematological tumors. *J Immunol* 186:1840-1848.

82. van der Veer, M. S., M. de Weers, B. van Kessel, J. M. Bakker, S. Wittebol, P. W. Parren, H. M. Lokhorst, and T. Mutis. 2011. Towards effective immunotherapy of myeloma: enhanced elimination of myeloma cells by combination of lenalidomide with the human CD38 monoclonal antibody daratumumab. *Haematologica* 96:284-290.

83. van der Veer, M. S., M. de Weers, B. van Kessel, J. M. Bakker, S. Wittebol, P. W. H. I. Parren, H. M. Lokhorst, and T. Mutis. 2011. The therapeutic human CD38 antibody daratumumab improves the anti-myeloma effect of newly emerging multi-drug therapies. *Blood Cancer Journal* 1:e41.

84. Hayashi, T., T. Hideshima, M. Akiyama, K. Podar, H. Yasui, N. Raje, S. Kumar, D. Chauhan, S. P. Treon, P. Richardson, and K. C. Anderson. 2005. Molecular mechanisms whereby immunomodulatory drugs activate natural killer cells: clinical application. *Br J Haematol* 128:192-203.

85. Tsavaris, N., C. Kosmas, M. Vadiaka, P. Kanelopoulos, and D. Boulamatsis. 2002. Immune changes in patients with advanced breast cancer undergoing chemotherapy with taxanes. *Br J Cancer* 87:21-27.

86. Lazar, G. A., W. Dang, S. Karki, O. Vafa, J. S. Peng, L. Hyun, C. Chan, H. S. Chung, A. Eivazi, S. C. Yoder, J. Vielmetter, D. F. Carmichael, R. J. Hayes, and B. I. Dahiyat. 2006. Engineered antibody Fc variants with enhanced effector function. *Proc Natl Acad Sci U S A* 103:4005-4010.

87. Awan, F. T., R. Lapalombella, R. Trotta, J. P. Butchar, B. Yu, D. M. Benson, Jr., J. M. Roda, C. Cheney, X. Mo, A. Lehman, J. Jones, J. Flynn, D. Jarjoura, J. R. Desjarlais, S. Tridandapani, M. A. Caligiuri, N. Muthusamy, and J. C. Byrd. 2010. CD19 targeting of chronic lymphocytic leukemia with a novel Fc-domain-engineered monoclonal antibody. *Blood* 115:1204-1213.

88. Ferrara, C., F. Stuart, P. Sondermann, P. Brunker, and P. Umana. 2006. The carbohydrate at FcgammaRIIIa Asn-162. An element required for high affinity binding to non-fucosylated IgG glycoforms. *J Biol Chem* 281:5032-5036.

89. Bologna, L., E. Gotti, M. Manganini, A. Rambaldi, T. Intermesoli, M. Introna, and J. Golay. 2011. Mechanism of action of type II, glycoengineered, anti-CD20 monoclonal antibody GA101 in B-chronic lymphocytic leukemia whole blood assays in comparison with rituximab and alemtuzumab. *J Immunol* 186:3762-3769.

90. Niwa, R., S. Hatanaka, E. Shoji-Hosaka, M. Sakurada, Y. Kobayashi, A. Uehara, H. Yokoi, K. Nakamura, and K. Shitara. 2004. Enhancement of the antibody-dependent cellular cytotoxicity of low-fucose IgG1 Is independent of FcgammaRIIIa functional polymorphism. *Clin Cancer Res* 10:6248-6255.

91. Peipp, M., J. J. Lammerts van Bueren, T. Schneider-Merck, W. W. Bleeker, M. Dechant, T. Beyer, R. Repp, P. H. van Berkel, T. Vink, J. G. van de Winkel, P. W. Parren, and T. Valerius. 2008. Antibody fucosylation differentially impacts cytotoxicity mediated by NK and PMN effector cells. *Blood* 112:2390-2399.

92. Paiva, M., H. Marques, A. Martins, P. Ferreira, R. Catarino, and R. Medeiros. 2008. FcgammaRIIa polymorphism and clinical response to rituximab in non-Hodgkin lymphoma patients. *Cancer Genet Cytogenet* 183:35-40.

3

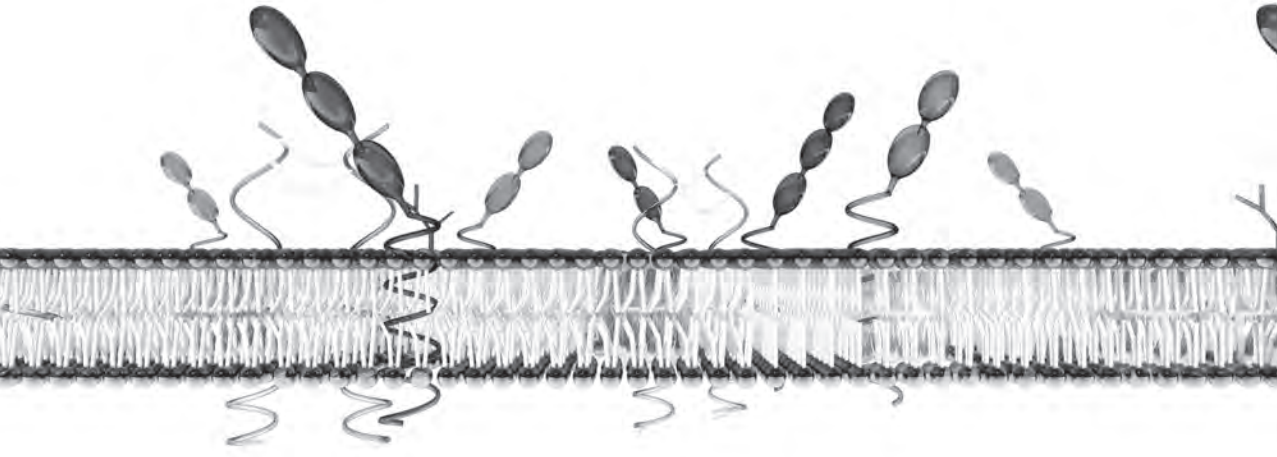

Crosstalk between human IgG isotypes and murine effector cells

Marije B. Overdijk[*], Sandra Verploegen[*], Antonio Ortiz Buijsse[*], Tom Vink[*], Jeanette H.W. Leusen[†], Wim K. Bleeker[*] and Paul W.H.I. Parren[*]

[*]Genmab, Utrecht, The Netherlands; [†]Immunotherapy Laboratory, Department of Immunology, University Medical Center, Utrecht, The Netherlands.

The Journal of Immunology, 2012, 189: 3430-3438

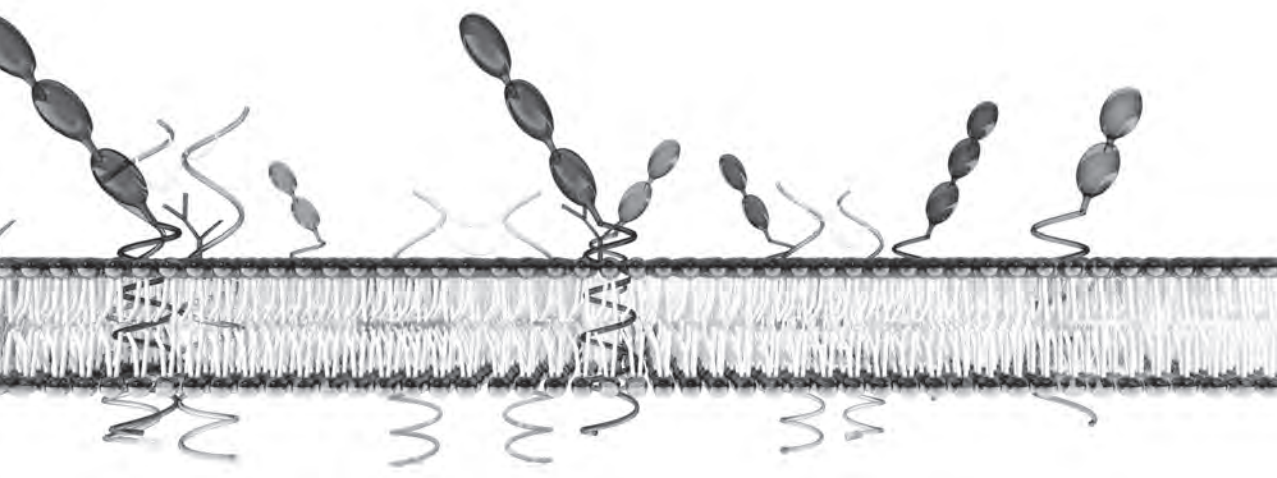

Abstract

Development of human therapeutic Abs has led to reduced immunogenicity and optimal interactions with the human immune system in patients. Humanization had as consequence that efficacy studies performed in mouse models, which represent a crucial step in preclinical development, are more difficult to interpret because gaps in our knowledge of the activation of murine effector cells by human IgG (hIgG) remain. We therefore developed full sets of human and mouse isotype variants of human Abs targeting epidermal growth factor receptor and CD20 to explore the crosstalk with mouse FcγRs (mFcγRs) and murine effector cells. Analysis of mFcγR binding demonstrated that hIgG1 and hIgG3 bound to all four mFcγRs, with hIgG3 having the highest affinity. hIgG1 nevertheless was more potent than hIgG3 in inducing antibody-dependent cellular cytotoxicity (ADCC) and antibody-dependent cellular phagocytosis (ADCP) with mouse NK cells, mouse polymorphonuclear leukocytes and mouse macrophages. hIgG4 bound to all mFcγRs except mFcγRIV and showed comparable interactions with murine effector cells to hIgG3. hIgG4 is thus active in the murine immune system, in contrast with its inert phenotype in the human system. hIgG2 bound to mFcγRIIb and mFcγRIII, and induced potent ADCC with mouse NK cells and mouse polymorphonuclear leukocytes. hIgG2 induced weak ADCC and, remarkably, was unable to induce ADCP with mouse macrophages. Finally, the isotypes were studied in s.c. and i.v. tumor xenograft models, which confirmed hIgG1 to be the most potent human isotype in mouse models. These data enhance our understanding of the crosstalk between hIgGs and murine effector cells, permitting a better interpretation of human Ab efficacy studies in mouse models.

Introduction

Therapeutic mAbs are an important class of agents for the treatment of cancer. The first developed therapeutic mAbs were of murine origin and, hence, mechanism of action (MoA) studies in mouse models were straightforward (1). Subsequently, chimeric, humanized and human (h) mAbs were developed to reduce the risk of immunogenicity in patients. The human IgG1 (hIgG) H chain constant domains (typically of the hIgG1 isotype) in these human(ized) mAbs provide optimal interactions with the human immune system and improved *in vivo* half-lives as an additional advantage. However, as a consequence they have become less adapted for studies in mouse models.

The engagement of immune effector mechanisms including antibody-dependent cellular cytotoxicity (ADCC) and antibody-dependent cellular phagocytosis (ADCP) by therapeutic Abs is dependent on the interaction of the IgG Fc domain with FcγRs on effector cells. There is a significant variation in the affinity of hIgG isotypes for individual hFcγRs (2, 3), which is reflected in their biological activities (4-6). Based on their affinity, hIgG1 and hIgG3 are considered to be the principal human isotypes for human activating FcγRs. In murine settings, they thus compare to mouse IgG2a (mIgG2a) and mIgG2b (7, 8). In humans there are five activating FcγRs; hFcγRI, hFcγRIIa, hFcγRIIc, hFcγRIIIa, hFcγRIIIb and one inhibitory FcγR, hFcγRIIb (2). Mice have 3 activating FcγRs; mouse FcγRI (mFcγRI), mFcγRIII, mFcγRIV and one inhibitory FcγR, mFcγRIIb (8).

Because efficacy studies in mouse models are a crucial step in preclinical development, and it is important to reliably translate such findings to the human system, a detailed understanding of the interaction of the murine immune system with human mAbs is essential. However, it has long been apparent that translation of findings across species is often problematic. Steplewski et al. (9), for example showed that an Ab of the hIgG4 isotype, which is inert with human effector cells, does induce ADCC of colorectal carcinoma cell lines by mouse macrophages and is equally potent to hIgG1 in a mouse *in vivo* model. These results were confirmed by Isaacs et al. (10). The limitations and risks for preclinical testing of human mAbs in mouse models was eloquently reviewed by Loisel et al. (11), who pointed out that in order to interpret the results correctly, it is critical to fully understand the interactions of human Abs with the murine immune system. Indeed, despite extensive research performed, important gaps in our knowledge still remain.

In our study we tackled this issue by use of full sets of human and mouse isotype variants of human mAbs targeting epidermal growth factor receptor (EGFR) and CD20, respectively. This allows us to exclude Ag- or epitope-dependent effects and draw general conclusions. We carefully mapped both the binding of these isotype panels to mFcγRs and their activity with murine effector cells in functional ADCC and ADCP assays. Finally, we studied the isotype-dependent efficacy in distinct mouse tumor models *in vivo* to complete our insight in the crosstalk of hIgGs with the murine cellular immune effector system.

Materials and Methods

Cell lines

A431-cells (human epidermoid cell line) were obtained from the Deutsche Sammlung von Mikroorganismen und Zelkulturen (cell line number ACC 91; Braunschweig, Germany). Daudi-cells (human Burkitt's lymphoma) were obtained from the American Type Culture Collection (ATCC no. CCL-213; Rockville, MD). Daudi cells were transfected by electroporation with gWIZ luciferase (Aldevron, Fargo, ND) and pPur vector (BD Biosciences, Alphen aan de Rijn, The Netherlands) in a 4:1 ratio and, after 48 h, puromycin was added for selecting a stably transfected clone (Daudi-luc). Both cell lines were cultured in RPMI 1640 medium (Lonza, Verviers, Belgium), supplemented with 10% heat-inactivated cosmic calf serum (CCS) (Hyclone, Logan, UT), 50 IU/ml penicillin, 50 μg/ml streptomycin (Lonza). The culture medium for the Daudi-cells was supplemented with 2 mM L-glutamin (Lonza) and 1 mM sodium pyruvate (Lonza). A431-cells were detached with 0.05% trypsin-EDTA (Invitrogen, Carlsbad, CA) in PBS (B.Braun, Melsungen, Germany). For *in vivo* tumor studies, cells were harvested when in log-phase and tested for EGFR or CD20 expression; mycoplasm contamination was excluded with a MycoAlert assay (Lonza).

Antibodies

Human anti-EGFR mAbs 2F8 (HuMax-EGFr, zalutumumab) and mAb 018 and human CD20 mAb 7D8 were generated by immunizing HuMAb mice (Medarex, Milpitas, CA) (12, 13). The variable regions of the immunoglobulin heavy chain

(VH) of anti-EGFR mAb 2F8 and mAb 018 and of CD20 mAb 7D8 were expressed recombinantly as hIgG1, hIgG2, hIgG3, hIgG4, mIgG1 and mIgG2a Abs. The human heavy chain constructs were co-expressed with the appropriate original human kappa light chain. For the mouse Abs, a corresponding construct with the mouse kappa light chain was used. All isotype batches contained less than 3.6% multimers as analyzed by high-performance size-exclusion chromatography (HP-SEC). For the hIgG1 isotype, Fc mutants were generated in which the site for N-linked glycosylation in the Fc domain was eliminated by mutating the asparagine at position 297 to glutamine. These mutants are referred to as mAb 2F8-hIgG1-N297Q, mAb 018-hIgG1-N297Q and mAb 7D8-hIgG1-N297Q. This mutation leads to loss of Fc glycosylation which results in abrogation of IgG FcR interactions and C1q binding, and thereby loss of ADCC and complement-dependent cytotoxicity (CDC) functions as previously described (14). The N297Q mutation was introduced using the QuikChange XL Site-Directed Mutagenesis Kit (Stratagene, La Jolla, CA), and mutagenesis was checked by sequencing (LGC Genomics, Berlin, Germany). IgG concentrations were determined by A280 measurements. An hIgG1 mAb, specific for keyhole limpet hemocyanin (HuMab-KLH), also generated in HuMab mice, was included in all experiments as an irrelevant mAb control. For the time-resolved fluorescence resonance energy transfer (TR-FRET) assay, 2F8-mIgG1 and 2F8-mIgG2a were labeled with Alexa Fluor 647 (Invitrogen), according to manufacturer's protocol.

TR-FRET

The TR-FRET assay was chosen, because it was demonstrated to be relatively insensitive to the presence of IgG aggregates in test samples. Thus, when comparing an IgG batch containing 1% multimers with a heat-aggregated IgG sample from the same batch containing 45% multimers, only a minor shift in the inhibition curve was observed (~factor 2, data not shown). Samples from the isotype batches were concentrated for this assay, which did not result in higher levels of aggregates (< 3.6%) except for 2F8-hIgG3 (~27%). Recombinant mFcγRI, mFcγRIIb, mFcγRIII and mFcγRIV (R&D Systems, Minneapolis, MN) were labeled with Eu-W1024 ITC Chelate (PerkinElmer, Waltham, MA) according to manufacturer's protocol. mFcγR binding was assessed by incubating mFcγR-Eu with serially diluted mAb solution for 30 min at room temperature (RT) followed by addition of mIgG1-A647, in the case of mFcγRIIb-Eu and mFcγRIII-Eu, or mIgG2a-A647, in the case of mFcγRI-Eu and mFcγRIV-Eu, and plates

were incubated for 2 h at RT. After 2 h, 30 µl sample was transferred to a 384w Optiplate White (PerkinElmer), and time-resolved fluorescence was measured at an emission of 665 nm upon excitation at 340 nm (Envision, PerkinElmer).

Mouse NK cell culture

Mouse NK (mNK) cells were isolated from the spleen of SCID mice (C.B.-17/IcrCrl-scid/scid; Charles River, Maastricht, The Netherlands). Isolated splenocytes were passed through a cell-strainer and cultured for 7 d at 37°C / 5% CO_2 in RPMI 1640 medium in the presence of 10% CCS/ 50 IU/ml penicillin, 50 µg/ml streptomycin and 1.7×10^3 U/ml recombinant human IL-2 (Peprotech, London, UK) at a concentration of 0.3×10^6 cells/ml. Cells were expanded once every 3 days by resuspending at 0.3×10^6 cells/ml in fresh medium. mNK cells were characterized on FACS with NKp46-PE (R&D Systems).

Isolation of mouse polymorphonuclear leukocytes

Mouse polymorphonuclear leukocyte (mPMN) counts in BALB/c (Charles River) mouse blood were enhanced by s.c. administration of 40 µg pegylated-G-CSF (Neulasta, Amgen, Thousand Oaks, CA). At day 4, mice were anesthetized with isoflurane (IsoFlo, Abbot Laboratories, Abbot Park, IL) and blood was collected via a cardiac puncture. mPMNs were characterized with GR-1-PerCP (BD Pharmingen, San Diego, CA) and counted on FACS with Trucount tubes (BD Pharmingen), demonstrating ~1.5×10^7 GR-1^+ cells per milliliter blood.

Bone marrow-derived mouse macrophage culture

Bone marrow was isolated from the hind legs of either wild type (WT) C57BL/6 mice (Janvier, Le Genest St Isle, France), FcγRI$^{-/-}$ (CD64 KO) mice, FcγRIII$^{-/-}$ (CD16 KO) mice (kindly provided by Dr. Jeanette Leusen), and FcγRI/III$^{-/-}$ (CD64/CD16 double KO) (kindly provided by Prof. Sjef Verbeek, Leiden University Medical Center, Leiden, The Netherlands) as reviewed by Otten et al. (15) by flushing the femurs. Bone marrow was brought over a cell-strainer and seeded in petri dishes in DMEM (Lonza) in the presence of 10% CCS/ 2 mM L-glutamine/ 50 IU/ml penicillin and 50 µg/ml streptomycin at a concentration of 1.25×10^5 cells/ml. Cells were cultured for 7 d at 37°C / 5%CO_2 in the presence of 50 U/ml M-CSF (ProSpec, Rehovot, Israel). For ADCC assays, cultured macrophages were stimulated with 250 U/ml IFNγ (BD Biosciences)/ 25 ng/ml LPS (Sigma-Aldrich, St. Louis, MO), 24 h before use. Macrophages were detached with versene

(Invitrogen) and characterized by FACS analysis for staining with F4/80-A488 (AbD Serotec, Oxford, U.K.) and CD80-PE (eBioscience, San Diego, CA).

ADCC

ADCC was evaluated in [^{51}Cr] release assay in which A431 or Daudi target cells (5×10^6 cells) were labeled with 100 µCi $Na_2{}^{51}CrO_4$ (Amersham Biosciences, Uppsala, Sweden) at 37°C for 1 h. Cells were washed twice with PBS and resuspended in culture medium at 1×10^5 cells/ml. A total of 5×10^3 labeled cells was added in 96-well plates and preincubated with mAb at a fixed mAb concentration (six replicates) for 15 min at RT. After the preincubation, either mNK cells (1×10^5/well, resulting in an effector:target (E:T) ratio of 20:1), mouse macrophages (1×10^5/well, resulting in an E:T of 20:1) or mPMNs (50 µl 2x diluted whole blood resulting in an E:T ratio of about 75:1) were added to the wells and incubated at 37°C for 4 h (mNK cells and mPMNs) or 24 h (mouse macrophages). Instead of mAb, culture medium was added to determine the background [^{51}Cr] release (negative control) and Triton-X-100 (1.6% final concentration; Sigma-Aldrich) was added to determine the maximal [^{51}Cr] release (positive control). Supernatants were collected and [^{51}Cr] release was measured in gamma counter [cpm]. Percentage of cellular cytotoxicity was calculated using the following formula: percentage specific lysis = (experimental release [cpm] – negative control [cpm])/(positive control [cpm] – negative control [cpm]) x100%.

ADCP

ADCP was determined by flow cytometry. Bone marrow-derived macrophages were seeded at 2.5×10^5 per well into 24-well plates and allowed to adhere overnight. Target Daudi cells were labeled with calcein-AM (Invitrogen) and added to the macrophages at a 1:1 E:T ratio in the presence of a fixed Ab concentration of 1 µg/ml. After a 4 h incubation at 37°C / 5%CO_2, target cells were washed away and macrophages were detached with versene and stained with F4/80-PE (AbD Serotec) and CD19-APC (DAKO, Glostrup, Denmark). ADCP was evaluated on a FACSCanto II flow cytometer (BD Biosciences) and defined as percentage of macrophages that had phagocytosed. Percentage of phagocytosis was calculated using the following gate settings: the percentage within the F4/80-positive cells that are calcein-AM$^+$ and CD19$^-$.

Mouse tumor xenograft models

All experiments were performed with 8- to 12-wk-old female SCID mice (C.B.-17/IcrCrl-scid/scid), purchased from Charles River (Maastricht, The Netherlands). Mice were housed in a barrier unit of the Central Laboratory Animal Facility (Utrecht, The Netherlands) and kept in filter-top cages with water and food provided ad libitum. Mice participating in experiments were checked at least twice a week for clinical signs of disease and discomfort. All experiments were approved by the Utrecht University Animal Ethics Committee.

Subcutaneous tumors were induced by inoculation of 5×10^6 A431 cells in the right flank of mice, tumor volumes were calculated from digital caliper measurements as 0.52 x length x width^2 (in mm^3). Experimental leukemia was induced by injecting 2.5×10^6 Daudi-luc cells into the tail vein. At weekly intervals, tumor growth was assessed using bioluminescence imaging. Before imaging, mice were anesthetized via isoflurane. Synthetic D-luciferin (Biothema, Handen, Sweden) was given i.p. at a dose of 125 mg/kg. Light was detected in a photon-counting manner over an exposure period of 5 min from the dorsal side, 10 min after luciferin administration, using the Photon Imager (Biospace Lab, Paris, France). During illumination, black and white images were made for anatomical reference; M3 vision software (Biospace Lab) was used for image analysis. MAb were injected i.p. at indicated time points at different dosing levels. During the study, heparinized blood samples were taken for determination of IgG levels in plasma using a Behring Nephelometer II (Siemens Healthcare Diagnostics, Erlangen, Germany).

Statistical analysis

Data analysis was performed using GraphPad Prism, version 5.0 (Graphpad, San Diego, CA) and Predictive Analytics Software Statistics 18.0 (SPSS, Chicago, IL). Data were reported as mean ± SEM Differences between groups were analyzed using one-way ANOVA followed by Tukey posttest (GraphPad Prism 5). Selected data was also analyzed using log-rank test (Predictive Analytics Software).

Results

Binding patterns of hIgG isotypes to mFcγRs

We studied the binding of the isotype panels of the anti-EGFR mAb 2F8 and CD20 mAb 7D8 to mFcγRI, mFcγRIIb, mFcγRIII and mFcγRIV in a TR-FRET binding competition assay. In this assay, binding to mFcγRI and mFcγRIV is studied via competition with 2F8-mIgG2a-A647 and binding to mFcγRIIb and mFcγRIII via competition with 2F8-mIgG1-A647. Fig. 1A shows the inhibition curves for the whole mAb 2F8 isotype panel. hIgG1 and hIgG3 compete for binding to all four mFcγRs. This indicates that both hIgG1 and hIgG3 compare with mIgG2a which showed a similar reactivity. hIgG4 also bound to all mFcγRs although binding to mFcγRIV was very weak, because it only competed at very high concentration. hIgG2 binding was restricted to mFcγRIIb and mFcγRIII, which is comparable with the binding pattern of mIgG1. The N297Q mutation in hIgG1, resulting in an absence of glycosylation in the Fc domain, led to loss of binding to all mFcγRs as expected.

The relative affinity of the hIgG isotypes for the different mFcγRs was also represented in a heat map (Fig. 1B) in which the different IgGs are classified on a color scale according to the relative differences in IC_{50}. Fig. 1B shows that the isotype panel of the CD20 mAb 7D8 gave similar results, except for hIgG3 binding to mFcγRIII. We cannot exclude that this is partially due to the high level of aggregates in the 2F8-hIgG3 sample and it therefore requires further study.

mFcγR binding pattern correlates with the ability to activate murine effector cells

Having the binding patterns of hIgG isotypes to mFcγRs established, we explored the interaction of the human isotypes with relevant murine effector cells in functional tumor cell killing assays including ADCC and ADCP. First, we confirmed that the binding characteristics of the hIgG isotype variants in each of the anti-EGFR mAb and CD20 mAb panels for their respective targets were similar (i.e., to the EGFR-expressing human epidermoid carcinoma cell line A431 and CD20-expressing human Burkitt's lymphoma Daudi cells, respectively; Supplemental Fig. 1).

Next, we studied ADCC with mNK cells that were obtained by culturing of mouse splenocytes in presence of IL-2. This yielded $NKp46^{+}$ mNK cells that expressed mFcγRIII as their exclusive FcγR (data not shown). All IgG isotypes induced ADCC with mNK cells. The anti-EGFR mAb panel clearly demonstrated

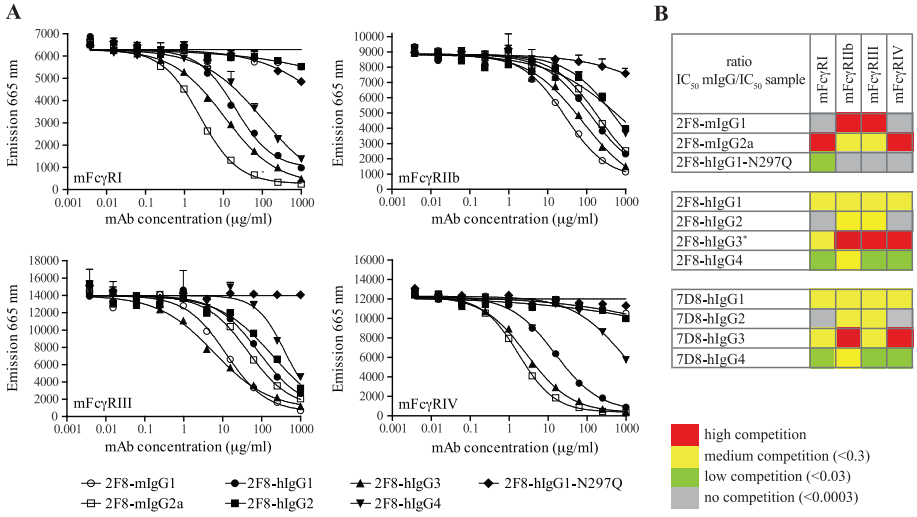

Figure 1. *Binding patterns of hIgG isotypes to mFcγR.* Binding of human and mIgG isotypes to recombinant mFcγR was analyzed in a TR-FRET inhibition assay. In this assay, serially diluted mAb compete with A647-labeled mIgG for binding to mFcγR, resulting in a decreased emission at 665nm. mFcγRI and mFcγRIV binding is assessed with 2F8-mIgG2a-A647, and mFcγRII and mFcγRIII with 2F8-mIgG1-A647. (A) Representative binding inhibition curves for each mFcγR of an IgG isotype panel of anti-EGFR mAb 2F8. (B) Heat map representing the relative mFcγR binding affinities for the IgG isotype panel. The IgGs are classified on a color scale according to the ratio of the observed IC_{50} and the IC_{50} of the competing mAb (i.e., 2F8-mIgG2a for mFcγRI and mFcγRIV and 2F8-mIgG1 for mFcγRIIb and mFcγRII). Asterisk signifies batch contained ~ 27% aggregates.

mIgG1 to be most potent in inducing mNK cell ADCC (Fig. 2A). This was less apparent for the CD20 mAb panel at the concentration used (Fig. 2B) but became clear at lower concentration (0.1 µg/ml; Supplemental Fig. 2). The overall specific lysis was lower for A431 cells (maximum lysis 22%; Fig. 2A) than for Daudi cells (maximum lysis 47%; Fig. 2B), but the trends were the same for both hIgG isotype panels. The observation that mNK ADCC is induced by all IgG isotypes correlates well with the mFcγR binding data, because all IgG isotypes demonstrated binding to mFcγRIII in the TR-FRET assay. An exception is the high affinity of hIgG3 for mFcγRs that did not result in increased mNK cell ADCC potency.

ADCC mediated by mPMN, which expressed mFcγRIIb, mFcγRIII and mFcγRIV, was studied by using whole blood of G-CSF-treated mice. No mPMN-induced ADCC of Daudi cells with the CD20 mAb isotype panel was observed (Fig. 2D), confirming the observation that PMN killing of target cells via ADCC is Ag-dependent as described previously by Elsässer et al. and Tiroch et al. (16, 17). In our previous studies we have confirmed this difference, where anti-EGFR mAb

2F8 could induce PMN ADCC whereas CD20 mAb 7D8 could not (13, 18). All anti-EGFR IgG isotypes were able to induce mPMN-mediated ADCC, with mIgG2a being the most potent, followed by mIgG1, hIgG1 and hIgG2 (Fig. 2C). hIgG3 and hIgG4 demonstrated only weak ADCC activity.

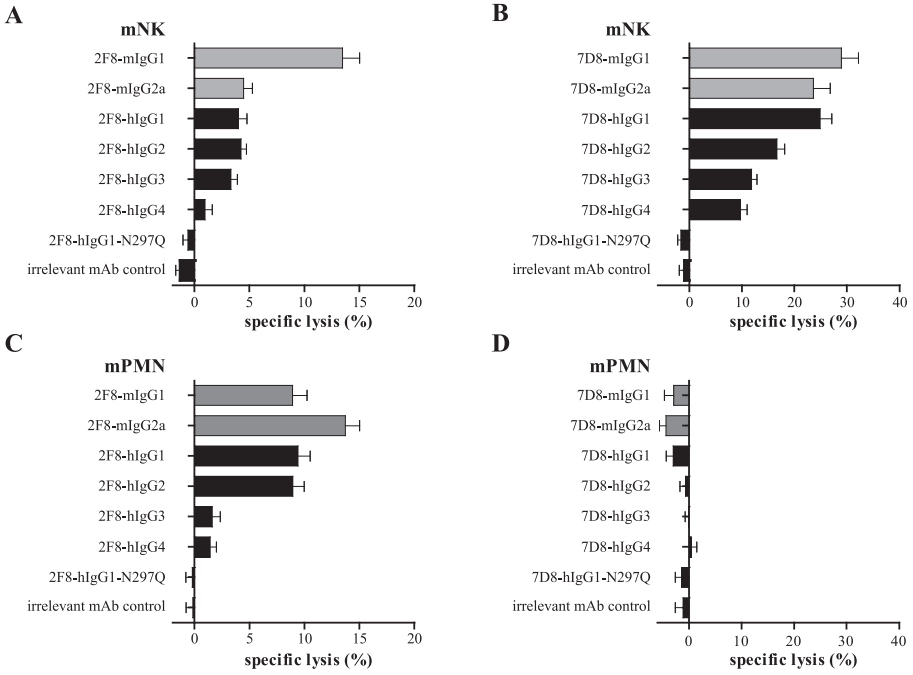

Figure 2. *hIgG1 and hIgG2 represent the most potent human isotypes to induce ADCC with mNK cells or mPMNs.* ADCC of A431 cells with a fixed 10 µg/ml concentration of the anti-EGFR mAb panel (A, C), and of Daudi cells for the CD20 mAb panel (B, D). (A, B) ADCC with mNK cells, E:T of 20:1. (C, D) ADCC with mPMN, E:T of 75:1. Data are shown as percentages specific lysis, which were calculated as described in *Materials and Methods*. Each bar shows mean ± SEM of three independent experiments.

Finally, mouse macrophages, which express all mFcγRs, were studied in ADCC (for the anti-EGFR mAb panel) and ADCP (for the CD20 mAb panel) assays. Bone marrow-derived macrophages were positive for F4/80 and CD80 and therefore represented mature and activated macrophages (data not shown). ADCC of A431 cells with the anti-EGFR mAb panel demonstrated that all IgG isotypes induced ADCC in which mIgG2a, hIgG1 and hIgG4 were the most and hIgG2 the least potent (Fig. 3A). Mouse macrophages were unable to induce ADCC of Daudi cells similar to the mPMNs, but did induce phagocytosis of Daudi cells induced by CD20 mAb 7D8. Activation of mouse macrophages by the CD20 isotype panel was therefore studied in an ADCP assay. All isotypes induced

phagocytosis of Daudi cells, in which hIgG1 demonstrated the highest and hIgG2 the lowest percentage phagocytosis (Fig. 3B).

Taken together, we demonstrated that opsonization of target cells with the different hIgG isotypes leads to activation of mNK cells, mPMNs and mouse macrophages. For activation of mNK cells and mPMNs the hIgG1 and hIgG2 were the most potent isotypes. hIgG1, hIgG3 and hIgG4 were the most potent in inducing ADCC and ADCP by mouse macrophages. In contrast hIgG2 was much weaker in activating mouse macrophages compared with its ability to engage mNK cells and mPMNs.

All human isotypes activate mouse macrophages, but act via different mFcγRs

Because mouse macrophages express all mFcγRs we checked which mFcγRs were crucial for induction of ADCC (for the anti-EGFR mAb panel) or ADCP (for the CD20 mAb panel). To study this, we made use of bone marrow-derived macrophages from mFcγR knockout mice. First, we studied the role of mFcγRIII by using macrophages from mFcγRIII$^{-/-}$ mice. Loss of mFcγRIII resulted in loss of ADCC/ADCP by mIgG1 and hIgG2 (Fig. 3C, 3D), which corresponded with the mFcγR binding data because mIgG1 and hIgG2 solely bound to the mFcγRIII within the group of activating mFcγRs (Fig. 1). Next we studied the role of mFcγRI by using macrophages from mFcγRI/III$^{-/-}$ mice (Fig. 3E). Additional loss of mFcγRI resulted in loss of ADCC via hIgG4, which was again consistent with the mFcγR binding data because hIgG4 bound mFcγRIV poorly (Fig. 1), which represented the only remaining activating mFcγR on the mFcγRI/III$^{-/-}$ mouse macrophages. Loss of mFcγRI and mFcγRIII did not result in loss of ADCC activity induced by hIgG1 and hIgG3, suggesting that both isotypes can act via mFcγRIV. This also corresponded with the mFcγR binding data, because hIgG1 as well as hIgG3 demonstrated intermediate to high binding to mFcγRIV (Fig. 1). From these data, we conclude that all human isotypes can activate murine macrophages to induce ADCC or ADCP, but they act via different mFcγRs.

hIgG1 is the most potent human isotype but is less potent than mIgG2a in mouse in vivo models

After we had established how the hIgG isotypes interacted with the murine effector cells *in vitro*, we studied the efficacy of the different isotypes *in vivo.* We used immune deficient SCID mice for these studies, because these mice are commonly used in preclinical studies, evaluating efficacy of non-cross-

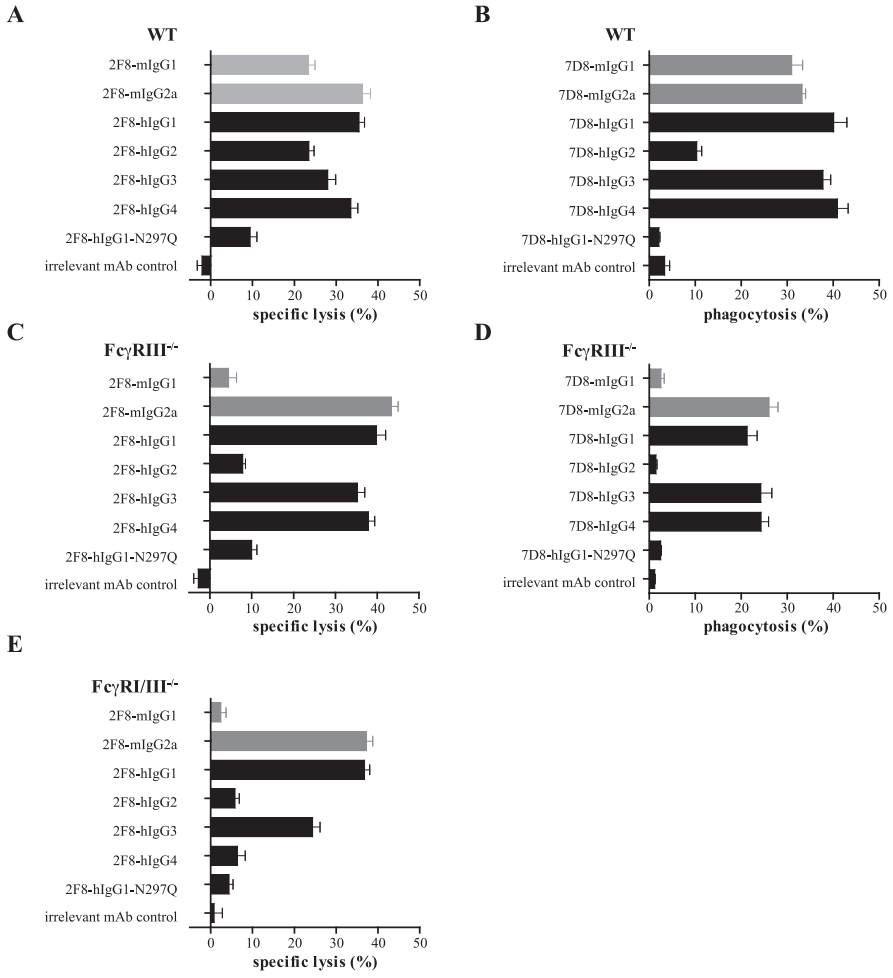

Figure 3. *All human isotypes activate mouse macrophages but act via different mFcγRs.* ADCC of A431 cells with a fixed 10 µg/ml concentration of the anti-EGFR mAb panel (A, C, E), E:T ratio of 20:1. ADCP of Daudi cells with a fixed 1 µg/ml concentration of the CD20 mAb panel (B, D), E:T ratio of 1:1. (A) ADCC and (B) ADCP with WT mouse macrophages. (C) ADCC and (D) ADCP with FcγRIII$^{-/-}$ mouse macrophages. (E) ADCC with FcγRI/III$^{-/-}$ mouse macrophages. Data shown for ADCC are percentages specific lysis which were calculated as described in Materials and Methods. Each bar shows mean ± SEM of three independent experiments. Data shown for ADCP are percentages F4/80^{+}/Calcein-AM^{+}/CD19^{-}-cells calculated as described in *Materials and Methods*. Each bar shows mean ± SEM of two independent experiments.

reactive human mAbs. Before performing the efficacy studies we determined the plasma clearance rates of the different hIgG isotypes in SCID mice, and no significant differences were found (Supplemental Fig. 4). Next, an additional anti-EGFR mAb isotype panel was tested in a s.c. A431 xenograft model. In this study, we made use of mAb 018, an anti-EGFR mAb that has ADCC induction as

its sole MoA (19). Mice were treated i.p. with 5 mg/kg mAb within 2 h after tumor challenge (Fig. 4A). The results of the treatment groups can be divided into four clusters, as observed in the Kaplan-Meier plot. The first cluster consists of the irrelevant mAb control group and the inert N297Q mutant of mAb 018, which demonstrated tumor outgrowth to ±800 mm^3 within 30 d. The hIgG1-N297Q mutant lacking Fc glycosylation therefore completely removed the antitumor effect of mAb 018, as shown previously (19). The second cluster demonstrated the weakest tumor inhibition: hIgG2 and hIgG3 ($p<0.05$, log-rank test at the time to progression, set at > 500 mm^3, compared with hIgG1-N297Q and irrelevant mAb control). The third cluster comprised hIgG4 and mIgG1, which showed intermediate antitumor effects ($p<0.01$ and $p<0.05$, log-rank test at time to progression, set at > 500 mm^3, compared with the previous cluster hIgG2 and hIgG3). The strongest antitumor effect was observed with mIgG2a and hIgG1 treatment ($p<0.001$ and $p<0.05$, log-rank test at time to progression, set at > 500 mm^3, compared with the previous cluster mIgG1 and hIgG4).

Second, we tested the CD20 mAb isotype panel in an i.v. Daudi-luc model. Mice were treated i.v. with 5 mg/kg mAb on day 5 and tumor development was assessed weekly by optical imaging (Fig. 4B). In this hematological model the same trend as in the previous experiment was observed, although no significant differences between the human isotypes were apparent. mIgG2a was significantly more potent than all the other isotypes ($p<0.05$, log-rank test at time to progression, set at a bioluminescence >50,000 cpm), and all isotypes differed significantly from 7D8-hIgG1-N297Q and irrelevant mAb control ($p<0.005$; log-rank test at time to progression, set at a bioluminescence >50,000 cpm).

To conclude, we have summarized our data on the interaction of the hIgG isotypes with murine effector cells to induce ADCC on tumor cells in a cartoon (Fig. 5, *left panel*). For better interpretation of the differences and/or similarities between mice and humans, literature data on the interaction of hIgG isotypes with human immune effector cells were depicted in a similar way (Fig. 5, *right panel*).

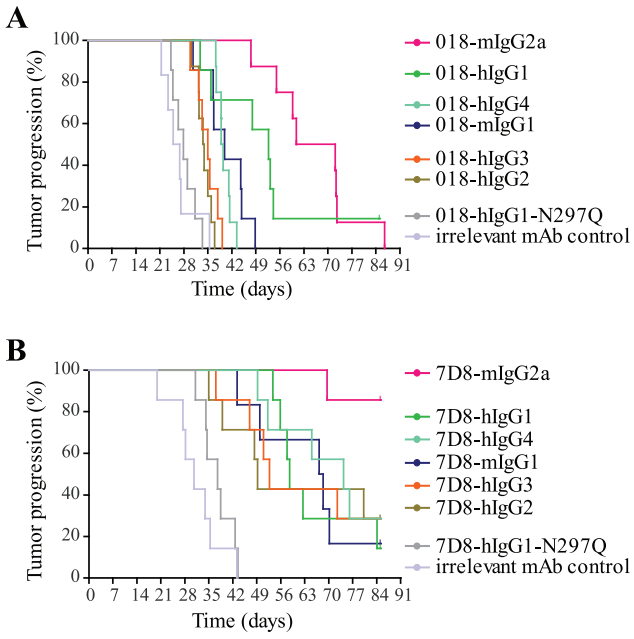

Figure 4. *hIgG1 is the most potent hIgG isotype in mouse in vivo models.* (A) s.c. inoculation of 5×10^6 A431 cells in groups of 8 mice, treatment with 100 µg/mouse (5mg/kg) anti-EGFR mAb at day 0. Kaplan-Meier plot (tumor progression, cutoff set at a tumor volume > 500 mm^3) is shown. (B) i.v. inoculation of 2.5×10^6 Daudi-luc cells in groups of 6 mice, treatment with 100 µg/mouse (5 mg/kg) CD20 mAb at day 5. Kaplan-Meier plot (tumor progression, cutoff set at a bioluminescence > 50.000 cpm) is depicted.

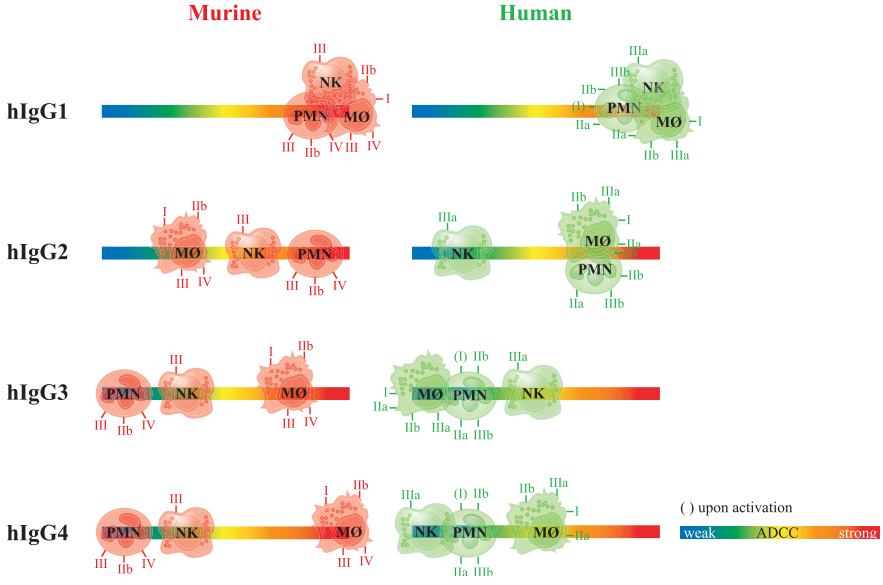

Figure 5. *Interaction of the hIgG isotypes with murine compared to human effector cells.* Cartoon depicting the relative potencies of the different hIgG isotypes to induce ADCC via murine (red) and human (green) effector cells. For the murine effector cells, the ranking is based on the findings from this study, and for the human effector cells, on literature findings on ADCC induction *in vitro* (9, 18, 28). The potencies of hIgG2, hIgG3 and hIgG4 are ranked against that of hIgG1 for each effector cell. Abbreviations: NK, NK cell; PMN, polymorphonuclear leukocyte; MØ, macrophage; roman ciphers represent the FcγRs.

Discussion

In this study, we evaluated the crosstalk between hIgG isotypes and murine effector cells to fill in gaps in our understanding. The hIgG1 isotype is the most commonly used isotype for Ab therapeutics and is, therefore, tested frequently in mouse models. We demonstrated that hIgG1 binds to all activating mFcγRs and is able to induce ADCC/ADCP with mNK cells and mouse macrophages. hIgG1 is also able to induce ADCC with mPMNs, although this is target-dependent because we observed this only for the anti-EGFR mAb. This pattern of hIgG1 corresponds with the profile of mIgG2a, which we confirmed to be the most potent IgG isotype in mice. ADCC/ADCP assays with mouse macrophages from different mFcγR$^{-/-}$ mice revealed hIgG1 to act via mFcγRIV. Notably, we do not exclude potential redundancy between the different activating mFcγRs, as demonstrated by Otten et al. (15) and Syed et al. (20) with a mIgG2a mAb. Furthermore, it should be considered that mFcγR expression levels might be influenced when one or more mFcγRs are knocked out, for example, mFcγRIV is upregulated in mFcγRIII$^{-/-}$ and mFcγRI/III$^{-/-}$ mice (20, 21).

The hIgG2 isotype is less frequently used for Ab therapeutics; currently, denosumab (against RANK-L) and panitumumab (against EGFR) are the only two approved and marketed hIgG2 mAbs. hIgG2 solely interacts with hFcγRIIa in which efficient binding is governed through a functional polymorphism of FcγRIIa amino acid 131 (4, 5). hIgG2 is often incorrectly described as being unable to activate human immune effector mechanisms (22, 23), Notably, however, a recent study by Schneider-Merck et al. (18) demonstrated that panitumumab can induce efficient myeloid cell-mediated, hFcγRIIa-dependent, ADCC. In our study we found hIgG2 to bind solely to mFcγRIIb and mFcγRIII, corresponding to the binding pattern of mIgG1. This mFcγR binding pattern led to ADCC induction with mNK cells and mPMNs. ADCC induction with mouse macrophages was very weak with hIgG2, corresponding to the data of Steplewski et al. (9). ADCP induction with hIgG2 on mouse macrophages was observed only at high mAb concentration, making hIgG2 an interesting tool to study the contribution of ADCP to the MoA of a mAb *in vivo*. ADCC/ADCP assays with mouse macrophages from mFcγRIII$^{-/-}$ mice revealed hIgG2 to act indeed solely via mFcγRIII. This might suggest that mFcγRIII on mouse macrophages is less contributing to ADCC/ADCP induction, because hIgG1, hIgG3 and hIgG4, which, next to mFcγRIII, also all bind to mFcγRI and/or mFcγRIV, induce stronger

ADCC with mouse macrophages compared with hIgG2. When extrapolating *in vivo* data from mouse models with hIgG2 to the human settings, it should be taken into account that, although mFcγRIII is described to be functionally similar to hFcγRIIa (24), hIgG2 activates both mNK cells and mPMNs but not macrophages, in mice, whereas in humans, only myeloid, but not NK, cells are activated to induce ADCC.

No therapeutic mAbs with the hIgG3 isotype have been approved for treatment to date, despite a higher affinity of hIgG3 for the activating hFcγRs (2). The major disadvantage described for hIgG3 is its weak hFcRn binding resulting in fast clearance, which was demonstrated to be dependent on the presence of hIgG1 (25). In our mouse models, no IgG was present and this might explain, next to mFcRn having a less stringent binding specificity (26), why we did not observe major differences in hIgG3 clearance compared with hIgG1 in mice. Several studies demonstrated that despite the higher affinity for the hFcγRs, compared with hIgG1, hIgG3 is much weaker in inducing ADCC than hIgG1 (6, 27, 28). We also demonstrated that hIgG3 has the highest relative affinity for each of the mFcγRs compared with the other hIgG isotypes. Strikingly, again this higher relative affinity did not result in stronger ADCC induction with the murine effector cells, which is, as mentioned earlier, also observed for human effector cells. Although mouse macrophages were equally potent in inducing ADCC via the hIgG3 and the hIgG1 isotype, mNK cells and mPMNs were less efficient in inducing ADCC via hIgG3 compared with hIgG1. Because we observed this phenomenon for two different targets, it is not likely to be target-dependent. Comparable findings have been obtained by Natsume et al. (27) for an hIgG3 variant of the CD20 mAb rituximab. They suggested that the less efficient ADCC induction by hIgG3 compared with hIgG1 might be caused by the longer hinge region of hIgG3. In their study they replaced the hinge region in hIgG3 with an hIgG1 hinge region, which indeed resulted in comparable ADCC induction by mononuclear cells as hIgG1. Mouse macrophages from FcγRI/III$^{-/-}$ mice revealed, comparable with hIgG1, that sole expression of mFcγRIV is sufficient for hIgG3 to induce ADCC. Again, redundancy between the activating mFcγRs cannot be excluded.

Finally hIgG4 was studied; this isotype has been applied in the clinic when activation of immune effector functions is undesired, because hIgG4 is described to be inert with human effector cells (6). An example is natalizumab (CD49d mAb), which is used in the treatment of Crohn's disease and multiple sclerosis.

In this study we showed that hIgG4 binds to mFcγRI, mFcγRIIb and mFcγRIII resulting in strong ADCC with mouse macrophages and weak ADCC induction with mNK cells and mPMNs. The ADCC induction by hIgG4 might be because of the fact that, in our models, there is no irrelevant IgG present to compete for binding to the high affinity mFcγRI. Similarly, activity of, usually inert, hIgG4 via hFcγRI was previously demonstrated in a very sensitive *in vitro* assay lacking the presence of irrelevant hIgG (5). However, efficacy of hIgG4 in mice was also demonstrated by Isaacs et al. (10) in WT mice, indicating that hIgG4 can compete with irrelevant mIgG for the binding to mFcγRI. hIgG4 has also been described to engage in Fab-arm exchange under physiological conditions in human serum (29). hIgG4 WT is able to Fab-arm exchange with mIgG3 (30), making it necessary to stabilize the hIgG4 hinge when using immunocompetent mice, which could likely be accomplished by introduction of a single point mutation (S228P) in the hIgG4 core hinge region (31-33). ADCC/ADCP assays with mFcγRI/III$^{-/-}$ mouse macrophages revealed that hIgG4 acts via mFcγRI to induce ADCC/ADCP. The weak ADCC induction with mNK cells indicates that hIgG4 can also act via mFcγRIII. We conclude that the hIgG4 is not an inert Ab isotype in mice. This combined with its instability in the presence of mIgG3 which potentially requires the use of hinge-stabilized ADCC-inert formats, like S228P/N297Q mutated nonglycosylated Abs, to test therapeutic hIgG4 mAbs in mouse models.

Finally, the therapeutic effect of all hIgG isotypes was studied *in vivo* in a solid tumor model and a hematological tumor model in SCID mice. In the solid tumor model with A431 cells we observed significant differences between some of the hIgG isotypes. We ranked the hIgG isotypes from strong tumor inhibition to weak tumor inhibition in the following order: hIgG1>hIgG4>hIgG2=hIgG3. The hematological model with the Daudi-luc cells revealed no clear differences between the hIgG isotypes. This might be because of the contribution of CDC, which has been excluded in the solid tumor model because we have shown that CDC is not a MoA for the anti-EGFR mAb in this model (19). In contrast, CDC has been shown to be part of the *in vivo* MoA for hIgG1 CD20 mAbs (34). To confirm whether this accounts for all hIgG isotypes, we compared the ability of the CD20 mAb isotypes to induce mouse C3 (mC3) deposition. At a subsaturating concentration of 2 μg/ml we did observe differences in the level of mC3 deposition between the different CD20 mAb isotypes, however at a saturating concentration of 10 μg/ml (which is reached in the *in vivo* studies), all mouse

and human isotypes induced comparable mC3 deposition (Supplemental Fig. 3). Therefore CDC as an additional MoA of the CD20 mAb isotypes may explain the smaller differences between the isotypes in the hematological model. We conclude that the *in vitro* data from hIgG1 was indicative for the *in vivo* results, because hIgG1 turned out to be the most potent human isotype. hIgG2, which is equally effective with mNK cells and mPMNs as hIgG1, but is ineffective with mouse macrophages, was able to inhibit tumor-growth, although it was less efficient compared with hIgG1 and hIgG4. This might indicate that in at least the solid tumor model mouse macrophages are the most important effector cells, because both hIgG1 and hIgG4 induce strong ADCC with these effector cells and hIgG2 is very weak in ADCC induction via mouse macrophages. Previous studies have also demonstrated, by using FcγRIII$^{-/-}$ mice or by depletion of mouse macrophages, that mouse macrophages are the strongest effector cells *in vivo* (35-37). In contrast, if mouse macrophages were the main effector cells in this model, we would expect hIgG3 to be at least as equally potent as hIgG4. This is however not the case and an explanation for the weak tumor inhibition by hIgG3 demands further investigation. Overall, although the *in vitro* data demonstrate clear differences between the different isotypes, the *in vivo* results show only small differences in efficacy. Nevertheless, a clear trend indicates hIgG1 to be the most potent human isotype in mouse models. The differences observed in the *in vitro* assays represent important guidance for translating the results with certain hIgG isotypes from mice to humans.

Considering that hIgG1 was found to be the most potent human isotype in mice, interacting similarly with murine and human effector cells, we conclude that mouse models are appropriate for evaluating Fc-mediated effects of hIgG1 mAb. However, it should be taken into account that hIgG1 was not as efficient as the mIgG2a isotype, suggesting that activation of cellular immune effector functions by hIgG1 might be underestimated in mouse models compared to humans. Because hIgG2 mAb activated a different set of effector cells in mice compared with humans, extrapolation of hIgG2 *in vivo* data to the human system requires great care. However, this means that hIgG2 can be used as a tool to study the role of ADCP as MoA of a hIgG1 mAb, by comparing its *in vivo* efficacy with that of a matched hIgG2. hIgG3 was found to be unable to induce strong ADCC activation with murine effector cells, despite the high relative affinity for mFcγRs, explaining poor *in vivo* efficacy. However, because this phenomenon is in accordance with observations using human effector cells, we consider

mouse models suitable for studying the efficacy of an hIgG3 mAb. Finally, hIgG4 potently activated mouse macrophages, whereas this activation is absent with human macrophages. Thus, mouse studies may lead to an overestimation of the efficacy of an hIgG4 mAb. We demonstrated that the N297Q mutation resulted in loss of binding to mFcγRs, making hIgG4-N297Q a suitable surrogate format for mouse models to evaluate the efficacy of an hIgG4 mAb. Taken together, our study provides a comprehensive and strong knowledge base for testing human mAb cell-mediated effector functions in mouse models and their extrapolation to the human system.

References

1. Stern, M., and R. Herrmann. 2005. Overview of monoclonal antibodies in cancer therapy: present and promise. *Crit Rev Oncol Hematol* 54:11-29.
2. Bruhns, P., B. Iannascoli, P. England, D. A. Mancardi, N. Fernandez, S. Jorieux, and M. Daeron. 2009. Specificity and affinity of human Fcgamma receptors and their polymorphic variants for human IgG subclasses. *Blood* 113:3716-3725.
3. van de Winkel, J. G., and C. L. Anderson. 1991. Biology of human immunoglobulin G Fc receptors. *J Leukoc Biol* 49:511-524.
4. Parren, P. W., P. A. Warmerdam, L. C. Boeije, J. Arts, N. A. Westerdaal, A. Vlug, P. J. Capel, L. A. Aarden, and J. G. van de Winkel. 1992. On the interaction of IgG subclasses with the low affinity Fc gamma RIIa (CD32) on human monocytes, neutrophils, and platelets. Analysis of a functional polymorphism to human IgG2. *J Clin Invest* 90:1537-1546.
5. Parren, P. W., P. A. Warmerdam, L. C. Boeije, P. J. Capel, J. G. van de Winkel, and L. A. Aarden. 1992. Characterization of IgG FcR-mediated proliferation of human T cells induced by mouse and human anti-CD3 monoclonal antibodies. Identification of a functional polymorphism to human IgG2 anti-CD3. *J Immunol* 148:695-701.
6. Bruggemann, M., G. T. Williams, C. I. Bindon, M. R. Clark, M. R. Walker, R. Jefferis, H. Waldmann, and M. S. Neuberger. 1987. Comparison of the effector functions of human immunoglobulins using a matched set of chimeric antibodies. *J Exp Med* 166:1351-1361.
7. Dijstelbloem, H. M., J. G. van de Winkel, and C. G. Kallenberg. 2001. Inflammation in autoimmunity: receptors for IgG revisited. *Trends Immunol* 22:510-516.
8. Nimmerjahn, F., P. Bruhns, K. Horiuchi, and J. V. Ravetch. 2005. FcgammaRIV: a novel FcR with distinct IgG subclass specificity. *Immunity* 23:41-51.
9. Steplewski, Z., L. K. Sun, C. W. Shearman, J. Ghrayeb, P. Daddona, and H. Koprowski. 1988. Biological activity of human-mouse IgG1, IgG2, IgG3, and IgG4 chimeric monoclonal antibodies with antitumor specificity. *Proc Natl Acad Sci U S A* 85:4852-4856.
10. Isaacs, J. D., M. R. Clark, J. Greenwood, and H. Waldmann. 1992. Therapy with monoclonal antibodies. An in vivo model for the assessment of therapeutic potential. *J Immunol* 148:3062-3071.
11. Loisel, S., M. Ohresser, M. Pallardy, D. Dayde, C. Berthou, G. Cartron, and H. Watier. 2007. Relevance, advantages and limitations of animal models used in the development of monoclonal antibodies for cancer treatment. *Crit Rev Oncol Hematol* 62:34-42.
12. Bleeker, W. K., J. J. Lammerts van Bueren, H. H. van Ojik, A. F. Gerritsen, M. Pluyter, M. Houtkamp, E. Halk, J. Goldstein, J. Schuurman, M. A. van Dijk, J. G. van de Winkel, and P. W. Parren. 2004. Dual mode of action of a human anti-epidermal growth factor receptor monoclonal antibody for cancer therapy. *J Immunol* 173:4699-4707.
13. Teeling, J. L., R. R. French, M. S. Cragg, J. van den Brakel, M. Pluyter, H. Huang, C. Chan, P. W. Parren, C. E. Hack, M. Dechant, T. Valerius, J. G. van de Winkel, and M. J. Glennie. 2004. Characterization of new human CD20 monoclonal antibodies with potent cytolytic activity against non-Hodgkin lymphomas. *Blood* 104:1793-1800.
14. Tao, M. H., and S. L. Morrison. 1989. Studies of aglycosylated chimeric mouse-human IgG. Role of carbohydrate in the structure and effector functions mediated by the human IgG constant region. *J Immunol* 143:2595-2601.
15. Otten, M. A., G. J. van der Bij, S. J. Verbeek, F. Nimmerjahn, J. V. Ravetch, R. H. Beelen, J. G. van de Winkel, and M. van Egmond. 2008. Experimental antibody therapy of liver metastases reveals functional redundancy between Fc gammaRI and Fc gammaRIV. *J Immunol* 181:6829-6836.
16. Elsasser, D., T. Valerius, R. Repp, G. J. Weiner, Y. Deo, J. R. Kalden, J. G. van de Winkel, G. T. Stevenson, M. J. Glennie, and M. Gramatzki. 1996. HLA class II as potential target antigen on malignant B cells for therapy with bispecific antibodies in combination with granulocyte colony-stimulating factor. *Blood* 87:3803-3812.
17. Tiroch, K., B. Stockmeyer, C. Frank, and T. Valerius. 2002. Intracellular domains of target antigens influence their capacity to trigger antibody-dependent cell-mediated cytotoxicity. *J Immunol* 168:3275-3282.

18. Schneider-Merck, T., J. J. Lammerts van Bueren, S. Berger, K. Rossen, P. H. van Berkel, S. Derer, T. Beyer, S. Lohse, W. K. Bleeker, M. Peipp, P. W. Parren, J. G. van de Winkel, T. Valerius, and M. Dechant. 2010. Human IgG2 antibodies against epidermal growth factor receptor effectively trigger antibody-dependent cellular cytotoxicity but, in contrast to IgG1, only by cells of myeloid lineage. *J Immunol* 184:512-520.
19. Overdijk, M. B., S. Verploegen, J. H. van den Brakel, J. J. Lammerts van Bueren, T. Vink, J. G. van de Winkel, P. W. Parren, and W. K. Bleeker. 2011. Epidermal Growth Factor Receptor (EGFR) Antibody-Induced Antibody-Dependent Cellular Cytotoxicity Plays a Prominent Role in Inhibiting Tumorigenesis, Even of Tumor Cells Insensitive to EGFR Signaling Inhibition. *J Immunol* 187:3383-3390.
20. Syed, S. N., S. Konrad, K. Wiege, B. Nieswandt, F. Nimmerjahn, R. E. Schmidt, and J. E. Gessner. 2009. Both FcgammaRIV and FcgammaRIII are essential receptors mediating type II and type III autoimmune responses via FcRgamma-LAT-dependent generation of C5a. *Eur J Immunol* 39:3343-3356.
21. Nimmerjahn, F., A. Lux, H. Albert, M. Woigk, C. Lehmann, D. Dudziak, P. Smith, and J. V. Ravetch. 2010. FcgammaRIV deletion reveals its central role for IgG2a and IgG2b activity in vivo. *Proc Natl Acad Sci U S A* 107:19396-19401.
22. Carter, P. J. 2006. Potent antibody therapeutics by design. *Nat Rev Immunol* 6:343-357.
23. Jefferis, R. 2007. Antibody therapeutics: isotype and glycoform selection. *Expert Opin Biol Ther* 7:1401-1413.
24. Nimmerjahn, F., and J. V. Ravetch. 2008. Fcgamma receptors as regulators of immune responses. *Nat Rev Immunol* 8:34-47.
25. Stapleton, N. M., J. T. Andersen, A. M. Stemerding, S. P. Bjarnarson, R. C. Verheul, J. Gerritsen, Y. Zhao, M. Kleijer, I. Sandlie, M. de Haas, I. Jonsdottir, C. E. van der Schoot, and G. Vidarsson. 2011. Competition for FcRn-mediated transport gives rise to short half-life of human IgG3 and offers therapeutic potential. *Nat Commun* 2:599.
26. Ober, R. J., C. G. Radu, V. Ghetie, and E. S. Ward. 2001. Differences in promiscuity for antibody-FcRn interactions across species: implications for therapeutic antibodies. *Int Immunol* 13:1551-1559.
27. Natsume, A., M. In, H. Takamura, T. Nakagawa, Y. Shimizu, K. Kitajima, M. Wakitani, S. Ohta, M. Satoh, K. Shitara, and R. Niwa. 2008. Engineered antibodies of IgG1/IgG3 mixed isotype with enhanced cytotoxic activities. *Cancer Res* 68:3863-3872.
28. Niwa, R., A. Natsume, A. Uehara, M. Wakitani, S. Iida, K. Uchida, M. Satoh, and K. Shitara. 2005. IgG subclass-independent improvement of antibody-dependent cellular cytotoxicity by fucose removal from Asn297-linked oligosaccharides. *J Immunol Methods* 306:151-160.
29. van der Neut Kolfschoten, M., J. Schuurman, M. Losen, W. K. Bleeker, P. Martinez-Martinez, E. Vermeulen, T. H. den Bleker, L. Wiegman, T. Vink, L. A. Aarden, M. H. De Baets, J. G. van de Winkel, R. C. Aalberse, and P. W. Parren. 2007. Anti-inflammatory activity of human IgG4 antibodies by dynamic Fab arm exchange. *Science* 317:1554-1557.
30. Lewis, K. B., B. Meengs, K. Bondensgaard, L. Chin, S. D. Hughes, B. Kjaer, S. Lund, and L. Wang. 2009. Comparison of the ability of wild type and stabilized human IgG(4) to undergo Fab arm exchange with endogenous IgG(4)in vitro and in vivo. *Mol Immunol* 46:3488-3494.
31. Angal, S., D. J. King, M. W. Bodmer, A. Turner, A. D. Lawson, G. Roberts, B. Pedley, and J. R. Adair. 1993. A single amino acid substitution abolishes the heterogeneity of chimeric mouse/human (IgG4) antibody. *Mol Immunol* 30:105-108.
32. Bloom, J. W., M. S. Madanat, D. Marriott, T. Wong, and S. Y. Chan. 1997. Intrachain disulfide bond in the core hinge region of human IgG4. *Protein Sci* 6:407-415.
33. Schuurman, J., G. J. Perdok, A. D. Gorter, and R. C. Aalberse. 2001. The inter-heavy chain disulfide bonds of IgG4 are in equilibrium with intra-chain disulfide bonds. *Mol Immunol* 38:1-8.
34. Boross, P., J. H. Jansen, S. de Haij, F. J. Beurskens, C. E. van der Poel, L. Bevaart, M. Nederend, J. Golay, J. G. van de Winkel, P. W. Parren, and J. H. Leusen. 2011. The in vivo mechanism of action of CD20 monoclonal antibodies depends on local tumor burden. *Haematologica* 96:1822-1830.
35. Bevaart, L., M. J. Jansen, M. J. van Vugt, J. S. Verbeek, J. G. van de Winkel, and J. H. Leusen. 2006. The high-affinity IgG receptor, FcgammaRI, plays a central role in antibody therapy of experimental melanoma. *Cancer Res* 66:1261-1264.

36. Nimmerjahn, F., and J. V. Ravetch. 2005. Divergent immunoglobulin g subclass activity through selective Fc receptor binding. *Science* 310:1510-1512.

37. Oflazoglu, E., I. J. Stone, L. Brown, K. A. Gordon, N. van Rooijen, M. Jonas, C. L. Law, I. S. Grewal, and H. P. Gerber. 2009. Macrophages and Fc-receptor interactions contribute to the antitumour activities of the anti-CD40 antibody SGN-40. *Br J Cancer* 100:113-117.

Supplemental Figures

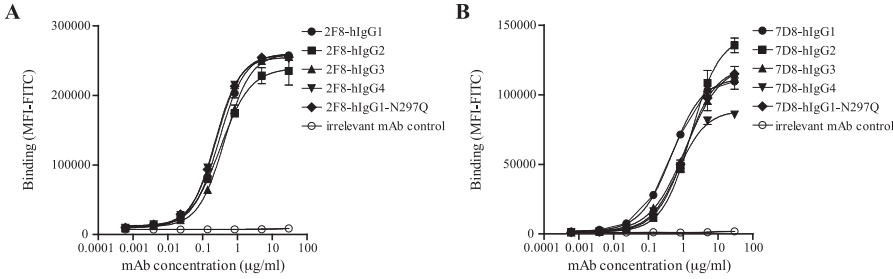

Supplemental Figure 1. *Similar binding curves of the different hIgG isotypes.* 1×10^5 cells were incubated with a serial dilution of the indicated mAb for 30 min at 4 degrees. Binding was detected with FITC labeled Rb anti-human gamma chain (DAKO, Glostrup, Denmark) and samples were measured on FACS CantoII. (A) Binding of anti-EGFR mAb 2F8 isotype panel to EGFR expressed on A431 cells. (B) Binding of CD20 mAb 7D8 isotype panel to CD20 expressed on Daudi cells. Data were analyzed using a four-parameter logistic curve fit. The mean fluorescence intensity (MFI) ± SEM is shown.

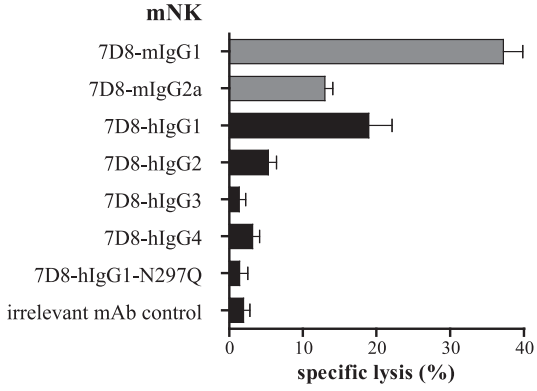

Supplemental Figure 2. *mIgG1 is most potent in inducing ADCC with mNK-cells.* ADCC of Daudi cells with a fixed Ab concentration of 0.1 µg/ml of the CD20 mAb panel. Data are shown as percentages specific lysis, which were calculated as described in *Materials and Methods*. Each bar shows mean ± SEM of three independent experiments.

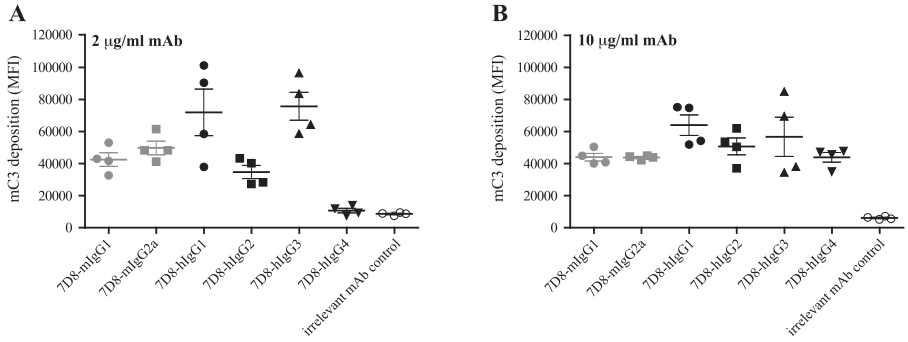

Supplemental Figure 3. *hIgG1 and hIgG3 represent the most potent hIgG isotypes for mouse C3 (mC3) deposition.* 1×10^4 Daudi cells were incubated for 15 min at RT with a serial dilution of the indicated CD20 mAb in RPMI 1640/0.1% BSA (Roche, Meylan, France) followed by addition of SCID mouse serum (1% final concentration). After 15 min incubation at 37 degrees mC3 binding was detected at 4 degrees with rat anti-mouse C3 (Hycult Biotech, Plymouth Meeting, PA) and PE labeled goat anti-rat Ig (BD Biosciences) and samples were measured on FACS Cantoll. (A) mC3 deposition at 2 μg/ml mAb concentration. (B) mC3 depostion at 10 μg/ml mAb concentration. Each bar shows mean ± SEM of two independent experiments.

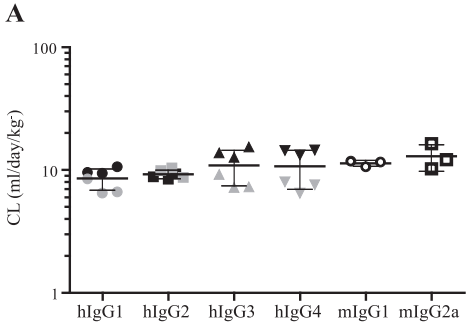

B

	CL (ml/day/kg)	$T_{1/2}$ (days)
hIgG1	8.5 (± 1.7)	17.2 (± 7.5)
hIgG2	9.2 (± 0.8)	19.1 (± 7.4)
hIgG3	10.9 (± 3.5)	10.2 (± 2.7)
hIgG4	10.7 (± 3.7)	13.9 (± 3.4)
mIgG1	11.3 (± 0.6)	8.4 (± 0.5)
mIgG2a	12.9 (± 3.2)	7.5 (± 2.8)

Supplemental Figure 4. *Comparable plasma clearance rates for the different hIgG isotypes.* Tumor-free SCID mice were dosed with 5 mg/kg anti-EGFR and 5 mg/kg CD20 mAb, 3 mice/group. Bloodsamples were taken at 10 min, 4 h, 1, 2, 7, 15 and 21 d after mAb dosing. Serum concentrations were determined in an ELISA. Recombinant EGFR or anti-idiotype specific mAb were used to coat 96-well Microlon ELISA plates (Greiner, Frickenhausen, Germany) for the anti-EGFR or the CD20 mAb panel, respectively. After blocking plates with ELISA buffer (PBS supplemented with 0.05% Tween-20 (Sigma-Aldrich) and 2% BSA), samples, serially diluted in ELISA buffer, were added and incubated for 1 h at RT. Plates were subsequently incubated with peroxidase labeled goat anti-human IgG Fc-specific Ig (Jackson, West Grace, PA) and developed with 2,2'-azino-bis (3-ethylbenzthiazoline-6-sulfonic acid) (ABTS; Roche Diagnostics, Mannheim, Germany). The reaction was stopped by adding oxalic acid (Sigma-Aldrich). Absorbance was measured in a microplate reader (Biotek, Winooski, VT, USA) at 405 nm. Area under curve (AUC) was calculated using the trapezoid rule for 0-21 days and the data from the anti-EGFR and CD20 panel were pooled. Tukey's Multiple Comparison Test revealed no significant differences in plasma clearance rates. (A) plasma clearance rate for the different isotypes. Black symbols represent data from the anti-EGFR mAb panel, grey symbols represent results from the CD20 mAb panel. (B) overview of plasma clearance rates (CL) and elimination half-lifes ($T_{1/2}$) ± SD.

4

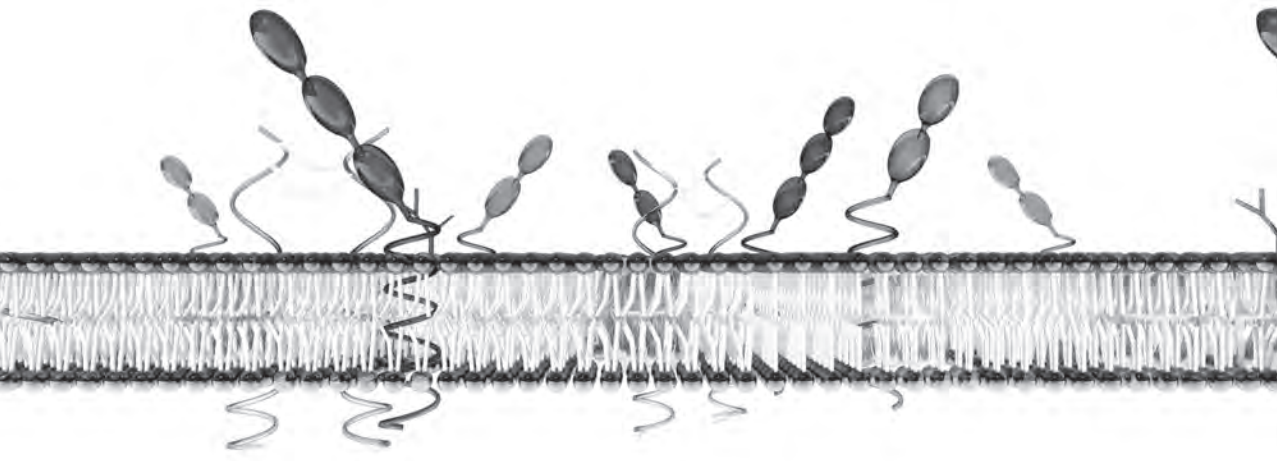

Phagocytosis is a potent mechanism of action for the therapeutic human monoclonal antibody daratumumab in lymphoma and multiple myeloma

Marije B. Overdijk[*], Sandra Verploegen[*], Marijn Bögels[†,‡], Marjolein van Egmond[†,‡], Jeroen J. Lammerts van Bueren[*], Tuna Mutis[§], Richard W.J. Groen[¶,‖], Anton C.M. Martens[¶,‖], Wim K. Bleeker[*] and Paul W.H.I. Parren[*]

[*]Genmab, Utrecht, The Netherlands; [†]Department of Molecular Cell Biology and Immunology, [‡]Department of Surgery, VU University Medical Center, Amsterdam, The Netherlands; [§]Department of Clinical Chemistry and Hematology, University Medical Center, Utrecht, The Netherlands; [¶]Department of Cell Biology and [‖]Department of Immunology, University Medical Center, Utrecht, The Netherlands.

Submitted

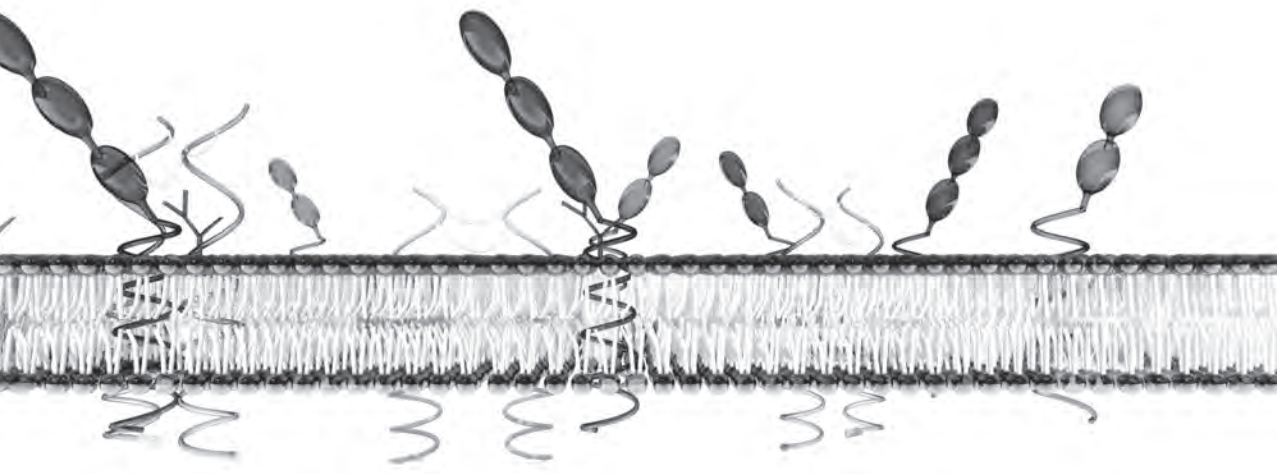

Abstract

Daratumumab (DARA) is a human CD38 antibody which has potential for therapy of hematological malignancies and is in clinical development for the treatment of multiple myeloma (MM). Here we demonstrate the importance of antibody-dependent cellular phagocytosis (ADCP) in DARA's mechanism of action. DARA was found to induce phagocytosis by mouse and human macrophages (mφ) of several MM and Burkitt's lymphoma (BL) cell lines *in vitro*. Live cell imaging revealed that ADCP occurred with high efficiency in which individual mφ were observed to rapidly engulf multiple tumor cells sequentially. Analyses with a phagocytosis-deficient DARA variant in subcutaneous solid tumor and intravenous leukemic xenograft mouse models revealed that ADCP also contributes to its *in vivo* mechanism of action. Finally, DARA was shown to induce ADCP of patient MM cells by human mφ which was of a similar magnitude as for MM and BL cell lines. In conclusion, we demonstrate that phagocytosis is a very fast and potent mechanism of action that contributes to DARA's activity against CD38-expressing hematological tumors such as lymphoma and multiple myeloma.

Introduction

Phagocytosis is an efficient and fast mechanism for the elimination of pathogens by the innate immune system. Phagocytosis can be induced via several pathways including those involving pathogen-associated molecular patterns (PAMPs), surface-bound complement factors and antibodies (Ab). Antibody-dependent cellular phagocytosis (ADCP) of IgG1-opsonized pathogens as well as cancer cells occurs via binding to Fcγ-receptors (FcγRs), specifically via the low-affinity FcγRs IIa and IIIa (1, 2). Macrophages (mφ) representing professional phagocytes are abundant in tumor stroma (3, 4) and ADCP by mφ might therefore be a very potent mechanism of action (MoA) of therapeutic Abs in cancer treatment.

By using different mouse strains or by depleting specific effector cell subsets, Uchida et al. showed that mφ were the main effector cells in the anti-tumor activity of CD20-targeting monoclonal Abs (mAbs) in the *in vivo* model studied (5). For SGN-30 (chimeric IgG1 CD30 mAb), SGN-40 (humanized IgG1 CD40 mAb) and a humanized CD70 mAb, which all induced ADCP *in vitro*, mφ were also shown to be the major effector cells *in vivo* (6-8). However, since mφ may also induce antibody-dependent cellular cytotoxicity (ADCC) (9), these studies did not discriminate between mφ-mediated ADCC or ADCP as the main MoA *in vivo*.

Daratumumab (DARA) is a human IgG1 mAb targeting CD38, a 46-kDa type II transmembrane glycoprotein which is expressed at relatively high levels on malignant cells in multiple myeloma (MM) (10). Currently, DARA is in clinical development for treatment of MM and was granted a Breakthrough Therapy Designation by the FDA for double-refractory MM patients on May 1, 2013. DARA is a mAb with multiple MoA, including the Fc-dependent effector mechanisms complement-dependent cytotoxicity (CDC) and NK-cell mediated ADCC (11). However, reminiscent of results with CD20-targeting mAbs (12, 13), we did not observe signs of cell lysis of leukemic target cells as evidence for ADCC when using mφ as effector cells (unpublished data).

Here, we explored DARA-induced ADCP of Burkitt's lymphoma (BL) and MM cell lines by mouse and human mφ *in vitro* and of patient-derived MM tumor cells by human mφ *ex vivo*. To distinguish ADCC from ADCP *in vivo*, we generated a DARA variant, which does not induce ADCP with mouse mφ. Our results showed that ADCP strongly contributes to the MoA of DARA *in vitro* and *in vivo.*

Materials and Methods

Cells

Raji, Ramos and Daudi-cells (human BL) were obtained from the ATCC (Rockville, MD). Wien-133 cells were kindly provided by Dr. Geoff Hale (BioAnaLab Limited, Oxford, UK). Daudi cells were transfected with gWIZ luciferase as previously described (12) (Daudi-luc). The MM cell lines UM-9, generated at the University Medical Center (Utrecht, the Netherlands) (14), and L363, obtained from the ATCC and gene-marked with GFP and luciferase marker genes (15), were transduced with human CD38 gene to obtain CD38 expression levels comparable to primary myeloma cells. For this the amphotropic Phoenix packaging cell line (Phoenix Ampho) was transfected, using calcium phosphate precipitation, with the pQCXIN vector in which the gene encoding human CD38 was inserted. These cell lines are referred to as UM9-CD38 and L363-CD38. Cells were cultured in IMDM medium (Lonza, Verviers, Belgium) (Wien-133) or RPMI 1640 medium (Lonza) (all other cell lines), supplemented with 10% heat-inactivated cosmic calf serum (CCS) (Hyclone, Logan, UT), 50 IU/ml penicillin (Lonza) and 50 μg/ml streptomycin (Lonza). The culture medium for Daudi, Daudi-luc and Ramos cells was supplemented with 2mM L-glutamine (Lonza) and 1mM sodium pyruvate (Lonza). Mononuclear cells (MNC) or peripheral blood mononuclear cells (PBMC) from MM patients isolated from the bone marrow, pleural fluid or blood respectively were obtained after informed consent and approval by the Medical Ethical Committee (University Medical Center, Utrecht, The Netherlands).

Antibodies

Human IgG1 CD38 mAb DARA was generated by immunization in a HuMAb mouse and produced as recombinant protein as described previously (11). DARA $F(ab')_2$ fragments were prepared via pepsin digestion (Sigma-Aldrich, St. Louis, MO). An IgG2 variant of DARA (DARA-IgG2) was constructed by cloning the variable region of the immunoglobulin heavy chain (V_H) of DARA into a human IgG2 backbone. The human heavy chain construct was co-expressed with the appropriate original human kappa light chain. Fc mutants were generated by mutating the lysine at position 322 to alanine; these mutants are referred to as DARA-K322A and DARA-IgG2-K322A. The mutations were introduced as described previously (12, 16). The human mAb IgG1 b12, specific for the HIV-1 gp120 envelope glycoprotein, generated as described previously (17), was

included in all experiments as an isotype control mAb. IgG concentrations were determined by A280 measurements.

Bone marrow-derived mouse macrophage culture

Bone marrow was isolated by flushing the femurs of female SCID mice (C.B-17/Icr-Prkdc^{scid}/Crl), purchased from Charles River (Maastricht, The Netherlands), filtered and subsequently cultured for 7 days in DMEM (Lonza) with 10% heat-inactivated CCS, 2 mM L-glutamine, 50 IU/ml penicillin, 50 μg/ml streptomycin (complete mφ medium) supplemented with 50 U/ml M-CSF (ProSpec, Rehovot, Israel) as described previously (12). Mφ were detached with 0.5 mM EDTA (versene, Invitrogen, Carlsbad, CA) and characterized by flow cytometry on a FACSCantoII (BD Biosciences, Franklin Lakes, NJ) for staining with F4/80-PE (Molecular Probes Inc, Paisley, UK), CD80-PE (eBioscience, San Diego, CA), CD64-PE and CD32/16-FITC (BD Biosciences).

Monocyte-derived human macrophage culture

PBMC were isolated from buffy coats obtained from regular blood bank donations (after informed consent, Sanquin Blood Bank, Utrecht, The Netherlands) using density separation with Lymphocyte Separation Medium (Lonza), followed by washing with PBS (B. Braun, Melsungen, Germany). Monocytes were isolated via negative selection from the PBMC fraction using the Dynabeads Untouched Human Monocytes isolation kit (Invitrogen). Isolated monocytes were cultured for 7 days in complete mφ medium supplemented with 10 ng/ml GM-CSF (Invitrogen). Mφ were detached with 0.1% trypsin-EDTA (Invitrogen) in PBS and characterized by flow cytometry (FACSCantoII) for staining with CD11b-PE, CD32-FITC, CD16-FITC (BD Biosciences) and CD64-FITC (Biolegend, San Diego, CA).

Flow cytometry

Numbers of cell surface CD38 molecules were determined with mouse-anti-human CD38 (BD Biosciences) and the Qifi kit (DAKO, Glostrup, Denmark). Samples were analyzed with flow cytometry (FACSCantoII).

ADCP

Mφ were seeded at 2.5×10^5 cells per well into 24-well plates and allowed to adhere O/N (mouse) or 48h (human). Target cells were labeled with calcein-AM (Invitrogen) and added to the mφ at an effector:target (E:T) ratio of 1:1 (mouse

mφ) or 2:1 (human mφ) in the presence of a fixed mAb concentration of 1 µg/ml. After 4 h incubation at 37°C/5%CO_2 the non-phagocytosed target cells were collected. Mφ were detached with 0.1% trypsin-EDTA and subsequently added to the collected non-phagocytosed target cells. The pooled cells were kept at 4°C and stained with either F4/80-PE (mouse mφ) or CD11b-PE (human mφ) and counterstained with either CD19-APC (DAKO) or CD138-APC (Beckman Coulter, Brea, CA) for the detection of non-phagocytosed BL or MM target cells respectively (in solution or attached to mφ). ADCP was evaluated with flow cytometry (FACSCantoII) and defined as percentage of mφ which had phagocytosed, referred to as percentage double positive (DP) mφ. The percentage DP mφ is defined by the following cell population: $F4/80^+$,$calcein^+$,$CD19^-$/$CD138^-$ (in case of mouse mφ) or $CD11b^+$,$calcein^+$,$CD19^-$/$CD138^-$ (in case of human mφ), in which the total mφ population ($F4/80^+$, or $CD11b^+$) was set as 100%.

In addition, the number of remaining target cells ($CD19^+$/$CD138^+$,$F4/80^-$ or $CD19^+$/$CD138^+$,$CD11^-$) was determined and the percentage of killed target cells in the presence of Ab compared to absence of Ab was calculated using the following formula: % killed target cells = 100 - ((100% × remaining target cells + Ab) / remaining target cells without Ab)

Live cell imaging

For live cell imaging, target cells and mouse mφ were incubated (1-10×10^6 cells/ml) in HBSS (Gibco, Carlsbad, CA) or complete mφ medium supplemented with 25 µg/ml DiB (Biotium, Hayward, CA) or 3,3'-dioctadecyloxacarbocyanine perchlorate (DiO, Molecular Probes Inc.) respectively for 30 minutes at 37˚C, and subsequently washed three times with complete mφ medium. Mφ were seeded at 2×10^5 cells/well into 8 wells ibiTreat µ-Slides (IBIDI, Munich, Germany) and allowed to adhere O/N. Real-time ADCP assays were performed with indicated E:T ratio's at a fixed mAb concentration and imaged with an Olympus CellR real-time live-imaging station (type IX81, UPLFLN 40 x O/1.3 lens, Münster, Germany). Pictures were taken every 20 seconds with an Olympus ColorView II camera for 30 minutes.

Mouse tumor xenograft models

Experiments were performed with 8-12 weeks old female SCID-BEIGE mice (C.B-17/IcrHsd-Prkdc ^{scid}Lys^{bg}), purchased from Harlan (Boxmeer, The Netherlands).

Mice were housed in a barrier unit of the Central Laboratory Animal Facility (Utrecht, The Netherlands) and kept in individually ventilated cages with water and food provided ad libitum. Mice included in experiments were checked at least twice a week for clinical signs of disease and discomfort. All experiments were approved by the Utrecht University animal ethics committee. Subcutaneous tumors were induced by inoculation of 20×10^6 Daudi-luc cells in BD Matrigel Basement Membrane Matrix High Concentration (BD Biosciences) in the right flank of mice and tumor volumes were calculated from digital caliper measurements as $0.52 \times \text{length} \times \text{width}^2$ (in mm^3). Experimental leukemia was induced by injecting 2.5×10^6 Daudi-luc cells into the tail vein. At weekly intervals, tumor growth was assessed using bioluminescence imaging on the Photon Imager (Biospace Lab, Paris, France). Before imaging, mice were anaesthetized via isoflurane and synthetic d-luciferin (Biothema, Handen, Sweden) was given i.p. at a dose of 125 mg/kg, M3 vision software (Biospace Lab) was used for image analysis. MAb were injected i.p. at day 0 at indicated dosing levels. During the study, heparinized blood samples were taken for determination of IgG levels in plasma using a Behring Nephelometer II (Siemens Healthcare Diagnostics, Erlangen, Germany).

Statistical analysis

Data analysis was performed using GraphPad Prism, vs 5.0 (Graphpad, San Diego, CA) and PASW Statistics 18.0 (SPSS Inc., Chicago, IL). Data were reported as mean ± SEM. Differences between groups were analyzed using Mantle-Cox log-rank test (PASW).

Results

Daratumumab (DARA) induces ADCP of BL and MM cell lines by mouse mφ

To explore the potential induction of phagocytosis by DARA, we set up a flow cytometric phagocytosis assay with mouse mφ and leukemic target cells. Bone marrow-derived mφ cultured in the presence of M-CSF were positive for F4/80 and CD80 and therefore represented mature and activated mφ (data not shown). Target cells were labeled with calcein-AM and incubated with the mouse mφ. To determine the percentage of mφ that engaged in phagocytosis, we assessed the number of F4/80 and calcein double-positive (DP) cells, which were negative for (surface) target cell markers (e.g. CD19). In addition, we calculated the

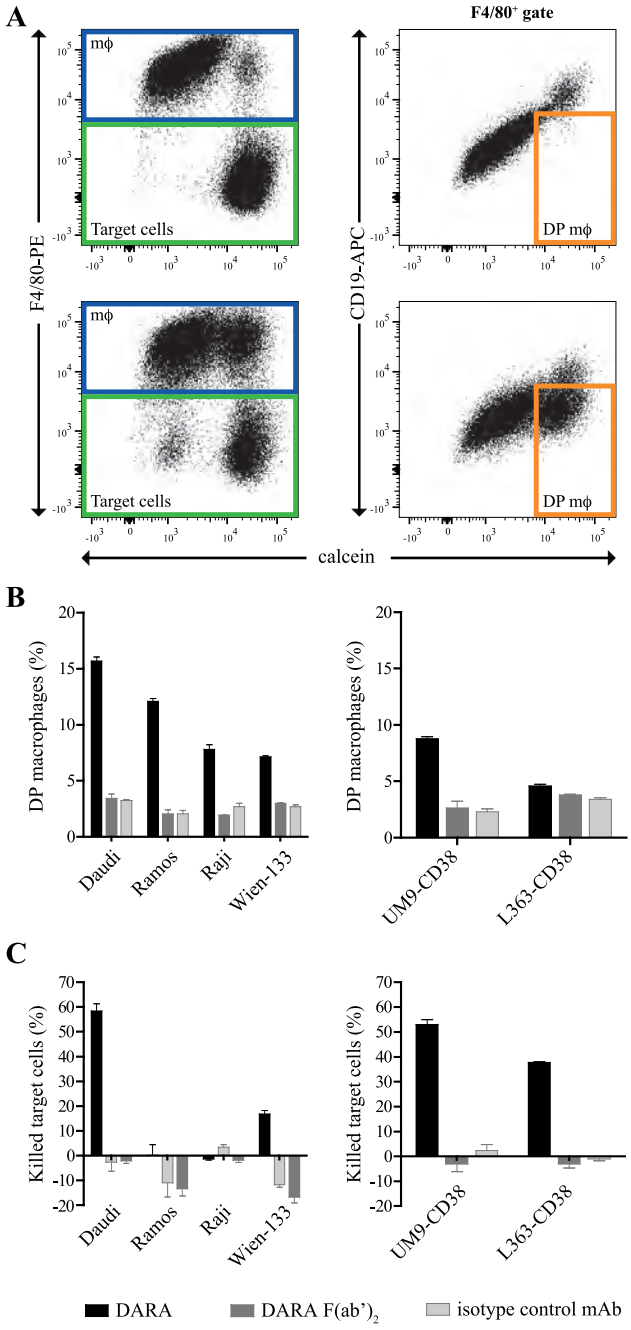

Figure 1. *Efficient ADCP of BL and MM cell lines by mouse macrophages.* ADCP of BL cell lines (*left panels*) or MM cell lines (*right panels*) by co-culture with mouse mφ for 4h with a fixed 6.7 μM concentration of mAb or $F(ab')_2$, E:T ratio of 1:1. (A) Representative flow cytometry plot of Daudi cells co-cultured with mouse mφ in the presence of isotype control mAb (*upper panel*) or DARA (*lower panel*). $F4/80^+$ mφ (blue

gate), F4/80$^-$ target cells (green gate) and F4/80$^+$,calcein$^+$,CD19$^-$ double positive (DP) mφ (orange gate) are indicated. (B) Percentage DP mφ characterized as F4/80$^+$,calcein$^+$,target Ag$^-$. C, Percentage killed target cells characterized as F4/80$^-$. Each bar shows mean ± SEM representative of three independent experiments.

percentage of cells killed in the incubation mixture from the difference between the initial and remaining numbers of target cells. To exclude additional killing mechanisms, like ADCC, which lead to loss of calcein through cell leakage, we included both calcein-negative and -positive cells when counting the number of target cells remaining. Fig. 1A shows representative flow cytometric plots of mouse mφ incubated with Daudi cells in the presence of an isotype control mAb (*upper panel*) or DARA (*lower panel*). F4/80$^+$ mφ, F4/80$^-$ target cells and F4/80$^+$,calcein$^+$ DP, CD19$^-$ mφ are indicated.

Fig. 1B (*left panel*) shows that the highest level of phagocytosis is observed for DARA-opsonized Daudi cells, followed by the Ramos, Raji and Wien-133 cells. Daudi and Wien-133 cells were killed effectively by the mφ as shown by the percentage target cells killed (Fig. 1C). For Ramos and Raji cells killing was observed in a low range (0-20%), even though CD38 expression and percentages of DP mφ obtained were similar compared to Daudi and Wien-133 cells (Fig. 1C; Table 1). No phagocytosis or killing was observed with DARA F(ab')$_2$ fragments and the isotype control indicating the effects to be Fc-dependent and target specific. To explore whether ADCP induction was dependent on CD38 expression levels, we compared the number of DP mφ and the percentage target cells killed for cell lines varying in CD38 expression levels (Table 1; Fig 1B,C). As shown, the parental MM cell lines UM9 and L363 with low CD38 expression were not susceptible to ADCP. However, phagocytosis and a high degree of cell kill was observed for CD38-transduced UM9-CD38 and L363-CD38 variants with high levels of CD38 expression which are in the range of what is observed for patient MM cells. These results suggest that ADCP and cell killing is related to CD38 expression levels. Nevertheless, additional factors are likely to play a role as large differences were also observed between target cell lines with comparable CD38 expression levels (e.g. comparing Daudi and Raji).

Table 1. No direct correlation between CD38 expression and ADCP

Cell Line	CD38 range (molecules/cell)	DP mφ range (%)	Killing range (%)
L363	50,000 ~ 100,000	0	0
UM9	100,000 ~ 150,000	0	0
Wien-133	100,000 ~ 150,000	5 - 20	0 - 40
Raji	150,000 ~ 350,000	7 - 15	0 - 10
Ramos	200,000 ~ 300,000	12 - 25	0 - 20
Daudi	200,000 ~ 400,000	12 - 40	29 - 79
UM9-CD38	350,000 ~ 600,000	5 - 8	2 - 50
L363-CD38	450,000 ~ 800,000	9 - 10	4 - 70

Ranges based on at least three independent experiments.

Live cell imaging demonstrates DARA-induced ADCP and serial engulfment of CD38+ target cells

With live cell imaging we showed ADCP to be the mechanism by which mouse mφ kill target cells. We frequently observed mφ which engulfed multiple target cells. In Fig. 2A and Supplemental movie 1, a time laps bright field microscopy is shown focusing on an individual mouse mφ (designated with an arrow) which sequentially engulfed five Daudi cells within a 15 min. period. Supplemental movies 2 and 4 show time laps imaging microscopy of co-cultures of DiO (green) labeled mouse mφ and DiB (blue) labeled Daudi or Ramos cells respectively in the presence of DARA. Daudi was more rapidly phagocytosed than the Ramos cells, despite equivalent CD38 expression, as demonstrated in a flow cytometric ADCP assay. During a 30 min. incubation, the percentage DP mφ (Fig. 2B) and the percentage of killed target cells (Fig. 2C) was two-three fold higher for Daudi than for Ramos target cells. No phagocytosis or cell killing was observed in the presence of the isotype control antibody (Fig. 2B,C, Supplemental movies 3 and 5). These real time data support that ADCP induction is a very rapid and efficient MoA of DARA.

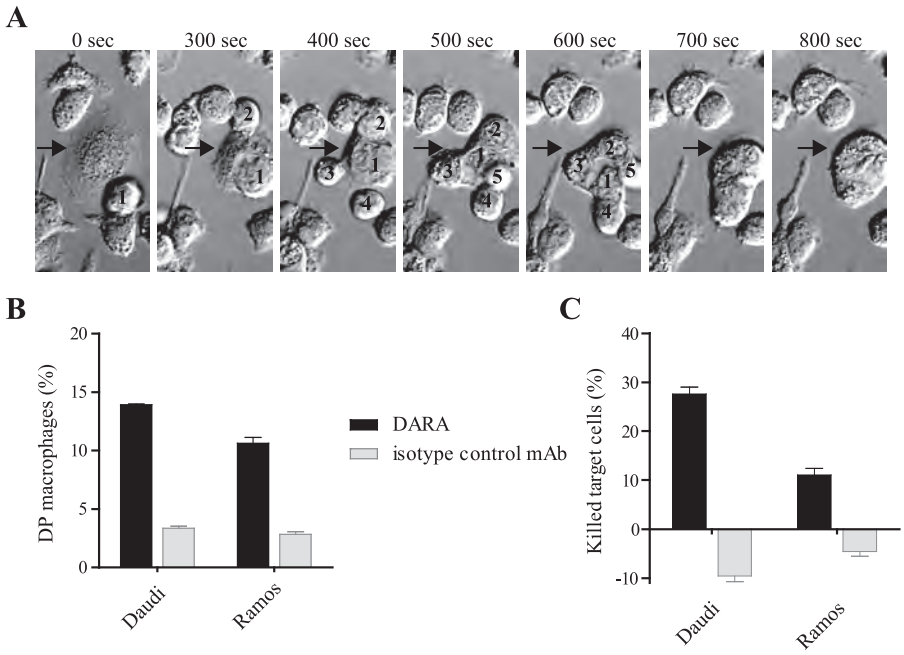

Figure 2. *Live cell imaging confirms ADCP as MoA of DARA and demonstrates mouse mφ to engulf multiple target cells.* Co-cultures of mouse mφ with target cells at a fixed DARA concentration of 1 μg/ml, E:T ratio 1:1. (A) Time laps imaging microscopy, bright field images of mouse mφ with Daudi cells (arrowhead points out mφ, numbers indicate Daudi cells). (B,C) Flow cytometry ADCP analysis of Daudi and Ramos after co-culture with mouse mφ for 30 minutes. (B) Percentage DP mφ characterized as F4/80^{+},calcein^{+},CD19^{-}. (C) Percentage killed target cells characterized as F4/80^{-}. Each bar shows mean ± SEM representative of two independent experiments.

ADCP contributes to the MoA of DARA in vivo

We previously demonstrated that the human IgG2 isotype shows weak to no phagocytosis with mouse mφ (12). Therefore, we compared DARA to a DARA-IgG2 isotype variant to study the contribution of ADCP to the *in vivo* MoA of DARA. To restrict *in vivo* effector cell activity to mouse mφ, we made use of immune-deficient SCID-BEIGE mice, which lack B, T and NK-cells. A potential contribution of CDC to therapy was eliminated by generating Fc mutants in which the lysine at position 322 was mutated to alanine (referred to as DARA-K322A and DARA-IgG2-K322A). Duncan et al. and Idusogie et al. showed K322 to be a critical residue for C1q binding and complement activation (18, 19) and we recently confirmed that the K322A mutation also leads to strongly reduced binding of mouse C1q (16). The K322A mutation itself did not affect ADCP induction or cell killing by DARA (Fig. 3A,B). In a subcutaneous Daudi-luc

tumor xenograft model (Fig. 3C), DARA-K322A provided significantly stronger inhibition of tumor growth than DARA-IgG2-K322A. Furthermore, in the experimental intravenous leukemic Daudi-luc xenograft model with treatment at the time of tumor challenge (Fig. 3D), DARA-K322A also demonstrated significantly stronger tumor growth inhibition than DARA-IgG2-K322A. Finally, DARA-K322A inhibited tumor growth in this model more strongly than DARA-IgG2-K322A in the therapeutic setting (treatment with 0.5 mg/kg at day 14) as shown in Supplemental Fig. 1. These data demonstrate that phagocytosis contributes to the *in vivo* MoA of DARA.

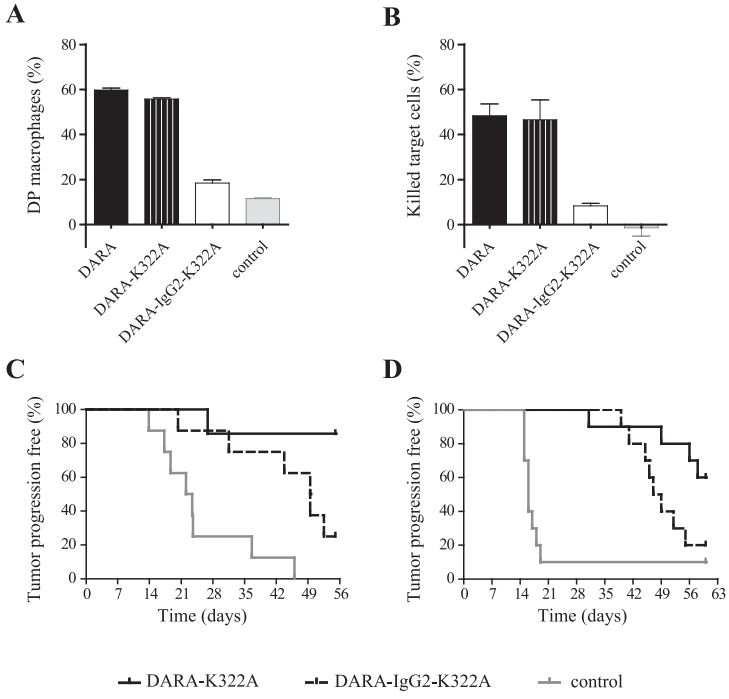

Figure 3. *DARA is more potent than DARA-IgG2 in a s.c and i.v. Daudi-luc SCID/BEIGE xenograft model.* (A,B) ADCP of Daudi cells by mouse mφ with a fixed mAb concentration of 1 µg/ml, E:T ratio of 1:1. Percentage double positive (DP) mφ characterized as F4/80^{+},calcein^{+},CD19^{-} (A) and percentage killed target cells characterized as F4/80^{-} (B). (C) s.c. inoculation of 20×10^{6} Daudi-luc cells with matrigel in groups of 8 mice, treatment with 250 µg/mouse (12.5 mg/kg) mAb at day 0. Kaplan-Meier plot (time to progression, cutoff set at a tumor volume > 800 mm^{3}) is shown (DARA-K322A vs DARA-IgG2-K322A p<0.004 Mantle-Cox log-rank test at time to progression). (D) i.v. inoculation of 2.5×10^{6} Daudi-luc cells in groups of 10 mice, treatment with 10 µg/mouse (0.5 mg/kg) mAb at day 0. Kaplan-Meier plot (time to progression, cutoff set at a bioluminescence > 50,000 cpm) is depicted (p<0.001 Mantle-Cox log-rank test at time to progression).

Efficient DARA-induced ADCP of patient MM cells

To translate our observations from mice to patients, we explored ADCP induction by DARA with human mφ. Monocytes isolated from healthy donors were cultured in the presence of GM-CSF and characterized as $CD11b^{+}$,$CD64^{+}$,$CD32^{+}$,$CD16^{+/-}$ mφ (data not shown). Firstly, we explored ADCP efficacy on cell lines by incubating human mφ with DARA and BL cell lines Daudi and Ramos or MM cell lines UM9-CD38 and L363-CD38. The percentage DP mφ and percentage target cells killed were determined with a similar method as for mouse mφ, with the exception that human mφ were detected by CD11b-PE staining. Fig. 4A shows the percentage DP mφ for BL (*left panel*) and MM cell line targets (*right panel*), and indicate that human mφ were able to phagocytose both cell types. The absence of DP mφ in the presence of DARA $F(ab')_2$ fragments confirms the effect to be Fc-mediated. Overall the percentage DP mφ is somewhat lower than with mouse mφ, whereas the percentage target cells killed (Fig. 4B) is comparable. Ramos cells appear to be more susceptible to killing by human mφ then by mouse mφ.

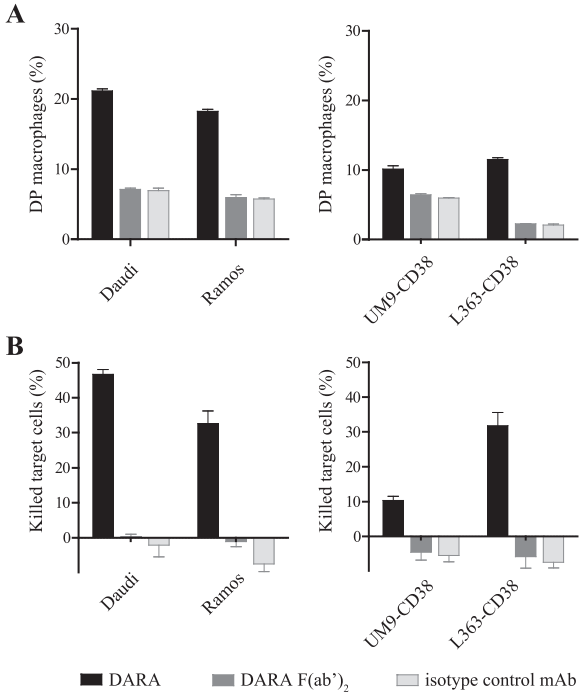

Figure 4. *Efficient ADCP by human macrophages on BL and MM cell lines.* ADCP of BL cell lines (*left panels*) or MM cell lines (*right panels*) by human mφ with a fixed 6.7 μM concentration of mAb, E:T ratio of 2:1. (A) Percentage double positive (DP) mφ characterized as $CD11b^{+}$,$calcein^{+}$,target Ag^{-}. (B) Percentage killed target cells characterized as $CD11b^{-}$. Each bar shows mean ± SEM representative of three independent experiments.

Secondly, we explored DARA-induced ADCP of patient MM cells obtained either from bone marrow (BM), pleural fluid or blood. The MM patient samples contained more than 80% plasma cells, characterized as CD138-APC positive cells. CD38 expression ranged from 10,000 to 550,000 molecules/cell (Table 2). Peripheral blood, from four different healthy donors for which the FcγRIIa and IIIa-polymorphisms were determined (Table 2), was used as a source for human mφ. As the potency of the human mφ differed between experiments e.g. due to differences in the FcγRIIa/IIIa polymorphisms, Daudi cells were included in each experiment as a reference.

Table 2. Overview MM patient samples and mφ donors

MM patient information			Mφ donor information	
Patient nr	**Origin**	**CD38 (molecules/ cell)**	**FcγRIIa polymorphism**	**FcγRIIIa polymorphism**
6	Blood	~ 10,000	H/R	V/F
10	BM	~ 60,000	H/R	F/F
4	BM	~ 70,000	H/R	V/F
9	BM	~ 80,000	H/R	F/F
8	BM	~ 100,000	H/R	F/F
7	BM	~ 220,000	H/R	V/F
3	BM	~ 230,000	H/H	V/F
5	Pleural fluid	~ 550,000	H/R	V/F

Fig. 5 shows the percentage DP mφ (A) and the percentage killed $CD138^+$ or $CD19^+$ target cells (B). DARA-induced ADCP was observed with cells from all patients, except patient 6. The $CD138^+$ cells of this MM patient were obtained from blood and only expressed very low levels of CD38 (~10,000 molecules/cell). MM cells from patients 3, 5 and 7, displayed high CD38 expression and, compared to Daudi in the same experiment, showed similar DP mφ whereas the number of killed cells was greater. Cells from patients 4, 8, 9 and 10, which displayed moderate CD38 expression, had a lower percentage of DP mφ compared to Daudi cells, but the percentage killing nonetheless was comparable. Based on these observations we conclude that ADCP is a powerful MoA of DARA for patient MM cells.

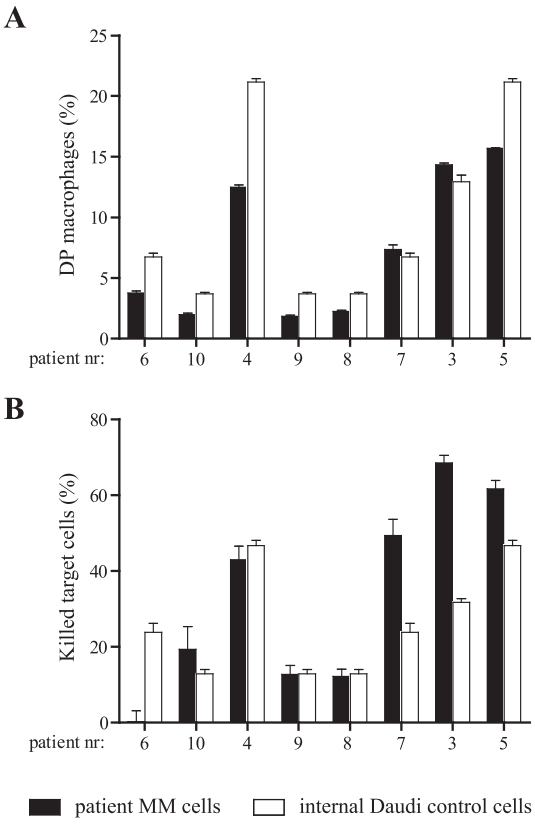

Figure 5. *Efficient ADCP of patient MM cells by human macrophages.* ADCP of MM patient material by human donor mφ with a fixed 1 μg/ml concentration of mAb, E:T ratio of 2:1. Black bars show mean ± SEM of triplicate samples for patient MM cells, while white bars show results for internal Daudi control cells observed in the same experiment. Patient samples are ordered on the x-axis according to their CD38 expression level, with patient 6 expressing low and patient 5 expressing high levels. (A) Percentage double positive (DP) mφ characterized as $CD11b^{+}$,$calcein^{+}$,$CD138^{-}$. (B) Percentage killed target cells characterized as $CD11b^{-}$, $CD138^{+}$. Background with isotype control mAb was < 8%.

Discussion

In this study we investigated the potency of DARA to induce phagocytosis and we showed that both murine and human mφ phagocytosed several BL and MM cell lines. ADCP by human mφ of patient MM cells appeared to be more efficient than for the MM cell lines. In two different *in vivo* models we showed that ADCP contributes to the MoA of DARA in reducing tumor growth.

Comparisons of different E:T ratios revealed that not all cultured mouse mφ are competent to phagocytose target cells, since only a maximum of ~40% of mouse mφ actively engulfed one or multiple target cells (data not shown).

Examining different target cell lines, we observed that the percentage DP mφ was more or less comparable for all cell lines, whereas there was a striking difference in the percentage of target cells killed. This difference might be due to the number of target cells engulfed per mφ or it might be due to a difference in rate of phagocytosis between cell lines. Overall, the percentage DP mφ reflects the ability of DARA to induce phagocytosis of a certain target cell. The percentage target cells killed is a measure of the efficacy of the ADCP.

Differences in the efficacy of ADCP against different target cell lines could not solely be explained by the CD38 expression level, which confirms previous findings of Leidi et al. (13). They compared ADCP by human mφ of rituximab (chimeric IgG1 CD20 mAb) opsonized B-chronic lymphocytic leukemia and Mantle cell lymphoma cells and found that CD20 expression did not impact ADCP significantly, as was also observed for ADCC (20). However, target expression was previously shown to significantly affect CDC (20, 21). Target cell size has been suggested to influence ADCP efficacy and Swanson and Hoppe (22) proposed a model for size-dependent transitions which may determine whether a target cell will be phagocytosed or not. Nevertheless, the size of the different BL and MM cells used in our study is comparable and therefore could not explain the difference in ADCP efficiency. In addition to target expression levels and target cell size, so-called 'don't eat me' signals on target cells play an important role in regulating phagocytosis. A prominent example is CD47, which inhibits phagocytosis via ligation to its receptor SIRPα on the phagocytic cell (23). CD47 is described to be up regulated on leukemic cells to avoid phagocytosis (24), which can be counterbalanced by the expression of calreticulin that gives a pro-phagocytic signal upon receptor binding (25, 26). However, human CD47 is not able to bind to mouse SIRPα (27, 28), and therefore also CD47 cannot be the cause for the difference in ADCP efficiency with mouse mφ on the different target cell lines. There might be other, yet undefined, regulators of phagocytosis and this needs further investigation.

With live cell imaging we observed that ADCP is a very fast mechanism, as we observed engulfment of up to five targets cells within 15 minutes by individual mφ. Chung et al. (29) studied the kinetics of ADCC induction via NK-cells induced by human immunodeficiency virus specific Abs. Degranulation and granzyme B loss, hallmarks of NK-cell mediated ADCC, peaked after 3 hours, therefore suggesting that ADCP is a faster killing mechanism than ADCC.

As mentioned earlier, *in vivo* studies demonstrating a role for mφ contributing

to the MoA of a mAb via mφ depletion, cannot discriminate ADCP from ADCC. Therefore, we compared efficacy of DARA with a matched IgG2 isotype variant, which did not induce ADCP by mouse mφ, in SCID-BEIGE mice which lack B, T and NK-cells. In addition, we do not expect an impact on efficacy of the DARA IgG1 and IgG2 variants due to differences in ADCC activity in this model, since we did not observe induction of ADCC of mφ by DARA (data not shown). Furthermore, we observed in a previous study with an epidermal growth factor receptor mAb that ADCC by polymorphonuclear leukocytes was similar (12). Finally, CDC is excluded in this *in vivo* model by using a K322A mutant for both isotypes. In both a subcutaneous as well as a leukemic intravenous Daudi xenograft model DARA induced significantly stronger tumor growth inhibition compared to the IgG2 variant. Our models therefore demonstrate a distinct role for mφ in the therapeutic effect of DARA as well as a contribution of ADCP to its *in vivo* MoA.

Due to the high potential of DARA in MM, we explored the efficacy of DARA-induced ADCP on patient MM cells with human mφ. ADCP was explored on patient samples derived from bone marrow, pleural fluid or blood. All patient samples expressing >60,000 CD38 molecules/cell were susceptible to ADCP. In each assay, Daudi cells were included as an internal control for the potency of the mφ batch. Macrophages which were FcγRIIIa 158-FF homozygous, this polymorphism is described to reduce binding to complexed IgG1, IgG3 and IgG4 (30), were found less potent in the ADCP assay compared to 158-F/V heterozygotes, confirming a role for FcγRIIIa in ADCP induction. The FcγRIIa 131 polymorphism was not found to affect ADCP efficacy by DARA, as expected (31). Furthermore, the percentage killed cells was higher for MM patient cells compared to control cells, whereas the percentage DP mφ were similar, suggesting that the patient samples are more efficiently and rapidly phagocytosed than the Daudi cells, however this needs further investigation.

For MM patient therapy, the current focus is on combination therapy of mAbs with immunomodulatory drugs (IMiDs) (32). IMiDs currently used, e.g. lenalidomide and pomalidomide, are described to enhance NK-cell mediated ADCC (33). Combining DARA with lenalidomide enhanced the elimination of MM cells (34). Enhancing mφ mediated ADCP might also be a powerful strategy in the treatment of MM. Due to the plasticity of mφ (35) IL-12 treatment has been shown to alter tumor growth promoting mφ, present in the tumor micro-environment, into a proimmunogenic/inflammatory profile (36) which might also enhance ADCP activity. Another approach is the combination with

drugs regulating pro-phagocytic signals. Anti-CD47 mAb has been shown to synergize with rituximab in the treatment of Non-Hodgkin lymphoma (37). CD47 is described to be highly expressed on $CD38^+$ MM cells (38), suggesting that inhibition of the CD47-SIRP alpha axis might be an interesting therapeutic approach in combination with DARA.

Overall, we have shown that DARA induces ADCP with mouse and human mφ on BL and MM cancer cell lines and MM patient cells. The enhanced efficacy of DARA-K322A versus DARA-IgG2-K322A in a subcutaneous and a leukemic intravenous xenograft tumor model suggest that ADCP also plays an important role *in vivo*. We conclude that ADCP is a potent mechanism of action for DARA.

Acknowledgement

The authors express their thanks to Berris van Kessel for technical assistance.

References

1. Manches, O., G. Lui, L. Chaperot, R. Gressin, J. P. Molens, M. C. Jacob, J. J. Sotto, D. Leroux, J. C. Bensa, and J. Plumas. 2003. In vitro mechanisms of action of rituximab on primary non-Hodgkin lymphomas. *Blood* 101:949-954.
2. Munn, D. H., M. McBride, and N. K. Cheung. 1991. Role of low-affinity Fc receptors in antibody-dependent tumor cell phagocytosis by human monocyte-derived macrophages. *Cancer Res* 51:1117-1123.
3. Mantovani, A., T. Schioppa, C. Porta, P. Allavena, and A. Sica. 2006. Role of tumor-associated macrophages in tumor progression and invasion. *Cancer Metastasis Rev* 25:315-322.
4. van der Bij, G. J., S. J. Oosterling, S. Meijer, R. H. Beelen, and M. van Egmond. 2005. The role of macrophages in tumor development. *Cell Oncol* 27:203-213.
5. Uchida, J., Y. Hamaguchi, J. A. Oliver, J. V. Ravetch, J. C. Poe, K. M. Haas, and T. F. Tedder. 2004. The innate mononuclear phagocyte network depletes B lymphocytes through Fc receptor-dependent mechanisms during anti-CD20 antibody immunotherapy. *J Exp Med* 199:1659-1669.
6. McEarchern, J. A., E. Oflazoglu, L. Francisco, C. F. McDonagh, K. A. Gordon, I. Stone, K. Klussman, E. Turcott, N. van Rooijen, P. Carter, I. S. Grewal, A. F. Wahl, and C. L. Law. 2007. Engineered anti-CD70 antibody with multiple effector functions exhibits in vitro and in vivo antitumor activities. *Blood* 109:1185-1192.
7. Oflazoglu, E., I. J. Stone, L. Brown, K. A. Gordon, N. van Rooijen, M. Jonas, C. L. Law, I. S. Grewal, and H. P. Gerber. 2009. Macrophages and Fc-receptor interactions contribute to the antitumour activities of the anti-CD40 antibody SGN-40. *Br J Cancer* 100:113-117.
8. Oflazoglu, E., I. J. Stone, K. A. Gordon, I. S. Grewal, N. van Rooijen, C. L. Law, and H. P. Gerber. 2007. Macrophages contribute to the antitumor activity of the anti-CD30 antibody SGN-30. *Blood* 110:4370-4372.
9. Schneider-Merck, T., J. J. Lammerts van Bueren, S. Berger, K. Rossen, P. H. van Berkel, S. Derer, T. Beyer, S. Lohse, W. K. Bleeker, M. Peipp, P. W. Parren, J. G. van de Winkel, T. Valerius, and M. Dechant. 2010. Human IgG2 antibodies against epidermal growth factor receptor effectively trigger antibody-dependent cellular cytotoxicity but, in contrast to IgG1, only by cells of myeloid lineage. *J Immunol* 184:512-520.
10. Lin, P., R. Owens, G. Tricot, and C. S. Wilson. 2004. Flow cytometric immunophenotypic analysis of 306 cases of multiple myeloma. *Am J Clin Pathol* 121:482-488.
11. de Weers, M., Y. T. Tai, M. S. van der Veer, J. M. Bakker, T. Vink, D. C. Jacobs, L. A. Oomen, M. Peipp, T. Valerius, J. W. Slootstra, T. Mutis, W. K. Bleeker, K. C. Anderson, H. M. Lokhorst, J. G. van de Winkel, and P. W. Parren. 2011. Daratumumab, a novel therapeutic human CD38 monoclonal antibody, induces killing of multiple myeloma and other hematological tumors. *J Immunol* 186:1840-1848.
12. Overdijk, M. B., S. Verploegen, A. Ortiz Buijsse, T. Vink, J. H. Leusen, W. K. Bleeker, and P. W. Parren. 2012. Crosstalk between human IgG isotypes and murine effector cells. *J Immunol* 189:3430-3438.
13. Leidi, M., E. Gotti, L. Bologna, E. Miranda, M. Rimoldi, A. Sica, M. Roncalli, G. A. Palumbo, M. Introna, and J. Golay. 2009. M2 macrophages phagocytose rituximab-opsonized leukemic targets more efficiently than m1 cells in vitro. *J Immunol* 182:4415-4422.
14. Kuipers, J., J. W. Vaandrager, D. O. Weghuis, P. L. Pearson, J. Scheres, H. M. Lokhorst, H. Clevers, and B. J. Bast. 1999. Fluorescence in situ hybridization analysis shows the frequent occurrence of 14q32.3 rearrangements with involvement of immunoglobulin switch regions in myeloma cell lines. *Cancer Genet Cytogenet* 109:99-107.
15. Rozemuller, H., E. van der Spek, L. H. Bogers-Boer, M. C. Zwart, V. Verweij, M. Emmelot, R. W. Groen, R. Spaapen, A. C. Bloem, H. M. Lokhorst, T. Mutis, and A. C. Martens. 2008. A bioluminescence imaging based in vivo model for preclinical testing of novel cellular immunotherapy strategies to improve the graft-versus-myeloma effect. *Haematologica* 93:1049-1057.
16. Overdijk, M. B., S. Verploegen, J. H. van den Brakel, J. J. Lammerts van Bueren, T. Vink, J. G. van de Winkel, P. W. Parren, and W. K. Bleeker. 2011. Epidermal Growth Factor Receptor (EGFR) Antibody-Induced Antibody-Dependent Cellular Cytotoxicity Plays a Prominent Role in Inhibiting Tumorigenesis, Even of Tumor Cells Insensitive to EGFR Signaling Inhibition. *J Immunol* 187:3383-3390.

17. Burton, D. R., J. Pyati, R. Koduri, S. J. Sharp, G. B. Thornton, P. W. Parren, L. S. Sawyer, R. M. Hendry, N. Dunlop, P. L. Nara, and et al. 1994. Efficient neutralization of primary isolates of HIV-1 by a recombinant human monoclonal antibody. *Science* 266:1024-1027.

18. Duncan, A. R., and G. Winter. 1988. The binding site for C1q on IgG. *Nature* 332:738-740.

19. Idusogie, E. E., L. G. Presta, H. Gazzano-Santoro, K. Totpal, P. Y. Wong, M. Ultsch, Y. G. Meng, and M. G. Mulkerrin. 2000. Mapping of the C1q binding site on rituxan, a chimeric antibody with a human IgG1 Fc. *J Immunol* 164:4178-4184.

20. van Meerten, T., R. S. van Rijn, S. Hol, A. Hagenbeek, and S. B. Ebeling. 2006. Complement-Induced Cell Death by Rituximab Depends on CD20 Expression Level and Acts Complementary to Antibody-Dependent Cellular Cytotoxicity. *Clinical Cancer Research* 12:4027-4035.

21. Golay, J., M. Lazzari, V. Facchinetti, S. Bernasconi, G. Borleri, T. Barbui, A. Rambaldi, and M. Introna. 2001. CD20 levels determine the in vitro susceptibility to rituximab and complement of B-cell chronic lymphocytic leukemia: further regulation by CD55 and CD59. *Blood* 98:3383-3389.

22. Swanson, J. A., and A. D. Hoppe. 2004. The coordination of signaling during Fc receptor-mediated phagocytosis. *J Leukoc Biol* 76:1093-1103.

23. Oldenborg, P. A., H. D. Gresham, and F. P. Lindberg. 2001. CD47-signal regulatory protein alpha (SIRPalpha) regulates Fcgamma and complement receptor-mediated phagocytosis. *J Exp Med* 193:855-862.

24. Jaiswal, S., C. H. Jamieson, W. W. Pang, C. Y. Park, M. P. Chao, R. Majeti, D. Traver, N. van Rooijen, and I. L. Weissman. 2009. CD47 is upregulated on circulating hematopoietic stem cells and leukemia cells to avoid phagocytosis. *Cell* 138:271-285.

25. Chao, M. P., S. Jaiswal, R. Weissman-Tsukamoto, A. A. Alizadeh, A. J. Gentles, J. Volkmer, K. Weiskopf, S. B. Willingham, T. Raveh, C. Y. Park, R. Majeti, and I. L. Weissman. 2010. Calreticulin is the dominant pro-phagocytic signal on multiple human cancers and is counterbalanced by CD47. *Sci Transl Med* 2:63ra94.

26. Martins, I., O. Kepp, L. Galluzzi, L. Senovilla, F. Schlemmer, S. Adjemian, L. Menger, M. Michaud, L. Zitvogel, and G. Kroemer. 2010. Surface-exposed calreticulin in the interaction between dying cells and phagocytes. *Ann N Y Acad Sci* 1209:77-82.

27. Subramanian, S., R. Parthasarathy, S. Sen, E. T. Boder, and D. E. Discher. 2006. Species- and cell type-specific interactions between CD47 and human SIRPalpha. *Blood* 107:2548-2556.

28. Takenaka, K., T. K. Prasolava, J. C. Wang, S. M. Mortin-Toth, S. Khalouei, O. I. Gan, J. E. Dick, and J. S. Danska. 2007. Polymorphism in Sirpa modulates engraftment of human hematopoietic stem cells. *Nat Immunol* 8:1313-1323.

29. Chung, A. W., E. Rollman, R. J. Center, S. J. Kent, and I. Stratov. 2009. Rapid degranulation of NK cells following activation by HIV-specific antibodies. *J Immunol* 182:1202-1210.

30. Koene, H. R., M. Kleijer, J. Algra, D. Roos, A. E. von dem Borne, and M. de Haas. 1997. Fc gammaRIIIa-158V/F polymorphism influences the binding of IgG by natural killer cell Fc gammaRIIIa, independently of the Fc gammaRIIIa-48L/R/H phenotype. *Blood* 90:1109-1114.

31. Parren, P. W., P. A. Warmerdam, L. C. Boeije, J. Arts, N. A. Westerdaal, A. Vlug, P. J. Capel, L. A. Aarden, and J. G. van de Winkel. 1992. On the interaction of IgG subclasses with the low affinity Fc gamma RIIa (CD32) on human monocytes, neutrophils, and platelets. Analysis of a functional polymorphism to human IgG2. *J Clin Invest* 90:1537-1546.

32. van de Donk, N. W., S. Kamps, T. Mutis, and H. M. Lokhorst. 2012. Monoclonal antibody-based therapy as a new treatment strategy in multiple myeloma. *Leukemia* 26:199-213.

33. Quach, H., D. Ritchie, A. K. Stewart, P. Neeson, S. Harrison, M. J. Smyth, and H. M. Prince. 2010. Mechanism of action of immunomodulatory drugs (IMiDS) in multiple myeloma. *Leukemia* 24:22-32.

34. van der Veer, M. S., M. de Weers, B. van Kessel, J. M. Bakker, S. Wittebol, P. W. Parren, H. M. Lokhorst, and T. Mutis. 2011. Towards effective immunotherapy of myeloma: enhanced elimination of myeloma cells by combination of lenalidomide with the human CD38 monoclonal antibody daratumumab. *Haematologica* 96:284-290.

35. Stout, R. D., S. K. Watkins, and J. Suttles. 2009. Functional plasticity of macrophages: in situ reprogramming of tumor-associated macrophages. *J Leukoc Biol* 86:1105-1109.

36. Watkins, S. K., N. K. Egilmez, J. Suttles, and R. D. Stout. 2007. IL-12 rapidly alters the functional profile of tumor-associated and tumor-infiltrating macrophages in vitro and in vivo. *J Immunol* 178:1357-1362.

37. Chao, M. P., A. A. Alizadeh, C. Tang, J. H. Myklebust, B. Varghese, S. Gill, M. Jan, A. C. Cha, C. K. Chan, B. T. Tan, C. Y. Park, F. Zhao, H. E. Kohrt, R. Malumbres, J. Briones, R. D. Gascoyne, I. S. Lossos, R. Levy, I. L. Weissman, and R. Majeti. 2010. Anti-CD47 antibody synergizes with rituximab to promote phagocytosis and eradicate non-Hodgkin lymphoma. *Cell* 142:699-713.

38. Kim, D., J. Wang, S. B. Willingham, R. Martin, G. Wernig, and I. L. Weissman. 2012. Anti-CD47 antibodies promote phagocytosis and inhibit the growth of human myeloma cells. *Leukemia* 26:2538-2545.

Supplemental Figure

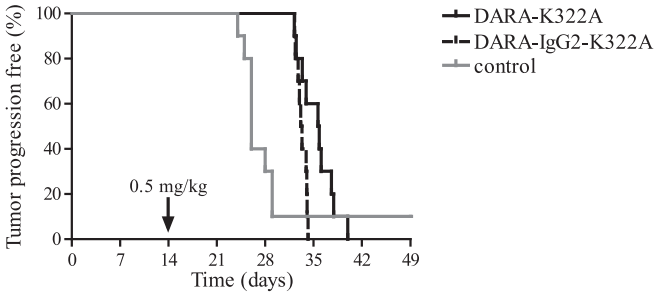

Supplemental Figure 1. *DARA is more potent than DARA-IgG2 in a therapeutic i.v. Daudi-luc SCID-BEIGE xenograft model.* Intravenous inoculation of 2.5×10^6 Daudi-luc cells in groups of 10 mice, treatment with 10 µg/mouse (0.5 mg/kg) mAb at day 14. Kaplan-Meier plot (time to progression, cutoff set at a bioluminescence > 500,000 cpm) is depicted ($p<0.012$ Mantle-Cox log-rank test at time to progression).

Supplemental Movies

Supplemental Movie 1. Time laps bright field microscopy focusing on an individual mouse mφ which sequentially engulfed five Daudi cells in the presence of 1 µg/ml DARA, E:T 3:1.

Supplemental Movie 2. Time laps imaging microscopy of DiO (green) labeled mouse mφ and DiB (blue) labeled Daudi cells in the presence of 1 µg/ml DARA, E:T 2:1.

Supplemental Movie 3. Time laps imaging microscopy of DiO (green) labeled mouse mφ and DiB (blue) labeled Daudi cells in the presence of 1 µg/ml isotype control mAb, E:T 2:1.

Supplemental Movie 4. Time laps imaging microscopy of DiO (green) labeled mouse mφ and DiB (blue) labeled Ramos cells in the presence of 1 µg/ml DARA, E:T 2:1.

Supplemental Movie 5. Time laps imaging microscopy of DiO (green) labeled mouse mφ and DiB (blue) labeled Ramos cells in the presence of 1 µg/ml isotype control mAb, E:T 2:1.

5

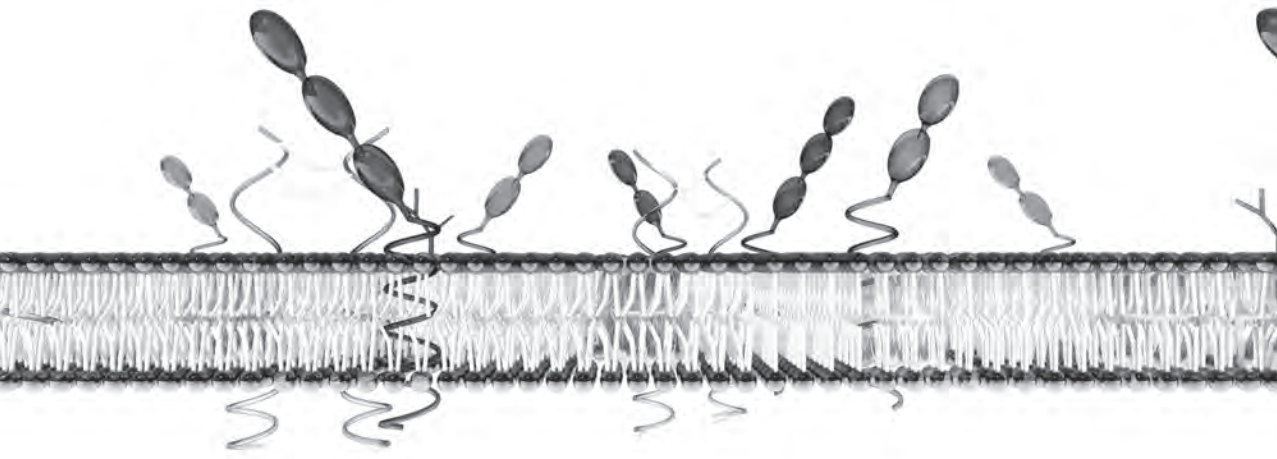

The therapeutic CD38 mAb daratumumab induces programmed cell death via Fc gamma receptor-mediated crosslinking

Marije B. Overdijk[*,¶], J.H. Marco Jansen[†,¶], Maaike Nederend[†], Jeroen J. Lammerts van Bueren[*], Richard W.J. Groen[‡], Paul W.H.I. Parren[*], Jeanette H.W. Leusen[†,‖], Peter Boross[†,‖]

[*]Genmab, Utrecht, The Netherlands; [†]Immunotherapy laboratory, Laboratory for Translational Immunology, [‡]Department of Cell Biology, University Medical Center, Utrecht, The Netherlands.

[¶], [‖]These authors contributed equally to this paper.

In preparation

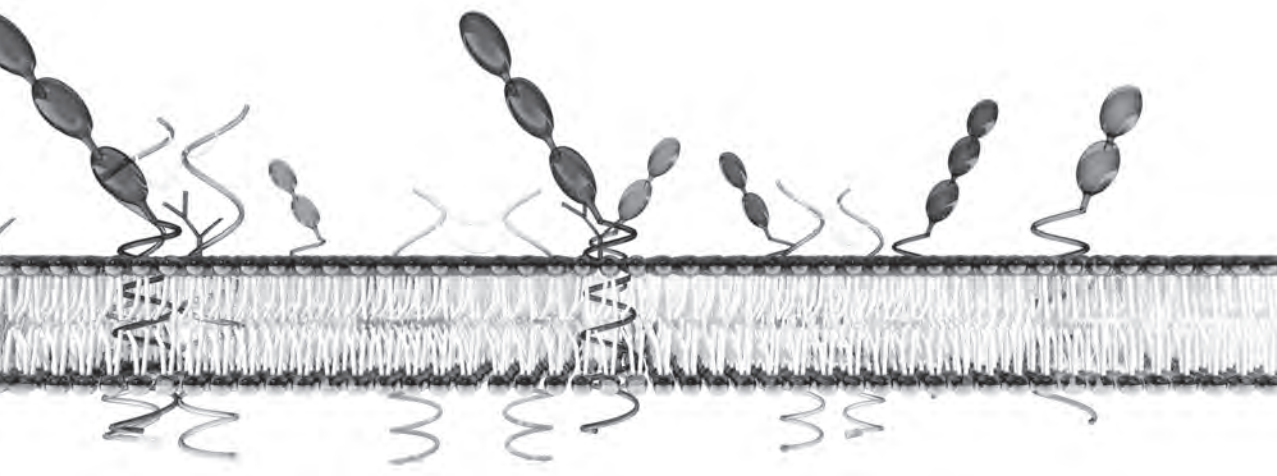

Abstract

Daratumumab (DARA) is a therapeutic human CD38 monoclonal antibody (mAb) with a broad-spectrum killing activity. Here, we show that DARA is able to induce programmed cell death (PCD) of several CD38 positive tumor cell lines when crosslinked via a secondary antibody or Fc gamma receptors (FcγRs). PCD induction by FcγR-expressing cells was observed over a broader DARA concentration range compared to crosslinking mediated by the secondary Ab. We found that activating as well as inhibitory FcγRs are able to induce DARA crosslinking-mediated PCD by comparing DARA efficacy in a peritoneal syngeneic *in vivo* model in FcRγ-chain knockout mice or transgenic NOTAM mice carrying a signaling-inactive FcRγ-chain. In conclusion, our *in vitro* and *in vivo* data show that FcγR-mediated crosslinking of DARA induces PCD of CD38 expressing MM tumor cells, and potentially adds to killing of tumor cells in patients.

Introduction

Programmed cell death (PCD) includes various pathways leading to cell death mediated by an intracellular program. PCD has been demonstrated to contribute to the anti-tumor effect of therapeutic monoclonal antibodies (mAbs). PCD can be induced by mAb binding to its antigen (Ag), as shown for the death-receptor 4 targeting mAb AY4 (1). Binding of this agonistic mAb leads to direct activation of the extrinsic apoptosis pathway. Crosslinking of surface Ags by mAbs may also induce PCD via a non-apoptotic pathway on tumor cells (2-5). This type of PCD was recently demonstrated to correlate with homotypic aggregation of the cells via cytoskeleton reorganization followed by lysosomal targeting and subsequent production of reactive oxygen species (6). PCD induction may be enhanced by crosslinking via a secondary Ab (7-9) or, more physiologically, by Fc gamma receptor (FcγR)-expressing cells (10). This suggests that FcγRs on e.g. tumor-associated leucocytes could provide a crosslinking scaffold for anti-tumor mAbs *in vivo*.

For mAbs targeting Ags from the tumor necrosis factor receptor (TNFR) superfamily it has been shown that their *in vivo* activity, either immunostimulatory effects or PCD induction, depends on binding to the inhibitory FcγRIIb (11-14). PCD induction of tumor cells by drozitumab (human IgG1 DR5 mAb) could also be mediated by crosslinking via activating FcγRs *in vitro* (15). However, drozitumab anti-tumor activity was strongly diminished in FcγRIIb$^{-/-}$ mice which only express activating FcγRs, though still significant compared to the control mAb. A potential contribution of ADCC to anti-tumor activity can, however, not be ruled out in this model. In the absence of activating FcγRs drozitumab anti-tumor activity was not affected, suggesting that FcγRIIb expression alone was sufficient for the anti-tumor effect of drozitumab *in vivo*.

Daratumumab (DARA) is a human IgG1 mAb that binds to CD38, which is expressed at relatively high levels on malignant cells in multiple myeloma (MM) (16). Multiple mechanisms of action have been observed for DARA, including the Fc-dependent effector mechanisms, complement-dependent cytotoxicity (CDC), antibody-dependent cellular cytotoxicity (ADCC) (17) and antibody-dependent cellular phagocytosis (ADCP) (manuscript submitted).

In this study we explored PCD induction on MM cell lines via FcγR-mediated crosslinking of DARA *in vitro*. PCD was defined by morphological changes resulting in clustering of cells, loss of mitochondrial membrane potential

(ΔΨm) and loss of membrane integrity. Phosphatidylserine translocation was included as a marker for the initiation of PCD. To investigate the contribution of the FcγRs in mediating DARA-crosslinking *in vivo*, we explored PCD induction in NOTAM (transgenic mice carrying a signaling-inactive FcRγ-chain) and FcRγ-chain knockout mice. Our results show that both inhibitory and activating FcγRs induced DARA crosslinking leading to phosphatidylserine translocation followed by cell death for a fraction of these cells.

Materials and methods

Cell culture

The MM cell lines UM-9, kindly provided by Prof. H.M. Lokhorst (18), and L363, obtained from the ATCC (Rockville, MD) and gene-marked with GFP and luciferase genes (19), were transduced with human CD38 gene to obtain CD38 expression levels comparable to primary myeloma cells. For this the amphotropic Phoenix packaging cell line (Phoenix Ampho) was transfected, using calcium phosphate precipitation, with the pQCXIN vector carrying the human CD38 gene. These cell lines are referred to as UM9-CD38 and L363-CD38 expressing CD38 in a range of 350,000 ~ 600,000 and 450,000 ~ 800,000 molecules/cell respectively as determined with Qifi analysis (QiFi kit, Dako, Glostrup, Denmark). IIA1.6 cells (mouse pre-B cell line, ATCC) were transfected with human FcγRI (hFcγRI) and human FcRγ-chain as described previously (20) and cells are referred to as IIA1.6-hFcγRI. EL4 cells (mouse lymphoma cell line, ATCC) were retrovirally transduced with GFP-IRES-luciferase construct as described previously (19). Subsequently the pQCXIN vector containing the gene encoding human CD38 was inserted as described for the MM cell lines. Cells were subcloned via limiting dilution resulting in a stable EL4-CD38 clone expressing 225,000 ~ 400,000 CD38 molecules/cell as determined with QuantiBrite analysis (BD biosciences, Franklin Lakes, NJ). All cells were cultured in RPMI 1640 (Life Technologies, Carlsbad, CA), 10% heat-inactivated fetal calf serum (FCS, Bodinco, Alkmaar, The Netherlands), 50 U/ml penicillin (Life Technologies) and 50 µg/ml streptomycin (Life Technologies). Culture medium for the IIA1.6-hFcγRI cells was supplemented with 2.5 µg/ml emthexate (Teva Pharmachemie, Haarlem, The Netherlands) and for the EL4-CD38 cells with 1 mg/ml geneticin (Life Technologies).

Antibodies and reagents

Human IgG1 CD38 mAb DARA was generated by immunization in HuMAb mice and was produced as recombinant protein as described previously (17). DARA-K322A, a Fc-mutant lacking complement activation was generated by mutating the lysine at position 322 to alanine as described previously (21, 22). The human mAb IgG1 b12, specific for the HIV-1 gp120 envelope glycoprotein generated as described previously (23), was included in all experiments as a control mAb. $F(ab')_2$ fragments of rabbit-anti-human IgG (Jackson ImmunoResearch, West Grove, PA) was used as a secondary Ab. $F(ab')_2$ fragments of the mouse FcγRIIb mAb K9.361 (kindly provided by Bioceros, Utrecht, the Netherlands) were generated according to manufacturer's instructions (Thermo Fisher Scientific, Waltham, MA). PE-labeled Annexin-V and viaprobe (7-AAD) were purchased from BD Biosciences and used according to the manufacturer's protocol. Briefly, cells were washed with binding buffer containing 10 mM HEPES (Merck, Darmstadt, Germany), 0.14 M NaCl (Merck) and 2.5 mM $CaCl_2$ (Riedel-de Haen, Seelze, Germany) followed by Annexin-V and 7-AAD staining in binding buffer at room temperature for 15 minutes. Mitochondrial membrane potential (ΔΨm) depolarization was measured with the MitoProbe DilC5(1) kit (Life Technologies), which was used according to the manufacturer's protocol. Briefly, after washing in phosphate buffered saline (PBS, Pharmacy University Medical Center, Utrecht, The Netherlands) cells were incubated for 20 minutes with 3 nM 1,1',3,3,3',3'-hexamethylindodicarbo - cyanine iodide (DilC5(1)) at 37 °C and 5% CO_2. Cells were washed twice with RPMI 1640 medium supplemented with 10% FCS and pen/strep to stop the DilC5(1) reaction. Numbers of cell surface CD38 molecules were determined with mouse-anti-human CD38 (BD Biosciences) and the Qifi kit (DAKO) or QuantiBRITE tubes (BD Biosciences).

CD38 crosslinking in vitro

UM9-CD38 and EL4-CD38 cells were labeled with CFSE (Life Technologies) according to the manufacturer's protocol. CFSE-labeled cells or GFP expressing L363-CD38 cells were seeded at 1.0×10^5 cells per well in 24-wells plates and incubated 30 minutes with varying concentrations of indicated mAb. Cell-bound CD38 Abs were crosslinked either with IIA1.6-hFcγRI or IIA1.6 cells at an effector:target (E:T) ratio of 1:1 or with 5μg/ml secondary Ab. Morphologic changes were visualized using the EVOS microscope (Advanced Microscopy Group, Life Technologies). PCD markers (Annexin-V, 7-AAD and ΔΨm

depolarization) were analyzed after 4 or 24 hours via flow cytometry using a FACS-Canto II (BD Biosciences). Number of $CFSE^+$/Annexin-V^+, $CFSE^+$/Annexin-V^+/7-AAD^+ and $CFSE^+$/DilC5(1)^{low} were calculated using FACS Diva software (BD Biosciences).

Mice

Experiments were performed with 8-19 weeks old FcRγ-chain knock-out ($FcR\gamma^{-/-}$) mice (24) and NOTAM mice (25) on a C57BL/6 background. Mice were bred at the specific pathogen free facility of the Central Animal Laboratory of Utrecht University and all experiments were approved by the local Animal Ethical Committee.

Syngeneic peritoneal mouse model

Mice were injected i.p. with 5×10^6 CFSE-labeled EL4-CD38 cells in 100 µl PBS and, directly after tumor cell inoculation, with 2 µg DARA-K322A or 100 µl PBS. To block FcγRIIb *in vivo*, 50 µg of $F(ab')_2$ fragments of the FcγRIIb mAb K9.361 was injected i.p. 30 minutes prior to tumor cell inoculation (blocking of FcγRIIb was confirmed on peritoneal effector cells via flow cytometry). Following 4h incubation the mice were euthanized and the peritoneum was washed with PBS containing 5 mM EDTA (Sigma-Aldrich, St. Louis, MO). Annexin-V and 7-AAD staining of the $CFSE^+$ EL4-CD38 cells was analysed by flow cytometry as described above.

Statistical analysis

Data analysis was performed using GraphPad Prism, version 5.0 (Graphpad, San Diego, CA). Data were reported as mean ± SD. Differences between groups were analyzed using Student's unpaired t-test or Bonferroni's multiple comparison test (p-value <0.05 was considered statistically significant).

Results

DARA induces PCD in MM cell lines after Ab-mediated crosslinking

We explored whether DARA causes PCD by crosslinking of CD38 on the MM cell lines L363 and UM9. These cell lines were transduced with CD38 to obtain expression levels in the range of those observed for patient MM cells. DARA-

opsonized L363-CD38 and UM9-CD38 cells were incubated for 24h at 37°C with a secondary Ab to induce crosslinking, which resulted in ΔΨm depolarization for both cell lines as shown by loss of DiIC5(1) staining (Fig. 1A). Furthermore, the number of Annexin-V positive cells (Fig. 1B) and 7-AAD positive cells (Fig. 1C) also increased compared to controls. PCD induction was most effective at the lower DARA concentration of 0.1 μg/ml. In the absence of secondary antibody we did not observe an increase of any of the PCD markers studied (data not shown).

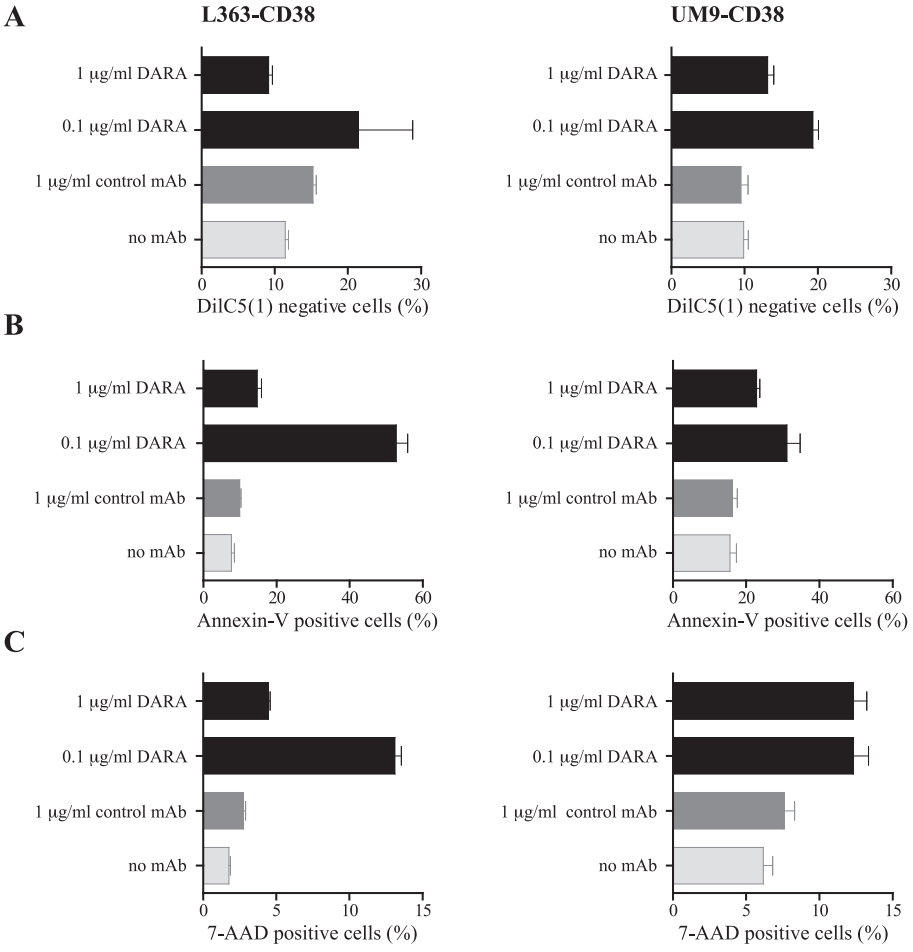

Figure 1. *DARA induces PCD in MM cells after Ab-mediated crosslinking.* PCD induction on GFP$^+$ L363-CD38 (*left panels*) or CFSE-labeled UM9-CD38 (*right panels*) after 24h incubation with indicated concentrations of DARA, control mAb or no mAb in the presence of a secondary Ab. Each bar shows mean ± SD representative of at least two independent experiments. Flow cytometric analysis of ΔΨm depolarization (A), percentage Annexin-V positive cells (B) and percentage 7-AAD positive (dead) cells (C).

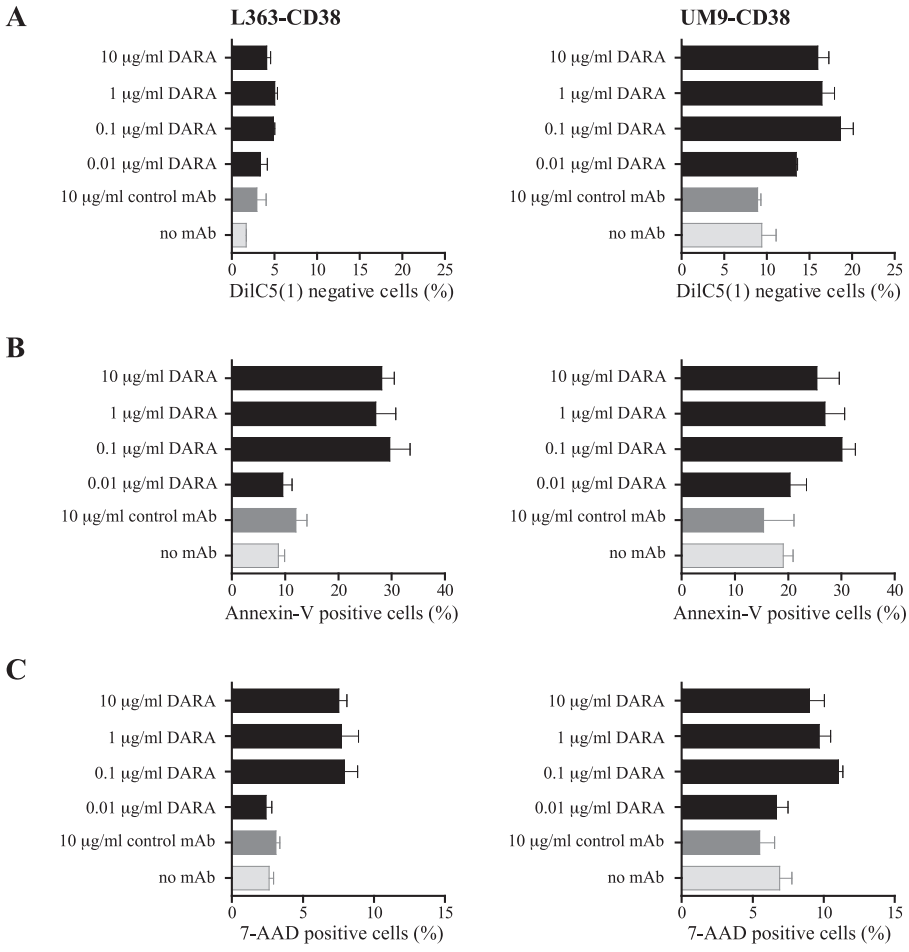

Figure 2. *DARA induces PCD in MM cell lines upon incubation with FcγRI-expressing cells.* GFP$^+$ L363-CD38 (*left panels*) and CFSE-labeled UM9-CD38 (*right panels*) cells were co-cultured with IIA1.6-hFcγRI cells (E:T = 1:1) in the presence of indicated concentration mAb for 24h. Each bar shows mean ± SD representative of three independent experiments. Flow cytometric analysis of ΔΨm depolarization (A), percentage Annexin-V positive cells (B) and percentage 7-AAD positive (dead) cells (C).

DARA induces PCD in MM cell lines after FcγRI-mediated crosslinking

To demonstrate DARA crosslinking-mediated PCD in a more physiological setting, we explored whether cells expressing FcγRs could induce PCD of DARA-opsonized target cells. We used a hFcγRI-transduced murine B-cell lymphoma cell line, IIA1.6-hFcγRI, which does not induce FcγR-mediated cell killing by ADCC (data not shown). DARA-opsonized L363-CD38 and UM9-CD38 cells were incubated for 24h with the IIA1.6-hFcγRI cells and subsequently analyzed by flow cytometry for the PCD markers. The incubation of DARA-opsonized

cells with human FcγRI-expressing cells resulted in ΔΨm depolarization (Fig. 2A), increase of Annexin-V positivity (Fig. 2B) and 7-AAD positive cells (Fig. 2C), confirming PCD induction via FcγR-expressing cells. As a control, incubation of DARA-opsonized L363-CD38 and UM9-CD38 cells with hFcγRI-negative IIA1.6 cells did not induce an increase of any of the PCD markers studied (data not shown), indicating that the effect is FcγR-mediated. Interestingly, the DARA concentration for effective hFcγRI-mediated PCD induction is observed over a broad concentration range, 0.1-10 µg/ml.

Incubation of L363-CD38 cells with DARA and a secondary Ab induced homotypic aggregation (Fig. 3, *left and middle panel*), which was previously observed to correlate with PCD for CD20 mAbs (2, 4, 26). Incubation of DARA-opsonized L363-CD38 cells with IIA1.6-hFcγRI cells resulted in similar morphologic changes (Fig. 3, *right panel*). In line with the results obtained with flow cytometry, FcγR-mediated clustering was effective over a broad concentration range, while secondary Ab-mediated clustering was restricted to a narrow concentration range (Fig. 3).

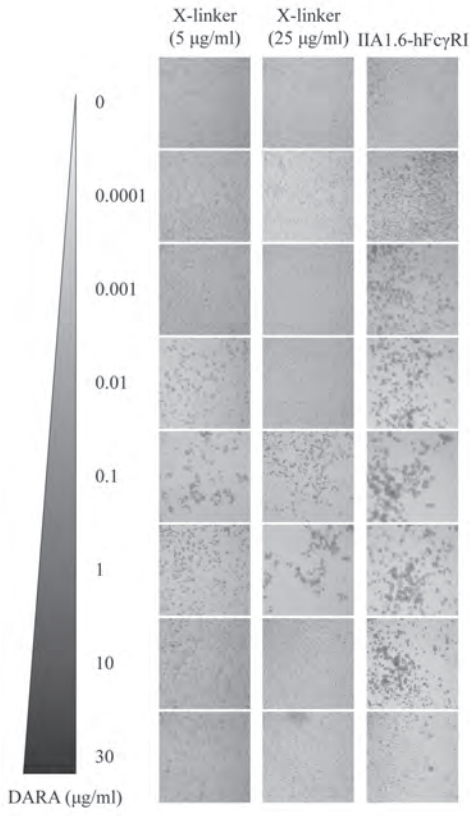

Figure 3. *Clustering of L363-CD38 after DARA crosslinking.* Bright field images of L363-CD38 cells after 24h incubation with a concentration range DARA in the presence of 5 or 25 µg/ml secondary Ab (*left and middle panel*) or IIA1.6-hFcγRI cells (E:T = 1:1) (*right panel*).

EL4-CD38 cells are sensitive for PCD induction after DARA crosslinking

To study FcγR-mediated DARA crosslinking *in vivo* in a syngeneic peritoneal mouse model, mouse EL4 lymphoma cells were transduced with human CD38. We first validated whether the EL4-CD38 cells were sensitive for PCD induction by DARA *in vitro*. Secondary Ab as well as the IIA1.6-hFcγRI cells supported induction of PCD in EL4-CD38 cells by DARA (Fig. 4A, B and Supplemental Fig. 1). FcγRI-mediated DARA crosslinking is also on the EL4-CD38 cells effective over a broad concentration range, while Ab-mediated crosslinking was restricted to a narrow window. Therefore, the DARA dose to study PCD induction *in vivo* was not expected to be critical.

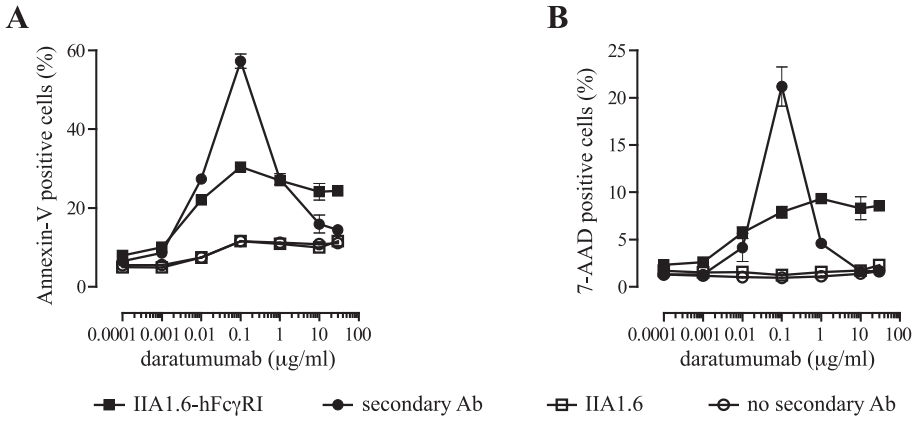

Figure 4. *EL4-CD38 cells sensitive for PCD induction after DARA crosslinking.* CFSE-labeled EL4-CD38 cells were co-cultured for 4h with a secondary Ab or IIA1.6-hFcγRI cells at an E:T ratio of 1:1 in the presence of a DARA concentration range. Flow cytometric analysis of percentage Annexin-V positive cells (A) or 7-AAD positive cells (B). Each line shows mean ± SD representative of two independent experiments.

Both inhibitory and activating FcγR can induce DARA crosslinking in vivo

To study the role of FcγR-mediated DARA-induced PCD *in vivo,* we made use of NOTAM and FcRγ-chain knockout (FcRγ$^{-/-}$) mice (Fig. 5A). NOTAM mice express an inactive FcR-associated γ-chain resulting in normal surface expression of all activating FcγRs, without signaling capacity (25). Leucocytes in the NOTAM mice are therefore capable of FcγR-mediated Ab crosslinking, without inducing cytotoxicity via ADCC. Leucocytes in the FcRγ$^{-/-}$ mice lack expression of all activating FcγRs and solely express the inhibitory FcγRIIb. To exclude *in vivo* CDC activity as a mechanism of action (MoA), we generated a Fc mutant of DARA in which the lysine at position 322 was mutated to alanine (referred to

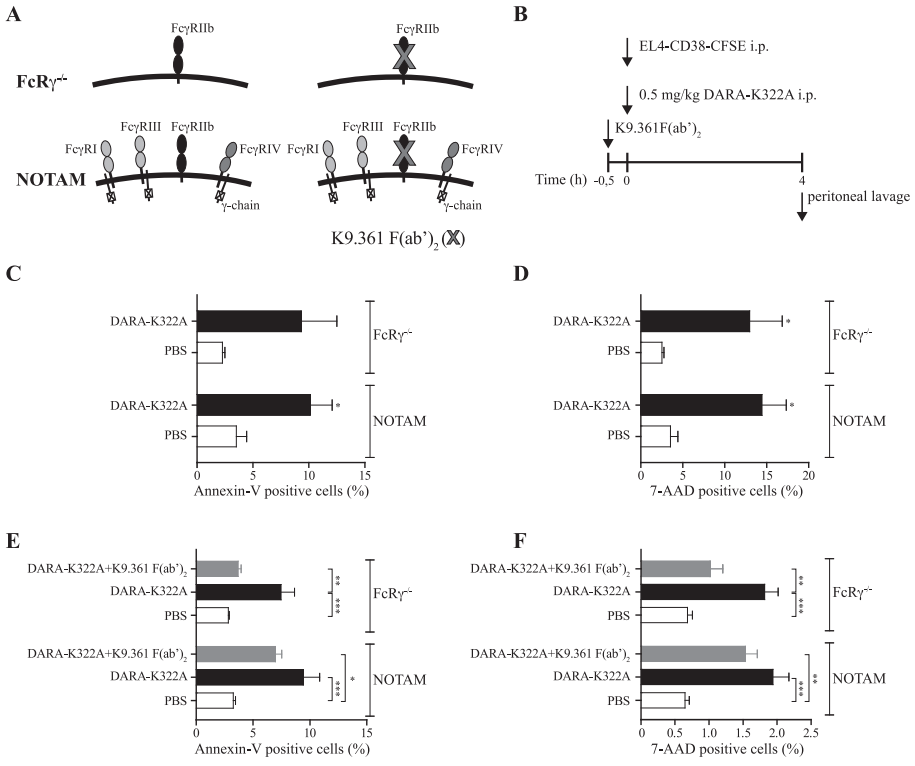

Figure 5. *In vivo PCD induction via both activating and the inhibitory FcγR.* NOTAM and FcRγ$^{-/-}$ mice were, as indicated, treated with FcγRIIb blocking F(ab')$_2$ fragments (K9.361 F(ab')$_2$) 30 min. prior to tumor cell inoculation (A). Subsequently, 5×10^6 CFSE labeled EL4-CD38 cells were inoculated i.p. followed by DARA-K322A (2 µg/mouse) or PBS treatment. After 4h tumor cells in the peritoneal wash were analyzed by flow cytometry (B). (C, E) Percentage Annexin-V positive cells. (D, F) Percentage 7-AAD positive cells. (4-6 mice/group; * p<0.05, ** p<0.01 unpaired t-test (C, E) or Bonferroni's multiple comparison test (D, F)).

as DARA-K322A). K322 was shown to be a critical residue for C1q binding and complement activation (27, 28) and we confirmed that the K322A mutation also leads to strongly reduced binding of mouse C1q (22). The K322A mutation itself did not affect FcγR-mediated PCD induction (Supplemental Fig. 2). CFSE-labeled EL4-CD38 cells were inoculated i.p. directly followed by treatment with 2 µg/mouse DARA-K322A. After 4h, the CFSE-labeled EL4-CD38 cells, harvested by peritoneal flush, were analyzed via flow cytometry for Annexin-V and 7-AAD staining (Fig. 5B). DARA-K322A induced an increase of Annexin-V positive cells and significantly increased the number of 7-AAD positive cells following 4h incubation in the FcRγ$^{-/-}$ mice (Fig. 5C, D, top bars). This indicates that DARA-K322A crosslinking via the inhibitory FcγRIIb can induce PCD *in vivo*. Also in

NOTAM mice, DARA-K322A treatment significantly increased the number of Annexin-V positive and 7-AAD positive cells (Fig. 5C, D, *bottom bars*). To explore whether PCD induction in the NOTAM mice occurred via both the activating and the inhibitory FcγRs, mice were pre-treated with FcγRIIb blocking $F(ab')_2$ fragments of mAb K9.361 (Fig. 5A). As expected, in FcR$\gamma^{-/-}$ mice, FcγR-mediated PCD via DARA-K322A was abolished after blocking FcγRIIb (Fig. 5E, F, top bars). In the NOTAM mice, significant PCD induction was still observed after blocking FcγRIIb, demonstrating that next to the inhibitory FcγRIIb, also the activating FcγRs can mediate *in vivo* DARA crosslinking leading to PCD (Fig. 5E, F, *bottom bars*).

Discussion

The aim of this study was to investigate whether DARA can induce PCD in CD38-expressing MM cells after crosslinking by FcγR-expressing cells. We demonstrated induction of PCD on MM cell lines *in vitro* by DARA, crosslinked via FcγRI. Using the non-complement-binding DARA-K322A mutant in a syngeneic peritoneal mouse model in NOTAM and FcR$\gamma^{-/-}$ mice, we showed that DARA-induced PCD can also occur *in vivo* and may be mediated by the inhibitory FcγRIIb as well as by activating FcγRs.

DARA-induced PCD was characterized by four phenotypic characteristics; phosphatidylserine translocation, loss of membrane integrity, loss of mitochondrial potential and morphological changes resulting in clustering of cells, and induced either by crosslinking secondary antibodies or cell surface-expressed FcγR. Crosslinking of DARA mediated by both secondary Ab and FcγRs induced PCD in the MM cell lines L363-CD38 and UM9-CD38, FcγR-mediated crosslinking was effective over a broader concentration range. This difference may be explained by a narrow optimum concentration of CD38 mAb required for secondary antibody crosslinking, while FcγR-mediated crosslinking may be less concentration-dependent as a result e.g. of diverse FcγR densities expressed on cells.

Loss of the mitochondrial membrane potential irreversibly results in cell death (29), while phosphatidylserine translocation is a reversible process (30). Indeed, the number of cells that lost the mitochondrial membrane potential corresponds with the number of 7-AAD positive cells, whereas the number of

Annexin-V positive cells was usually higher. However, the relatively high number of Annexin-V positive cells, indicating phosphatidylserine translocation, may substantially enhance efficacy of other MoA of DARA. Phosphatidylserine translocation may opsonize cells for phagocytosis, since phosphatidylserine is recognized by scavenger receptors on macrophages. We previously observed DARA to be highly potent in phagocytosis induction (manuscript submitted), therefore phosphatidylserine translocation induced by FcγR-mediated crosslinking could potentially further increase phagocytosis. This may well represent an effective MoA under conditions when complement is depleted or the NK cells are exhausted (31, 32).

DARA-induced PCD was further characterized by morphologic changes resulting in clustering of the cells. This cell clustering was demonstrated to correlate with PCD induction for several therapeutic mAbs (2, 4, 6, 33, 34). In literature there is debate whether the observed cell death associated with cell clustering is actually caused by mAb-induced PCD, and not an artifact of disruption of these cell clusters by analytical methods (35). To address this question, analysis of cell death without disrupting the cell clusters have been performed and confirmed PCD induction by these mAbs (9, 36).

The *in vivo* contribution of DARA-induced PCD mediated via FcγR-dependent crosslinking was explored in a syngeneic peritoneal mouse model. To exclude a possible role for CDC we made use of a K322A mutant of DARA. When treating FcRγ$^{-/-}$ mice, which only express the inhibitory FcγRIIb, with the DARA-K322A mutant, a significant induction of Annexin-V positive and 7-AAD positive tumor cells was observed. Blocking of FcγRIIb in this model abolished the DARA-K322A induced effect, confirming *in vivo* PCD induction to be FcγR-dependent and feasible via FcγRIIb alone. DARA-induced PCD via crosslinking by the inhibitory FcγRIIb might be relevant at tumor sites where only FcγRIIb expressing cells, e.g. B-cells or liver sinusoidal endothelial cells reside. Also, primary mature MM cells have been shown to express FcγRIIb (37), suggesting that the MM cells might also mediate DARA crosslinking themselves without a requirement for accessory cells, as was shown for CD40 mAb (15). PCD may therefore be an effective MoA of DARA in bulky tumors to which access of effector cells may be limited (38) or under conditions of immune-suppression due to high MM tumor load or concomitant therapy in the bone marrow.

NOTAM mice express all FcγRs, however, due to their deficient γ-chain signaling, leucocytes in the NOTAM mice are unable to induce cytotoxicity via

ADCC or ADCP (25). A significant induction of Annexin-V positive and 7-AAD positive cells was also observed in NOTAM mice. Blocking of FcγRIIb in NOTAM mice did not completely abolish induction of PCD, as after DARA treatment, still a significant induction of Annexin-V positive and 7-AAD positive cells was observed. Accordingly, we hereby show, for the first time, *in vivo* induction of PCD by an Ab, which is mediated via crosslinking by the activating FcγRs.

FcγR-mediated crosslinking may be induced via various FcγR-expressing cells like polymorphonuclear cells (PMN), NK-cells, monocytes, macrophages, dendritic cells, platelets, B-cells, and endothelial cells. In this study, we observed after 4h both F4/80$^+$ macrophages as well as GR1$^+$PMNs in the peritoneal cavity (data not shown), suggesting a role for both effector cell types in DARA-induced PCD.

In summary, we have shown *in vitro* PCD induction by DARA via FcγR-mediated crosslinking on CD38 expressing MM cell lines. We demonstrated *in vivo* that the inhibitory FcγR as well as the activating FcγRs facilitate crosslinking of DARA on tumor cells to engage PCD induction. From these findings, we conclude that PCD induction via FcγR-mediated crosslinking is a MoA for DARA. However, the underlying mechanism of the PCD induction and the contribution to the overall anti-tumor effect *in vivo* requires further investigation.

Acknowledgements

The authors express their thanks to Daniëlle Jacobs and Lukas Oomen for technical assistance and to Michel de Weers for scientific input.

References

1. Lee, B. S., S. U. Kang, H. S. Hwang, Y. S. Kim, E. S. Sung, Y. S. Shin, Y. C. Lim, and C. H. Kim. 2012. An agonistic antibody to human death receptor 4 induces apoptotic cell death in head and neck cancer cells through mitochondrial ROS generation. *Cancer Lett* 322:45-57.
2. Alduaij, W., A. Ivanov, J. Honeychurch, E. J. Cheadle, S. Potluri, S. H. Lim, K. Shimada, C. H. T. Chan, A. Tutt, S. A. Beers, M. J. Glennie, M. S. Cragg, and T. M. Illidge. 2011. Novel type II anti-CD20 monoclonal antibody (GA101) evokes homotypic adhesion and actin-dependent, lysosome-mediated cell death in B-cell malignancies. *Blood* 117:4519-4529.
3. Cerisano, V., Y. Aalto, S. Perdichizzi, G. Bernard, M. C. Manara, S. Benini, G. Cenacchi, P. Preda, G. Lattanzi, B. Nagy, S. Knuutila, M. P. Colombo, A. Bernard, P. Picci, and K. Scotlandi. 2004. Molecular mechanisms of CD99-induced caspase-independent cell death and cell-cell adhesion in Ewing's sarcoma cells: actin and zyxin as key intracellular mediators. *Oncogene* 23:5664-5674.
4. Ivanov, A., S. A. Beers, C. A. Walshe, J. Honeychurch, W. Alduaij, K. L. Cox, K. N. Potter, S. Murray, C. H. Chan, T. Klymenko, J. Erenpreisa, M. J. Glennie, T. M. Illidge, and M. S. Cragg. 2009. Monoclonal antibodies directed to CD20 and HLA-DR can elicit homotypic adhesion followed by lysosome-mediated cell death in human lymphoma and leukemia cells. *J Clin Invest* 119:2143-2159.
5. Mateo, V., E. J. Brown, G. Biron, M. Rubio, A. Fischer, F. L. Deist, and M. Sarfati. 2002. Mechanisms of CD47-induced caspase-independent cell death in normal and leukemic cells: link between phosphatidylserine exposure and cytoskeleton organization. *Blood* 100:2882-2890.
6. Honeychurch, J., W. Alduaij, M. Azizyan, E. J. Cheadle, H. Pelicano, A. Ivanov, P. Huang, M. S. Cragg, and T. M. Illidge. 2012. Antibody-induced nonapoptotic cell death in human lymphoma and leukemia cells is mediated through a novel reactive oxygen species-dependent pathway. *Blood* 119:3523-3533.
7. Chaouchi, N., A. Vazquez, P. Galanaud, and C. Leprince. 1995. B cell antigen receptor-mediated apoptosis. Importance of accessory molecules CD19 and CD22, and of surface IgM cross-linking. *J Immunol* 154:3096-3104.
8. Ghetie, M. A., E. M. Podar, A. Ilgen, B. E. Gordon, J. W. Uhr, and E. S. Vitetta. 1997. Homodimerization of tumor-reactive monoclonal antibodies markedly increases their ability to induce growth arrest or apoptosis of tumor cells. *Proc Natl Acad Sci U S A* 94:7509-7514.
9. Mattes, M. J., R. B. Michel, D. M. Goldenberg, and R. M. Sharkey. 2009. Induction of apoptosis by cross-linking antibodies bound to human B-lymphoma cells: expression of Annexin V binding sites on the antibody cap. *Cancer Biother Radiopharm* 24:185-193.
10. Shan, D., J. A. Ledbetter, and O. W. Press. 1998. Apoptosis of malignant human B cells by ligation of CD20 with monoclonal antibodies. *Blood* 91:1644-1652.
11. Chuntharapai, A., K. Dodge, K. Grimmer, K. Schroeder, S. A. Marsters, H. Koeppen, A. Ashkenazi, and K. J. Kim. 2001. Isotype-dependent inhibition of tumor growth in vivo by monoclonal antibodies to death receptor 4. *J Immunol* 166:4891-4898.
12. Li, F., and J. V. Ravetch. 2011. Inhibitory Fcgamma receptor engagement drives adjuvant and anti-tumor activities of agonistic CD40 antibodies. *Science* 333:1030-1034.
13. White, A. L., H. T. Chan, A. Roghanian, R. R. French, C. I. Mockridge, A. L. Tutt, S. V. Dixon, D. Ajona, J. S. Verbeek, A. Al-Shamkhani, M. S. Cragg, S. A. Beers, and M. J. Glennie. 2011. Interaction with FcgammaRIIB is critical for the agonistic activity of anti-CD40 monoclonal antibody. *J Immunol* 187:1754-1763.
14. Xu, Y., A. J. Szalai, T. Zhou, K. R. Zinn, T. R. Chaudhuri, X. Li, W. J. Koopman, and R. P. Kimberly. 2003. Fc gamma Rs modulate cytotoxicity of anti-Fas antibodies: implications for agonistic antibody-based therapeutics. *J Immunol* 171:562-568.
15. Wilson, N. S., B. Yang, A. Yang, S. Loeser, S. Marsters, D. Lawrence, Y. Li, R. Pitti, K. Totpal, S. Yee, S. Ross, J. M. Vernes, Y. Lu, C. Adams, R. Offringa, B. Kelley, S. Hymowitz, D. Daniel, G. Meng, and A. Ashkenazi. 2011. An Fcgamma receptor-dependent mechanism drives antibody-mediated target-receptor signaling in cancer cells. *Cancer Cell* 19:101-113.
16. Lin, P., R. Owens, G. Tricot, and C. S. Wilson. 2004. Flow cytometric immunophenotypic analysis of 306 cases of multiple myeloma. *Am J Clin Pathol* 121:482-488.

17. de Weers, M., Y. T. Tai, M. S. van der Veer, J. M. Bakker, T. Vink, D. C. Jacobs, L. A. Oomen, M. Peipp, T. Valerius, J. W. Slootstra, T. Mutis, W. K. Bleeker, K. C. Anderson, H. M. Lokhorst, J. G. van de Winkel, and P. W. Parren. 2011. Daratumumab, a novel therapeutic human CD38 monoclonal antibody, induces killing of multiple myeloma and other hematological tumors. *J Immunol* 186:1840-1848.

18. Kuipers, J., J. W. Vaandrager, D. O. Weghuis, P. L. Pearson, J. Scheres, H. M. Lokhorst, H. Clevers, and B. J. Bast. 1999. Fluorescence in situ hybridization analysis shows the frequent occurrence of 14q32.3 rearrangements with involvement of immunoglobulin switch regions in myeloma cell lines. *Cancer Genet Cytogenet* 109:99-107.

19. Rozemuller, H., E. van der Spek, L. H. Bogers-Boer, M. C. Zwart, V. Verweij, M. Emmelot, R. W. Groen, R. Spaapen, A. C. Bloem, H. M. Lokhorst, T. Mutis, and A. C. Martens. 2008. A bioluminescence imaging based in vivo model for preclinical testing of novel cellular immunotherapy strategies to improve the graft-versus-myeloma effect. *Haematologica* 93:1049-1057.

20. Van Vugt, M. J., I. E. Van den Herik-Oudijk, and J. G. Van de Winkel. 1998. FcgammaRIa-gamma-chain complexes trigger antibody-dependent cell-mediated cytotoxicity (ADCC) in CD5+ B cell/macrophage IIA1.6 cells. *Clin Exp Immunol* 113:415-422.

21. Overdijk, M. B., S. Verploegen, A. Ortiz Buijsse, T. Vink, J. H. Leusen, W. K. Bleeker, and P. W. Parren. 2012. Crosstalk between human IgG isotypes and murine effector cells. *J Immunol* 189:3430-3438.

22. Overdijk, M. B., S. Verploegen, J. H. van den Brakel, J. J. Lammerts van Bueren, T. Vink, J. G. van de Winkel, P. W. Parren, and W. K. Bleeker. 2011. Epidermal Growth Factor Receptor (EGFR) Antibody-Induced Antibody-Dependent Cellular Cytotoxicity Plays a Prominent Role in Inhibiting Tumorigenesis, Even of Tumor Cells Insensitive to EGFR Signaling Inhibition. *J Immunol* 187:3383-3390.

23. Burton, D. R., J. Pyati, R. Koduri, S. J. Sharp, G. B. Thornton, P. W. Parren, L. S. Sawyer, R. M. Hendry, N. Dunlop, P. L. Nara, and et al. 1994. Efficient neutralization of primary isolates of HIV-1 by a recombinant human monoclonal antibody. *Science* 266:1024-1027.

24. Takai, T., M. Li, D. Sylvestre, R. Clynes, and J. V. Ravetch. 1994. FcR gamma chain deletion results in pleiotrophic effector cell defects. *Cell* 76:519-529.

25. de Haij, S., J. H. Jansen, P. Boross, F. J. Beurskens, J. E. Bakema, D. L. Bos, A. Martens, J. S. Verbeek, P. W. Parren, J. G. van de Winkel, and J. H. Leusen. 2010. In vivo cytotoxicity of type I CD20 antibodies critically depends on Fc receptor ITAM signaling. *Cancer Res* 70:3209-3217.

26. Chan, H. T., D. Hughes, R. R. French, A. L. Tutt, C. A. Walshe, J. L. Teeling, M. J. Glennie, and M. S. Cragg. 2003. CD20-induced lymphoma cell death is independent of both caspases and its redistribution into triton X-100 insoluble membrane rafts. *Cancer Res* 63:5480-5489.

27. Duncan, A. R., and G. Winter. 1988. The binding site for C1q on IgG. *Nature* 332:738-740.

28. Idusogie, E. E., L. G. Presta, H. Gazzano-Santoro, K. Totpal, P. Y. Wong, M. Ultsch, Y. G. Meng, and M. G. Mulkerrin. 2000. Mapping of the C1q binding site on rituxan, a chimeric antibody with a human IgG1 Fc. *J Immunol* 164:4178-4184.

29. Zamzami, N., P. Marchetti, M. Castedo, C. Zanin, J. L. Vayssiere, P. X. Petit, and G. Kroemer. 1995. Reduction in mitochondrial potential constitutes an early irreversible step of programmed lymphocyte death in vivo. *J Exp Med* 181:1661-1672.

30. Henson, P. M., D. L. Bratton, and V. A. Fadok. 2001. The phosphatidylserine receptor: a crucial molecular switch? *Nat Rev Mol Cell Biol* 2:627-633.

31. Bhat, R., and C. Watzl. 2007. Serial killing of tumor cells by human natural killer cells--enhancement by therapeutic antibodies. *PLoS One* 2:e326.

32. Beurskens, F. J., M. A. Lindorfer, M. Farooqui, P. V. Beum, P. Engelberts, W. J. M. Mackus, P. W. H. I. Parren, A. Wiestner, and R. P. Taylor. 2012. Exhaustion of Cytotoxic Effector Systems May Limit Monoclonal Antibody-Based Immunotherapy in Cancer Patients. *The Journal of Immunology* 188:3532-3541.

33. Mössner, E., P. Brünker, S. Moser, U. Püntener, C. Schmidt, S. Herter, R. Grau, C. Gerdes, A. Nopora, E. van Puijenbroek, C. Ferrara, P. Sondermann, C. Jäger, P. Strein, G. Fertig, T. Friess, C. Schüll, S. Bauer, J. Dal Porto, C. Del Nagro, K. Dabbagh, M. J. S. Dyer, S. Poppema, C. Klein, and P. Umaña. 2010. Increasing the efficacy of CD20 antibody therapy through the engineering of a new type II anti-CD20 antibody with enhanced direct and immune effector cell–mediated B-cell cytotoxicity. *Blood* 115:4393-4402.

34. Bologna, L., E. Gotti, M. Manganini, A. Rambaldi, T. Intermesoli, M. Introna, and J. Golay. 2011. Mechanism of action of type II, glycoengineered, anti-CD20 monoclonal antibody GA101 in B-chronic lymphocytic leukemia whole blood assays in comparison with rituximab and alemtuzumab. *J Immunol* 186:3762-3769.

35. Golay, J., L. Bologna, P. A. Andre, F. Buchegger, J. P. Mach, L. Boumsell, and M. Introna. 2010. Possible misinterpretation of the mode of action of therapeutic antibodies in vitro: homotypic adhesion and flow cytometry result in artefactual direct cell death. *Blood* 116:3372-3373; author reply 3373-3374.

36. Cragg, M. S., W. Alduaij, C. Klein, P. Umana, M. J. Glennie, and T. M. Illidge. 2010. Response: novel lysosomal-dependent cell death following homotypic adhesion occurs within cell aggregates. *Blood* 116:3373-3374.

37. Zheng, X., S. Abroun, K. Otsuyama, H. Asaoku, and M. M. Kawano. 2006. Heterogeneous expression of CD32 and CD32-mediated growth suppression in human myeloma cells. *Haematologica* 91:920-928.

38. Gong, Q., Q. Ou, S. Ye, W. P. Lee, J. Cornelius, L. Diehl, W. Y. Lin, Z. Hu, Y. Lu, Y. Chen, Y. Wu, Y. G. Meng, P. Gribling, Z. Lin, K. Nguyen, T. Tran, Y. Zhang, H. Rosen, F. Martin, and A. C. Chan. 2005. Importance of cellular microenvironment and circulatory dynamics in B cell immunotherapy. *J Immunol* 174:817-826.

Supplemental Figures

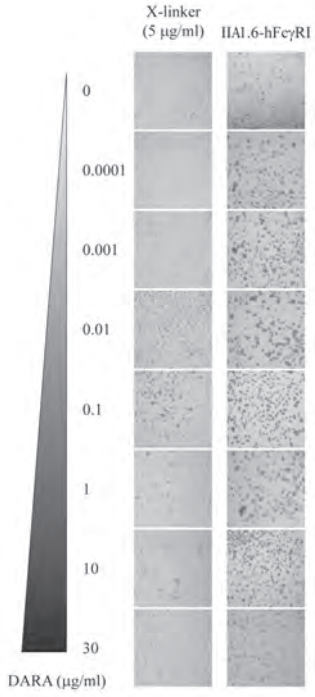

Supplemental Figure 1. Clustering of EL4-CD38 after DARA crosslinking. Bright field images of EL4-CD38 cells after 24h incubation with a concentration range DARA in the presence of 5 µg/ml secondary Ab or IIA1.6-hFcγRI cells (E:T 1:1).

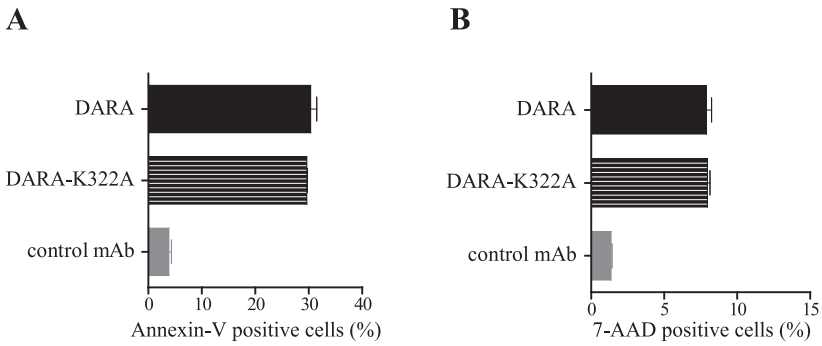

Supplemental Figure 2. DARA-K322A mutation is not affecting FcγR-mediated PCD induction. CFSE labeled EL4-CD38 cells were co-cultured for 4h with IIA1.6-hFcγRI cells at an E:T ratio of 1:1 in the presence of a fixed mAb concentration of 0.1 µg/ml. Flow cytometric analysis of percentage Annexin-V positive cells (A) or 7-AAD positive cells (B). Each bar shows mean ± SD representative of at least two independent experiments.

6

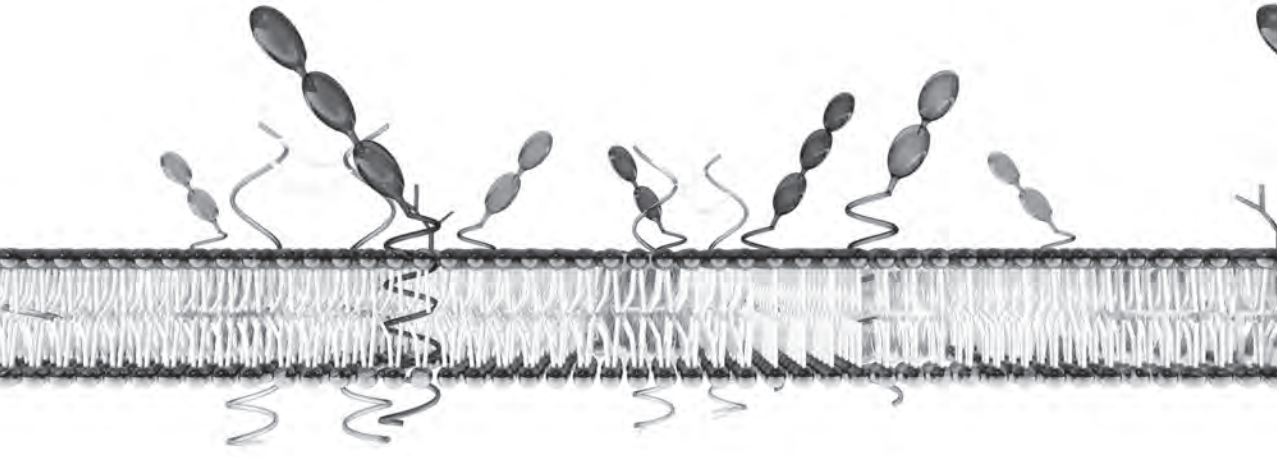

Epidermal growth factor receptor (EGFR) antibody-induced antibody-dependent cellular cytotoxicity plays a prominent role in inhibiting tumorigenesis, even of tumor cells insensitive to EGFR signaling inhibition

Marije B. Overdijk[*], Sandra Verploegen[*], Jeroen H. van den Brakel[*], Jeroen J. Lammerts van Bueren[*], Tom Vink[*], Jan G.J. van de Winkel[*†], Paul W.H.I. Parren[*] and Wim K. Bleeker[*]

[*]Genmab, Utrecht, The Netherlands; [†]Immunotherapy Laboratory, Department of Immunology, University Medical Center, Utrecht, The Netherlands.

The Journal of Immunology, 2011, 187: 3383-3390

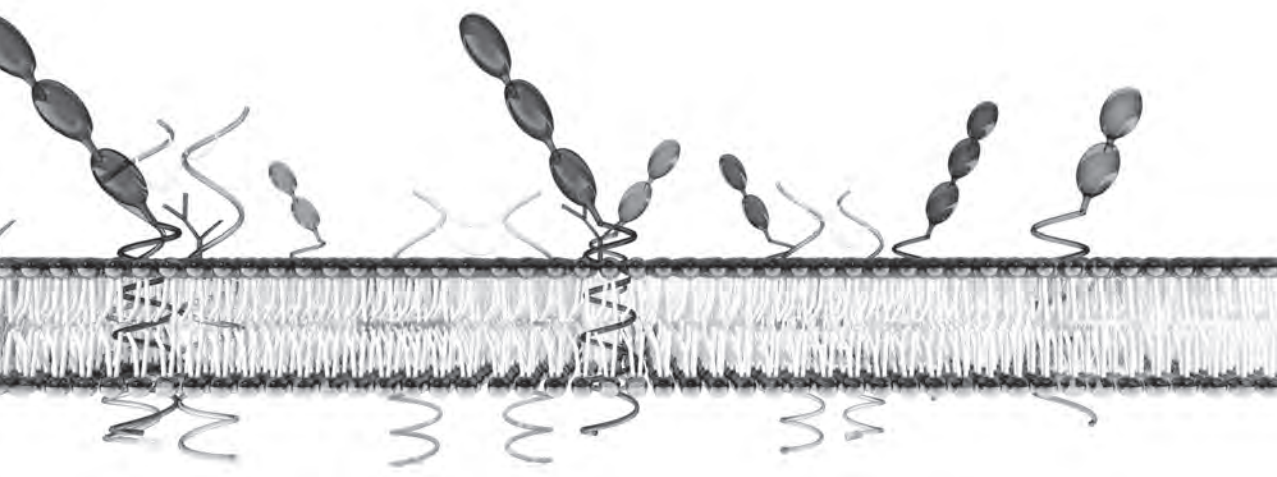

Abstract

Antibody-dependent cellular cytotoxicity (ADCC) is recognized as a prominent cytotoxic mechanism for therapeutic mAbs *in vitro*. However, the contribution of ADCC to *in vivo* efficacy, particularly for treatment of solid tumors, is still poorly understood. For zalutumumab, a therapeutic epidermal growth factor receptor (EGFR)-specific mAb currently in clinical development, previous studies have indicated signaling inhibition and ADCC induction as important therapeutic mechanisms of action. To investigate the *in vivo* role of ADCC, a panel of EGFR-specific mAbs lacking specific functionalities was generated. By comparing zalutumumab with mAb 018, an EGFR-specific mAb that induced ADCC with similar potency, but did not inhibit signaling, we observed that ADCC alone was insufficient for efficacy against established A431 xenografts. Interestingly, however, both zalutumumab and mAb 018 prevented tumor formation upon early treatment in this model. Zalutumumab and mAb 018 also completely prevented outgrowth of lung metastases, in A431 and MDA-MB-231-luc-D3H2LN experimental metastasis models, already when given at nonsaturating doses. Finally, tumor growth of mutant KRAS-expressing A431 tumor cells, which were resistant to EGFR signaling inhibition, was completely prevented by early treatment with zalutumumab and mAb 018, whereas ADCC-crippled N297Q-mutated variants of both mAbs did not show any inhibitory effects. In conclusion, ADCC induction by EGFR-specific mAbs represents an important mechanism of action in preventing tumor outgrowth or metastasis *in vivo,* even of cancers insensitive to EGFR signaling inhibition.

Introduction

Monoclonal Abs targeting cancer cells represent an important class of drugs whose action depends on the engagement of multiple mechanisms of action (MoA). First, mAbs may block target functionality via, for example, receptor downmodulation or ligand blockade. Second, mAbs can induce immune effector functions such as complement-mediated cytotoxicity (CDC) or antibody-dependent cellular cytotoxicity (ADCC). Many studies have shown *in vitro* that therapeutic mAbs can effectively induce ADCC (1-5). The *in vivo* relevance of *in vitro* observed ADCC activity is difficult to delineate because more than one MoA can be involved in the *in vivo* anti-tumor effects of therapeutic mAbs.

Evidence for the role of ADCC was gained from studies on FcγR polymorphisms, which influence the affinity of FcγR for IgG, in patients, in relation to mAb efficacy. *In vitro* studies showed that effector cells expressing the high-affinity FcγRIIIa-158V/V genotype induce higher levels of target cell killing with rituximab (MabThera, anti-CD20) compared with effector cells expressing the low-affinity FcγRIIIa-158F/F genotype (6). Clinical observations in non-Hodgkin's lymphoma patients showed rituximab to be most efficient in patients with the high-affinity FcγRIIIa-158V/V genotype (7, 8). Additionally, metastatic breast cancer patients treated with trastuzumab (Herceptin, anti-HER2) showed that patients with the FcγRIIIa-158V/V genotype responded better to therapy (9). These clinical studies indicate that ADCC represents a relevant MoA for rituximab and trastuzumab *in vivo*. For cetuximab (Erbitux, anti-epidermal growth factor receptor [EGFR]) contradictory results have been published on the importance of ADCC as MoA in metastatic colorectal cancer patients. Zhang et al. (10) showed that cetuximab-treated patients with low-affinity FcγRIIIa genotypes had longer progression-free survival than did high-affinity carriers, whereas Bibeau et al. (11) showed the opposite, that is, patients with high-affinity FcγRIIIa genotypes had longer progression-free survival. The reason for the discrepancy between these two studies regarding FcγRIIIa polymorphism and progression-free survival remains unclear.

Murine xenograft models have been crucial for establishing ADCC as a MoA. Clynes et al. (12) demonstrated the importance of ADCC for efficacy of rituximab and trastuzumab using FcR γ-chain$^{-/-}$ mice, which have no functional activating FcγR. No anti-tumor effect of the mAbs was observed in these mice, demonstrating the importance of IgG-FcγR interactions in inhibition of tumor growth.

Currently, due to the discrepancy in clinical results for cetuximab, it remains to be established whether ADCC induction contributes to the *in vivo* efficacy of EGFR-specific mAbs. The present study addresses the *in vivo* MoA of zalutumumab, a human IgG1 mAb specific for human EGFR, previously demonstrated to have a dual MoA namely signaling inhibition and ADCC (13). To distinguish ADCC induction from signaling inhibition we generated a matched set of EGFR-specific mAbs, including one mAb with ADCC induction and one mAb with signaling inhibition as the sole MoA. We studied the effects of this mAb panel in several mouse tumor xenograft models, mimicking either metastatic colonization or solid tumor growth. Using these tools, we obtained a better insight into when, where, and at what mAb dose, ADCC induction plays a role in the treatment of solid tumors with EGFR-specific mAbs.

Materials and Methods

Cell lines

A431 cells (epidermoid cell line), were obtained from DSMZ (Braunschweig, Germany; cell line no. ACC 91). The A431-luciferase clone L18 cell line (further referred to as A431-luc) was generated by stable transfection of the A431 cells with gWIZ luciferase (construct from Gene Therapy Systems, San Diego). MDA-MB-231-luc-D3H2LN cells (adenocarcinoma, mammary gland, further referred to as MDA-MB-231-luc) were obtained from Caliper Life Sciences (Hopkinton, MA). A431-KRAS4b^{G12V} cells were provided by Thomas Valerius [University Hospital Schleswig-Holstein and Christian-Albrechts-University Kiel, Kiel, Germany (14)]. A431 cells were cultured in RPMI 1640 medium (Lonza, Verviers, Belgium), supplemented with 10% heat-inactivated Cosmic Calf Serum (CCS) (HyClone, Logan, UT), 50 IU/ml penicillin, and 50 μg/ml streptomycin (Lonza). The growth medium for the A431-KRAS4b^{G12V} cells was supplemented with 0.7 mg/ml hygromycin B (Invitrogen, Carlsbad, CA). MDA-MB-231-luc cells were cultured in DMEM medium (Lonza), supplemented with 10% heat-inactivated CCS, 50 IU/ml penicillin, 50 μg/ml streptomycin, 1 mM sodium pyruvate (Lonza), and 0.1 mM nonessential amino acids (Invitrogen). Cells were detached with 0.05% trypsin-EDTA (Invitrogen) in PBS (B.Braun, Melsungen, Germany). For *in vivo* tumor studies, cells were harvested in log phase and tested for EGFR expression and potential mycoplasm contamination.

Antibodies

The human IgG1, κ, EGFR-specific mAb zalutumumab (HuMax-EGFr, clone 2F8) and mAb 018 were generated by immunizing HuMAb-mice™ (Medarex, Milpitas, CA) and produced as recombinant proteins as described previously (13). The N297Q mutation in the Fc part of zalutumumab and mAb 018, referred to as zalu-N297Q and mAb 018-N297Q and the K322A mutation in zalutumumab, referred to as zalu-K322A, were introduced using the QuikChange XL site-directed mutagenesis kit (Stratagene, La Jolla, CA). Mutagenesis was checked by sequencing (LGC Genomics, Berlin, Germany). IgG concentrations were determined by A280 measurements. Human IgG1, κ mAb specific for keyhole limpet hemocyanin (HuMAb-KLH), also generated in HuMAb mice was included in all experiments as isotype control mAb.

Flow cytometry

EGFR binding was assessed by incubating EGFR-expressing cells with serial dilutions of mAb in PBS, 0.05% BSA (Roche, Meylan, France), and 0.02% sodium azide (Sigma-Aldrich, St. Louis, MO), at 4°C for 30 min. Cells were washed and incubated with FITC-conjugated $F(ab')_2$ fragments of goat anti-human κ light chain (BD Biosciences, Aalst, Belgium) at 4°C for 30 min in the dark. Samples were analyzed by FACS analysis (FACSCantoII; BD Biosciences).

EGFR phosphorylation inhibition assay

Inhibition of EGFR autophosphorylation was evaluated in a two-step assay using the A431 cell line as described previously (15). In short, cells starved overnight were incubated with serially diluted EGFR-specific mAbs. After 60 min incubation, 50 ng/ml recombinant human EGF (Invitrogen) was added and incubated for 30 min. Cells lysates were transferred to ELISA plates and EGFR was captured with mouse EGFR-specific mAb (mAb EGFR1; BD Pharmingen, San Diego, CA). Phosphorylated EGFR was detected using europium-labeled mouse mAb, specific for phosphorylated tyrosines (mAb Eu-N1 P-Tyr-100; PerkinElmer, Boston, MA).

Proliferation inhibition assay

The ability of EGFR-specific mAbs to inhibit tumor cell proliferation was tested in a proliferation assay as described previously (15). A431 cells were seeded at a density of 500 cells per well in 96-well culture plates. EGFR-specific mAbs were

added in serial dilutions in culture medium and cultured for 5 d. Alamar Blue (20µl: Invitrogen) was used for measuring vital cell mass.

Isolation of PBMCs from human blood

PBMCs were isolated from buffy coats obtained from regular blood bank donations (after informed consent; Sanquin Blood Bank, Utrecht, The Netherlands) using density separation with lymphocyte separation medium (Lymphoprep, Lonza), followed by washing with PBS to remove platelets.

Culture of bone marrow-derived mouse macrophages

Bone marrow was isolated from the hind legs of SCID mice by flushing the femurs. Bone marrow was passed through a cell strainer and seeded in petri dishes (58 cm^2) with 10 ml/petri dish at 1.25×10^5 cells/ml in DMEM medium containing 10% CCS, 2mM L-glutamin (Lonza), 50 IU/ml penicillin, and 50 µg/ml streptomycin. Cells were cultured with 50 U/ml M-CSF (Prospec, Rehovot, Israel) at 37°C and 5% CO_2 for 7 d. Cultured macrophages were stimulated with 250 U/ml IFNγ (BD Biosciences) and 25 ng/ml LPS (Sigma-Aldrich) 24 h prior to use. Macrophages were detached with Versene (Invitrogen) and characterized by FACS analysis for staining with F4/80-A488 (AbD Serotec, Oxford, U.K.) and CD80-PE (eBioscience, San Diego, CA).

Antibody-dependent cellular cytotoxicity

ADCC was evaluated in a ^{51}Cr-release assay in which A431 target cells (5×10^6 cells) were labeled with 100 µCi $Na_2{}^{51}CrO_4$ (Amersham Biosciences, Uppsala, Sweden) at 37°C for 1 h. Cells were washed twice with PBS and resuspended in culture medium at 1×10^5 cells/ml. Labeled cells (5×10^3) were added in 96-well plates and preincubated with mAb (room temperature, 15 min). In the ADCC assay with human PBMCs, mAbs were added in 5-fold serial dilutions in culture medium (triplicate wells) and 5×10^5 PBMCs/well. In the ADCC assay with mouse macrophages, a fixed mAb concentration of 10 µg/ml was used (six replicates) and 1×10^5 mouse macrophages per well. Instead of mAb, culture medium was added to determine the background ^{51}Cr release (negative control), and Triton-X-100 (Sigma-Aldrich) (1.6% final concentration) was added to determine the maximal ^{51}Cr release (positive control). After 24 h incubation at 37°C supernatants were collected and ^{51}Cr release was measured in a gamma counter (cpm). Percentage of cellular cytotoxicity was calculated using the following formula: percentage

specific lysis = [experimental release (cpm) – negative control (cpm)]/[positive control (cpm) – negative control (cpm)) x100%.

Mouse tumor xenograft models

SCID mice (C.B.-17/IcrCrl-scid/scid) were purchased from Charles River (Maastricht, The Netherlands). All experiments were performed with 8- to 12-wk-old female mice. Mice were housed in a barrier unit of the Central Laboratory Animal Facility (Utrecht, The Netherlands) and kept in filter-top cages with water and food provided *ad libitum*. Mice were checked at least twice a week for clinical signs of disease and discomfort. All experiments were approved by the Utrecht University Animal Ethics Committee. Subcutaneous tumors were induced by inoculation of 5×10^6 A431 cells or 1×10^6 A431-KRAS4b^{G12V} cells in the right flank of mice. Tumor volumes were calculated from digital caliper measurements as $0.52 \times \text{length} \times \text{width}^2$ (mm^3). Experimental lung metastases were induced by injecting 1×10^6 A431-luc cells or 0.25×10^6 MDA-MB-231-luc cells into the tail vein. At weekly intervals, tumor growth was assessed using bioluminescence imaging. Before imaging, mice were anesthetized by i.p. injection of a mix of ketamine (Vétoquinol, Lure cedex, France), xylazine (Eurovet Animal Health, Cuijk, The Netherlands), and atropine (Eurovet Animal Health). Synthetic D-luciferin (Biothema, Handen, Sweden) was given i.p. at a dose of 125 mg/kg. Light was detected in a photon-counting manner over an exposure period of 5 min from the dorsal side (A431-luc cells) or from the ventral side (MDA-MB-231-luc cells), 10 min after luciferin administration, using a VersArray 1300B CCD camera (Roper Scientific, Vianen, The Netherlands; A431-luc model) or the Photon Imager (Biospace Lab, Paris, France; MDA-MB-231-luc model). During illumination, black-and-white images were made for anatomical reference. Metavue software (Universal Imaging, Downingtown, PA) was used for data collection and image analysis of the A431-luc model. M3 Vision software (Biospace Lab) was used for image analysis of the MDA-MB-231-luc model. mAbs were injected i.p. at indicated time points at four different dosing levels: 2 µg/mouse (0.1 mg/kg), 10 µg/mouse (0.5 mg/kg), 100 µg/mouse (5 mg/kg), and 1 mg/mouse (50 mg/kg). During the study, heparinized blood samples were taken for determination of human IgG levels in plasma using a Behring Nephelometer II (Siemens Healthcare Diagnostics, Erlangen, Germany).

Statistical analysis

Data analysis was performed using GraphPad Prism 5.0 (GraphPad Software, San Diego, CA) and PASW Statistics 18.0 (SPSS, Chicago, IL). Data were reported as means ± SEM. Differences between groups were analyzed using one-way ANOVA followed by a Tukey posttest (GraphPad Prism 5.0). Selected data were also analyzed using log-rank test (PASW Statistics 18.0).

Results

In vitro characterization of EGFR-specific Abs

To study the differential roles of signaling inhibition and ADCC induction by EGFR-specific mAbs, four mAbs with different functionalities were developed. Next to zalutumumab, the EGFR-specific mAb 018, which binds EGFR at a different epitope, was used (16). mAb 018 induces ADCC but does not inhibit EGFR phosphorylation and proliferation of A431 cells (see below). From both zalutumumab and mAb 018, mutants were generated in which the site for N-linked glycosylation in the Fc domain was eliminated by mutating the asparagine at position 297 to glutamine, referred to as zalu-N297Q and mAb 018-N297Q. This mutation leads to loss of Fc glycosylation, which results in abrogation of IgG Fc receptor interactions and C1q binding, and thereby of ADCC and CDC functions as previously described (17).

By flow cytometric analyses on A431 cells, the binding characteristics of zalutumumab, mAb 018, and their N297Q mutants were demonstrated to be similar. Half-maximal binding concentrations (EC_{50}) for zalutumumab and zalu-N297Q were 0.36 µg/ml (95% confidence interval [CI], 0.22-0.59 µg/ml) and 0.37 µg/ml (95% CI, 0.22-0.64 µg/ml) and for mAb 018 and mAb 018-N297Q, 1.4 µg/ml (95% CI, 0.84-2.34 µg/ml) and 1.9 µg/ml (95% CI, 1.27-2.88 µg/ml) (Fig. 1A).

The capacity to induce ADCC in A431 cells was comparable for mAb 018 (EC_{50} of 0.03 µg/ml, 95% CI, 0.02-0.05 µg/ml) and zalutumumab (EC_{50} of 0.04 µg/ml, 95% CI, 0.01-0.14 µg/ml). Both N297Q mutants were unable to induce ADCC, consistent with their loss of FcγR binding (Fig. 1B). As expected, the N297Q mutation did not affect zalutumumab's ability to inhibit signaling, as both Abs demonstrated a similar inhibition of EGFR phosphorylation. mAb 018 and mAb 018-N297Q did not inhibit EGF-induced phosphorylation (Fig. 1C). Finally, we demonstrated that zalutumumab and zalu-N297Q inhibited proliferation,

whereas mAb 018 and mAb 018-N297Q did not (Fig. 1D). Previously, it had been observed that neither zalutumumab alone nor mAb 018 alone was able to induce CDC with human complement (16).

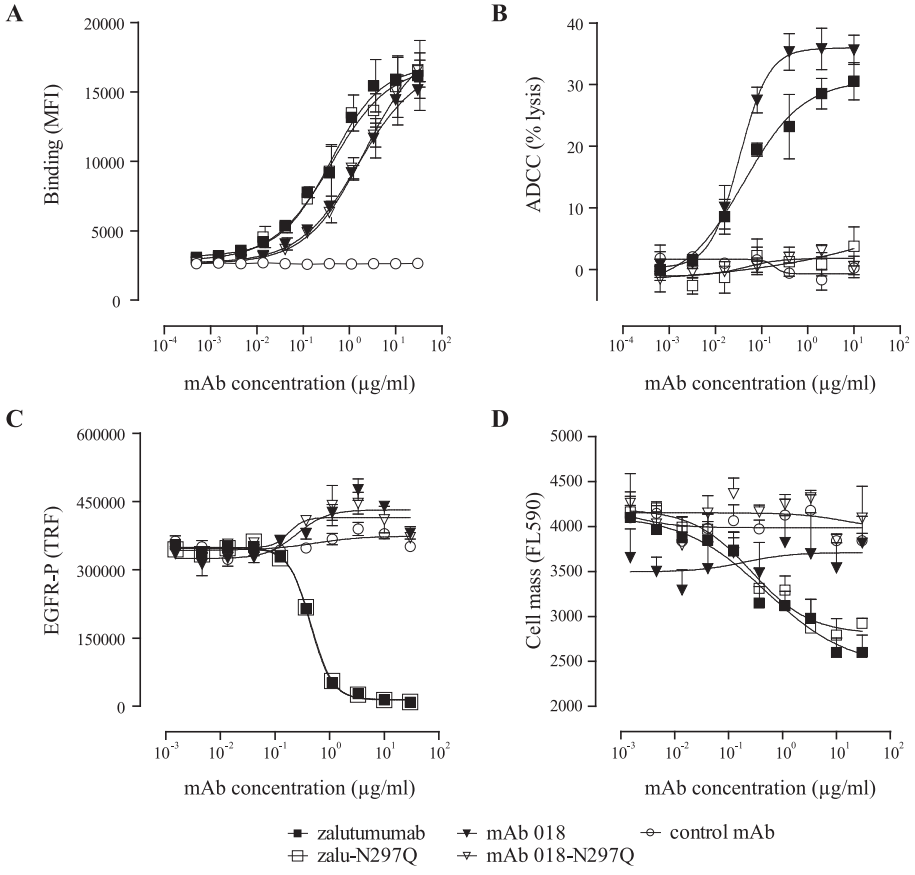

Figure 1. *Development of a panel of EGFR-specific mAbs with distinct functionalities*. (A) Binding of zalutumumab, zalu-N297Q, mAb 018, and mAb 018-N297Q to cell-associated EGFR on A431 cells analyzed by flow cytometry; data were analyzed using a four-parameter logistic curve fit. Shown is the mean fluorescence intensity (MFI). (B) The capacity of the different mAb to induce ADCC analyzed in ^{51}Cr release assay using human PBMCs as effector cells and A431 cells as target cells. Data shown are percentages specific lysis, calculated as described in *Materials and Methods*. (C) mAb-induced inhibition of EGFR phosphorylation in A431 cells upon stimulation with EGF measured in an EGFR phosphorylation inhibition assay. Data shown are time-resolved fluorescences (TRF). (D) Inhibition of A431 cell proliferation determined in a proliferation inhibition assay using Alamar Blue staining. Each data point represents mean ± SEM of triplicates, and experiments shown are representative of at least two independent experiments.

Taken together, we generated a well-assorted panel of EGFR-specific mAbs in which zalutumumab inhibits signaling and induces ADCC, mAb 018 solely induces ADCC, zalu-N297Q only inhibits EGFR signaling, and mAb 018-N297Q is inert for both MoA. This matched set of mAbs with a unique combination of MoA allowed us to focus on the differential role of ADCC in xenograft models.

Zalutumumab and mAb 018 are functional in ADCC with murine effector cells

Because we employed a mouse model to study the *in vivo* impact of ADCC, we first checked the interaction of our mAbs with mouse effector cells *in vitro*. Bone marrow-derived macrophages were used, since they are important effector cells expressing all FcγRs. The cultured macrophages were positive for F4/80-A488 and CD80-PE, and they therefore represent mature and activated macrophages (data not shown). To study ADCC, mouse macrophages were incubated with ^{51}Cr-labeled A431 cells in an E:T ratio of 20:1 in the presence of saturating mAb concentrations (10 µg/ml). As expected, zalutumumab and mAb 018 induced a comparable percentage of specific lysis of A431 cells with mouse macrophages (mean ± SEM, 23.8 ± 2.5 and 22.0 ± 1.8%), whereas the N297Q mutants were inactive in ADCC (Fig. 2). These results were confirmed by using mouse NK cells and mouse neutrophils as effector cells (data not shown).

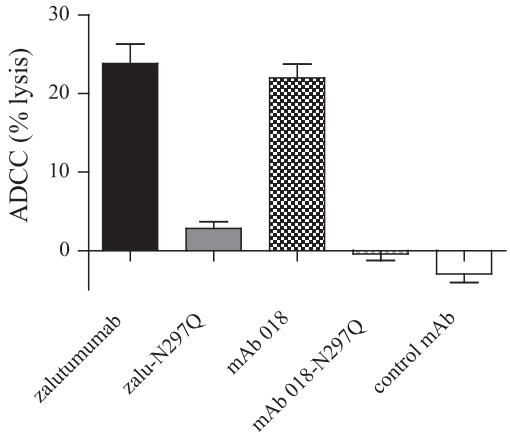

Figure 2. *Zalutumumab and mAb 018 are functional in an ADCC assay with murine effector cells*. The capacity of the different mAbs to induce ADCC was analyzed in ^{51}Cr release assay using mouse bone marrow-derived macrophages as effector cells, and A431 cells as target cells. mAbs were tested at a concentration of 10 µg/ml with six replicates. Data represent mean ± SEM of three independent experiments.

Inhibition of signaling or induction of ADCC is sufficient to prevent tumor growth upon early treatment in A431 s.c. xenografts

Knowing that both zalutumumab and mAb 018 can induce ADCC with mouse effector cells, we tested these mAbs and their N297Q mutants in an A431 xenograft model. Mice were treated i.p. with 5 mg/kg mAb within 2 h after tumor induction (early treatment). Zalutumumab and zalu-N297Q were both found capable of inhibiting tumor growth ($p<0.001$; one-way ANOVA, day 26), indicating signaling inhibition alone to be sufficient to inhibit tumor growth upon early treatment (Fig. 3A). mAb 018 was also capable of inhibiting tumor growth ($p<0.001$; one-way ANOVA, day 26), indicating that also ADCC alone suffices for inhibition of tumor growth in this experimental setting (Fig. 3B). The N297Q mutation completely removed the anti-tumor effect of mAb 018, confirming mAb 018 indeed to be inactive *in vivo* in the absence of its capability to induce ADCC.

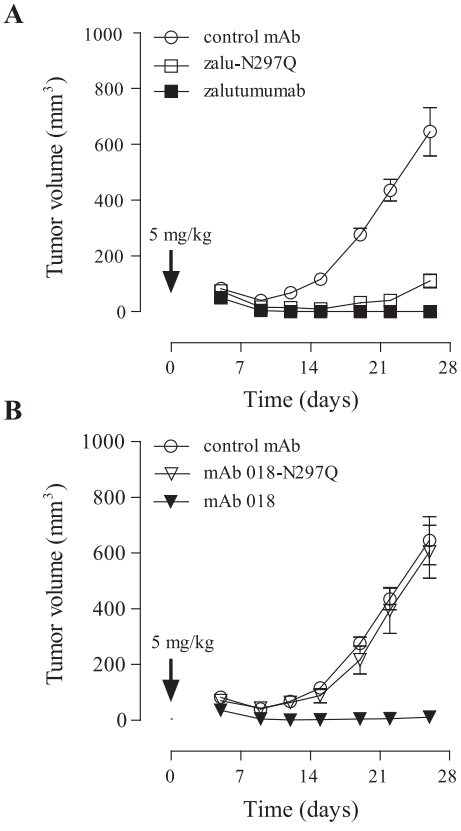

Figure 3. *Early treatment with mAb 018-N297Q does not prevent tumor growth*. Eight mice per group were injected s.c. with 5×10^6 A431 cells. mAb (5 mg/kg) was administered within 2 h after tumor inoculation. Tumor volumes were calculated as described in *Materials and Methods*. (A) Efficacy of zalutumumab and zalu-N297Q. (B) Efficacy of mAb 018 and mAb 018-N297Q. Data shown are mean tumor volumes ± SEM.

Impact of dosing and timing on zalutumumab and mAb 018 efficacy in A431 s.c. xenografts

Having established the different functionalities of our EGFR-specific Ab panel *in vivo*, the influence of dosing and timing on efficacy was examined. First, 0.5 mg/kg and 5 mg/kg mAb doses were tested in early treatment (Fig. 4A). Dosing of 0.5 mg/kg zalutumumab or mAb 018, leading to expected maximum plasma concentrations of 5 µg/ml (18), resulted in a delay in tumor growth ($p<0.001$; one-way ANOVA, day 21). This suggests that ADCC is already effective at mAb doses that are not expected to fully saturate EGFR with mAbs. At a dose of 5 mg/kg, both zalutumumab and mAb 018 completely inhibited tumor growth ($p<0.001$; one-way ANOVA, day 21).

Additionally, the impact of timing on the role of ADCC was studied in established tumor models in which we examined efficacy of zalutumumab and mAb 018 on variable tumor volumes. A delay in tumor growth was observed when mice with tumor volumes of 80-100 mm^3 (days 2-4) were treated with 0.5 or 5 mg/kg mAb ($p<0.05$ and $p<0.001$; one-way ANOVA, days 24 and 18, respectively). Complete inhibition of tumor growth, however, was no longer observed (Fig. 4B). At a tumor volume of 200 mm^3 (day 15) mice were treated with a repeated dose of 50 mg/kg mAb, which is expected to give full target saturation in established tumors (13). Treatment with mAb 018 did not inhibit tumor growth in this setting, whereas complete abrogation of tumor growth with zalutumumab ($p<0.01$; one-way ANOVA, day 29) was observed (Fig. 4C).

Taken together, these data indicate that at an early time point in tumor development, ADCC as the only MoA is capable of reducing tumor growth and that low mAb concentrations are sufficient. In contrast, inhibition of EGFR signaling is required for inhibiting established tumors with a large tumor volume, where ADCC induction alone is ineffective.

Both zalutumumab and mAb 018 are effective at low doses in experimental metastasis models

Because ADCC has been an effective MoA upon early treatment, we hypothesized that ADCC might be very effective in killing metastasizing tumor cells. Therefore, the efficacy of ADCC as a MoA was studied in two different experimental metastasis models in which tumor cells colonize the lungs. Development was assessed weekly by optical imaging. First, early treatment with 0.5 mg/kg mAb was tested in the i.v. A431-luc model. Tumor development of A431-luc cells in

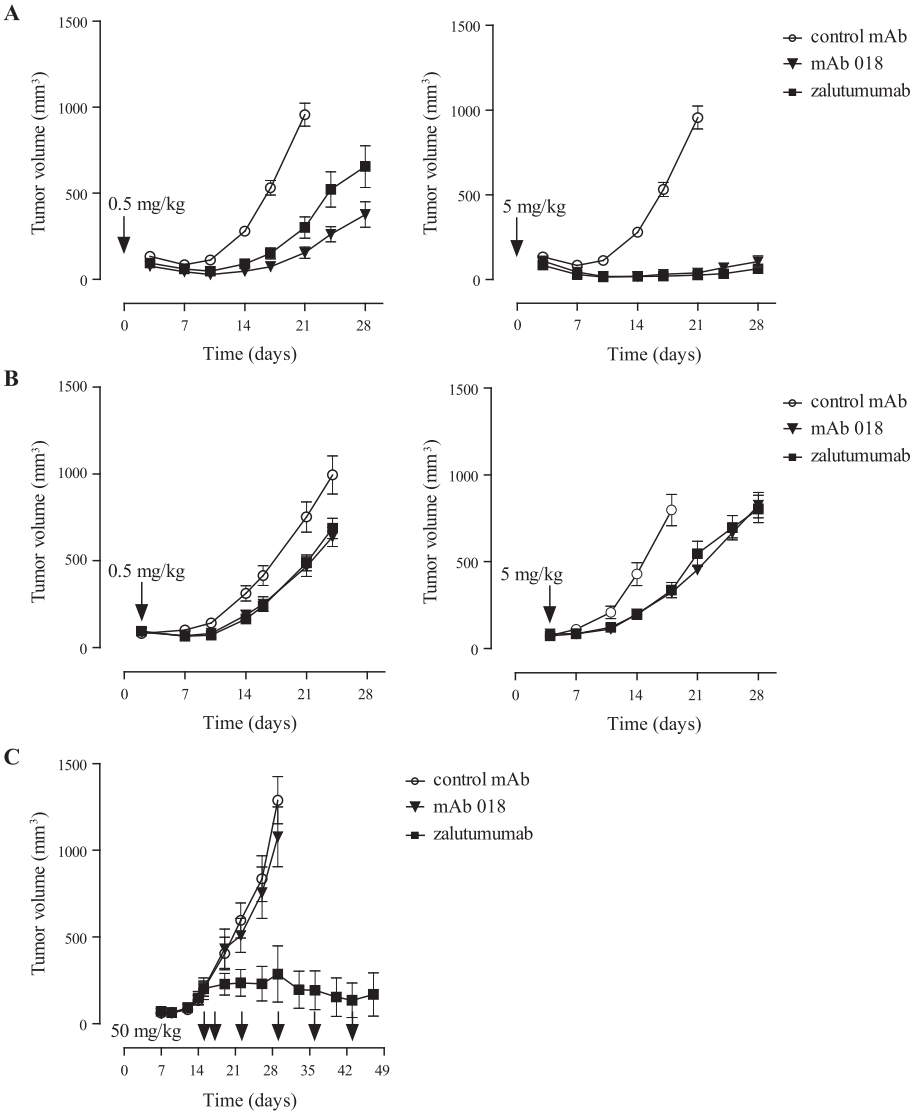

Figure 4. *Effect of dose level and timing of dosing on the efficacy of zalutumumab and mAb 018 in an A431 s.c. xenograft model*. Tumors were induced by s.c. inoculation of 5×10^6 A431 cells. (A) Single treatment at day 0 with 0.5mg/kg (*left panel*) or 5 mg/kg (*right panel*) mAb; eight mice per group. (B) Single treatment with 0.5 mg/kg (*left panel*) or 5 mg/kg (*right panel*) mAb when tumor volume was ~80-100 mm^3; nine mice per group. (C) Repeated treatment with 50 mg/kg mAb when average tumor volume was 200 mm^3; six mice per group. Data shown are mean tumor volumes ± SEM.

the lungs became visible at day 23, and starting from day 43 tumor volume enhanced exponentially in the control group. The light intensities of A431-luc cells at day 49 are shown in Fig. 5A. Tumor growth was completely inhibited

upon treatment with zalutumumab or mAb 018 ($p<0.01$ and $p<0.05$; log-rank test, progression-free set at < 200.000 counts). These results were confirmed in a second model in which mice were injected i.v. with MDA-MB-231-luc cells. To evaluate the dose requirements, mAb 018 was tested in this model at different dose levels. Tumor development became visible at day 21 and tumor volume enhanced exponentially in the control group, whereas in the mAb 018-treated mice a delay in tumor growth was observed. The light intensity of the MDA-MB-231-luc cells in the lungs at day 33 in the mAb 018-treated groups was ~10- to 18-fold lower than in the group treated with control mAb (Fig. 5B). Even a low dose of 0.1 mg/kg mAb 018 was able to significantly delay tumor progression ($p<0.05$; log-rank test, progression-free set at < 5000 cpm).

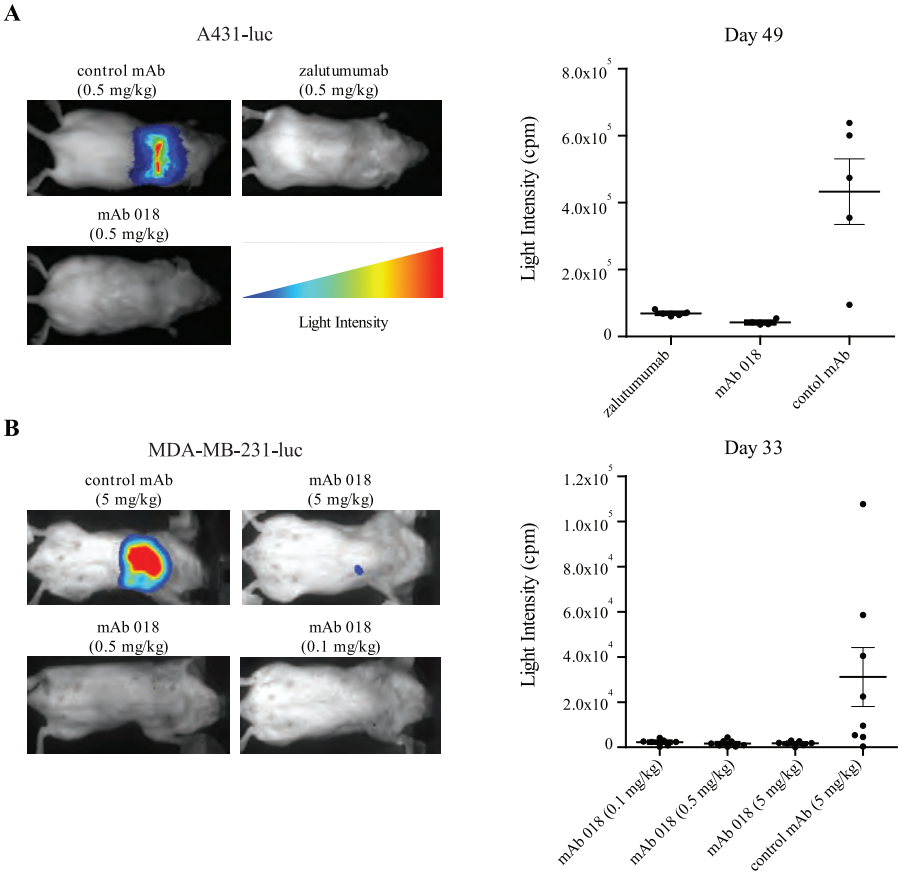

Figure 5. *Both zalutumumab and mAb 018 are effective at low dose in experimental metastasis models.* A431-luc cells (1×10^6) or MDA-MB-231-luc cells (0.25×10^6) were injected i.v.; five and eight mice per group, respectively. Mice were treated at day 0 at indicated dose levels. (A) A431-luc model, single treatment using 0.5 mg/kg mAb. Bioluminescence image at day 49, one representative mouse per

group, dorsal view (*left panel*) and light intensity at day 49 (*right panel*). (B) MDA-MB-231-luc model, single treatment at day 0 using 0.1, 0.5, and 5 mg/kg mAb. Bioluminescence image at day 33, one representative mouse per group, ventral view (*left panel*) and light intensity at day 33 (*right panel*). Data shown are mean light intensity ± SEM.

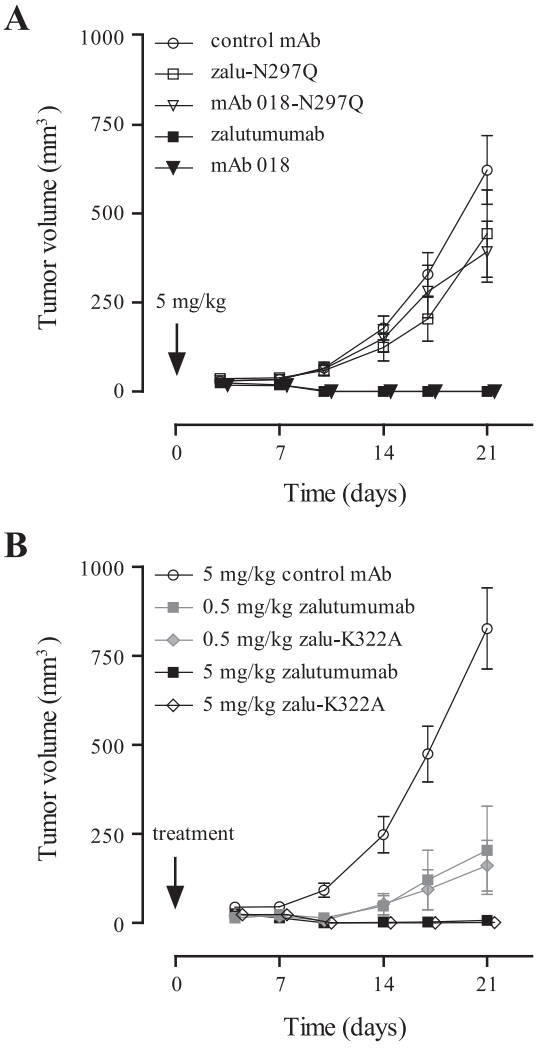

Figure 6. *Both zalutumumab and mAb 018 are capable of inhibiting growth of tumor cells expressing mutant KRAS.* Eight mice per group were inoculated s.c. with 1×10^6 A431-KRAS4b^{G12V} cells, which are insensitive for EGFR signaling inhibition. (A) Single treatment at day 0 with 5mg/kg mAb. (B) Single treatment at day 0, at indicated dose levels. Data shown are mean tumor volumes ± SEM.

Both zalutumumab and mAb 018 are effective on tumors resistant to inhibition of EGFR signaling

The data so far indicate that ADCC occurs independently of effects on signaling. This is further supported by the fact that proliferation of the MDA-MB-231-luc cell line was found to be insensitive to EGFR signaling inhibition *in vitro* (Supplemental Fig. 1), but *in vivo* growth of this cell line can be delayed with

EGFR-specific mAb. To further evaluate ADCC efficacy in tumors insensitive to EGFR signaling inhibition we used A431-KRAS4b^{G12V} cells. Schlaeth et al. (14) demonstrated previously that an A431 cell line stably transfected with oncogenic KRAS4b^{G12V} remained sensitive to ADCC, but not to EGFR signaling inhibition, *in vitro*. To study this *in vivo*, we treated mice with a single dose of 5 mg/kg mAb after s.c. A431-KRAS4b^{G12V} tumor inoculation. Indeed, both zalutumumab and mAb 018 were able to inhibit tumor growth completely ($p<0.001$; one-way ANOVA, day 21; Fig. 6A). The N297Q mutation completely removed the anti-tumor effects from zalutumumab and mAb 018, confirming that ADCC is indeed an effective MoA against A431-KRAS4b^{G12V} tumor cells *in vivo*, which are insensitive to EGFR signaling inhibition.

No major role for CDC as MoA of zalutumumab in mice

So far, we assumed that CDC does not play a role in the anti-tumor effects of zalutumumab or mAb 018 in mouse models, because no CDC induction was observed in assays with human serum (16). To confirm that this also holds true in a mouse model we used a zalutumumab Fc mutant in which the lysine at position 322 was mutated to alanine, referred to as zalu-K322A. Duncan and Winter (19) suggested that the K322 position in mouse IgG2b is located in the binding site for C1q. Furthermore, Idusogie et al. (20) showed that the K322 position is also in human IgG1 the epicenter for human, rabbit and guinea pig C1q binding. To extend this to mice, we confirmed that the K322A mutation also leads to strongly reduced binding of mouse C1q (Supplemental Fig. 2A). Furthermore, we showed that this mutation leads to loss of CDC of human cells induced by human IgG1 mAb in mouse serum (Supplemental Fig. 2B). Having established loss of CDC by the K322A mutation with mouse complement, we compared zalutumumab and zalu-K322A in an *in vivo* model in which we treated A431-KRAS4b^{G12V} s.c. xenografts within 2 h after tumor inoculation with 0.5 or 5 mg/kg mAb. If CDC was an additional MoA of zalutumumab *in vivo*, a reduced effect on tumor growth inhibition by zalu-K322A would be expected. However, zalu-K322A was as effective in tumor inhibition as zalutumumab, and therefore we can exclude CDC as a major MoA of zalutumumab (Fig. 6B).

In conclusion, we have demonstrated that ADCC induction by EGFR-specific mAbs alone is sufficient for preventing tumor outgrowth, even of tumor cells which are insensitive to EGFR signaling inhibition.

Discussion

To evaluate the *in vivo* role of ADCC in the anti-tumor effects of zalutumumab, a matched set of EGFR-specific mAb was generated. Each EGFR-specific mAb displayed a different MoA, permitting us to distinguish between ADCC and signaling inhibition. We evaluated the efficacy of these EGFR-specific mAbs in several murine xenograft models to answer the questions when, where, and at what mAb dose levels ADCC induction may play a role in the treatment of solid tumors with therapeutic mAbs.

Previous work already demonstrated a role for ADCC in preventing tumor growth. The data from Clynes et al. (12) was confirmed by De Haij et al. (5) in a recent study in mice deficient in FcR γ-chain signaling (NOTAM mice). In these mice, tumor growth was no longer inhibited by rituximab. These studies established ADCC as MoA, but did not address the questions under which conditions it is effective and how it relates to other potential MoA. To clarify these questions, we treated mice at different time points of tumor development. Early treatment (at day 0) in a s.c. A431 xenograft model completely inhibited tumor growth with ADCC (mAb 018) and/or signaling inhibition (zalu-N297Q) as MoA (zalutumumab has both MoA). Treatment at a time point on which the tumors were established but still had a small tumor volume was less effective, but still resulted in a delay of tumor growth by ADCC induction or inhibition of signaling. However, growth of established tumor with a large tumor volume (day 15) was only inhibited by a signaling blocking mAb (zalutumumab) at high dose (50 mg/kg). mAb 018, a mAb with only ADCC as a MoA, did not reduce growth of established tumors. These results demonstrate ADCC to be especially effective in early treatment, suggesting that nonestablished tumors, in particular, are susceptible to eradication via ADCC. This is consistent with and explains the previous finding of Clynes et al. (12) and de Haij et al. (5) who employed nonestablished tumor models for their experiments.

To investigate what EGFR-specific mAb dose level is required to induce efficient ADCC, mice were treated with three different mAb doses. A dose of 0.5 mg/kg is expected to yield a maximum plasma concentration of 5 µg/ml, which gives incomplete receptor saturation according to *in vitro* binding data. Doses of 5 and 50 mg/kg are expected to yield maximum plasma concentrations of 50 and 500 µg/ml, which both give full receptor saturation *in vitro*. In the current study, a single dose of 0.5 mg/kg mAb at day 0 was sufficient to strongly

inhibit tumor development via ADCC as the only MoA. We conclude that EGFR saturation is not required for effective ADCC induction *in vivo*. This conclusion is supported by a study in FcγRIIB knockout mice, in which it was shown that mice deficient in the inhibitory receptor, FcγRIIB, had complete inhibition of tumor growth already at submaximal trastuzumab doses (12).

The importance of ADCC in the treatment of hematological tumors with mAb has been shown in several studies (21). A role for ADCC in the treatment of solid tumors with mAb is less clear. An exception is trastuzumab, which is used for the treatment of solid tumors and for which ADCC has been described as an important MoA (22). In this study, we demonstrate that s.c. growth of a solid tumor can only be inhibited via ADCC when mAb treatment is started shortly after tumor induction. These results suggest that ADCC by EGFR-specific mAbs has no or limited impact on an established solid tumor mass. In experimental metastasis models, in which A431-luc cells or MDA-MB-231-luc cells were inoculated i.v., complete inhibition or a delay, respectively, of tumor growth by ADCC as single MoA was observed, even at a single low dose of 0.1 mg/kg mAb. These data suggest that tumor cells must be easily accessible for the therapeutic mAb and/or effector cells to be effectively depleted via ADCC. Ineffectiveness of the immune system to access xenografts was shown by Yu et al. (23) who observed, upon i.v. injection of light-emitting microorganisms in mice bearing MCF-7 human metastatic mammary carcinoma tumors, that the primary breast tumor and metastasis in the left breast were colonized by bacteria 2 d after injection. Eight days after injection the bacteria were no longer detectable in the metastasis, but they were present in the primary tumor for over 45 d. These results indicate that the tumor microenvironment is an immune-privileged site. Comparable findings have been obtained by Gong et al. (24) for B cell clearance by CD20 targeting Ab. Using a human CD20 transgenic mouse model they observed that upon administration of CD20-specific mAb, circulating B cells were rapidly cleared through the reticuloendothelial system, but B cells residing within the marginal zone compartment were only partially cleared. The partial clearance of B cells from the marginal zone was mediated by CDC induction, indicating that the mAb did reach this compartment. Clearance of the remaining resistant B-cells required trafficking of these cells through the circulation. Our results, showing that zalutumumab can inhibit tumor growth of an established solid tumor via signaling inhibition, demonstrate that indeed the therapeutic mAb does reach the tumor. These data imply that an established

solid tumor protects itself from ADCC, not by excluding the therapeutic mAb, but by excluding the effector cells from the tumor microenvironment. Protection from the tumor against the immune system can be overcome by enhancing the affinity of therapeutic mAb for activating FcγR. Junttila et al. (25) showed that enhanced affinity of trastuzumab for FcγR resulted in enhanced anti-tumor effects in established solid tumors *in vivo*. Enhancing the affinity of mAb for activating FcγR may well lead to enhanced capture of effector cells in the tumor microenvironment.

In the process of metastasis, tumor cells seem to be better accessible for the immune effector cells, as indicated by the observation that bacteria are cleared from the metastasis after 8 d (23) and the low dose of mAb 018 we needed to strongly diminish the experimental lung metastases . We suggest ADCC to represent a powerful MoA in inhibiting metastasis, and several studies with trastuzumab support this hypothesis. In a mouse xenograft model where the primary tumor does no longer respond to trastuzumab treatment, there was a reduction in circulating tumor cells (26). Furthermore, a clinical study with trastuzumab showed that therapy-resistant CK-19 mRNA-positive disseminated occult breast cancer cells in the peripheral blood and bone marrow can be effectively targeted by trastuzumab administration (27).

Finally, the question was addressed whether ADCC is effective in tumors insensitive to EGFR signaling inhibition due to mutations downstream of EGFR. An *in vitro* study from Schlaeth et al. (14) showed that tumor cells expressing mutant KRAS, which results in cells insensitive to EGFR signaling inhibition, can be effectively killed via ADCC. In this study, we studied the role of ADCC induction on tumor growth of MDA-MB-231-luc cells and A431-KRAS4b^{G12V} cells *in vivo*. The MDA-MB-231-luc tumor cells originated from a metastatic site in a MDA-MB-231 xenograft are described to be insensitive to EGF stimulation (28). *In vitro* proliferation demonstrated these cells indeed to be insensitive to EGFR signaling inhibition via zalutumumab. Tumor growth of an i.v. MDA-MB-231-luc tumor model could be delayed via mAb 018 treatment, even at a dose of 0.1 mg/kg, indicating again that full receptor saturation is not nessecary for ADCC activity. No complete tumor growth inhibition was observed in contrast to the A431-luc experimental metastatic model also not at a dose of 5 mg/kg mAb 018. The fact that MDA-MB-231-luc cells are not fully sensitive to ADCC needs further investigation, but might be due to a lower EGFR density on the MDA-MB-231-luc cells or due to a higher expression of ADCC suppressor

proteins. Early treatment (day 0) with 5 mg/kg zalutumumab or mAb 018 in a s.c. A431-KRAS4b^{G12V} tumor model completely prevented tumor growth. Zalu-N297Q and mAb 018-N297Q, which lack ADCC activity, were not able to inhibit tumor growth, and treatment with zalu-K322A did not result in an abrogation of the anti-tumor effect, indicating that CDC has no major role in the EGFR-specific mAb anti-tumor effect of A431-KRAS4b^{G12V} cells. This demonstrates that growth of tumor cells insensitive to EGFR signaling inhibition can be inhibited completely *in vivo* by induction of solely ADCC.

In conclusion, our study supports ADCC induction by EGFR-specific mAbs, such as zalutumumab, to represent a powerful MoA in metastasis, as well as early stages of tumor development, even in cancers insensitive to EGFR signaling inhibition due to, for example, KRAS mutations. ADCC, therefore, is likely an important MoA for treatment of solid tumors via the prevention of metastasis.

Acknowledgements

We thank Gemma M. Rigter and Marieke A. Stoel for technical assistance.

References

1. Cooley, S., L. J. Burns, T. Repka, and J. S. Miller. 1999. Natural killer cell cytotoxicity of breast cancer targets is enhanced by two distinct mechanisms of antibody-dependent cellular cytotoxicity against LFA-3 and HER2/neu. *Exp Hematol* 27:1533-1541.
2. Hale, G., M. Clark, and H. Waldmann. 1985. Therapeutic potential of rat monoclonal antibodies: isotype specificity of antibody-dependent cell-mediated cytotoxicity with human lymphocytes. *J Immunol* 134:3056-3061.
3. Reff, M. E., K. Carner, K. S. Chambers, P. C. Chinn, J. E. Leonard, R. Raab, R. A. Newman, N. Hanna, and D. R. Anderson. 1994. Depletion of B cells in vivo by a chimeric mouse human monoclonal antibody to CD20. *Blood* 83:435-445.
4. Sliwkowski, M. X., J. A. Lofgren, G. D. Lewis, T. E. Hotaling, B. M. Fendly, and J. A. Fox. 1999. Nonclinical studies addressing the mechanism of action of trastuzumab (Herceptin). *Semin Oncol* 26:60-70.
5. de Haij, S., J. H. Jansen, P. Boross, F. J. Beurskens, J. E. Bakema, D. L. Bos, A. Martens, J. S. Verbeek, P. W. Parren, J. G. van de Winkel, and J. H. Leusen. 2010. In vivo cytotoxicity of type I CD20 antibodies critically depends on Fc receptor ITAM signaling. *Cancer Res* 70:3209-3217.
6. Dall'Ozzo, S., S. Tartas, G. Paintaud, G. Cartron, P. Colombat, P. Bardos, H. Watier, and G. Thibault. 2004. Rituximab-dependent cytotoxicity by natural killer cells: influence of FCGR3A polymorphism on the concentration-effect relationship. *Cancer Res* 64:4664-4669.
7. Cartron, G., L. Dacheux, G. Salles, P. Solal-Celigny, P. Bardos, P. Colombat, and H. Watier. 2002. Therapeutic activity of humanized anti-CD20 monoclonal antibody and polymorphism in IgG Fc receptor FcgammaRIIIa gene. *Blood* 99:754-758.
8. Weng, W. K., and R. Levy. 2003. Two immunoglobulin G fragment C receptor polymorphisms independently predict response to rituximab in patients with follicular lymphoma. *J Clin Oncol* 21:3940-3947.
9. Musolino, A., N. Naldi, B. Bortesi, D. Pezzuolo, M. Capelletti, G. Missale, D. Laccabue, A. Zerbini, R. Camisa, G. Bisagni, T. M. Neri, and A. Ardizzoni. 2008. Immunoglobulin G fragment C receptor polymorphisms and clinical efficacy of trastuzumab-based therapy in patients with HER-2/neu-positive metastatic breast cancer. *J Clin Oncol* 26:1789-1796.
10. Zhang, W., M. Gordon, A. M. Schultheis, D. Y. Yang, F. Nagashima, M. Azuma, H. M. Chang, E. Borucka, G. Lurje, A. E. Sherrod, S. Iqbal, S. Groshen, and H. J. Lenz. 2007. FCGR2A and FCGR3A polymorphisms associated with clinical outcome of epidermal growth factor receptor expressing metastatic colorectal cancer patients treated with single-agent cetuximab. *J Clin Oncol* 25:3712-3718.
11. Bibeau, F., E. Lopez-Crapez, F. Di Fiore, S. Thezenas, M. Ychou, F. Blanchard, A. Lamy, F. Penault-Llorca, T. Frebourg, P. Michel, J. C. Sabourin, and F. Boissiere-Michot. 2009. Impact of Fc{gamma}RIIa-Fc{gamma}RIIIa polymorphisms and KRAS mutations on the clinical outcome of patients with metastatic colorectal cancer treated with cetuximab plus irinotecan. *J Clin Oncol* 27:1122-1129.
12. Clynes, R. A., T. L. Towers, L. G. Presta, and J. V. Ravetch. 2000. Inhibitory Fc receptors modulate in vivo cytoxicity against tumor targets. *Nat Med* 6:443-446.
13. Bleeker, W. K., J. J. Lammerts van Bueren, H. H. van Ojik, A. F. Gerritsen, M. Pluyter, M. Houtkamp, E. Halk, J. Goldstein, J. Schuurman, M. A. van Dijk, J. G. van de Winkel, and P. W. Parren. 2004. Dual mode of action of a human anti-epidermal growth factor receptor monoclonal antibody for cancer therapy. *J Immunol* 173:4699-4707.
14. Schlaeth, M., S. Berger, S. Derer, K. Klausz, S. Lohse, M. Dechant, G. A. Lazar, T. Schneider-Merck, M. Peipp, and T. Valerius. 2010. Fc-engineered EGF-R antibodies mediate improved antibody-dependent cellular cytotoxicity (ADCC) against KRAS-mutated tumor cells. *Cancer Sci* 101:1080-1088.
15. Peipp, M., J. J. Lammerts van Bueren, T. Schneider-Merck, W. W. Bleeker, M. Dechant, T. Beyer, R. Repp, P. H. van Berkel, T. Vink, J. G. van de Winkel, P. W. Parren, and T. Valerius. 2008. Antibody fucosylation differentially impacts cytotoxicity mediated by NK and PMN effector cells. *Blood* 112:2390-2399.
16. Dechant, M., W. Weisner, S. Berger, M. Peipp, T. Beyer, T. Schneider-Merck, J. J. Lammerts van Bueren, W. K. Bleeker, P. W. Parren, J. G. van de Winkel, and T. Valerius. 2008. Complement-dependent tumor cell lysis triggered by combinations of epidermal growth factor receptor antibodies. *Cancer Res* 68:4998-5003.

17. Tao, M. H., and S. L. Morrison. 1989. Studies of aglycosylated chimeric mouse-human IgG. Role of carbohydrate in the structure and effector functions mediated by the human IgG constant region. *J Immunol* 143:2595-2601.

18. Lammerts van Bueren, J. J., W. K. Bleeker, H. O. Bogh, M. Houtkamp, J. Schuurman, J. G. van de Winkel, and P. W. Parren. 2006. Effect of target dynamics on pharmacokinetics of a novel therapeutic antibody against the epidermal growth factor receptor: implications for the mechanisms of action. *Cancer Res* 66:7630-7638.

19. Duncan, A. R., and G. Winter. 1988. The binding site for C1q on IgG. *Nature* 332:738-740.

20. Idusogie, E. E., L. G. Presta, H. Gazzano-Santoro, K. Totpal, P. Y. Wong, M. Ultsch, Y. G. Meng, and M. G. Mulkerrin. 2000. Mapping of the C1q binding site on rituxan, a chimeric antibody with a human IgG1 Fc. *J Immunol* 164:4178-4184.

21. Castillo, J., E. Winer, and P. Quesenberry. 2008. Newer monoclonal antibodies for hematological malignancies. *Exp Hematol* 36:755-768.

22. Arnould, L., M. Gelly, F. Penault-Llorca, L. Benoit, F. Bonnetain, C. Migeon, V. Cabaret, V. Fermeaux, P. Bertheau, J. Garnier, J. F. Jeannin, and B. Coudert. 2006. Trastuzumab-based treatment of HER2-positive breast cancer: an antibody-dependent cellular cytotoxicity mechanism? *Br J Cancer* 94:259-267.

23. Yu, Y. A., S. Shabahang, T. M. Timiryasova, Q. Zhang, R. Beltz, I. Gentschev, W. Goebel, and A. A. Szalay. 2004. Visualization of tumors and metastases in live animals with bacteria and vaccinia virus encoding light-emitting proteins. *Nat Biotechnol* 22:313-320.

24. Gong, Q., Q. Ou, S. Ye, W. P. Lee, J. Cornelius, L. Diehl, W. Y. Lin, Z. Hu, Y. Lu, Y. Chen, Y. Wu, Y. G. Meng, P. Gribling, Z. Lin, K. Nguyen, T. Tran, Y. Zhang, H. Rosen, F. Martin, and A. C. Chan. 2005. Importance of cellular microenvironment and circulatory dynamics in B cell immunotherapy. *J Immunol* 174:817-826.

25. Junttila, T. T., K. Parsons, C. Olsson, Y. Lu, Y. Xin, J. Theriault, L. Crocker, O. Pabonan, T. Baginski, G. Meng, K. Totpal, R. F. Kelley, and M. X. Sliwkowski. 2010. Superior in vivo efficacy of afucosylated trastuzumab in the treatment of HER2-amplified breast cancer. *Cancer Res* 70:4481-4489.

26. Barok, M., M. Balazs, P. Nagy, Z. Rakosy, A. Treszl, E. Toth, I. Juhasz, J. W. Park, J. Isola, G. Vereb, and J. Szollosi. 2008. Trastuzumab decreases the number of circulating and disseminated tumor cells despite trastuzumab resistance of the primary tumor. *Cancer Lett* 260:198-208.

27. Bozionellou, V., D. Mavroudis, M. Perraki, S. Papadopoulos, S. Apostolaki, E. Stathopoulos, A. Stathopoulou, E. Lianidou, and V. Georgoulias. 2004. Trastuzumab administration can effectively target chemotherapy-resistant cytokeratin-19 messenger RNA-positive tumor cells in the peripheral blood and bone marrow of patients with breast cancer. *Clin Cancer Res* 10:8185-8194.

28. Davidson, N. E., E. P. Gelmann, M. E. Lippman, and R. B. Dickson. 1987. Epidermal growth factor receptor gene expression in estrogen receptor-positive and negative human breast cancer cell lines. *Mol Endocrinol* 1:216-223.

29. de Weers, M., Y. T. Tai, M. S. van der Veer, J. M. Bakker, T. Vink, D. C. Jacobs, L. A. Oomen, M. Peipp, T. Valerius, J. W. Slootstra, T. Mutis, W. K. Bleeker, K. C. Anderson, H. M. Lokhorst, J. G. van de Winkel, and P. W. Parren. 2011. Daratumumab, a novel therapeutic human CD38 monoclonal antibody, induces killing of multiple myeloma and other hematological tumors. *J Immunol* 186:1840-1848.

Supplemental Figures

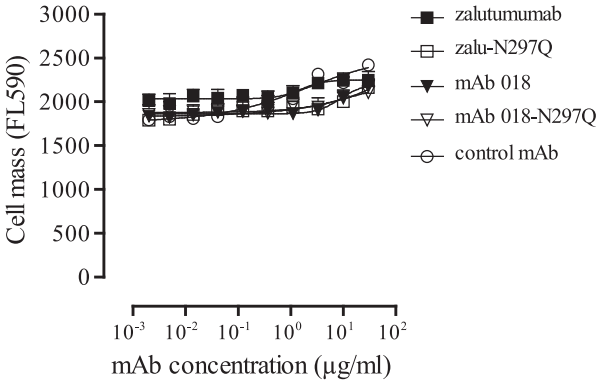

Supplemental Figure 1. *MDA-MB-231-luc cells are not sensitive for EGFR signaling inhibition.* (A) Proliferation-inhibition assay using Alamar Blue staining of MDA-MB-231-luc was performed as indicated in *Materials and Methods*. Initial cell number was adapted to obtain exponential growth in the assay. Each data point represents mean ± SEM of triplicates and the experiment shown is representative of two independent experiments. In each experiment A431 cells were included as positive control, which demonstrated more than 50% inhibition with zalutumumab which is consistent with the data shown in Fig. 1D.

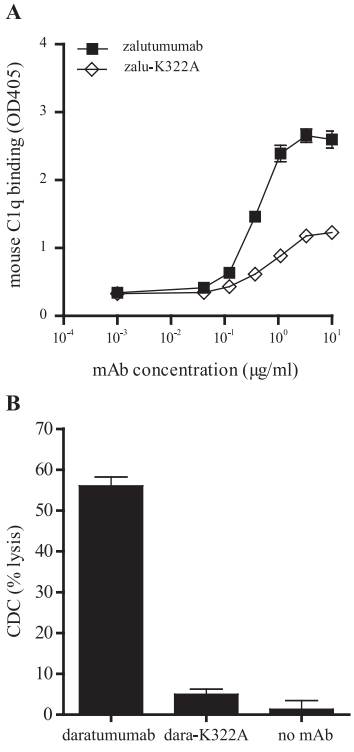

Supplemental Figure 2. *Strongly reduced C1q binding and CDC induction by human IgG1-K322A mutant with mouse serum.* (A) Binding of zalutumumab and zalu-K322A to mouse C1q was analyzed by ELISA. For this, 1% mouse serum was incubated in 96-well plates coated with a serially diluted human IgG1 mAb. After washing, mouse C1q was detected using biotinylated rabbit-anti-mouse C1q (Cedarlane, Burlington, Canada) and streptavidin-HRP (Sanquin), shown is the OD405. (B) Because A431 cells are insensitive for *in vitro* CDC induced by EGFR-specific Abs, as previously demonstrated (13, 16), we used a Burkitt's lymphoma cell line in combination with daratumumab, a human IgG1 antibody against CD38 which potently induces CDC (29) to demonstrate that a K322A mutation in human IgG1 abrogates CDC with mouse serum. A ^{51}Cr release assay was used to study the CDC-inducing capacity of the CD38-specific mAb daratumumab and the dara-K322A mutant. For this, ^{51}Cr labeled Daudi target cells were dispensed into 96-well plates ($2.5x10^3$ cells per well) and pre-incubated with 1 µg/mL mAb (RT, 15 min) followed by 60 min incubation at 37°C in the presence of 12.5% mouse serum. Data shown are percentages specific lysis, calculated as described in *Materials and Methods*. Each data point represents mean ± SEM of triplicates and experiments shown are representative of two independent experiments.

7

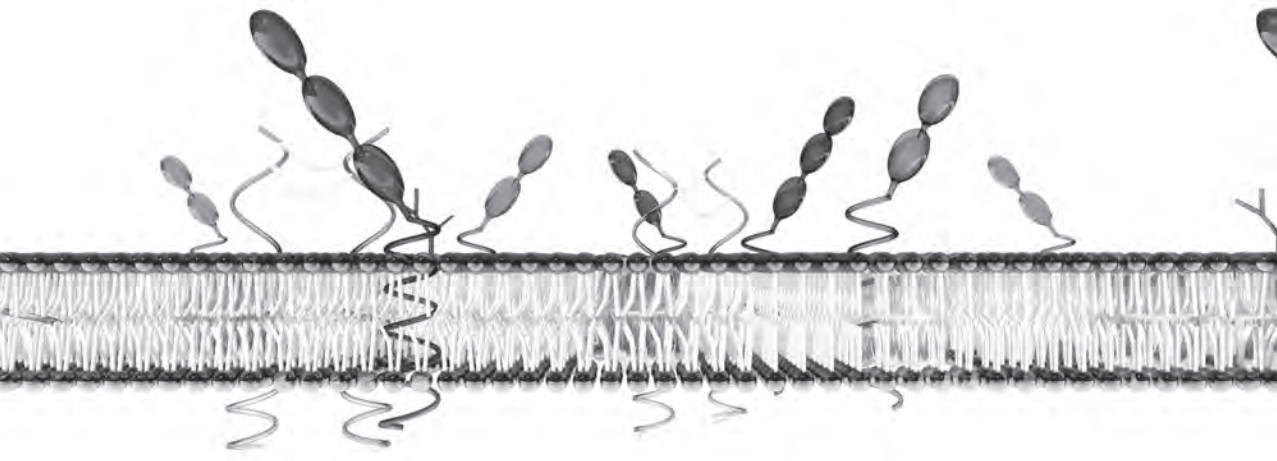

Epidermal growth factor receptor as target for peri-operative monoclonal antibody treatment of colon carcinoma

Marijn Bögels[1,2,#], Marije B. Overdijk[3#], Rens Braster[1], Nuray Gül[1], Wim K. Bleeker[3], Sandra Verploegen[3], Paul W.H.I. Parren[3] and Marjolein van Egmond[1,2]

[1]Department of Molecular Cell Biology and Immunology, VU University Medical Center, Amsterdam, the Netherlands, [2]Department of Surgery, VU University Medical Center, Amsterdam, the Netherlands, [3]Genmab, Utrecht, The Netherlands

[#] These authors contributed equally to this paper.

In preparation

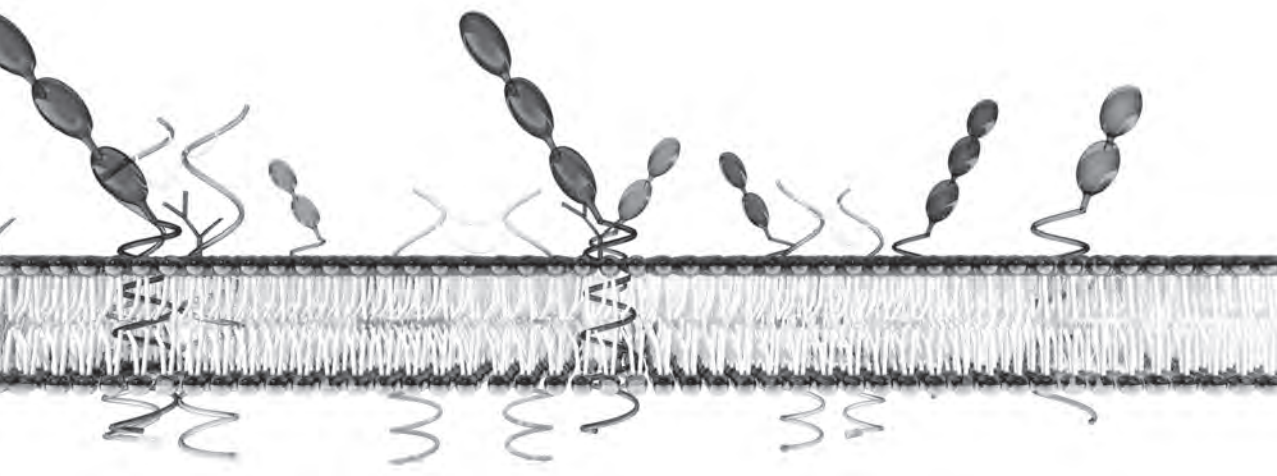

Abstract

The primary treatment of patients with restricted colorectal cancer (CRC) is surgical resection of the colorectal tumor. However, the trauma inflicted by surgical procedures during excision of the primary tumor, has been shown to be associated with risk of developing distant metastases, mostly in the liver. It has been hypothesized that antibody-dependent cellular phagocytosis (ADCP) of antibody-opsonized tumor cells by Kupffer cells in the liver might prevent the formation of such surgery-induced metastases. Here we assess whether treatment with a monoclonal antibody (mAb) against epidermal growth factor receptor (EGFR), which is expressed on ~80% of human CRC, may be used to prevent surgery-induced liver metastasis. To address this question we made use of zalutumumab, a human IgG1 EGFR mAb. Zalutumumab efficiently induced ADCP of epidermoid and CRC tumor cells *in vitro* with both mouse and human macrophages (mφ). Live cell imaging demonstrated that zalutumumab-mediated ADCP led to lysosomal degradation of tumor cells within the mφ phagosome. The potency of ADCP was dependent on EGFR expression but independent of mutations in downstream EGFR kinases KRAS or BRAF. Finally, we showed efficient *in vivo* ADCP by Kupffer cells of zalutumumab-opsonized human EGFR-expressing murine colon carcinoma cell line (C26-hEGFR) accompanied by a reduction of free tumor cells in the liver. In conclusion, we suggest that EGFR is a promising target candidate for peri-operative mAb treatment of patients to prevent surgery-induced liver metastasis of CRC.

Introduction

Surgical excision of the primary tumor is the basis of curative therapy for colorectal cancer (CRC) and critical for improved survival (1, 2). Remarkably, 10-25% of patients without detectable colorectal liver metastases at time of diagnosis, develop distant metastases after removal of the primary tumor (3). These metastases are thought to arise from circulating tumor cells (4-6), which have been detected in 10-70% of the patients (7). In addition, over the years evidence has accumulated, which supports that trauma, inflicted by surgical procedures to excise the primary tumor, is associated with the risk of developing metastases (1, 8-10). Studies in animal models showed that the dissemination of tumor cells from a solid tumor into the circulation is enhanced after manipulation of the primary tumor (11, 12). By mimicking surgical procedures in syngeneic *in vivo* models, we previously demonstrated that surgical trauma induced a systemic effect resulting in enhanced tumor cell adhesion of circulating tumor cells (13, 14). The surgical trauma did not stimulate growth of already adhered tumor cell clusters.

The peri-operative period is an attractive window of opportunity for eliminating the disseminated circulating tumor cells, and engagement of anti-tumor immune responses via monoclonal antibodies (mAbs) might be a promising approach (9). Therapeutic mAbs can inhibit or reduce tumor growth by one or multiple mechanisms of action (15). Studies with mAbs mainly focus on tumor regression in patients with larger primary or metastatic tumor masses (16, 17). Research on the effects of mAb therapy to prevent new distant recurrences of disease is however sparse. We previously showed that post-operative treatment of rats with a mAb directed against rat CC531s colon carcinoma cells prevented surgery-induced liver metastases (18). Furthermore, we demonstrated in *in vivo* experiments that prevention of surgery-induced metastases via mAb treatment was dependent on the presence of macrophages (mφ) and Fc-gamma receptors (FcγRs) (18, 19). In 1998, Rietmuller et al. (20) described the post-operative effect of an EpCAM-targeting murine mAb in patients in which the primary CRC tumor was resected. The occurrence of distant metastases was reduced, albeit only in ~30% of the treated patients. The low response rate is suggested to be due to the heterogenic EpCam expression and the development of an Ab response targeting the therapeutic mouse Ab (HAMA response).

As epidermal growth factor receptor (EGFR) expression is up-regulated in ~80% of colorectal cancer patients (21, 22), EGFR might represent a suitable

target for peri-operative therapy of CRC patients without any evidence of distant metastases (e.g. stage I/II cancer). Zalutumumab is a human IgG1 EGFR mAb, previously demonstrated to have a dual mechanism of action, namely through signaling inhibition and antibody-dependent cellular cytotoxicity (ADCC) (23). Zalutumumab has been shown, in pre-clinical studies, to be able to inhibit tumor growth in early stages of tumor development and in metastasis solely via ADCC (24) and therefore represents an interesting tool to study the potency of EGFR as a target in peri-operative therapy of CRC patients.

In this study we investigated zalutumumab induced antibody-dependent cellular phagocytosis (ADCP) of epidermoid and CRC cell lines, and whether this is impacted by the EGFR expression level and mutations in EGFR downstream kinases BRAF and KRAS. Finally, we explored the *in vivo* efficacy of peri-operative treatment with zalutumumab in a syngeneic *in vivo* liver metastasis model.

Materials and methods

Antibodies

The human IgG1, κ, EGFR-specific mAb zalutumumab was generated by immunizing HuMAb mice (Medarex, Milpitas, CA) and produced as recombinant proteins as described previously (23). The N297Q mutation in the Fc part of zalutumumab, referred to as zalu-N297Q was introduced using the QuikChange XL site-directed mutagenesis kit (Stratagene, La Jolla, CA). Mutagenesis was checked by sequencing (LGC Genomics, Berlin, Germany). IgG concentrations were determined by A280 measurements. A human IgG1, λ, against hepatitis C E2 envelope protein was included in all experiments as control mAb (25).

Cells

HT29, HCT116, RKO (human colon carcinoma), A431 (human vulvar carcinoma), L929 (murine fibroblast) and C26 (murine colon carcinoma) were all obtained at the ATCC (Rockville, MD). C26 wild-type (WT) cells were transfected with 1 μg human EGFR construct (hEGFR in pUSE/amp/neo vector, Upstate biotechnology, Lake Placid NY)) using the Fugene-6 transfection system (Roche Applied Science, Basel, Switzerland) according to manufacture's instructions. EGFR positive cells were selected 48h after transfection by incubating cells with 3.5 mg/ml geneticin (G418, Invitrogen, Paisley, UK). C26 expressing hEGFR were sorted using a MoFlo XDP flow cytometry cell sorter (Beckman Coulter

Inc, Miami, FL) into C26-hEGFR-1, C26-hEGFR-2 and C26-hEGFR-3 clones with low, intermediate and high EGFR expression respectively. Cells were resorted every 2 weeks with a minimum of 10 sorting rounds to obtain stable C26-hEGFR cell lines. Cells were cultured under standard incubator conditions in RPMI 1640 medium (Invitrogen) (L929 and C26) or DMEM medium (Invitrogen) (all other cell lines), supplemented with 10% heat inactivated fetal calf serum (FCS, Lonza, Verviers, Belgium), 100 U/ml penicillin (Lonza), 100 µg/ml streptomycin (Lonza) and 200 µM L-glutamin (Lonza) (further referred to as complete RPMI or DMEM medium respectively) The culture medium for C26-hEGFR cells was supplemented with 3.5 mg/ml geneticin. Cell suspensions were prepared by enzymatic detachment using trypsin-EDTA solution (Invitrogen). Viability was assessed by trypan blue exclusion and always exceeded 95%.

Mouse L929 cell conditioned medium

Murine L929 cells secrete macrophage-colony stimulating factor (M-CSF) and were used to produce L929 cell conditioned medium (LCM) to differentiate mφ. L929 cells were grown to confluency, after which medium was changed with fresh complete RPMI medium. Cells were subsequently grown for 7 days after which LCM was harvested, centrifuged at 4750g for 10 minutes, filtered through 0.2 µm filters and stored at -20˚C until further use.

Bone marrow-derived mouse macrophage culture

WT balb/c mice were bred and maintained at the Central Animal Facility of the VU University Medical Center (VUmc, Amsterdam, The Netherlands) under standard conditions. Bone marrow (BM) was harvested from freshly isolated femur, tibia and humerus. BM was flushed and single cell suspensions were made by passing BM cell suspension through a sterile 70 µm filter (BD Falcon, Bedford, MA). Macrophages were differentiated by incubating BM cells for 7 days with complete DMEM medium, supplemented with 15% LCM (referred to as complete mφ medium). Macrophages were harvested after a 15 minute incubation with trypsin-EDTA and subsequent scraping using a cell scraper.

Monocyte-derived human macrophage culture

Buffy coats were obtained within 24h after blood collection (Sanquin, Amsterdam, The Netherlands) from healthy listed blood donors who gave informed consent according to the guidelines of the medical ethical committee

of the VUmc. Peripheral blood mononuclear cells (PBMCs) were isolated using density separation with lymfoprep (Nyegaard, Oslo, Norway), followed by washing with PBS (B.Braun, Melsungen, Germany) supplemented with autologous serum and reconstituted in complete DMEM. Human monocytes were isolated from the PBMCs using a Percoll gradient (GE Healthcare, Uppsala, Sweden) (46.1 % Percoll, 0.15 mM NaCl). Isolated monocytes were seeded in 10 cm^2 plastic cell culture petri-dishes (10-15×10^6 cells/dish) in complete DMEM medium, supplemented with 10 ng/ml human granulocyte macrophage-colony stimulating factor (GM-CSF, ImmunoTools, Friesoythe, Germany) and cultured for 7 days. Cultured mφ were harvested by incubation with trypsin-EDTA and subsequent scraping using a cell scraper.

Flow cytometry

Numbers of cell surface EGFR molecules were determined with mouse-anti-human EGFR (BD Biosciences) and the Qifi kit (DAKO, Glostrup, Denmark). Samples were analyzed with flow cytometry (FacsCalibur, BD, San Jose, CA).

Fluorescent labeling cells

For *in vitro* ADCP assays tumor cells or mφ were harvested and incubated (1-10×10^6 cells/ml) in complete DMEM medium supplemented with either 2.5 µg/ml 1,1'-dioctadecyl-3,3,3',3'-tetramethylindocarbocyanine perchlorate (DiI, Sigma-Aldrich, St. Louis, MO) or 2.5 µg/ml 3,3'-dioctadecyloxacarbocyanine perchlorate (DiO, Molecular Probes Inc, Paisley, UK) for 30 minutes at 37˚C, and subsequently washed three times with complete DMEM. Alternatively, mφ were labeled with the Lyso-ID Red lysosomal staining (Enzo Biochem Inc, Farmingdale, NY), according to the manufacturer's instructions.

Antibody-dependent cellular phagocytosis (ADCP)

DiO labeled mφ were seeded at 4×10^5 cells/well into 24-well plates and allowed to adhere O/N. DiI labeled tumor cells were co-cultured with the adhered mφ for 24h at 37˚C at an effector to target (E:T) ratio of 15:1 in the presence of indicated mAb concentration. All cells were detached using trypsin-EDTA and subsequent scraping using a cell scraper. ADCP was evaluated with flow cytometry and defined by the number of remaining tumor cells (percentage DiI^+ cells) and the number of double positive (DP) mφ (percentage DiI^+,DiO^+ cells). The number of remaining tumor cells and DP mφ after co-culture without mAb were set at 100%.

Live cell imaging

DiO or Lyso-ID Red labeled mφ were seeded at 2×10^5 cells/well in 8-well ibiTreat µ-Slides (IBIDI, Munich, Germany) and allowed to adhere O/N. DiI or DiO labeled tumor cells were added at an E:T ratio of 3:1 in the presence of 1 µg/ml zalutumumab or control mAb. Live cell imaging was done using the Olympus CellR real-time live-imaging station (type IX81, UPLFLN 40 x O/1.3 lens, Münster, Germany). Pictures were taken every 3 min with an Olympus ColorView II camera for 3-6h, followed by a 6 min interval for 18-21h. Additionally, random pictures were taken after 24h.

Mouse tumor models

Experiments were performed with male WT balb/c mice. The Committee for Animal Research of the VUmc approved all experiments, according to institutional and national guidelines. Induction of liver metastasis was done as previously described (18). In short, 1.5×10^6 DiI labeled C26-hEGFR-3 cells were inoculated under anesthesia in a mesenteric vein after laparotomy. Directly after tumor cell inoculation 100 µg/mouse (5mg/kg) mAb was given intraperitoneally (i.p.) before closing the abdomen. Mice were sacrificed after 24h and livers were snap frozen for microscopic analysis.

Fluorescence microscopy

Cryostat tissue sections of 5 µm were fixed for 10 min in acetone and air-dried. Slides were incubated for 1h with F4/80-FITC (Serotec, Oxford, UK) at 4˚C in a humidified tissue chamber. After washing, nuclei were stained with Hoechst (10 µg/ml, Molecular Probes). Sections were washed, mounted and examined with a Leica DM6000B fluorescence microscope (Leica Microsystems, Heidelberg,Germany). The number of free tumor cells and phagocytosed tumor cells was determined by analyzing, on average, 42 randomly selected fields per liver sample for each animal. The total number of tumor cells (both free and phagocytosed) counted within the selected fields was set at 100%.

Statistical analysis

Data was analyzed with Bonferroni-Post Hoc test, preceded by one way ANOVA test for comparison of multiple groups. Significance was accepted at $p < 0.05$.

Results

Antibody-dependent cellular phagocytosis of epidermoid tumor cells by zalutumumab

To explore whether ADCP could be induced by a human mAb targeting EGFR, we set-up a flow cytometric assay with murine mφ and an epidermoid cell line A431 expressing high levels of EGFR (>500,000 molecules/cell, Table 1).

Table 1. EGFR expression

Cell line	EGFR expression (molecules/cell)
C26-hEGFR-1	< 2,000
RKO	~ 3,000
C26-hEGFR-2	~ 15,000
C26-hEGFR-3	~ 40,000
HT29	~ 40,000
HCT116	~ 40,000
A431	> 500,000

A serial dilution of either zalutumumab or a control mAb was assessed and the percentage remaining target cells and double positive (DP) mφ determined. Zalutumumab did not inhibit EGFR signaling in the selected concentration range (1 to 100 ng/ml; Supplemental Fig. 1A). Fig. 1A shows representative flow cytometry plots of mouse mφ co-cultured with A431 cells in the presence of 100 ng/ml control mAb (*left plot*) or zalutumumab (*right plot*) in which DiI^-/DiO^+ mφ, DiI^+/DiO^- target cells and DiO^+/DiI^+ double positive (DP) mφ are indicated. Zalutumumab concentrations above 0.1 ng/ml reduced the number of A431 cell cells (Fig. 1B) and increased the number of DP mφ (Fig. 1C) after O/N incubation.

Live cell imaging revealed ADCP of whole A431 cells on average within 60 minutes by mφ in the presence of 1 μg/ml zalutumumab (Supplementary video 1). Bright field microscopy is shown of a mφ (designated with an arrow) and an A431 cell (designated with an asterisk) (Fig. 2A, *left picture*) and subsequently engulfment of this A431 cell by the mφ (Fig. 2A, *right picture*) in the presence of zalutumumab. No tumor cell uptake was observed in the presence of a control mAb even after prolonged imaging, indicating ADCP to be target dependent (Fig. 2B, and Supplementary video 2).

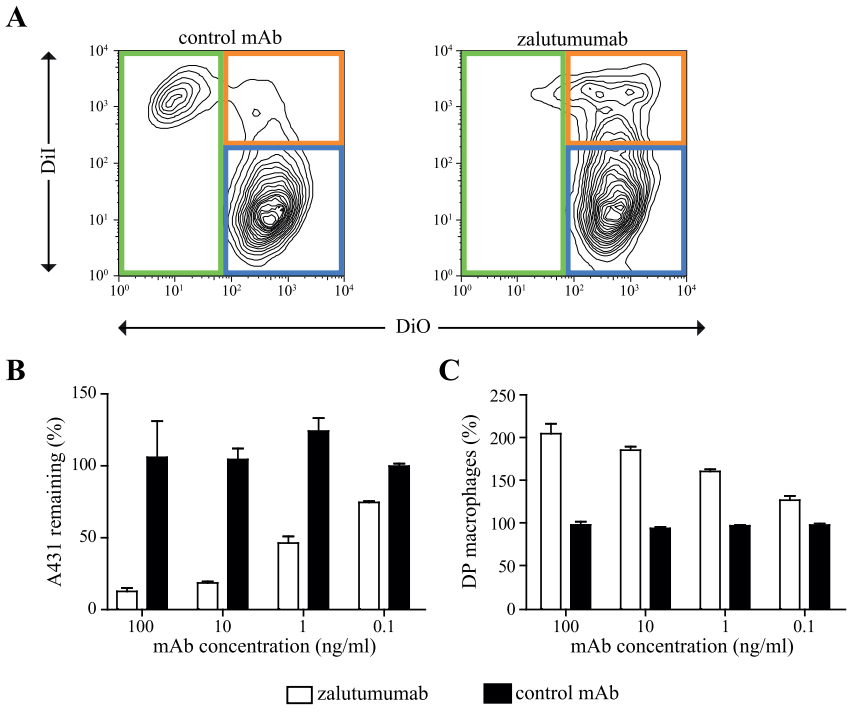

Figure 1. *Zalutumumab-induced ADCP of epidermoid tumor cells.* Flow cytometry analysis of ADCP induction of A431 cells by co-cultures with mouse mφ for 24h with a serial dilution of zalutumumab or control mAb, E:T ratio 15:1. (A) Representative flow cytometry plots of co-cultures in the presence of control mAb (*left plot*) or zalutumumab (*right plot*). DiI^-/DiO^+ mφ (blue gate), DiI^+/DiO^- target cells (green gate) and DiI^+/DiO^+ double positive (DP) mφ (orange gate) are indicated. (B) Percentage remaining A431 cells characterized as DiI^+/DiO^- cells. (C) Percentage DP mφ characterized as DiI^+/DiO^+ cells. The lowest concentration of control mAb is set as 100%. Each bar shows mean ± SD representative of at least 3 independent experiments.

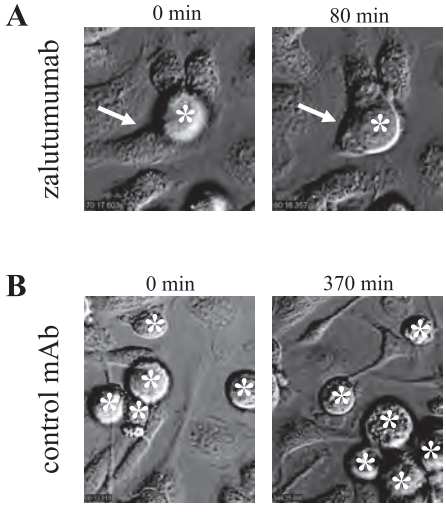

Figure 2. *Live cell imaging shows ADCP induction of A431 cells by zalutumumab.* Phagocytosis of A431 cells by mφ in the presence of 1 μg/ml mAb, E:T ratio 3:1. (A) Bright field images of engulfment of an individual A431 cell by a mφ in the presence of zalutumumab. (B) Bright field images of A431 cells and mφ in the presence of control mAb. Arrow points to mφ, asterisks indicate A431 cells.

Antibody-dependent cellular phagocytosis of tumor cells by macrophages leads to sequential lysosomal degradation

To explore whether tumor cells are degraded in the lysosomes, mφ were labeled with the acidic organelle-specific dye Lyso-ID, which becomes red fluorescent in acidic lysosomes. Macrophages engulfed one to three whole A431 cells in the presence of zalutumumab. Interestingly, the lysosomes fused sequentially with the different tumor cell containing phagosomes within an individual mφ (Fig. 3A, Supplemental Fig. 2 and Supplemental videos 3,4). The lysosomes seemed to fuse with the first phagosome they encountered. Fig. 3A shows that within 1h after addition of tumor cells to the mφ in the presence of zalutumumab, lysosomes were recruited towards the first A431 containing phagosome (indicated with number 1). Then 2.5h later, lysosomes fused with the second A431 containing phagosome (indicated with number 2). The first A431 cell is degraded and acidity of phagosome declines after 5h (indicated with an asterisk), whereas degradation of the second A431 containing-phagosome still persists. After 24h all detectable A431 tumor cells were degraded in the presence of zalutumumab and tumor cell debris was observed within mφ (Fig. 3B). Co-cultures in the presence of control mAb neither led to ADCP of tumor cells nor lysosomal activity (Fig. 3C, Supplementary video 5) and after 24h large tumor cell clusters were observed, indicative for outgrowth of the tumor cells (data not shown).

Zalutumumab-dependent phagocytosis of tumor cells by macrophages is independent of mutations in KRAS or BRAF, but depends on levels of EGFR expression

Mutations in genes encoding KRAS and BRAF kinases downstream of EGFR in tumor cells have been demonstrated to hamper the responsiveness of CRC cells to EGFR mAb treatment (26). We therefore explored whether efficiency in ADCP induction by zalutumumab is affected by mutations in the EGFR signaling pathway. Flow cytometric analyses of ADCP induction by zalutumumab on KRAS-mutated HCT116 cells (Fig. 4A,B) and BRAF mutated HT29 cells (Fig. 4C,D) showed a dose-dependent decrease of tumor cells and an increase in DP mφ after 24h incubation. Incubation with the control mAb did not induce tumor cell killing or DP mφ on the mutated cell lines (Fig. 4A-D), showing the effect to be target specific. To translate our findings to human cells, we also explored ADCP by human mφ. Zalutumumab induced ADCP of HCT116 and HT29 cells by human mφ which was of a similar magnitude compared to ADCP by mouse mφ (Fig. 4E,F).

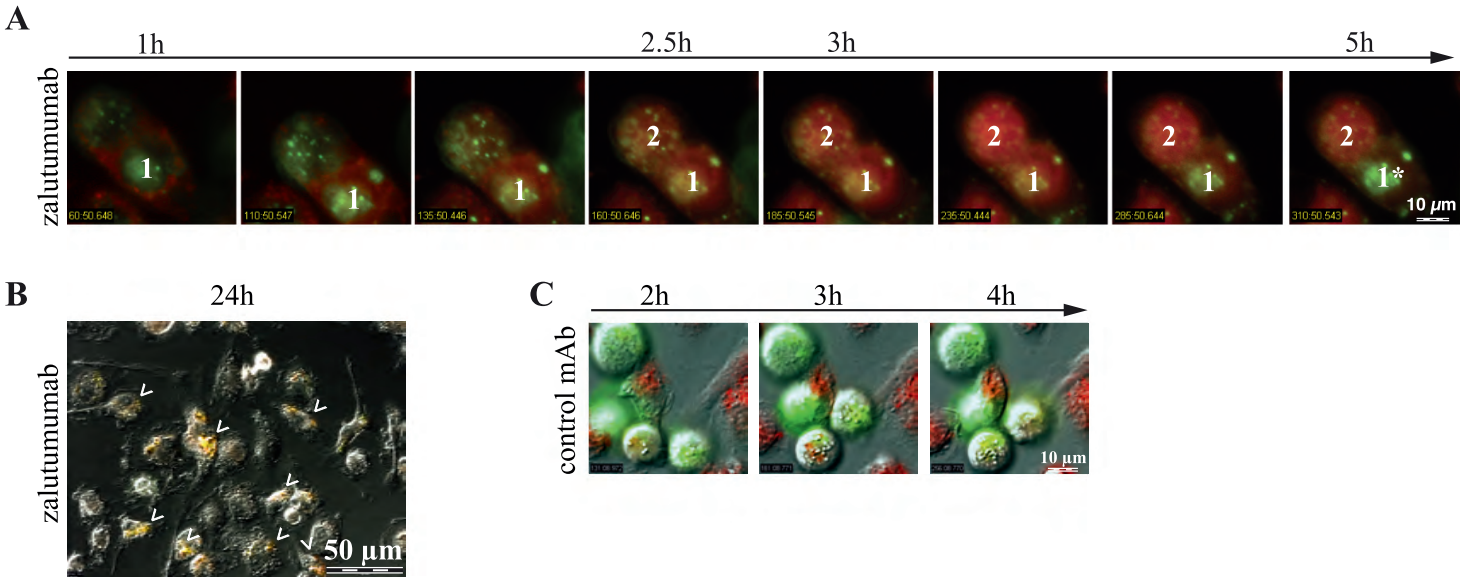

Figure 3. *Live cell imaging shows sequential lysosomal degradation of ingested tumor cells upon EGFR mAb-mediated ADCP.* Live cell imaging microscopy of co-cultures with DiO-labeled A431 cells (green) and acidic organelle-specific dye stained mφ (red) in the presence of 1 µg/ml mAb, E:T ratio 3:1. (A) Time lapse fluorescent images of sequential lysosomal targeting of two engulfed A431 cells. Numbers indicate the tumor cells to which the lysosomes are recruited, asterisk indicates degraded tumor cell. (B) Fluorescent image after 24h incubation in the presence of zalutumumab (arrowheads indicate degraded tumor cells). (C) Time lapse microscopy images of A431 cells in the presence of control mAb.

RKO cells, a human CRC cell line without downstream EGFR mutations, but with low EGFR expression (~3,000 molecules/cell) was not phagocytosed in the presence of zalutumumab (data not shown). We therefore investigated the minimal level of EGFR expression required for ADCP induction. To exclude confounding effects from factors other than EGFR expression, we stably transfected murine C26 colon carcinoma cells with human EGFR (hEGFR) and obtained three clones, referred to as C26-hEGFR-1, C26-hEGFR-2, C26-hEGFR-3, expressing <2,000, ~15,000 or ~40,000 molecules/cell hEGFR, respectively (Table 1). EGFR signaling was not functional in these clones as shown in a proliferation inhibition assay (Supplemental Fig. 1B). Flow cytometric analysis of ADCP induction by mouse mφ via zalutumumab on the C26-hEGFR clones showed a decrease of tumor cells and an increase of DP mφ for all three hEGFR expressing clones (Fig. 5A,B). However, the effect on C26-hEGFR-1 and C26-hEGFR-2 cells was marginal, indicating that an EGFR expression level above 15,000 molecules/cell is required for good ADCP. The control mAb had no effect on killing or DP mφ for all C26-hEGFR clones (Fig. 5A,B), demonstrating the effects to be target-dependent.

Peri-operative treatment with zalutumumab leads to ADCP via Kupffer cells in the mouse liver

Next, we explored whether zalutumumab induced ADCP *in vivo*. We generated a mutant in which the site for N-linked glycosylation in the Fc domain was eliminated through mutation of the asparagine at position 297 to glutamine (zalu-N297Q). This mutation leads to loss of FcγR binding (27) and zalu-N297Q was previously shown to be unable to induce ADCC (24). We confirmed in a flow cytometry ADCP assay with mouse mφ and C26-hEGFR-3 cells that the N297Q mutation also led to strongly reduced ADCP, since there was almost no killing (Fig. 6A) and no induction of DP mφ (Fig. 6B). We studied whether peri-operative treatment with either 5 mg/kg zalutumumab, zalu-N297Q or a control mAb, directly after a laparotomy and inoculation of DiI labeled C26-hEGFR-3 cells in a mesenteric vein, was able to induce ADCP. After 24h, livers were snap-frozen and cryostat tissue sections were stained with F4/80-FITC to identify the Kupffer cells. Liver sections were scored blinded for free DiI^+ C26-hEGFR-3 cells and for $F4/80^+/DiI^+$ DP Kupffer cells. In the zalutumumab-treated mice there was a significant reduction of free DiI^+ C26-hEGFR-3 cells and a significant increase in DP Kupffer cells. This effect was significantly reduced in the zalu-N297Q treated group, indicating that the effect was Fc-mediated. Overall, data showed in this

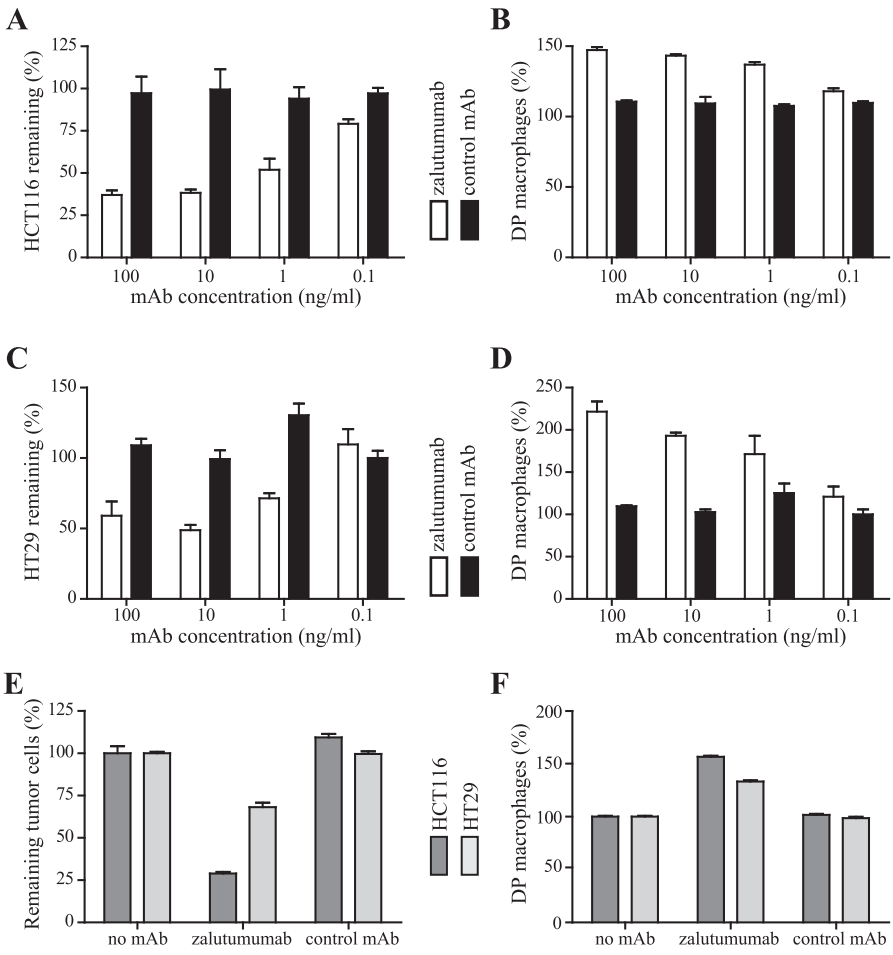

Figure 4. *ADCP induction is independent of mutations in EGFR downstream kinases.* Flow cytometry analysis of ADCP induction of KRAS mutated HCT116 cells (A,B) or BRAF mutated HT29 cells (C,D) by co-culture with mouse mφ (A-D) or human mφ (E,F) for 24h with different concentrations of zalutumumab or control mAb, E:T ratio 15:1. (A,C,E) Percentage remaining tumor cells characterized as DiI^{+}/DiO^{-} cells. (B,D,F) Percentage double positive (DP) mφ characterized as DiI^{+}/DiO^{+} cells. The lowest concentration of control mAb is set as 100%. Each bar shows mean ± SD representative of at least 3 independent experiments.

study supports that peri-operative treatment with an EGFR targeting mAb, like zalutumumab, might be able to reduce outgrowth of disseminated circulating tumor cells.

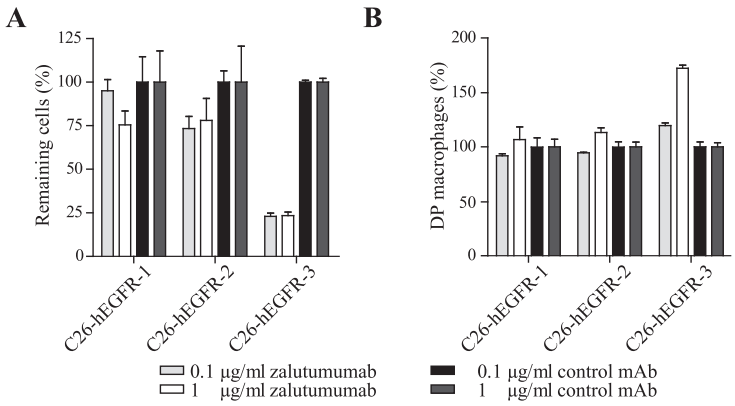

Figure 5. *ADCP induction is dependent on EGFR expression level.* Flow cytometry analysis of ADCP induction of C26-hEGFR clones with different hEGFR expression levels, by co-culture with mouse mφ for 24h with indicated concentration of zalutumumab or control mAb, E:T ratio 15:1. (A) Percentage remaining tumor cells characterized as DiI^+/DiO^- cells. (B) Percentage double positive (DP) mφ characterized as DiI^+/DiO^+ cells. The lowest concentration of control mAb is set as 100%. Each bar shows mean ± SD representative of at least 3 independent experiments

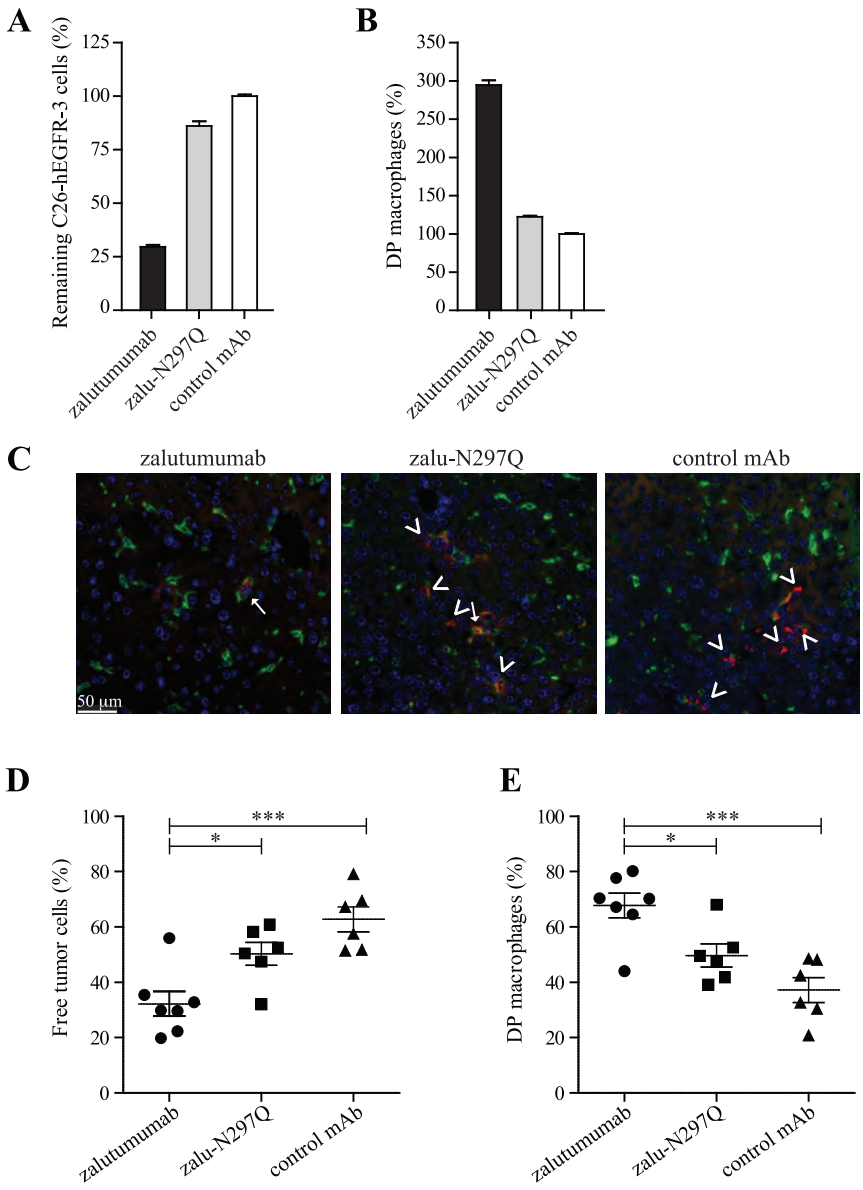

Figure 6. *Peri-operative treatment with EGFR mAb leads to ADCP via kupffer cells in vivo.* (A) Percentage remaining C26-hEGFR-3 cells, and (B) percentage DP mφ after 24h co-culture with mouse mφ in the presence of indicated mAbs at 0.1 µg/ml. (C-E) Syngeneic experimentally induced liver metastasis model via inoculation of 1.5×10^6 DiI labeled C26-EGFR-3 cells in a mesenteric vein, peri-operative treatment with 100 µg/mouse (5 mg/kg). (C) Representative fluorescent microscopy images of the liver are shown stained for F4/80$^+$ mφ (green), DiI$^+$ tumor cells (red) and Hoechst stained nuclei (blue) (arrows indicate DP mφ, arrowheads indicate free tumor cells). (D) Percentage free DiI$^+$ tumor cells scored. (E) Percentage DP DiI$^+$/F4/80$^+$ mφ scored. (* $p<0.05$, *** $p<0.001$ Bonferroni's multiple comparison test).

Discussion

In this study we explored the potential use of an EGFR-targeting mAb for peri-operative treatment of patients to inhibit surgery-induced metastasis of CRC. We demonstrated potent ADCP induction by zalutumumab, an EGFR mAb, of EGFR-expressing epidermoid and CRC cell lines, including CRC cell lines with mutations in genes encoding kinases downstream of EGFR. ADCP induction was dependent on EGFR expression level and was shown to lead to sequential lysosomal degradation of the tumor cells. In a syngeneic *in vivo* experimental liver metastasis model induction of ADCP by Kupffer cells was observed upon peri-operative zalutumumab treatment.

EGFR-targeting mAbs have been shown to inhibit proliferation, by blocking of EGF binding and EGFR down modulation, and to induce ADCC (28, 29). ADCP induction of ovarian cancer cells has recently been shown for cetuximab (chimeric IgG1 EGFR mAb) (30), though ADCP induction by other EGFR mAbs has not been reported. We now demonstrate a dose-dependent induction of ADCP by zalutumumab of the epidermoid cell line A431, starting at a dose of 1 ng/ml. Live cell imaging showed that the mouse mφ engulfed multiple tumor cells rapidly, which were fused sequentially with the lysosomal compartment. Complete degradation of all engulfed tumor cells was taking up to 24h.

Mutations in EGFR downstream kinases have been shown to inhibit cetuximab treatment of CRC (31). We previously demonstrated that post-operative treatment with a tumor-specific mAb prevented surgery-induced liver metastasis mainly via ADCP by Kupffer cells and monocytes in the liver (18). Therefore, signaling inhibition by the EGFR-targeting mAb is likely not necessary for therapeutic efficacy in peri-operative treatment. We showed ADCP occurs with both HCT116 cells, containing a KRAS mutation, and HT29 cells, containing a BRAF mutation, indicating that EGFR-mediated killing of human CRC cells by mφ is independent of the KRAS or BRAF mutational status of tumor the cells.

ADCC induction has been shown to already induce a maximal effect at very low EGFR expression (>5,000 molecules/cell) on lung cancer cell lines (28). The low threshold for ADCC has also been shown for EGFR targeting mAbs in other studies (23, 32, 33). In this study we still found detectable ADCP induction at low EGFR expression (~15,000 molecules/cell). The strength of ADCP induction with a cell line with 40,000 molecules/cell (C26-hEGFR-3, Fig. 5) was comparable to that with a cell line with > 500,000 molecules/cell (A431, Fig. 1). Therefore, we suggest that optimal

ADCP efficacy on CRC cell lines is already reached at 40,000 EGFR molecules/cell, although expression of regulators of phagocytosis on different cell lines may influence this threshold.

Finally, we explored whether zalutumumab was effective *in vivo* after peri-operative treatment of C26-hEGFR-3 cells in an experimentally induced liver metastasis model. The peri-operative zalutumumab treatment significantly reduced the number of C26-hEGFR-3 cells in the liver after 24h and the percentage DP Kupffer cells was significantly increased. This effect was significantly reduced with the zalu-N297Q mutant, confirming that this process was Fc-dependent. The small effect of zalu-N297Q on the number of C26-hEGFR-3 cells and percentage DP Kupffer cells is probably due to residual FcγRI binding (34).

In conclusion, EGFR, which is up-regulated in ~80% of colorectal cancer patients (35), represents an excellent candidate for mAb prevention of surgery-induced metastases formation in patients undergoing resection of primary CRC. Furthermore, it might also be a promising target for eliminating circulating tumor cells in CRC patients, which have been proposed as an independent prognostic factor for survival of CRC patients (5, 36). Currently, two EGFR mAbs are approved for the treatment of (metastasized) CRC, cetuximab and panitumumab (human IgG2 EGFR mAb). We previously showed that the human IgG2 isotype poorly induces ADCP (37) and therefore panitumumab is not a suitable candidate for peri-operative treatment of CRC patients. Cetuximab has been shown to induce ADCP (30) and represents a candidate for peri-operative treatment. Drawbacks however, may be the immunogenicity risk profile, as cetuximab is a mouse/human chimeric Ab, and cetuximab has been shown to induce allergic reactions (38, 39). This study provides a proof of concept for peri-operative treatment with zalutumumab, which has been evaluated for the treatment of patients with squamous cell carcinoma of the head and neck (SCCHN) (40). We hypothesize that patients undergoing resection for primary CRC may greatly benefit from peri-operative treatment with zalutumumab, as this will induce elimination of disseminated tumor cells by the myeloid mononuclear network in the liver.

References

1. Coffey, J. C., M. J. Smith, J. H. Wang, D. Bouchier-Hayes, T. G. Cotter, and H. P. Redmond. 2006. Cancer surgery: risks and opportunities. *Bioessays* 28:433-437.
2. Weitz, J., M. Koch, J. Debus, T. Hohler, P. R. Galle, and M. W. Buchler. 2005. Colorectal cancer. *Lancet* 365:153-165.
3. Sutcliffe, R. P., and S. Bhattacharya. 2011. Colorectal liver metastases. *Br Med Bull* 99:107-124.
4. Cohen, S. J., C. J. Punt, N. Iannotti, B. H. Saidman, K. D. Sabbath, N. Y. Gabrail, J. Picus, M. Morse, E. Mitchell, M. C. Miller, G. V. Doyle, H. Tissing, L. W. Terstappen, and N. J. Meropol. 2008. Relationship of circulating tumor cells to tumor response, progression-free survival, and overall survival in patients with metastatic colorectal cancer. *J Clin Oncol* 26:3213-3221.
5. Cohen, S. J., C. J. Punt, N. Iannotti, B. H. Saidman, K. D. Sabbath, N. Y. Gabrail, J. Picus, M. A. Morse, E. Mitchell, M. C. Miller, G. V. Doyle, H. Tissing, L. W. Terstappen, and N. J. Meropol. 2009. Prognostic significance of circulating tumor cells in patients with metastatic colorectal cancer. *Ann Oncol* 20:1223-1229.
6. Guller, U., P. Zajac, A. Schnider, B. Bosch, S. Vorburger, M. Zuber, G. C. Spagnoli, D. Oertli, R. Maurer, U. Metzger, F. Harder, M. Heberer, and W. R. Marti. 2002. Disseminated single tumor cells as detected by real-time quantitative polymerase chain reaction represent a prognostic factor in patients undergoing surgery for colorectal cancer. *Ann Surg* 236:768-775; discussion 775-766.
7. Gervasoni, A., M. T. Sandri, R. Nascimbeni, L. Zorzino, M. C. Cassatella, L. Baglioni, S. Panigara, M. Gervasi, D. Di Lorenzo, and O. Parolini. 2011. Comparison of three distinct methods for the detection of circulating tumor cells in colorectal cancer patients. *Oncol Rep* 25:1669-1703.
8. Coffey, J. C., J. H. Wang, M. J. Smith, D. Bouchier-Hayes, T. G. Cotter, and H. P. Redmond. 2003. Excisional surgery for cancer cure: therapy at a cost. *Lancet Oncol* 4:760-768.
9. van der Bij, G. J., S. J. Oosterling, R. H. Beelen, S. Meijer, J. C. Coffey, and M. van Egmond. 2009. The perioperative period is an underutilized window of therapeutic opportunity in patients with colorectal cancer. *Ann Surg* 249:727-734.
10. Halsted, W. S. 1907. I. The Results of Radical Operations for the Cure of Carcinoma of the Breast. *Ann Surg* 46:1-19.
11. Liotta, L. A., J. Kleinerman, and G. M. Saidel. 1974. Quantitative relationships of intravascular tumor cells, tumor vessels, and pulmonary metastases following tumor implantation. *Cancer Res* 34:997-1004.
12. Nishizaki, T., T. Matsumata, T. Kanematsu, C. Yasunaga, and K. Sugimachi. 1990. Surgical manipulation of VX2 carcinoma in the rabbit liver evokes enhancement of metastasis. *J Surg Res* 49:92-97.
13. Raa, S. T., S. J. Oosterling, N. P. van der Kaaij, M. P. van den Tol, R. H. Beelen, S. Meijer, C. H. van Eijck, J. R. van der Sijp, M. van Egmond, and J. Jeekel. 2005. Surgery promotes implantation of disseminated tumor cells, but does not increase growth of tumor cell clusters. *J Surg Oncol* 92:124-129.
14. van der Bij, G. J., S. J. Oosterling, M. Bogels, F. Bhoelan, D. M. Fluitsma, R. H. Beelen, S. Meijer, and M. van Egmond. 2008. Blocking alpha2 integrins on rat CC531s colon carcinoma cells prevents operation-induced augmentation of liver metastases outgrowth. *Hepatology* 47:532-543.
15. Oldham, R. K., and R. O. Dillman. 2008. Monoclonal antibodies in cancer therapy: 25 years of progress. *J Clin Oncol* 26:1774-1777.
16. Scott, A. M., J. P. Allison, and J. D. Wolchok. 2012. Monoclonal antibodies in cancer therapy. *Cancer Immun* 12:14.
17. Veronese, M. L., and P. J. O'Dwyer. 2004. Monoclonal antibodies in the treatment of colorectal cancer. *Eur J Cancer* 40:1292-1301.
18. van der Bij, G. J., M. Bogels, M. A. Otten, S. J. Oosterling, P. J. Kuppen, S. Meijer, R. H. Beelen, and M. van Egmond. 2010. Experimentally induced liver metastases from colorectal cancer can be prevented by mononuclear phagocyte-mediated monoclonal antibody therapy. *J Hepatol* 53:677-685.
19. Otten, M. A., G. J. van der Bij, S. J. Verbeek, F. Nimmerjahn, J. V. Ravetch, R. H. Beelen, J. G. van de Winkel, and M. van Egmond. 2008. Experimental antibody therapy of liver metastases reveals functional redundancy between Fc gammaRI and Fc gammaRIV. *J Immunol* 181:6829-6836.

20. Riethmuller, G., E. Holz, G. Schlimok, W. Schmiegel, R. Raab, K. Hoffken, R. Gruber, I. Funke, H. Pichlmaier, H. Hirche, P. Buggisch, J. Witte, and R. Pichlmayr. 1998. Monoclonal antibody therapy for resected Dukes' C colorectal cancer: seven-year outcome of a multicenter randomized trial. *J Clin Oncol* 16:1788-1794.

21. Messa, C., F. Russo, M. G. Caruso, and A. Di Leo. 1998. EGF, TGF-alpha, and EGF-R in human colorectal adenocarcinoma. *Acta Oncol* 37:285-289.

22. Porebska, I., A. Harlozinska, and T. Bojarowski. 2000. Expression of the tyrosine kinase activity growth factor receptors (EGFR, ERB B2, ERB B3) in colorectal adenocarcinomas and adenomas. *Tumour Biol* 21:105-115.

23. Bleeker, W. K., J. J. Lammerts van Bueren, H. H. van Ojik, A. F. Gerritsen, M. Pluyter, M. Houtkamp, E. Halk, J. Goldstein, J. Schuurman, M. A. van Dijk, J. G. van de Winkel, and P. W. Parren. 2004. Dual mode of action of a human anti-epidermal growth factor receptor monoclonal antibody for cancer therapy. *J Immunol* 173:4699-4707.

24. Overdijk, M. B., S. Verploegen, J. H. van den Brakel, J. J. Lammerts van Bueren, T. Vink, J. G. van de Winkel, P. W. Parren, and W. K. Bleeker. 2011. Epidermal Growth Factor Receptor (EGFR) Antibody-Induced Antibody-Dependent Cellular Cytotoxicity Plays a Prominent Role in Inhibiting Tumorigenesis, Even of Tumor Cells Insensitive to EGFR Signaling Inhibition. *J Immunol* 187:3383-3390.

25. Habersetzer, F., A. Fournillier, J. Dubuisson, D. Rosa, S. Abrignani, C. Wychowski, I. Nakano, C. Trepo, C. Desgranges, and G. Inchauspe. 1998. Characterization of human monoclonal antibodies specific to the hepatitis C virus glycoprotein E2 with in vitro binding neutralization properties. *Virology* 249:32-41.

26. Benvenuti, S., A. Sartore-Bianchi, F. Di Nicolantonio, C. Zanon, M. Moroni, S. Veronese, S. Siena, and A. Bardelli. 2007. Oncogenic activation of the RAS/RAF signaling pathway impairs the response of metastatic colorectal cancers to anti-epidermal growth factor receptor antibody therapies. *Cancer Res* 67:2643-2648.

27. Tao, M. H., and S. L. Morrison. 1989. Studies of aglycosylated chimeric mouse-human IgG. Role of carbohydrate in the structure and effector functions mediated by the human IgG constant region. *J Immunol* 143:2595-2601.

28. Kurai, J., H. Chikumi, K. Hashimoto, K. Yamaguchi, A. Yamasaki, T. Sako, H. Touge, H. Makino, M. Takata, M. Miyata, M. Nakamoto, N. Burioka, and E. Shimizu. 2007. Antibody-Dependent Cellular Cytotoxicity Mediated by Cetuximab against Lung Cancer Cell Lines. *Clinical Cancer Research* 13:1552-1561.

29. Schneider-Merck, T., J. J. Lammerts van Bueren, S. Berger, K. Rossen, P. H. van Berkel, S. Derer, T. Beyer, S. Lohse, W. K. Bleeker, M. Peipp, P. W. Parren, J. G. van de Winkel, T. Valerius, and M. Dechant. 2010. Human IgG2 antibodies against epidermal growth factor receptor effectively trigger antibody-dependent cellular cytotoxicity but, in contrast to IgG1, only by cells of myeloid lineage. *J Immunol* 184:512-520.

30. Sommariva, M., M. de Cesare, A. Meini, A. Cataldo, N. Zaffaroni, E. Tagliabue, and A. Balsari. 2013. High efficacy of CpG-ODN, Cetuximab and Cisplatin combination for very advanced ovarian xenograft tumors. *J Transl Med* 11:25.

31. Lièvre, A., J.-B. Bachet, V. Boige, A. Cayre, D. Le Corre, E. Buc, M. Ychou, O. Bouché, B. Landi, C. Louvet, T. André, F. Bibeau, M.-D. Diebold, P. Rougier, M. Ducreux, G. Tomasic, J.-F. Emile, F. Penault-Llorca, and P. Laurent-Puig. 2008. KRAS Mutations As an Independent Prognostic Factor in Patients With Advanced Colorectal Cancer Treated With Cetuximab. *Journal of Clinical Oncology* 26:374-379.

32. Kawaguchi, Y., K. Kono, K. Mimura, H. Sugai, H. Akaike, and H. Fujii. 2007. Cetuximab induce antibody-dependent cellular cytotoxicity against EGFR-expressing esophageal squamous cell carcinoma. *Int J Cancer* 120:781-787.

33. Lopez-Albaitero, A., S. C. Lee, S. Morgan, J. R. Grandis, W. E. Gooding, S. Ferrone, and R. L. Ferris. 2009. Role of polymorphic Fc gamma receptor IIIa and EGFR expression level in cetuximab mediated, NK cell dependent in vitro cytotoxicity of head and neck squamous cell carcinoma cells. *Cancer Immunol Immunother* 58:1853-1864.

34. Nesspor, T. C., T. S. Raju, C. N. Chin, O. Vafa, and R. J. Brezski. 2012. Avidity confers FcgammaR binding and immune effector function to aglycosylated immunoglobulin G1. *J Mol Recognit* 25:147-154.

35. Cunningham, D., Y. Humblet, S. Siena, D. Khayat, H. Bleiberg, A. Santoro, D. Bets, M. Mueser, A. Harstrick, C. Verslype, I. Chau, and E. Van Cutsem. 2004. Cetuximab monotherapy and cetuximab plus irinotecan in irinotecan-refractory metastatic colorectal cancer. *N Engl J Med* 351:337-345.

36. Rahbari, N. N., M. Aigner, K. Thorlund, N. Mollberg, E. Motschall, K. Jensen, M. K. Diener, M. W. Buchler, M. Koch, and J. Weitz. 2010. Meta-analysis shows that detection of circulating tumor cells indicates poor prognosis in patients with colorectal cancer. *Gastroenterology* 138:1714-1726.

37. Overdijk, M. B., S. Verploegen, A. Ortiz Buijsse, T. Vink, J. H. Leusen, W. K. Bleeker, and P. W. Parren. 2012. Crosstalk between human IgG isotypes and murine effector cells. *J Immunol* 189:3430-3438.

38. Chung, C. H., B. Mirakhur, E. Chan, Q. T. Le, J. Berlin, M. Morse, B. A. Murphy, S. M. Satinover, J. Hosen, D. Mauro, R. J. Slebos, Q. Zhou, D. Gold, T. Hatley, D. J. Hicklin, and T. A. Platts-Mills. 2008. Cetuximab-induced anaphylaxis and IgE specific for galactose-alpha-1,3-galactose. *N Engl J Med* 358:1109-1117.

39. Lammerts van Bueren, J. J., T. Rispens, S. Verploegen, T. van der Palen-Merkus, S. Stapel, L. J. Workman, H. James, P. H. van Berkel, J. G. van de Winkel, T. A. Platts-Mills, and P. W. Parren. 2011. Anti-galactose-alpha-1,3-galactose IgE from allergic patients does not bind alpha-galactosylated glycans on intact therapeutic antibody Fc domains. *Nat Biotechnol* 29:574-576.

40. Machiels, J. P., S. Subramanian, A. Ruzsa, G. Repassy, I. Lifirenko, A. Flygare, P. Sorensen, T. Nielsen, S. Lisby, and P. M. Clement. 2011. Zalutumumab plus best supportive care versus best supportive care alone in patients with recurrent or metastatic squamous-cell carcinoma of the head and neck after failure of platinum-based chemotherapy: an open-label, randomised phase 3 trial. *Lancet Oncol* 12:333-343.

Supplemental Figures

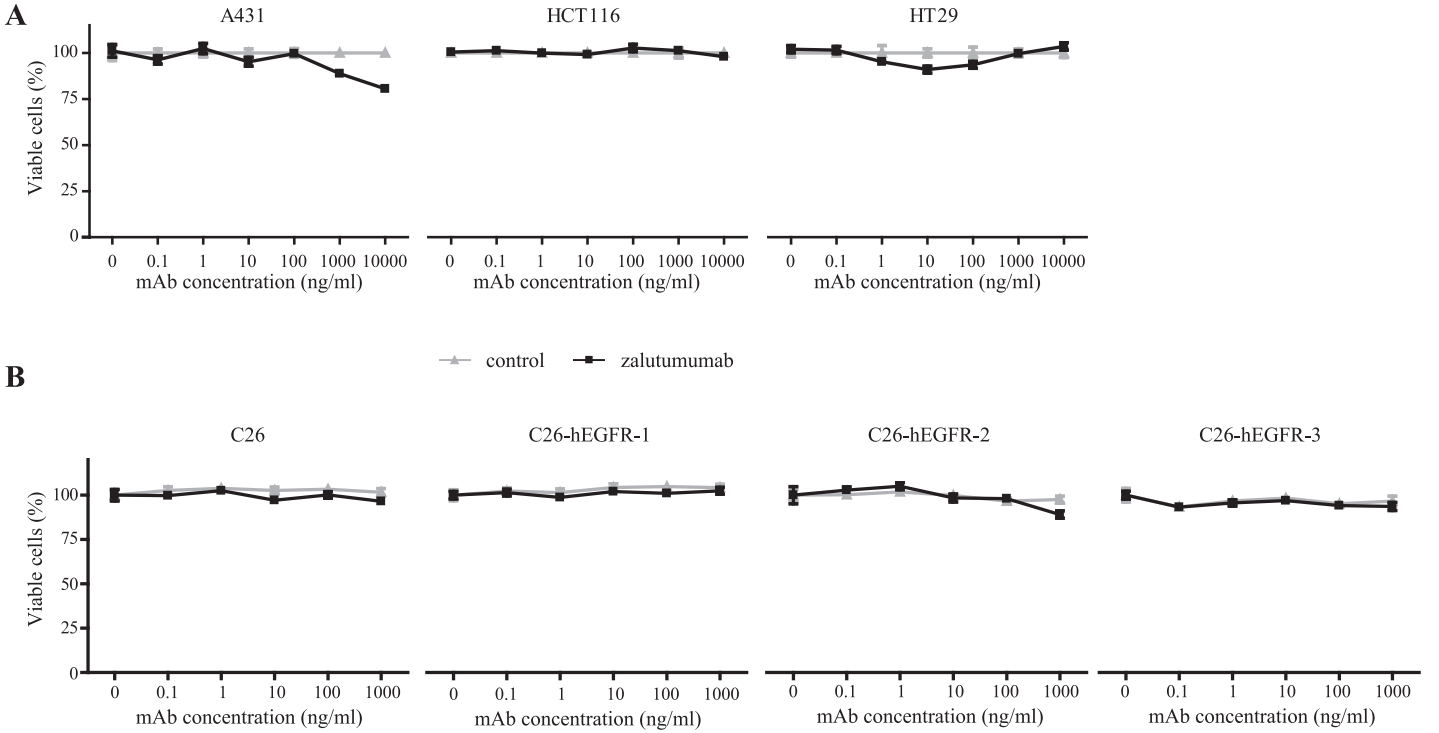

Supplemental Figure 1. *Inhibition of EGFR signaling via zalutumumab.* Cell viability was evaluated, following 24h incubation with mAb, by measuring vital cell mass using a MTT assay. Cells were incubated with 0.5 mg/ml MTT for 1-2h at 37°C, converted MTT by viable cells into formazan was measured at 450 nm in a plate reader (Biorad, Hercules, CA). (A) Cell viability after 24h incubation at 37°C with a concentration range of zalutumumab or control mAb on A431, HCT116 and HT29 cells. (B) Cell viability after 24h incubation at 37°C with a concentration range of zalutumumab or control mAb on C26-hEGFR clones with different EGFR expression levels.

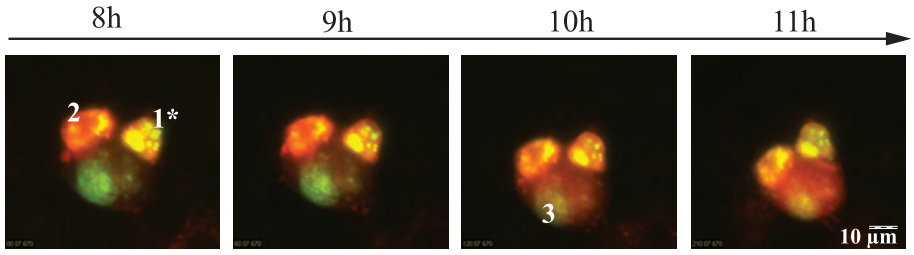

Supplemental Figure 2. *Live cell imaging shows sequential lysosomal degradation upon EGFR mAb-mediated ADCP.* Live cell imaging microscopy of co-cultures of red acidic organelle-specific dye stained mφ (red) and DiO-labeled A431 (green) cells in the presence of zalutumumab. Time laps fluorescent microscopy started 8 h after addition of A431 cells to the mφ, three A431 tumor cells were engulfed by an individual mφ. The first tumor cell (1*) is already degraded and acidity of phagosome declines. Lysosomes fused with a second phagosome (2) and after approximately 10h lysosomes fuse with last tumor cell containing phagosome (3).

Supplemental Videos

Supplemental Video 1. Time laps imaging microscopy of DiO (green) labeled mouse mφ and DiI (red) labeled A431 cells in the presence of 1 µg/ml zalutumumab, E:T 3:1.

Supplemental Video 2. Time laps imaging microscopy of DiO (green) labeled mouse mφ and DiI (red) labeled A431 cells in the presence of 1 µg/ml control mAb, E:T 3:1.

Supplemental Video 3. Time laps imaging microscopy of acidic organelle-specific dye (red) labeled mouse mφ and DiO (green) labeled A431 cells in the presence of 1 µg/ml zalutumumab, E:T 3:1. Time lapse fluorescent images of sequential lysosomal targeting of two engulfed A431 cells

Supplemental Video 4. Time laps imaging microscopy of acidic organelle-specific dye (red) labeled mouse mφ and DiO (green) labeled A431 cells in the presence of 1 μg/ml zalutumumab, E:T 3:1. Time laps fluorescent microscopy started 8 h after addition of A431 cells to the mφ, three A431 tumor cells were engulfed by an individual mφ

Supplemental Movie 5. Time laps imaging microscopy of acidic organelle-specific dye (red) labeled mouse mφ and DiO (green) labeled A431 cells in the presence of 1 μg/ml control mAb, E:T 3:1.

8

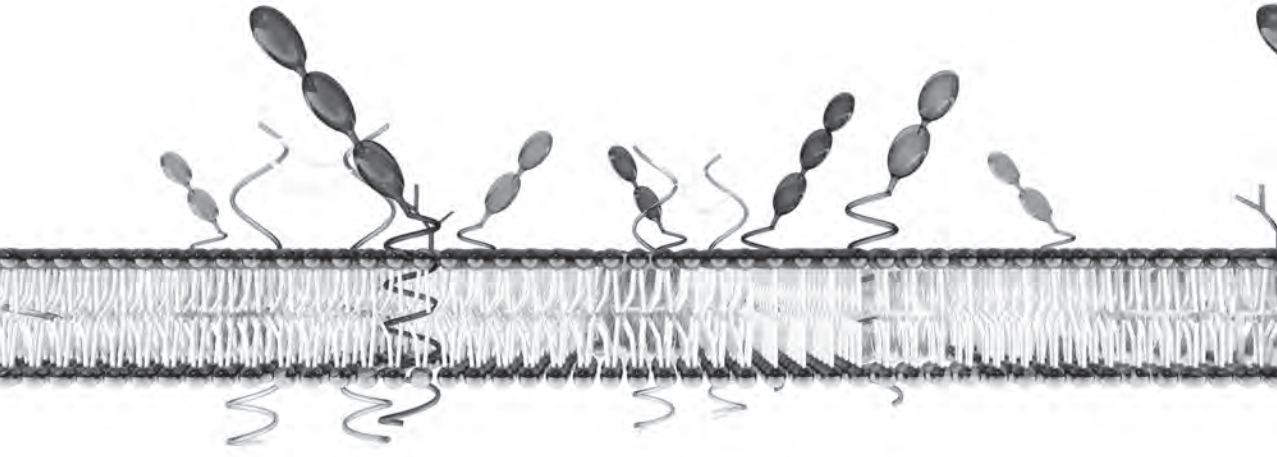

General discussion

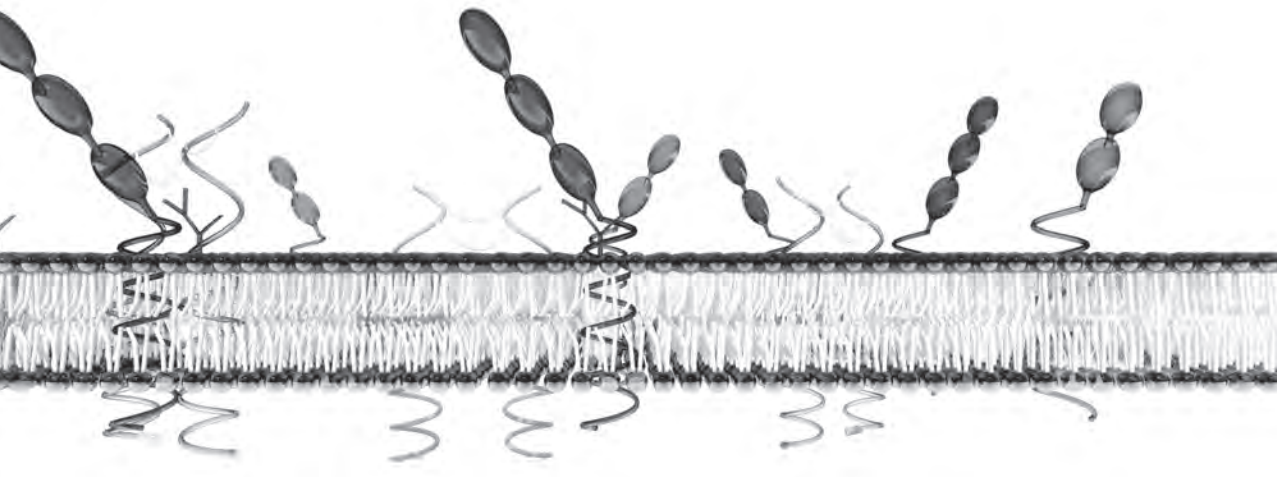

The specificity of cancer therapy has been improved by the development of monoclonal antibodies (mAbs) targeting tumor antigens (Ags). Therapeutic antibodies exert their anti-tumor activity via multiple mechanisms of action (MoA) mediated by the Fab (fragment antigen binding)-regions and/or the Fc (fragment crystallizable)-region of the mAb. Binding of the Fc-region to Fc-gamma receptors (FcγRs) expressed on immune effector cells, initiates directed cell-mediated killing of tumor cells. This ability is thought to contribute to the clinical efficacy of therapeutic Abs and represents an aspect in which Abs are differentiated from other therapeutic molecules, including small chemical entities or non-antibody biologics. The aim of this thesis was to study the FcγR-mediated effects of therapeutic mAbs to gain insight into which, when and where FcγR-mediated antibody effector functions contribute to anti-tumor activity.

FcγR-mediated mechanisms of action of therapeutic mAbs

An important contribution for FcγR-mediated effector functions of therapeutic mAbs in the therapy of cancer has been demonstrated both in pre-clinical studies and clinical trials (reviewed in **Chapter 2**). In pre-clinical studies, the evidence is based on experiments with mice lacking FcγR expression, via the use of antibody mutants or by the specific depletion of effector cells. In clinical trials the evidence is drawn from analyzing the correlation between clinical outcome and functional FcγR polymorphisms resulting in either high or low affinity for the Fc-region of the therapeutic mAb. However, despite intensive research over the past decade, important gaps in our knowledge remain. In this thesis, questions related to the role of FcγR-mediated mechanisms for *in vitro* and *in vivo* killing of tumor cells were addressed using two therapeutic human mAbs, zalutumumab and daratumumab, which are in different stages of clinical development. Daratumumab (a human IgG1 CD38 mAb) was previously shown to potently induce complement-dependent cytotoxicity (CDC) and FcγR-mediated antibody-dependent cellular cytotoxicity (ADCC) (1). We have now demonstrated two additional FcγR-mediated mechanisms of action (MoA) for this mAb; antibody-dependent cellular phagocytosis (ADCP, **Chapter 4**) and programmed cell death via mAb crosslinking (PCD, **Chapter 5**). Also for

zalutumumab (a human IgG1 mAb against the epidermal growth factor receptor (EGFR)) we demonstrated that ADCP represents a potent MoA (**Chapter 7**) in addition to the previously described FcγR-mediated ADCC and Fab-mediated effects including ligand inhibition and EGFR down modulation (2, 3). We studied the conditions that influence the efficacy of FcγR-mediated mechanisms and how they relate to non-FcγR-mediated MoA. In the next paragraphs, the impact of the tumor microenvironment, and the timing and level of antibody dosing on the anti-tumor effects of FcγR-mediated effector functions are discussed (Fig. 1).

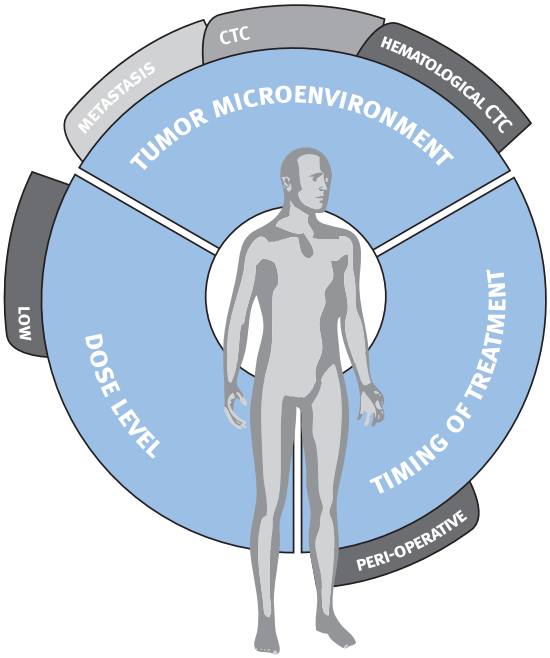

Figure 1. *Factors contributing to efficacy of FcγR-mediated anti-tumor activity in the treatment of cancer patients with therapeutic mAbs.* (CTC: circulating tumor cells).

Tumor microenvironment

Malignant tumors can be subdivided into two main categories; hematological and solid tumors. Hematological tumors are derived from myeloid (granulocytes, erythrocytes, thrombocytes, macrophages, mast cells) or lymphoid (B-, T-, NK-cells) cells and include three major classes; leukemia, myeloma and lymphoma. Leukemic cells primarily reside in the blood and bone marrow (BM) and are derived from either myeloid or lymphoid cells. Myeloma is a disease resulting from the abnormal growth of plasma B-cells, which accumulate in the BM and

usually have a low presence in the blood. Lymphoma cells originate from B- or T-cells and are primarily located in the BM and lymphoid organs. Furthermore, lymphomas can progress into bulky disease which has manifestations with solid-tumor like characteristics. Solid tumors are generally defined as an abnormal mass of cancer cells derived from either epithelial cells (carcinomas) or connective tissue (sarcomas).

The tumor microenvironment, including e.g. fibroblasts, epithelial cells, blood vessels and extracellular matrix, is critical for tumorigenesis, invasion and metastasis of both hematological and solid tumors (4, 5). Inflammation within the tumor microenvironment has also been described to regulate tumor development by attracting tumor associated macrophages (TAM), myeloid derived suppressor cells (MDSC) and T-regulatory (T-reg) cells into the tumor microenvironment (6, 7). These TAM and MDSC have been shown to be potent suppressors of protective anti-tumor immune responses (8, 9). In addition, T-reg cells have been described to suppress adaptive and innate immune responses (7, 10). The presence of these immunosuppressive cells in the tumor microenvironment has been correlated with a poor disease prognosis (11, 12). Interestingly, evidence for differences in cellular immunity between distinct tumor sites also comes from infectious disease studies. Thus, bacterial clearance in primary and metastatic tumors has been compared in a metastatic mammary carcinoma xenograft mouse model. Bacteria colonized the primary breast tumor and the metastases two days after intravenous (i.v.) injection and were efficiently cleared from metastatic sites but not in the primary breast tumor after 6 days (13). These findings indicate the tumor microenvironment of solid tumors to constitute an immune-privileged site; a condition that may also apply to bulky tumors in hematological disease and which may impact FcγR-mediated tumor killing by therapeutic mAbs. In **Chapter 6** we showed that ADCC or ADCP induction by EGFR mAbs alone was indeed insufficient to inhibit solid tumor growth. The absence of anti-tumor activity by therapeutic mAbs was not due to inability to penetrate tumors, since Fab-mediated signaling inhibition by zalutumumab was effective in a solid tumor (**Chapter 6**), consistent with earlier observations (2).

It has been documented that FcγR-mediated PCD contributes significantly to the anti-tumor effects of therapeutic mAbs targeting Ags from the tumor necrosis factor receptor (TNFR) superfamily (14, 15). This mechanism may, therefore, well play a role in the treatment of solid or bulky tumors by

other mAbs, such as daratumumab, that induce crosslinking-mediated PCD (**Chapter 5**). For example FcγRIIb-expressing liver sinusoidal endothelial cells in the liver, documented to be involved in the clearance of small immune complexes (16), might initiate mAb crosslinking-mediated PCD. Furthermore, crosslinking-mediated PCD may also occur during interactions between tumor cells themselves under conditions where these express FcγRs.

Numerous studies have demonstrated an important role for ADCC in Ab induced anti-tumor effects in hematological diseases (17). In **Chapter 4** we explored the contribution of ADCP in hematological disease by comparing the anti-tumor effect of a variant of daratumumab capable of ADCC/ADCP induction with that of a variant that could solely induce ADCC in a mouse xenograft model of Burkitt's lymphoma. We demonstrated a significant contribution of ADCP in the anti-tumor activity of daratumumab, which suggested that hematological circulating tumor cells (CTC) may be effectively cleared by the reticuloendothelial system. This is supported by studies using IgG-opsonized circulating erythrocytes for which rapid FcγR-dependent clearance in the liver and spleen by macrophages has been documented (18, 19). In addition, in a mouse model employing engraftment of human bone environment and multiple myeloma (MM) cells from a late-stage patient with an aggressive phenotype, effective daratumumab-mediated anti-tumor activity on CTCs and tumor cells residing in murine BM has been observed (20). Notably, MM cells residing in the human hematopoietic niche, were not susceptible to daratumumab treatment, possibly linked to the existence of an immune privileged site within the BM tumor microenvironment of these aggressive MM cells.

Timing of treatment

The tumor microenvironment plays an important role in the efficacy of FcγR-mediated effector functions. Treatment of solid or bulky tumors employing these effector functions alone would therefore be expected to have a limited impact. However, in **Chapter 6** we showed FcγR-mediated cytotoxicity to be sufficient for EGFR mAb to inhibit early carcinoma tumor development in a mouse xenograft model. These results indicate that during mAb treatment of patients with a solid tumor the FcγR-mediated MoA may have an impact on depletion of CTCs and prevention of metastases. This is supported by **Chapter 7**, exploring the potency of peri-operative treatment with EGFR mAbs in depletion

of dissected CTCs, or prevention of metastasis development via FcγR-mediated mechanisms. For the treatment of patients with hematological tumors the timing of treatment is expected to be less critical, albeit that in late stage disease FcγR-mediated effector functions may only impact CTCs.

Dose level

The Fab and Fc-mediated MoA have been demonstrated to exhibit different dose requirements. ADCC induction by zalutumumab is efficient at <5% EGFR occupancy, whereas Fab-mediated signaling inhibition requires ~100% receptor occupancy (2) (**Chapter 6**). We demonstrated that a low dose (~5- 30% occupancy) was sufficient for all FcγR-mediated effector functions; ADCP (**Chapter 4, 7**), FcγR-mediated PCD induction (**Chapter 5**) and ADCC (**Chapter 6**). Dose-effect relationships for both zalutumumab and daratumumab are schematically depicted in Fig. 2.

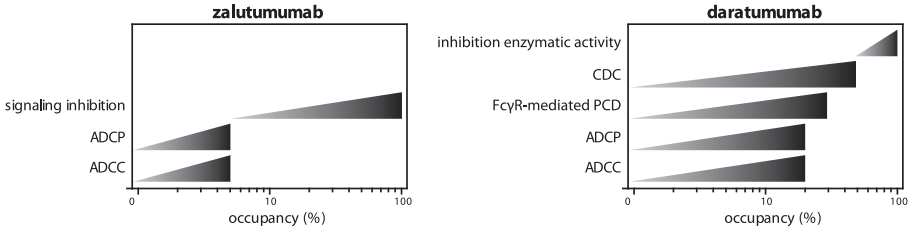

Figure 2. *Schematic representation of dose-effect relationships for different mechanisms of action of zalutumumab (left) and daratumumab (right).* Occupancy to give maximal effect is depicted. Data are based on findings in this thesis, Bleeker et al. and de Weers et al. (1, 2). Inhibition of CD38 ecto-enzyme activity represents our own unpublished data.

Occupancy is dependent on mAb affinity for the target and mAb concentration. As there may be a relatively large concentration gradient between the blood and the interstitial space in established tumors, high plasma concentrations and consequently high dose levels are generally required to achieve full target occupancy in solid tumors, whereas full target occupancy on CTCs in the blood is achieved at much lower doses. Potent Fc-mediated anti-tumor activity by daratumumab was indeed already evident at a dose of 0.5 μg/kg during early treatment of an i.v. Burkitt's lymphoma systemic xenograft mouse model (1). Treatment performed 14 days after tumor establishment required a higher daratumumab concentration for effective tumor growth inhibition, which may be due to the higher tumor load and manifestations of bulky disease. Furthermore, the efficacy of Fc-mediated

MoA by ofatumumab (a human IgG1 CD20 mAb (21)) in non-human primates was shown to require a lower concentration for depletion of circulating B-cells compared to depletion of B-cells which reside in the BM or lymphoid tissues (22). These data support FcγR-mediated anti-tumor activity on CTCs, derived from either hematological malignancies or from a solid tumor, to require only low non-saturating mAb doses.

The anti-tumor activity of therapeutic mAbs which depend on Fc-mediated cytotoxicity, as described for daratumumab and zalutumumab, is likely impacted by the availability of effector reservoirs. For the CD20 mAbs ofatumumab and rituximab, it has been described that exhaustion of complement factors or effector cells may impact mAb therapy in cancer patients (23, 24). Notably, the magnitude of complement depletion and subsequent *in vitro* inhibition of complement-mediated lysis by CD20 mAbs was dependent on antibody doses. High dosing resulting in exaggerated complement activation, complement depletion and a reduction of maximal killing, whereas low dosing resulted in complement sparing and greater overall effects. On a similar note, since FcγR-mediated effector functions already trigger maximal effects at low mAb doses, low dosing schemes may be attractive in order to maximize the therapeutic contribution of FcγR-mediated functions while avoiding potential effector cell exhaustion via exaggerated triggering.

Pre-clinical *in vivo* models

Pre-clinical studies in mouse models are of central importance in the development of therapeutic mAbs. Genetically engineered mouse models resulting in spontaneous tumor development are regularly used for cancer research (25). Unfortunately, these are often not suitable for studies with mAbs due to lack of cross reactivity of therapeutic mAbs with the murine target. Human tumor xenografts grown in immune deficient mice are thus frequently used for pre-clinical studies with therapeutic mAbs. Nowadays, most therapeutic mAbs contain human constant domains to provide optimal interactions with the human immune system (26). However, due to differences between human and murine FcγRs (**Chapter 1**) mouse xenograft models provide challenges to study the impact of FcγR-mediated effector functions in antibody therapy studies. Mouse models engrafted with a human immune system may provide

an alternative to evaluate effector functions.

Humanized mouse models can be established in immune-deficient mice by engraftment of peripheral blood mononuclear cells (PBMC) or hematopoietic stem cells (HSC). Within such models there is a wide diversity due to several factors; e.g. source of the human immune cells used, route of inoculation of the cells, as well as the specific mouse (host) strain (27, 28). Humanized models with engraftment of PMBC represent fast and easy models, though changes in the different cellular subsets over time, and development of graft-versus-host disease may complicate interpretation of pre-clinical studies. Engraftment with HSC does result in expansion of the different cellular subsets, ongoing hematopoiesis and human immune cells were demonstrated functionally active (28-30). Optimization of such models currently takes place to further enhance engraftment of human immune cells, resulting in improved development of their natural function and cellular distribution. Major limitations of these models are the complexity, reproducibility and the time consuming nature. Studies focusing on FcγR-mediated MoA may not require such complex models and an alternative might be provided by FcγR-humanized mouse models generated through transgenic expression. In the FcγR humanized mouse model all human FcγR transgenes have been inserted into the genome of an FcRα-chain null mouse, which lacks expression of murine FcγRs (31). Immune cells of these mice display a human FcγR expression pattern comparable to that in humans. A disadvantage of this model is the immune competent nature of the mice. Xenografted tumors can thus not be used and cross reactivity of mAb with murine targets, or the development of murine cancer cell lines expressing human targets is required. Therapy with human antibodies, in addition, may induce anti-drug antibodies providing additional limitations. Overall, these humanized mouse models have significant shortcomings and may not necessarily represent an improvement over xenograft models. For this reason, we evaluated crosstalk between human IgG isotypes and murine effector cells in **Chapter 3** to provide a comprehensive knowledge base for testing human mAb FcγR-mediated cytotoxicity in xenograft mouse models. We showed human IgG1 to be the most potent human isotype for inducing FcγR-mediated cytotoxicity by NK-cells, neutrophils and macrophages in mice. These results document xenograft models to represent appropriate pre-clinical models to study efficacy of human IgG1. A lower efficacy compared to mouse IgG2a suggests anti-tumor activity may be underestimated in xenograft models. Human IgG4 potently induces

FcγR-mediated cytotoxicity with mouse macrophages, whereas this activation is absent with human macrophages. IgG4 may thus be less suitable for pre-clinical studies in xenograft models. Overall, we suggest that a better understanding of the activation of murine effector cells by human IgG isotypes is essential for interpretation of data and extrapolation to the human system.

For new mAb formats, developed to enhance anti-tumor efficacy, the selection of an appropriate mouse model is complex. One method to improve FcγR-mediated mAb activity is glyco-engineering, which refers to modifications made in the carbohydrate moieties in the antibody Fc-domains. Removing the fucose moiety from the IgG oligosaccharide for example, enhances the binding to human FcγRIIIa, resulting in enhanced NK-cell mediated ADCC activity (32, 33). In mice removal of fucose from IgG is mainly affecting binding to mouse FcγRIV (34, 35), which is only expressed on mouse myeloid cells and thus affects FcγR-mediated activity of monocytes, macrophages and neutrophils, instead of NK-cells as shown for humans. The use of xenograft mouse models for pre-clinical studies with afucosylated mAbs are problematic due to this discrepancy and a humanized model is suggested more appropriate, as shown for afucosylated trastuzumab (a humanized IgG1 HER2 mAb). Enhanced efficacy for afucosylated trastuzumab compared to fucosylated trastuzumab was shown in an orthotopic breast xenograft model in a humanized mouse model expressing human FcγRIIIa (36). Similar difficulties for choosing an appropriate mouse model are encountered with other novel Ab formats. We conclude that the experimental question addressed in an animal model should fully dictate the choice of an appropriate mouse model, rather than attempting to recapitulate the human biological process entirely.

Perspectives

As discussed in this thesis, FcγR-mediated effector functions of therapeutic mAbs are potent mechanisms of action in the anti-tumor activity. Strategies to enhance FcγR-mediated cytotoxicity may further improve the efficacy of therapeutic mAbs for cancer. There are four key interface areas to enhance FcγR-mediated cytotoxicity; affinity for the activating FcγRs, mAb format, localization of the tumor cells and activation status of effector cells (Fig. 3).

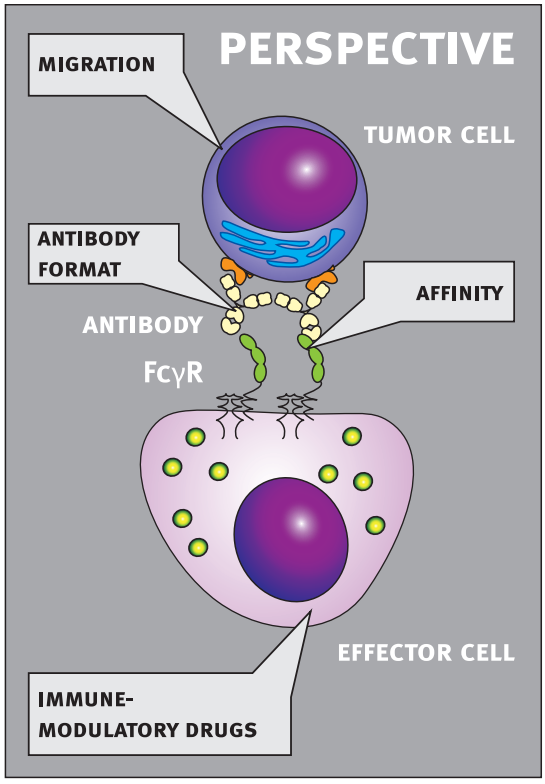

Figure 3. *Interfaces to enhance FcγR-mediated anti-tumor activity.*

The affinity for activating FcγRs can be enhanced by modifying the Fc-domain of therapeutic mAbs. This can be achieved by amino acid mutations in the Fc-region (Fc-engineering) or by glyco-engineering (37, 38). Fc-enhanced mAbs may overcome the immune-privileged environment in solid or bulky tumors, as shown for an Fc-engineered CD19 mAb (39). Furthermore, enhanced affinity may result in increased cytotoxicity in the circulation at even lower mAb doses, or under conditions in which tumor penetration and retention are impaired (40). A second approach to enhance FcγR-mediated cytotoxicity is adaptation of mAb format. An example is the construction of bispecific mAb targeting both the tumor cells and activating FcγRs on effector cells (41, 42). The third interface is to induce migration of tumor cells into the circulation, since FcγR-mediated cytotoxicity may be most potent in circulation. This can be achieved via combination therapy with drugs promoting redistribution of tumor cells into the circulation, as described for the bruton tyrosine kinase (BTK) inhibitor ibrutinib in combination with rituximab (43). Furthermore, mAbs interfering

with adhesion or homing of tumor cells may promote redistribution of tumor cells into circulation, as was demonstrated for an anti-alpha-2 integrin mAb (44). Finally, combination therapy with immune modulatory drugs (IMiDs) enhancing the activity of effector cells may improve FcγR-mediated anti-tumor activity. For example IMiDs enhancing NK-cell activity (45) enhance mAb mediated anti-tumor activity (46-50). IMiDs may, furthermore, activate tumor-associated macrophages to augment FcγR-mediated cytotoxicity in the tumor microenvironment of solid tumors, as shown for Vadimezan (DMXAA) (51) or IL12 treatment (52).

In conclusion, a better understanding of the different mechanisms of action of therapeutic mAbs, including FcγR-mediated mechanisms studied in this thesis, should stimulate the development of more effective therapeutic approaches for cancer. Furthermore, detailed knowledge of the anti-tumor mechanisms initiated by therapeutic antibodies provides rationales for effective combination therapies of mAbs and other agents. These may bring the ultimate goal of turning cancer into a chronic or curable disease within reach in the coming decades.

References

1. de Weers, M., Y. T. Tai, M. S. van der Veer, J. M. Bakker, T. Vink, D. C. Jacobs, L. A. Oomen, M. Peipp, T. Valerius, J. W. Slootstra, T. Mutis, W. K. Bleeker, K. C. Anderson, H. M. Lokhorst, J. G. van de Winkel, and P. W. Parren. 2011. Daratumumab, a novel therapeutic human CD38 monoclonal antibody, induces killing of multiple myeloma and other hematological tumors. *J Immunol* 186:1840-1848.
2. Bleeker, W. K., J. J. Lammerts van Bueren, H. H. van Ojik, A. F. Gerritsen, M. Pluyter, M. Houtkamp, E. Halk, J. Goldstein, J. Schuurman, M. A. van Dijk, J. G. van de Winkel, and P. W. Parren. 2004. Dual mode of action of a human anti-epidermal growth factor receptor monoclonal antibody for cancer therapy. *J Immunol* 173:4699-4707.
3. Lammerts van Bueren, J. J., W. K. Bleeker, H. O. Bogh, M. Houtkamp, J. Schuurman, J. G. van de Winkel, and P. W. Parren. 2006. Effect of target dynamics on pharmacokinetics of a novel therapeutic antibody against the epidermal growth factor receptor: implications for the mechanisms of action. *Cancer Res* 66:7630-7638.
4. Allen, M., and J. Louise Jones. 2011. Jekyll and Hyde: the role of the microenvironment on the progression of cancer. *J Pathol* 223:162-176.
5. Zhou, J., K. Mauerer, L. Farina, and J. G. Gribben. 2005. The role of the tumor microenvironment in hematological malignancies and implication for therapy. *Front Biosci* 10:1581-1596.
6. Colotta, F., P. Allavena, A. Sica, C. Garlanda, and A. Mantovani. 2009. Cancer-related inflammation, the seventh hallmark of cancer: links to genetic instability. *Carcinogenesis* 30:1073-1081.
7. Mantovani, A., P. Allavena, A. Sica, and F. Balkwill. 2008. Cancer-related inflammation. *Nature* 454:436-444.
8. Mantovani, A., S. Sozzani, M. Locati, P. Allavena, and A. Sica. 2002. Macrophage polarization: tumor-associated macrophages as a paradigm for polarized M2 mononuclear phagocytes. *Trends Immunol* 23:549-555.
9. Sica, A., and V. Bronte. 2007. Altered macrophage differentiation and immune dysfunction in tumor development. *J Clin Invest* 117:1155-1166.
10. O'Garra, A., and P. Vieira. 2004. Regulatory T cells and mechanisms of immune system control. *Nat Med* 10:801-805.
11. Bindea, G., B. Mlecnik, W. H. Fridman, and J. Galon. 2011. The prognostic impact of anti-cancer immune response: a novel classification of cancer patients. *Semin Immunopathol* 33:335-340.
12. Bindea, G., B. Mlecnik, W. H. Fridman, F. Pages, and J. Galon. 2010. Natural immunity to cancer in humans. *Curr Opin Immunol* 22:215-222.
13. Yu, Y. A., S. Shabahang, T. M. Timiryasova, Q. Zhang, R. Beltz, I. Gentschev, W. Goebel, and A. A. Szalay. 2004. Visualization of tumors and metastases in live animals with bacteria and vaccinia virus encoding light-emitting proteins. *Nat Biotechnol* 22:313-320.
14. Li, F., and J. V. Ravetch. 2012. A general requirement for FcgammaRIIB co-engagement of agonistic anti-TNFR antibodies. *Cell Cycle* 11:3343-3344.
15. White, A. L., H. T. Chan, R. R. French, S. A. Beers, M. S. Cragg, P. W. Johnson, and M. J. Glennie. 2013. FcgammaRIotalotaB controls the potency of agonistic anti-TNFR mAbs. *Cancer Immunol Immunother* 62:941-948.
16. Ganesan, L. P., J. Kim, Y. Wu, S. Mohanty, G. S. Phillips, D. J. Birmingham, J. M. Robinson, and C. L. Anderson. 2012. FcgammaRIIb on liver sinusoidal endothelium clears small immune complexes. *J Immunol* 189:4981-4988.
17. Castillo, J., E. Winer, and P. Quesenberry. 2008. Newer monoclonal antibodies for hematological malignancies. *Exp Hematol* 36:755-768.
18. Kabbash, L., J. Esdaile, S. Shenker, F. Decary, D. Danoff, A. Fuks, and J. Shuster. 1987. Reticuloendothelial system Fc receptor function in systemic lupus erythematosus: effect of decreased sensitization on clearance of autologous erythrocytes. *J Rheumatol* 14:487-489.
19. Schreiber, A. D., and M. M. Frank. 1972. Role of antibody and complement in the immune clearance and destruction of erythrocytes. I. In vivo effects of IgG and IgM complement-fixing sites. *J Clin Invest* 51:575-582.

20. Groen, R. W., W. A. Noort, R. A. Raymakers, H. J. Prins, L. Aalders, F. M. Hofhuis, P. Moerer, J. F. van Velzen, A. C. Bloem, B. van Kessel, H. Rozemuller, E. van Binsbergen, A. Buijs, H. Yuan, J. D. de Bruijn, M. de Weers, P. W. Parren, J. J. Schuringa, H. M. Lokhorst, T. Mutis, and A. C. Martens. 2012. Reconstructing the human hematopoietic niche in immunodeficient mice: opportunities for studying primary multiple myeloma. *Blood* 120:e9-e16.
21. Teeling, J. L., R. R. French, M. S. Cragg, J. van den Brakel, M. Pluyter, H. Huang, C. Chan, P. W. Parren, C. E. Hack, M. Dechant, T. Valerius, J. G. van de Winkel, and M. J. Glennie. 2004. Characterization of new human CD20 monoclonal antibodies with potent cytolytic activity against non-Hodgkin lymphomas. *Blood* 104:1793-1800.
22. Bleeker, W. K., M. E. Munk, W. J. Mackus, J. H. van den Brakel, M. Pluyter, M. J. Glennie, J. G. van de Winkel, and P. W. Parren. 2008. Estimation of dose requirements for sustained in vivo activity of a therapeutic human anti-CD20 antibody. *Br J Haematol* 140:303-312.
23. Beurskens, F. J., M. A. Lindorfer, M. Farooqui, P. V. Beum, P. Engelberts, W. J. M. Mackus, P. W. H. I. Parren, A. Wiestner, and R. P. Taylor. 2012. Exhaustion of Cytotoxic Effector Systems May Limit Monoclonal Antibody-Based Immunotherapy in Cancer Patients. *The Journal of Immunology* 188:3532-3541.
24. Kennedy, A. D., P. V. Beum, M. D. Solga, D. J. DiLillo, M. A. Lindorfer, C. E. Hess, J. J. Densmore, M. E. Williams, and R. P. Taylor. 2004. Rituximab infusion promotes rapid complement depletion and acute CD20 loss in chronic lymphocytic leukemia. *J Immunol* 172:3280-3288.
25. Richmond, A., and Y. Su. 2008. Mouse xenograft models vs GEM models for human cancer therapeutics. *Dis Model Mech* 1:78-82.
26. Ruuls, S. R., J. J. Lammerts van Bueren, J. G. van de Winkel, and P. W. Parren. 2008. Novel human antibody therapeutics: the age of the Umabs. *Biotechnol J* 3:1157-1171.
27. Shultz, L. D., M. A. Brehm, J. V. Garcia-Martinez, and D. L. Greiner. 2012. Humanized mice for immune system investigation: progress, promise and challenges. *Nat Rev Immunol* 12:786-798.
28. Shultz, L. D., F. Ishikawa, and D. L. Greiner. 2007. Humanized mice in translational biomedical research. *Nat Rev Immunol* 7:118-130.
29. Becker, P. D., N. Legrand, C. M. van Geelen, M. Noerder, N. D. Huntington, A. Lim, E. Yasuda, S. A. Diehl, F. A. Scheeren, M. Ott, K. Weijer, H. Wedemeyer, J. P. Di Santo, T. Beaumont, C. A. Guzman, and H. Spits. 2010. Generation of human antigen-specific monoclonal IgM antibodies using vaccinated "human immune system" mice. *PLoS One* 5.
30. Coughlan, A. M., S. J. Freeley, and M. G. Robson. 2012. Humanised mice have functional human neutrophils. *J Immunol Methods* 385:96-104.
31. Smith, P., D. J. DiLillo, S. Bournazos, F. Li, and J. V. Ravetch. 2012. Mouse model recapitulating human Fcgamma receptor structural and functional diversity. *Proc Natl Acad Sci U S A* 109:6181-6186.
32. Shields, R. L., J. Lai, R. Keck, L. Y. O'Connell, K. Hong, Y. G. Meng, S. H. Weikert, and L. G. Presta. 2002. Lack of fucose on human IgG1 N-linked oligosaccharide improves binding to human Fcgamma RIII and antibody-dependent cellular toxicity. *J Biol Chem* 277:26733-26740.
33. Shinkawa, T., K. Nakamura, N. Yamane, E. Shoji-Hosaka, Y. Kanda, M. Sakurada, K. Uchida, H. Anazawa, M. Satoh, M. Yamasaki, N. Hanai, and K. Shitara. 2003. The absence of fucose but not the presence of galactose or bisecting N-acetylglucosamine of human IgG1 complex-type oligosaccharides shows the critical role of enhancing antibody-dependent cellular cytotoxicity. *J Biol Chem* 278:3466-3473.
34. Nimmerjahn, F., and J. V. Ravetch. 2005. Divergent immunoglobulin g subclass activity through selective Fc receptor binding. *Science* 310:1510-1512.
35. Scallon, B., S. McCarthy, J. Radewonuk, A. Cai, M. Naso, T. S. Raju, and R. Capocasale. 2007. Quantitative in vivo comparisons of the Fc gamma receptor-dependent agonist activities of different fucosylation variants of an immunoglobulin G antibody. *Int Immunopharmacol* 7:761-772.
36. Junttila, T. T., K. Parsons, C. Olsson, Y. Lu, Y. Xin, J. Theriault, L. Crocker, O. Pabonan, T. Baginski, G. Meng, K. Totpal, R. F. Kelley, and M. X. Sliwkowski. 2010. Superior in vivo efficacy of afucosylated trastuzumab in the treatment of HER2-amplified breast cancer. *Cancer Res* 70:4481-4489.
37. Kaneko, E., and R. Niwa. 2011. Optimizing therapeutic antibody function: progress with Fc domain engineering. *BioDrugs* 25:1-11.

38. Schlaeth, M., S. Berger, S. Derer, K. Klausz, S. Lohse, M. Dechant, G. A. Lazar, T. Schneider-Merck, M. Peipp, and T. Valerius. 2010. Fc-engineered EGF-R antibodies mediate improved antibody-dependent cellular cytotoxicity (ADCC) against KRAS-mutated tumor cells. *Cancer Sci* 101:1080-1088.

39. Horton, H. M., M. J. Bernett, E. Pong, M. Peipp, S. Karki, S. Y. Chu, J. O. Richards, I. Vostiar, P. F. Joyce, R. Repp, J. R. Desjarlais, and E. A. Zhukovsky. 2008. Potent in vitro and in vivo activity of an Fc-engineered anti-CD19 monoclonal antibody against lymphoma and leukemia. *Cancer Res* 68:8049-8057.

40. Adams, G. P., R. Schier, A. M. McCall, H. H. Simmons, E. M. Horak, R. K. Alpaugh, J. D. Marks, and L. M. Weiner. 2001. High affinity restricts the localization and tumor penetration of single-chain fv antibody molecules. *Cancer Res* 61:4750-4755.

41. Kellner, C., J. Bruenke, H. Horner, J. Schubert, M. Schwenkert, K. Mentz, K. Barbin, C. Stein, M. Peipp, B. Stockmeyer, and G. H. Fey. 2011. Heterodimeric bispecific antibody-derivatives against CD19 and CD16 induce effective antibody-dependent cellular cytotoxicity against B-lymphoid tumor cells. *Cancer Lett* 303:128-139.

42. Wallace, P. K., J. L. Romet-Lemonne, M. Chokri, L. H. Kasper, M. W. Fanger, and C. E. Fadul. 2000. Production of macrophage-activated killer cells for targeting of glioblastoma cells with bispecific antibody to FcgammaRI and the epidermal growth factor receptor. *Cancer Immunol Immunother* 49:493-503.

43. Burger, J. A., M. J. Keating, W. G. Wierda, J. Hoellenriegel, A. Ferrajoli, S. Faderl, S. Lerner, G. Zacharian, X. Huang, D. F. James, J. J. Buggy, H. M. Kantarjian, and S. M. O'Brien. 2012. The Btk Inhibitor Ibrutinib (PCI-32765) in Combination with Rituximab Is Well Tolerated and Displays Profound Activity in High-Risk Chronic Lymphocytic Leukemia (CLL) Patients. *ASH Annual Meeting Abstracts* 120:187-.

44. van der Bij, G. J., S. J. Oosterling, M. Bogels, F. Bhoelan, D. M. Fluitsma, R. H. Beelen, S. Meijer, and M. van Egmond. 2008. Blocking alpha2 integrins on rat CC531s colon carcinoma cells prevents operation-induced augmentation of liver metastases outgrowth. *Hepatology* 47:532-543.

45. Hayashi, T., T. Hideshima, M. Akiyama, K. Podar, H. Yasui, N. Raje, S. Kumar, D. Chauhan, S. P. Treon, P. Richardson, and K. C. Anderson. 2005. Molecular mechanisms whereby immunomodulatory drugs activate natural killer cells: clinical application. *Br J Haematol* 128:192-203.

46. Awan, F. T., R. Lapalombella, R. Trotta, J. P. Butchar, B. Yu, D. M. Benson, Jr., J. M. Roda, C. Cheney, X. Mo, A. Lehman, J. Jones, J. Flynn, D. Jarjoura, J. R. Desjarlais, S. Tridandapani, M. A. Caligiuri, N. Muthusamy, and J. C. Byrd. 2010. CD19 targeting of chronic lymphocytic leukemia with a novel Fc-domain-engineered monoclonal antibody. *Blood* 115:1204-1213.

47. Benson, D. M., Jr., C. E. Bakan, S. Zhang, S. M. Collins, J. Liang, S. Srivastava, C. C. Hofmeister, Y. Efebera, P. Andre, F. Romagne, M. Blery, C. Bonnafous, J. Zhang, D. Clever, M. A. Caligiuri, and S. S. Farag. 2011. IPH2101, a novel anti-inhibitory KIR antibody, and lenalidomide combine to enhance the natural killer cell versus multiple myeloma effect. *Blood* 118:6387-6391.

48. Reddy, N., F. J. Hernandez-Ilizaliturri, G. Deeb, M. Roth, M. Vaughn, J. Knight, P. Wallace, and M. S. Czuczman. 2008. Immunomodulatory drugs stimulate natural killer-cell function, alter cytokine production by dendritic cells, and inhibit angiogenesis enhancing the anti-tumour activity of rituximab in vivo. *Br J Haematol* 140:36-45.

49. Tai, Y. T., H. M. Horton, S. Y. Kong, E. Pong, H. Chen, S. Cemerski, M. J. Bernett, D. H. Nguyen, S. Karki, S. Y. Chu, G. A. Lazar, N. C. Munshi, J. R. Desjarlais, K. C. Anderson, and U. S. Muchhal. 2012. Potent in vitro and in vivo activity of an Fc-engineered humanized anti-HM1.24 antibody against multiple myeloma via augmented effector function. *Blood* 119:2074-2082.

50. Wu, L., M. Adams, T. Carter, R. Chen, G. Muller, D. Stirling, P. Schafer, and J. B. Bartlett. 2008. lenalidomide enhances natural killer cell and monocyte-mediated antibody-dependent cellular cytotoxicity of rituximab-treated CD20+ tumor cells. *Clin Cancer Res* 14:4650-4657.

51. Fridlender, Z. G., A. Jassar, I. Mishalian, L. C. Wang, V. Kapoor, G. Cheng, J. Sun, S. Singhal, L. Levy, and S. M. Albelda. 2013. Using macrophage activation to augment immunotherapy of established tumours. *Br J Cancer* 108:1288-1297.

52. Watkins, S. K., N. K. Egilmez, J. Suttles, and R. D. Stout. 2007. IL-12 rapidly alters the functional profile of tumor-associated and tumor-infiltrating macrophages in vitro and in vivo. *J Immunol* 178:1357-1362.

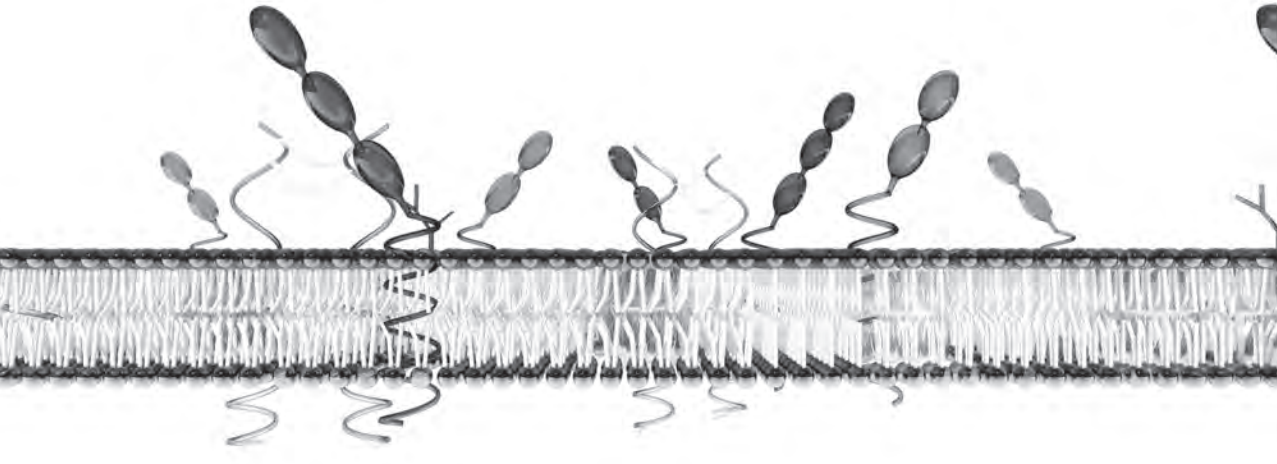

Summary
Nederlandse samenvatting voor niet-ingewijden
Dankwoord
Curriculum Vitae
List of publications

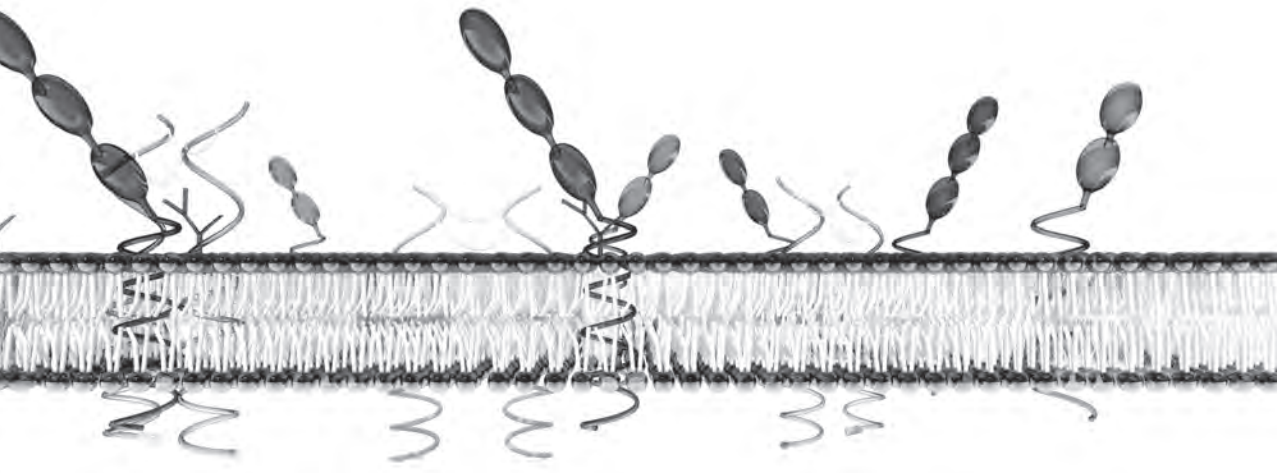

Summary

The high specificity of antibodies (Abs) combined with their ability to engage multiple mechanisms of action (MoA) makes them attractive agents for the treatment of cancer. The Fab (fragment antigen binding)-mediated specific binding to antigens (Ag) on the tumor cells results in coating of tumor cells, so-called opsonization. Opsonization leads to activation of an immune response via the clustered Fc (fragment crystallizable)-regions of the Abs. Binding to Fc-gamma receptors (FcγRs) expressed on immune effector cells may induce antibody-dependent cellular cytotoxicity (ADCC) and/or antibody-dependent cellular phagocytosis (ADCP). Non-cellular immune response is activated by binding of proteins of the complement system to the clustered Fc-region leading to complement-dependent cytotoxicity (CDC). This thesis addresses the FcγR-mediated effects of therapeutic monoclonal Abs (mAbs) to gain insight into which, when and where FcγR-mediated Ab effector functions contribute to anti-tumor activity.

The **first Chapter** provides an introduction on general Ab biology and functionality. Furthermore, a rationale why Abs represent attractive agents for treatment of cancer, a class of malignant diseases characterized by unregulated cell growth. **Chapter 2** addresses the therapeutic monoclonal antibodies (mAbs) currently approved for use in cancer therapy with emphasis on the role of FcγR polymorphisms in Ab therapeutic efficacy. FcγR polymorphic variants have an amino acid substitution, which impacts the affinity for IgG and subsequently the FcγR-mediated effector functions. The correlation between certain functional FcγR polymorphisms and clinical responses provides evidence for the role of FcγR-mediated effector functions in the clinical efficacy of unmodified mAbs. However, because multiple factors in addition to FcγR polymorphisms modulate clinical efficacy, FcγR polymorphisms currently do not seem to provide useful predictive biomarkers for patient selection.

In **Chapter 3** the interaction between human IgG isotypes, IgG1, IgG2, IgG3 and IgG4 and murine effector cells was explored. *In vitro* and *in vivo* studies demonstrated that human IgG1 is the most potent human isotype in activating mouse effector cells. Taken together, these data on interactions between human IgG isotypes and murine effector cells permit a better interpretation of human antibody efficacy studies in mouse xenograft models.

Chapter 4 focusses on the contribution of FcγR-mediated phagocytosis in the

MoA of daratumumab (DARA), a human IgG1 CD38 mAb. *In vitro* data showed both Burkitt's lymphoma and multiple myeloma (MM) cell lines to be susceptible for DARA-induced ADCP with murine and human macrophages. Furthermore, DARA induced potent ADCP with human macrophages and cells derived from MM patients, a bone marrow cancer in which DARA is currently clinically evaluated. Human IgG2 was demonstrated in **Chapter 3** to be incapable of inducing ADCP with mouse macrophages. Therefore, efficacy of an IgG2-variant of DARA was compared with DARA in xenograft mouse models to study the *in vivo* contribution of ADCP. These studies revealed ADCP to contribute to the *in vivo* MoA of DARA. These data support ADCP to represent one of the MoA for DARA.

The study in **Chapter 5** demonstrated DARA-induced FcγR-mediated programmed cell death (PCD) in MM cell lines. Inhibitory as well as activating FcγRs were shown to mediate DARA-induced PCD in a peritoneal syngeneic *in vivo* model. The underlying mechanism of the PCD induction and the contribution to the overall anti-tumor effect *in vivo* requires further investigation.

The role of ADCC in tumor inhibition by epidermal growth factor receptor (EGFR) mAbs was studied in **Chapter 6**. With a matched set of EGFR-specific mAbs, each with a unique MoA, we could distinguish between FcγR-mediated ADCC and Fab-mediated signaling inhibition. Comparing efficacy in several *in vivo* xenograft mouse models documented ADCC as MoA of EGFR targeting mAbs to play a key role during metastasis, and in early stages of tumor development.

FcγR-mediated tumor inhibition by EGFR-targeting mAbs in metastasis and early stages of tumor development prompted the study in **Chapter 7** to explore the potential of EGFR-targeting mAbs for peri-operative treatment of colorectal cancer (CRC). *In vitro* studies showed induction of ADCP by zalutumumab, a human IgG1 EGFR mAb, of an epidermoid cell line and CRC cell lines. ADCP induction was independent of EGFR downstream mutations. Peri-operative treatment of an experimentally induced liver metastasis mouse model showed significant zalutumumab induced ADCP *in vivo*.

In conclusion, the work described in this thesis on FcγR-mediated anti-tumor mechanisms of therapeutic mAbs showed multiple factors e.g. tumor microenvironment, tumor origin, timing of mAb treatment and antibody dose level to impact antibody therapeutic efficacy. The contribution of these factors is discussed in **Chapter 8**. A thorough understanding of anti-tumor mechanisms initiated by therapeutic mAbs will provide better rationales for more effective cancer combination therapies with mAbs and other agents.

Nederlandse samenvatting voor niet-ingewijden

Inleiding in Kanker

Het woord kanker is afgeleid van het Latijnse woord 'cancer', dat letterlijk vertaald krab betekent. De ziekte werd vroeger herkend aan de rode gezwollen bloedvaten rondom de kankergezwellen die deden denken aan de pootjes van een krab. Kanker is de verzamelnaam voor alle ziekten die worden gekenmerkt door kwaadaardige ongecontroleerde celdeling. Kankergezwellen worden ook wel tumoren genoemd. Kwaadaardige tumoren kunnen ontstaan door genetische defecten of door omgevingsfactoren, zoals blootstelling aan de zon (UV-straling), roken, dieet, chemicaliën, virussen en stress. Tumoren kunnen worden onderverdeeld in grofweg twee categorieën: hematologische en solide tumoren. **Hematologische tumoren** ontstaan uit bloedvormende cellen en circuleren in het bloed of bevinden zich in organen waarin afweercellen zich ophouden, de lymfoïde organen (bv de milt en de lymfeklieren). **Solide tumoren** ontstaan meestal uit epitheelcellen (bedekkende cellen) die zich aan elkaar hechten, waardoor er een stevige tumormassa ontstaat. **Uitzaaiing** of metastasering ontstaat als tumorcellen op een plek in het lichaam groeien, die verschilt van de plek waar de tumor ontstond.

Bestraling, chemotherapie en het chirurgisch verwijderen van de tumor (wanneer mogelijk) vormen vaak de basis van kanker behandeling. Met name bestraling en chemotherapie brengen niet alleen schade toe aan kwaadaardige cellen, maar ook aan gezonde lichaamscellen, met alle problemen van dien. Nieuwe therapieën zijn er daarom op gericht om schade aan omliggende gezonde lichaamscellen zoveel mogelijk te beperken. Dit kan door de medicijnen zo te maken, dat ze doelgericht op tumorcellen afgaan en daardoor alleen tumorcellen onschadelijk maken, of in ieder geval hun groei remmen.

Antistoffen als onderdeel van het afweersysteem

Het afweersysteem (immuunsysteem) zorgt voor de bescherming, **immuunrespons** genoemd, tegen ziekteverwekkers zoals virussen en bacteriën. B-cellen zijn onderdeel van het immuunsysteem, behoren tot de witte bloedcellen en worden gevormd in het beenmerg (in holtes van botten). Na activatie gaan B-cellen **antistoffen** uitscheiden, deze antistoffen bevatten twee domeinen: het Fab-domein en het Fc-domein (Fig. 1, linker plaatje). Het **Fab-domein** bindt aan speciale moleculen, **antigenen**, op het oppervlak van

ziekteverwekkers (Fig. 1, rechter plaatje). Het **Fc-domein** is het constante domein, dat de antistof klasse bepaalt. De mens heeft vijf verschillende antistofklassen. In de benaming staat Ig voor immuunglobuline, met een extra letter voor de klasse: IgA, IgD, IgE, IgG en IgM. De meest voorkomende klasse in de bloedbaan is **IgG.** IgG antistoffen kunnen verder worden onderverdeeld in vier typen: IgG1, IgG2, IgG3 en IgG4.

Antistoffen spelen een belangrijk rol in de afweer tegen ziekteverwekkers, en hierin zijn zowel het Fab-domein als het Fc-domein onontbeerlijk. Binding van het Fab-domein aan het antigeen op de ziekteverwekker kan bijvoorbeeld infectie van gezonde cellen door ziekteverwekkers blokkeren. Na binding van antistoffen aan ziekteverwekkers, kan met het Fc-domein het immuunsysteem sterk worden geactiveerd. Deze Fc-domeinen kunnen namelijk worden herkend door afweercellen in het lichaam. Op het oppervlak van afweercellen (witte bloedcellen) zitten 'herkennings-eiwitten' die binden aan het Fc-domein van antistoffen, zogenaamde Fc-gamma receptoren (**Fcγ-receptoren**). Na binding van het Fc-domein aan Fcγ-receptoren worden afweercellen geactiveerd om de ziekteverwekker, waaraan de antistof is gebonden, te doden. Dit kan bijvoorbeeld door het uitscheiden van stoffen die gaatjes maken in de ziekteverwekker, waardoor deze sterft (Fig. 2, linker plaatje). Het doden van ziekteverwekkers met behulp van antistoffen en afweercellen staat bekend onder de Engelse afkorting **ADCC**, dat *antibody-dependent cellular cytotoxicity* betekent. Binding aan Fcγ-receptoren kan ook het signaal geven aan de afweercel om de ziekteverwekker op te eten en te verteren; dit heet fagocytose (Fig. 2, middelste plaatje). Fagocytose die plaats vindt met behulp van antistoffen staat bekend onder de Engelse afkorting **ADCP**, dat *antibody-dependent cellular phagocytosis* betekent. Naast de cel-gebonden Fcγ-receptoren zitten er ook nog losse (niet cel-gebonden) eiwitten in de bloedbaan. Dit zijn de zogenaamde complement factoren, die ook kunnen binden aan het Fc-domein van antistoffen (Fig. 2, rechter plaatje). Binding van complement factoren zorgt voor de vorming van kanalen (gaatjes) in de ziekteverwekker, en omdat hier geen activatie van afweercellen voor nodig is, werkt deze manier bijzonder snel. Deze vorm van celdoding staat bekend onder de Engelse afkorting **CDC**, dat *complement-mediated cytotoxicity* betekent. In **Hoofdstuk 1** van dit proefschrift geef ik meer details over antistofbiologie en de verschillende manieren waarop antistoffen kunnen werken.

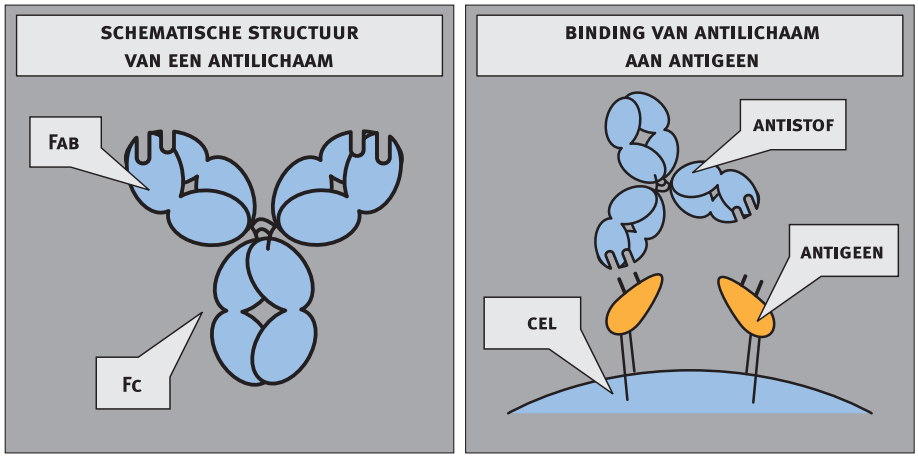

Figuur 1. *Schematische weergave van de opbouw van een antistof (links) en binding aan een antigeen (rechts).*

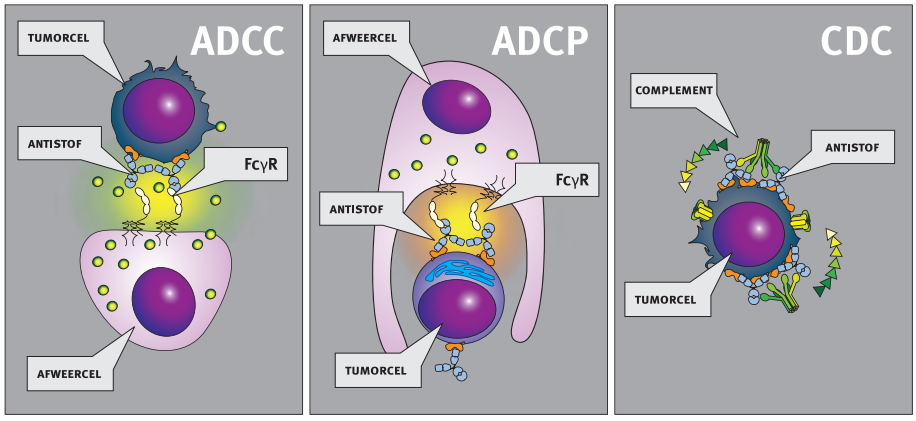

Figuur 2. *Schematische weergave van antistof gemedieerde activatie van het immuunsysteem.* Afkortingen; ADCC, antibody-dependent cellular cytotoxicity; ADCP, antibody-dependent cellular phagocytosis; CDC, complement-dependent cytotoxicity.

Antistoffen als therapie

De specifieke herkenning van antigenen en de verschillende werkingsmechanismen van antistoffen om ziekteverwekkers te doden, maken antistoffen ook interessant voor de behandeling van tumoren. Het lichaam maakt zelf geen antistoffen tegen tumorcellen, omdat het lichaam deze cellen niet ziet als ziekteverwekkers; het zijn immers lichaamseigen cellen. Tegenwoordig kunnen we in het laboratorium antistoffen maken, die doelgericht antigenen op tumorcellen kunnen herkennen. Wanneer antistoffen gebonden zijn aan

tumorcellen, kan het afweersysteem worden geactiveerd tegen de tumorcellen.

De eerste therapeutische antistoffen waren afkomstig van muizen. Omdat het menselijk lichaam antistoffen afkomstig van muizen als lichaamsvreemd ziet, bouwt het lichaam daar een afweer tegen op. Deze muizen antistoffen werken daardoor niet zo heel goed. Om deze afweer te verminderen, werden technieken ontwikkeld om antistoffen te ontwikkelen die van de mens afkomstig zijn. Zo werden zogenaamde chimere antistoffen ontwikkeld (Fab-domein van de muis, Fc-domein van de mens), en later zogenaamde gehumaniseerde antistoffen (met een klein stukje van het Fab-domein van de muis, en de rest van de antistof van de mens). Uiteindelijk lukte het in de jaren '90 om volledig menselijke antistoffen te maken. Er waren in januari 2013 vijftien therapeutische monoklonale antistoffen goedgekeurd als medicijn voor de behandeling van kanker, allemaal van de IgG klasse. De naamgeving van therapeutische antistoffen is zo vastgelegd, dat hieraan kan worden gezien voor welke tumor indicatie het medicijn als eerste is goedgekeurd en van welk organisme de antistof afkomstig is (Tabel 1).

Tabel 1. Generieke naamgeving therapeutische antistoffen

Prefix	Tumor indicatie		bron		Suffix
Variabel, 4 letters	-co(l) -	dikke darm tumor	-o-	muis	-mab
	-me(l)-	Melanoma	-xi-	chimeer	
	-ma(r)-	borstklier tumor	-zu-	gehumaniseerd	
	-go(t)-	testis tumor	-u-	volledig menselijk	
	-go(v)-	eierstok tumor			
	-pr(o)-	prostaat tumor			
	-tu(m)-	gemengde tumor			
	-li(m)-	immuun systeem			

Promotieonderzoek

In dit proefschrift is er onderzoek gedaan naar de rol van Fcγ-receptoren op afweercellen bij het doden en opruimen van tumorcellen, nadat er antistoffen aan zijn gebonden. **Hoofdstuk 2** geeft een overzicht van alle therapeutische antistoffen die goedgekeurd zijn voor de behandeling van kanker en de rol van anti-tumoreffecten die via Fcγ-receptoren op afweercellen verlopen, bij het doden en opruimen van tumorcellen.

Voordat patiënten behandeld kunnen worden met therapeutische antistoffen moet er eerst in diermodellen worden aangetoond dat het kandidaat medicijn veilig en werkzaam is. Hiervoor wordt vaak gebruik gemaakt van muismodellen. Om de resultaten met menselijke antistoffen in muizen goed te kunnen begrijpen is er in **Hoofdstuk 3** gekeken hoe menselijke antistoffen binden aan Fcγ-receptoren op afweercellen van de muis en hoe deze afweercellen vervolgens geactiveerd worden. In de mens is de IgG1 variant het beste in het activeren van afweercellen door binding aan Fcγ-receptoren; dit is daarom ook de meest gebruikte variant voor therapeutische antistoffen. In de muis bleek menselijk IgG1 ook het best in staat tot activatie van afweercellen, maar menselijk IgG4, dat niet of nauwelijks menselijke afweercellen kan activeren, kon wel de macrofagen (een type afweercel) van de muis activeren. Een menselijke IgG4 antistof gedraagt zich dus anders in de muis dan in de patiënt. Door het in kaart brengen van de interactie tussen menselijke IgG antistoffen en afweercellen van de muis, kunnen studies met therapeutische antistoffen in muis modellen beter geïnterpreteerd worden. In **Hoofdstuk 4** is vervolgens aangetoond dat fagocytose (ADCP) door macrofagen een bijdrage levert aan het anti-tumor effect op verschillende soorten tumoren door een therapeutische antistof die CD38 herkent (**daratumumab**; dara=prefix, tum=gemengde tumor, u=volledig menselijk, mab=monoklonale antistof). Met deze informatie kan er een betere keuze gemaakt worden voor een combinatie therapie van daratumumab met een additioneel medicijn, bv een medicijn dat zorgt voor de aanwezigheid van meer geactiveerde macrofagen om ADCP te versterken. Binding van antistoffen aan een Fcγ-receptor kan ook een signaal aan de tumorcel geven, waardoor de kankercel de opdracht krijgt dood te gaan. Dit wordt geprogrammeerde celdood (PCD) genoemd. Dit fenomeen is in **Hoofdstuk 5** onderzocht voor daratumumab. In **Hoofdstuk 6** is aangetoond dat als een therapeutische antistof alleen ADCC kan gebruiken als werkingsmechanisme, het heel moeilijk is om de groei van solide tumoren te remmen of deze kleiner te maken. Bij de behandeling van solide tumoren blijkt ADCC alleen effectief in het voorkomen van uitzaaiingen en in de vroege fase van tumorontwikkeling. In **Hoofdstuk 7** is daarom gekeken of een therapeutische antistof uitzaaiingen kan voorkomen, wanneer deze wordt gegeven tijdens een operatie om de primaire tumor te verwijderen. Inderdaad waren in dit geval immuunresponsen waarbij Fcγ-receptoren betrokken zijn, effectief bij het voorkomen van uitzaaiingen.

De gedetailleerde onderzoeken in dit proefschrift naar anti-tumor effecten van antistoffen die via Fcγ-receptoren verlopen, hebben laten zien dat deze door veel factoren wordt beïnvloed. De plek waar de tumor zit, de tumor origine, in welke fase de behandeling plaats vindt en hoeveel therapeutische antistof er gegeven wordt, zijn een aantal van deze factoren. Hoe deze precies invloed hebben op Fcγ-receptor gemedieerde effecten is besproken in de algemene discussie in **Hoofdstuk 8**. Hoe meer we te weten komen over verschillende werkingsmechanismen van therapeutische antistoffen, des te beter we in de toekomst kunnen bepalen met welke therapeutische antistoffen of andere medicijnen deze gecombineerd kunnen worden om zo van kanker een chronische of zelfs geneesbare ziekte te kunnen maken.

Dankwoord

Jaaaaaaaaaaaaa, eindelijk tijd voor het dankwoord! Dit proefschrift heb ik natuurlijk niet in mijn eentje gemaakt, daarom zijn er heel wat bedankjes nodig. Ik zal starten met de belangrijkste, dank aan al mijn Genmab collega's! Ik zie Genmab als een groot team en ook dit proefschrift is het resultaat van dit fijne teamwerk. Ik kan jullie helaas niet allemaal persoonlijk noemen, maar ik hoop dat iedereen zich bij Genmab aangesproken voelt als ik zeg: **BEDANKT!**

Dan zijn er de drie wijze mannen die mij afgelopen vier jaar enorm veel geleerd hebben. Te beginnen mijn promotor, Jan bedankt dat je mij de kans hebt gegeven om deze uitdaging aan te gaan binnen Genmab. De directe begeleiding heb je overgedragen aan mijn co-promotoren, maar jouw oneindige enthousiasme was voor mij een grote stimulans. Ik had de luxe om begeleid te worden door twee co-promotoren. Allereerst Wim, jouw enorme rust en je droge humor waren de perfecte combinatie om mijn ongeduldigheid in toom te houden. Vanaf het begin tot het einde heb je mij begeleid, ik heb ontzettend veel van je geleerd al deze jaren, super bedankt! Paul, de eerste twee jaar was je begeleiding nog wat meer op de achtergrond, maar de laatste twee jaar werd het steeds intensiever. De discussies die we hebben gehad en al je hulp met het schrijven waren zeer waardevol voor mij. Ik hoop dat ik de komende jaren ook nog veel van je mag leren. Bedankt voor al je hulp en dat je je aan mijn strakke planningen hebt gehouden!

Sandra, tjsa waar moet ik beginnen om jou te bedanken. Het voelt alsof je mij aan de hand hebt genomen vanaf het sollicitatiegesprek, en je me daarna niet meer los hebt gelaten! En wat ben ik daar blij mee! Toen ik bij Genmab kwam werken was ik zoekende welke kant ik op wilde gaan. Jij hebt mij het zelfvertrouwen gegeven en het duwtje in de juiste richting om toch promotie onderzoek te gaan doen. Ik heb genoten van onze 'aftik' meetingen (heerlijk efficiënt), samen op congres en natuurlijk de borreltjes na werktijd. Antonio, je hebt een belangrijke bijdrage geleverd aan de crosstalk studie. Echter, jouw belangrijkste bijdrage aan dit proefschrift is, dat je regelmatig voor de nodige ontspanning hebt gezorgd. Een bakkie, een gezellig babbeltje, een luisterend oor en natuurlijk altijd de gezellige vrijdagmiddagborrel! Je stond zelfs met een flesje champagne klaar toen onze cover was geaccepteerd. Al met al heb ik dus

het geluk dat ik twee super collega's, maar tegelijkertijd ook twee super goede vrienden naast mij heb staan als paranimfen, thanks allebei!

Mijn promotie onderzoek heb ik uit mogen voeren binnen de Translational Research & Pharmacology groep, oftewel bij de TRP-ers Jeroen, Ilse, Marcel, Antonio, Ingrid, Wim en Sandra! Wat een feestje was dat en ik mis jullie nu al! Bedankt voor al jullie hulp! Hopelijk kan ik af en toe nog als freelance TRP-er aansluiten voor een gezellige maandagochtend meeting (hoe moet ik anders mijn chocolade-levels op peil houden…). Ik wil hierbij ook graag nog een oud TRP-er bedanken, Judith. Lange tijd was jij de TRP manager en jij hebt er destijds heel wat bloed, zweet en tranen ingestoken, zodat ik mijn promotieonderzoek binnen TRP kon uitvoeren. Mijn studente Marieke, wat een berg werk heb jij verzet! Het heeft niet tot een apart hoofdstuk geleid, maar jouw werk was zeer belangrijk ter ondersteuning. Bedankt voor je inzet.

Dan ben ik aangekomen bij mijn lieve kamergenoten Ilse, Joyce, Marlies, Maayke, Soeniel, en oud-kamer genoten Teun, Martin, Lukas en Fleur. Onder andere de geweldige woordgrappen van Teun en Martin, de heerlijke taarten en 'slechte' kerstversiering van Joyce, de chocolade van Ilse, de Friese inslag van Marlies, de hindoeïstische gebruiken van Soeniel en het Engelse taalgebruik van Maayke, maakten dat ik altijd met een glimlach de kamer binnenkwam. Thanks allemaal!

De zalu en dara experts Jeroen LvB en Michel, enorm bedankt voor alle hulp. Heerlijke vraagbaken zijn jullie allebei, ik heb veel van jullie geleerd!

Bart en Patrick, mijn mede junior-scientisten, bedankt voor alle tips en discussies. Heel galant dat jullie een dame voor laten gaan, maar ik reken erop dat ik snel een biertje op jullie promoties kan drinken!

De 'popkes' van het eerste uur, Agnes, Inge, Joyce en Wendy, bedankt voor alle gezelligheid tijdens de lunches en buiten werktijd!

Joost, super bedankt voor al je hulp met illustrator, de posters en alle prachtige illustraties voor mijn introductie, discussie en samenvatting! En ook voor je geduld met mij. Ik wens je heel veel succes met je eigen graphic design bureau *scicomvisuals*!

Hoofdstukken 5 en 7 van dit proefschrift zijn het resultaat van twee hele leuke samenwerkingen, waaruit ik veel heb geleerd. Jeanette, Marco en Peter, bedankt voor jullie inzet, discussies en gezelligheid tijdens congressen! Marjolein en Marijn, met jullie heb ik heel wat uurtjes in de donkere kamer achter de microscoop doorgebracht en als operatie assistente van Marijn in het GDL. Bedankt voor alle gezelligheid, tips en leerzame discussies, hopelijk kunnen we binnenkort deze studie afronden met mooie *in vivo* data erbij!

Minstens zo belangrijk tijdens promotie onderzoek is de ontspanning en gezelligheid naast het werk!

Lieven meiden, Esther, Magda, Margarite, Marijke, Rinske, en Linda bedankt voor alle gezellige mailtjes, sms-jes, whatsapp-jes en borrels. Bedankt dat jullie er zijn en alvast bedankt voor alle gezelligheid die nog gaat komen (citaat van Rins en Magda)!

Tennis ladies, het is altijd een feestje om een dagje met jullie op de tennisbaan door te brengen! Nicole, je staat altijd voor mij (en voor Valtho!) klaar, in goede en slechte tijden. Thanks lieverd!

Dan zijn er de Rotterdammers, geloof dat ik jullie voornamelijk moet bedanken voor het feit dat ik Roel mocht meenemen naar Utrecht! Jajajajahjahjahjahjahhjahhjahhjahhhjaahhhh…..…

Rien en Arna, bedankt voor al jullie interesse in mijn onderzoek, voor de fijne werkplekjes bij jullie en alle gezelligheid!

Berber, ik ben er trots op om jouw naamgenote te zijn. Het is dan wel geen Friese literatuur geworden, maar hopelijk zie je jouw schrijvers genen hier toch een beetje in terug.

Jolmer, Jildou en Riksta, wat een mazzelkont ben ik met een lieve grote broer en zulke lieve grote zussen! Rikkie, wij zijn het Utrechtse Overdijk-front en daardoor heb je een speciaal plekje. Je staat, samen met Colin, letterlijk dag en nacht voor mij klaar, je bent mijn zus en mijn beste vriendin!

Lieve mem en heit, jullie zeggen weleens dat jullie trots zijn op jullie kroost, maar ik hoop dat jullie weten dat ik ook enorm trots ben op jullie! Ik heb de afgelopen jaren uiteraard veel gehad aan de analytische genen van mem en de medische genen van heit! Heit, ik waardeer je enorme interesse in mijn onderzoek en ben onder de indruk van je inzet om alle details te begrijpen. Eens een arts altijd een arts, soms tot vervelends aan toe…. Bedankt voor jullie onvoorwaardelijke steun en alles wat jullie mij hebben meegegeven!

Als laatste wil ik mijn aller liefste bedanken. Lieve Roel, ik ben er super trots op dat jij de cover van mijn proefschrift hebt gemaakt. Op deze manier is jouw enorme bijdrage, die je op de achtergrond hebt geleverd aan dit proefschrift, toch nog een beetje zichtbaar geworden. Heb je lief!

Curriculum Vitae

Marije Berber Overdijk was born on January 6, 1980 in Sneek, The Netherlands. After finishing high school (Voortgezet Wetenschappelijk Onderwijs, VWO) at the RSG Magister Alvinus in Sneek in 1998 she studied at the Hanzehogeschool Groningen Higher Laboratory education (Biologie en Medisch Laboratoriumonderzoek). In 2002 she received her bachelor's degree and continued her research at the University Groningen, where she had performed her internship. In January 2003 she started as a research technician at the Faculty of Veterinary Medicine, University Utrecht, Department of Infectious Diseases and Immunology, focusing on trancytosis of *Mycobacterium avium* ssp. *paratuberculosis*. In July 2005 she switched to the Academic Medical Center, Amsterdam, Department Pathology. Here her work focused on the role of WNT-signaling in Multiple Myeloma. From April 2007 she is employed at Genmab where she initially started as a research associate, working on the discovery and development of new therapeutic antibodies. In January 2009 she was promoted to senior research associate and in July 2009 she started a PhD study in the Translational Research & Pharmacology group under supervision of dr. W. Bleeker, dr. P. Parren and Prof. dr. J. v.d. Winkel, in which she studied the Fc-gamma receptor mediated effector functions of therapeutic antibodies. The results of these studies are reported in this thesis. She will continue working at Genmab as scientist in the Antibody science department.

List of publications

1. **Overdijk, M. B.**, S. Verploegen, W. K. Bleeker, and P. W. Parren. 2013. Chapter 13, Role of IgG Fc receptors in monoclonal antibody therapy of Cancer. 2014. *Antibody Fc: Linking Adaptive and Innate Immunity*, page 239-255, ISBN 9780123948021.

2. **Overdijk, M. B.,** S. Verploegen, A. Ortiz Buijsse, T. Vink, J. H. Leusen, W. K. Bleeker, and P. W. Parren. 2012. Crosstalk between human IgG isotypes and murine effector cells. *J Immunol* 189:3430-3438.

3. Santema, W., P. van Kooten, A. Hoek, M. Leeflang, **M. Overdijk**, V. Rutten, and A. Koets. 2011. Hsp70 vaccination-induced antibodies recognize B cell epitopes in the cell wall of Mycobacterium avium subspecies paratuberculosis. *Vaccine* 29:1364-1373.

4. **Overdijk, M. B.**, S. Verploegen, J. H. van den Brakel, J. J. Lammerts van Bueren, T. Vink, J. G. van de Winkel, P. W. Parren, and W. K. Bleeker. 2011. Epidermal Growth Factor Receptor (EGFR) Antibody-Induced Antibody-Dependent Cellular Cytotoxicity Plays a Prominent Role in Inhibiting Tumorigenesis, Even of Tumor Cells Insensitive to EGFR Signaling Inhibition. *J Immunol* 187:3383-3390.

5. Groen, R. W., M. F. de Rooij, K. A. Kocemba, R. M. Reijmers, A. de Haan-Kramer, **M. B. Overdijk,** L. Aalders, H. Rozemuller, A. C. Martens, P. L. Bergsagel, M. J. Kersten, S. T. Pals, and M. Spaargaren. 2011. N-cadherin-mediated interaction with multiple myeloma cells inhibits osteoblast differentiation. *Haematologica* 96:1653-1661.

6. Koets, A., W. Santema, H. Mertens, D. Oostenrijk, M. Keestra, **M. Overdijk**, R. Labouriau, P. Franken, A. Frijters, M. Nielen, and V. Rutten. 2010. Susceptibility to paratuberculosis infection in cattle is associated with single nucleotide polymorphisms in Toll-like receptor 2 which modulate immune responses against Mycobacterium avium subspecies paratuberculosis. *Prev Vet Med* 93:305-315.

7. Santema, W., **M. Overdijk,** J. Barends, J. Krijgsveld, V. Rutten, and A. Koets. 2009. Searching for proteins of Mycobacterium avium subspecies paratuberculosis with diagnostic potential by comparative qualitative proteomic analysis of mycobacterial tuberculins. *Vet Microbiol* 138:191-196.

8. Groen, R. W., M. E. Oud, E. J. Schilder-Tol, **M. B. Overdijk,** D. ten Berge, R. Nusse, M. Spaargaren, and S. T. Pals. 2008. Illegitimate WNT pathway activation by beta-catenin mutation or autocrine stimulation in T-cell malignancies. *Cancer Res* 68:6969-6977.

9. Koets, A., A. Hoek, M. Langelaar, **M. Overdijk,** W. Santema, P. Franken, W. Eden, and V. Rutten. 2006. Mycobacterial 70 kD heat-shock protein is an effective subunit vaccine against bovine paratuberculosis. *Vaccine* 24:2550-2559.

10. Langelaar, M. F., C. N. Weber, **M. B. Overdijk**, K. E. Muller, A. P. Koets, and V. P. Rutten. 2005. Cytokine gene expression profiles of bovine dendritic cells after interaction with Mycobacterium avium ssp. paratuberculosis (M.a.p.), Escherichia coli (E. coli) or recombinant M.a.p. heat shock protein 70. *Vet Immunol Immunopathol* 107:153-161.